Novel approaches to Boron-directed functionalisation of organic molecules

Usman Hamza Shabbir

A dissertation presented to

UNIVERSITY COLLEGE LONDON

in partial fulfilment of the requirements for the degree of

DOCTOR OF PHILOSOPHY

UCL Department of Chemistry
20 Gordon Street
London
WC1H 0AJ

Declaration

I, Usman H. Shabbir, confirm that the work presented in this thesis is my own. Where information has been derived from other sources, I confirm this has been acknowledged in the thesis.

……..

Abstract

This thesis is aimed at exploiting the potential of boron compounds for: developing novel boron-directed C–H functionalisation; the synthesis of novel five-membered heterocyclic boron ring systems and in the design of a method for mono-*N*-methylation of primary amines.

Chapter 1 provides an introductory review of the synthetic uses of boron and the medicinal applications of boron-containing compounds.

Chapter 2 begins with a detailed overview into transition-metal catalysed directed C–H functionalisation. This is followed by an investigation of existing and novel boron scaffolds for their suitability in transition-metal catalysed functionalisation of unreactive C–H bonds. Various well-established directing groups (DGs) were incorporated leading to B(DG)-linked scaffolds which were then attached to a range of unsaturated and saturated aliphatic and cyclic systems containing inert C–H bonds. After extensive investigation into regioselectivity transforming inert C–H bonds to more attractive C–C bonds, it was found that a fine balance needed to be struck between B-scaffold stability and reactivity towards C–H functionalisation conditions.

Chapter 3 opens with a review in the role of boron as part of a frustrated Lewis pair (FLP) as well as its applications in metal-free chemical transformations. This is followed by an investigation into the use of halomethylboronates in the synthesis of novel heterocyclic systems, through acting as a FLP. This novel reaction was optimised, and 3 different vectors of functional group attachment were explored resulting in a diverse spectrum of highly functionalised boron-centred spiro compounds. The use of halomethylboronates in the mono-*N*-methylation of primary amines was also studied to identify how to overcome the low methylation yields previously reported in the group.

Impact statement

Boron plays a pivotal role in synthetic chemistry, providing a range of applications that have rendered it an indispensable tool for chemists. Its unique properties, including the capacity to form diverse chemical bonds and participate in various transformations, make it an element of great interest for further investigation to unlock additional applications.

Our work on boron-directed C–H functionalisation highlighted the delicate balance required for maintaining the stability of boron-containing scaffolds while ensuring reactivity towards C–H functionalisation conditions. Our results hold the potential to inspire the development of more informed strategies in the synthesis of boron-based scaffolds that can direct the functionalisation of simple building blocks to yield complex compounds.

We also report an optimised method using a low-cost organoboron reagent to form novel and highly functionalised diazaboroles, which have the potential for use in medicinal chemistry, as building blocks for organic synthesis, or as chiral auxiliaries. Moreover, we have explored a strategy for the mono-*N*-methylation of primary amines using the same boron reagent. These discoveries establish a groundwork for refining this method into a high-yielding monoalkylation reaction, which we envision will hold significant value for the pharmaceutical industry. A 2006 assessment of reactions utilised at GSK, Pfizer, and AstraZeneca in process chemistry, determined heteroatom alkylation as the most prevalent reaction class, reinforcing the potential impact of our findings in this industry.[†]

[†] Carey, J. S.; Laffan, D.; Thomson, C. & Williams, M. T. Analysis of the reactions used for the preparation of drug candidate molecules. *Org. Biomol. Chem*. **4**, 2337–2347 (2006).

Acknowledgements

I am deeply grateful to Tom Sheppard for his exceptional guidance throughout my PhD journey, particularly during the challenging times of the Covid-19 pandemic. His infectious enthusiasm and optimistic outlook were incredibly uplifting, providing perfect support during the setbacks I faced in my experiments. Your mentorship has been instrumental in shaping both my academic and personal growth, for which I will always be indebted. Thank you also to Carl Mallia, my industrial supervisor at AstraZeneca. His assistance in extending my industrial placement in Macclesfield not only accelerated my research progress but also allowed me to savour the serene beauty of the countryside, surrounded by sheep, cows and green fields.

To my viva examiners, Alex and Vijay, thank you for your time in reviewing my thesis and for the engaging discussion on my research. Special mention to Vijay for the candid conversations in the corridors, lab, and office which I always enjoyed being a part of. Your gesture of sharing oranges in the office showed your commitment to a healthy workspace and dispelled my scurvy concerns. Less healthy but much appreciated was the chocolate ice cream you kindly purchased for the whole lab, etched in my memory for its distinctive appearance. I hope soon you'll forget about the retirement letter that was accidentally sent your way due to a mistyped email address.

Moving on to the current members in the Sheppard group, starting from none other than Phyllida. Despite dedicating a significant number of hours to swimming, her boundless energy and delightful company have been an absolute joy. With her knack for vandalising fumehoods and spreading amusing CIB rumours, I can't help but wonder who the next target of her mischievous antics will be. That brings me to Nat, who recently joined the Sheppard group and has been a pleasure to work alongside, despite her questionable taste in Taylor Swift's music. I hope her friend soon get the hang of travelling on a bus properly.

Matt P. has been an incredibly invaluable member of the Sheppard group, not least for ensuring the lab is fully functional and his valiant attempts to sort out waste collection despite the waste man's lack of organisation. I dread to think how the KLB will cope without you when you leave. I will also miss my boron comrade, Richard, and his expert knowledge in all things boron. I wish you well in your collaboration with the Powner group despite your betrayal to the dark side. I also express gratitude to Helen Allan, who has kept the lab running smoothly.

I must also say a few words about past members of the Sheppard group, starting with Nehaal. I've always admired your impeccable fashion taste and highly appreciated your advice for the

ACS conference in USA. Though my experience across the pond might not have matched the intensity of your thrilling schedule, I could enjoy other delights in California. In addition, while I did not have much lab overlap with my other boron comrade, Matt C., due to the pandemic and industrial placements, conversations with him were always intellectually stimulating.

Another long-standing member of the Sheppard group, Rachel, has been a steadfast companion throughout my PhD journey. It is she whom I must thank for joining me in playing badminton during the first year of my PhD – I believe we're due for another match soon. Dave, too, was an excellent colleague, sought after by everyone in the lab for his endless wisdom and advice. His departure from the lab to pursue greener pastures is still deeply felt. Additionally, another member of the group, Sahra, spearheaded a streamlined lab transformation, including the revival of the Kardex system, which unfortunately is broken as I write this.

I am grateful to all members of the Baker and Chudasama groups, particularly the subset Faker Bakers. An integral part of this group is Roshni, whose presence illuminated the lab during the challenging times of Covid and beyond, mirroring the literal translation of her name. Thank you for being a founder of the Saturday lunch crew, initiating countless bakery breaks, organising lab socials, and hosting numerous events at your house for us all – you made the PhD a much more enjoyable experience.

Also, thank you to Muhammed, who is not only a founder of the infamous Burger Boys™, but a constant source of calm during my hectic PhD. Given his inclination for adrenaline-inducing automobile adventures, I wish you all the best with the new passenger in your married life. Another founder, Mikesh, has been a great pleasure to work alongside. Whilst he was quite reserved when he started, I am pleased he opened up and became a key part of the lab. Thank you for organising the renowned treasure hunts, of which many decisions were controversial.

Despite plenty of pranks played on her, some of which were borderline traumatic, Léa has always maintained her cheerful spirit. Thank you for bringing joy and positivity to the lab. I hope you will share your many memorable 365 experiences with your new colleagues, and I eagerly anticipate the day when you settle the £10 debt which has accrued significant interest.

This brings me to Léa's new colleague and a former member of our lab, Alina, who symbolises the work-hard (how early were you waking up?) and play-hard (haram falcon tubes?) ethos. Sadly, I'm still haunted by the rum-filled chocolates you kindly offered after you returned from Poland. I hope the lingering trace amounts will leave my bloodstream soon.

Yanbo, I'd like to express my gratitude for your incredible patience, especially when I was frequently late for our meetings at Kings Cross station before our lab socials. I am grateful you didn’t threaten me with your knife(s) especially since I may or may not have been involved in the freeze-drying of your teddy bear. I wish you well in your influencer career in China.

I'd also like to extend my thanks to Lula, whom I'm delighted to keep encountering during my NMR visits to the CIB. Our catchups are always enjoyable, and I'm saddened that these spontaneous meetups are coming to an end. To Faiza, with a fashion sense rivalling that of Nehaal's, thank you for inviting me to your special day, it remains an unforgettable memory.

To the surviving Bakers Charlie and Matt D., even though our time together was short, it was nevertheless sweet and I'm grateful for sharing my remaining lab time with both of you. I hope your mischievous laptop pranks continue, though I must admit I'm still dealing with the aftermath of my laptop being haunted by random sounds that I find great difficulty to identify.

Moving on to the Chudasama group, I must start with Ioanna who is probably the most hard-working person I know. Her can-do attitude is something I strive to attain. I hope that the last stretch of your PhD is drama-free and avoids any handling of liquid nitrogen. Her partner in crime, Clíona, is one of the kindest individuals in the lab. She is always happy to help, particularly with completing certain 'stalking' requests. Your excellent but equally worrying skill for uncovering hidden truths about people's lives might just qualify you for a role in the secret service if you fancy a career change after the PhD.

An honourable mention to Steven and Toby, who are two of the most wholesome colleagues I worked alongside. Steven, may your golfing adventures continue to match the prowess of Tiger Woods himself. Toby, your PI and I both look forward to the day when your wild weekend parties might become a bit more restrained.

I am also indebted to my friends across the road at the CIB, providing me with much-needed breaks from the KLB. It has been great catching up in various corridors, lifts, Nyholm room for lunches as well as dinners with cuisines ranging from Japanese to Lebanese. While there are several in the KLB eager to know who you are, for both my safety and your privacy, names have been redacted to prevent any explosive reactions from keen colleagues in the KLB.

Lastly, I want to express eternal gratitude to my family for their constant support throughout my studies. In particular, I am grateful to my mum with the endless supplies of home-cooked food, which have provided me with the much-needed energy to complete this PhD. Thank you.

Contents

Abbreviations

Ac	Acetyl
AQ	8-Aminoquinoline
dan	1,8-Diaminonapthalene
dab	1,2-Diaminobenzene
DCC	*N*,*N*'-Dicyclohexylcarbodiimide
DCE	1,2-Dichloroethane
DCM	Dichloromethane
DFT	Density functional theory
DG	Directing group
DIPEA	*N*,*N*-Diisopropylethylamine
DMAP	4-Dimethylaminopyridine
DMF	*N*,*N*-Dimethylformamide
DMSO	Dimethylsulfoxide
Eq.	Equivalent(s)
GC	Gas Chromatography
h	Hours
HFIP	1,1,1,3,3,3-Hexafluoroisopropanol
HOBt	1-Hydroxybenzotriazole hydrate
Mes	Mesityl
MIDA	*N*-Methyliminodiacetic acid
MS	Molecular sieves
NBS	*N*-Bromosuccinamide
NMR	Nuclear Magnetic Resonance

PA	Picolinamide
Pin	Pinacol
Piv	Pivalate
ppm	Parts per million
pza	2-Pyrazol-5-ylaniline
rt	Room temperature
SAR	Structure activity relationship
SM	Starting material
S_N2	Bimolecular nucleophilic substitution
S_NAr	Nucleophilic aromatic substitution
tAmOH	*tert*-Amyl alcohol
TFA	Trifluoroacetic acid
THF	Tetrahydrofuran
TLC	Thin layer chromatography
TsOH	*p*-Toluenesulfonic acid
TAME	*tert*-Amyl methyl ether

1 An overview of boron chemistry

1.1 Introduction to boron

In the domain of synthetic organic chemistry, boron has emerged as a versatile element, drawing attention for its unique properties and diverse applications. Boron's distinct electronic configuration and its capacity to form a range of compounds have positioned it as a valuable component in various transformations. This introductory review will shed light on the role boron plays in organic synthesis and medicinal chemistry.

Boron possesses three valence electrons and exhibits a ground state electron configuration of $1s^2 2s^2 2p^1$. It is not uncommon to observe boron forming stable trivalent compounds such as BF_3 without a full octet, where the central boron atom adopts sp^2 hybridization with a vacant p-orbital. As a result, these compounds share isoelectronic similarities with carbocations.

The distinctive properties of trivalent boron compounds mainly stem from the unoccupied p-orbital on the boron atom, rendering these compounds Lewis acidic. This property has been exploited in various reactions – which will be discussed in this overview and in subsequent chapters.

Compounds belonging to the category of organoboron compounds encompass at least one carbon-to-boron bond, such as boranes, borinic acids and borinic esters. Other boron compounds, while not strictly classified as organoboron compounds, are also employed in synthesis. These include borate (boric) esters and boron trihalides, featuring three halogens bonded to boron. Borate esters, being trivalent, consist of three alkoxy groups attached to boron (**Figure 1**). Boronic acids and boronic (boronate) esters stand out as some of the most extensively researched and synthetically valuable organoboron compounds, largely due to their role in the Suzuki reaction.

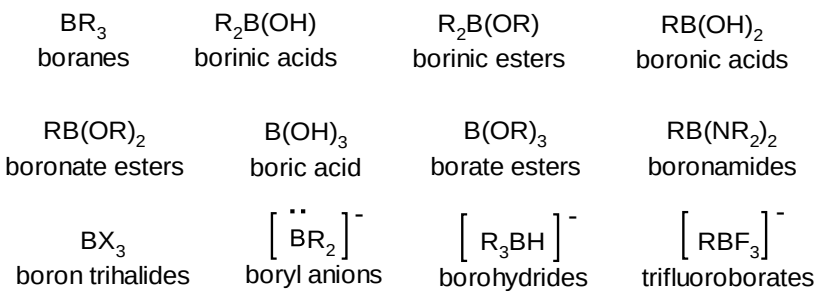

***Figure 1**. Examples of boron-containing compounds.*

1.2 Boron-based catalysis

Boranes are often employed as strong Lewis acids by virtue of their empty p-orbital and are commonly used as catalysts since they enhance the reactivity of organic compounds via coordination to Lewis basic sites.[1–5]

Given the theme of C–H activation in a later chapter in this work, it is apt to note that metal-free catalytic C–H silylation of aromatic substrates **1** with hydrolysilanes **2** could be achieved with the halogenated triarylborane $B(C_6F_5)_3$ under mild reaction conditions (**Scheme 1**).[6]

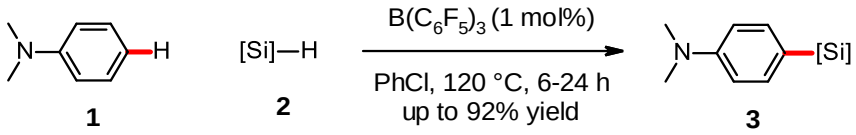

***Scheme 1**. Boron-catalysed C(sp^2)–H bond silylation.*

Within our group, borate esters were employed as simple catalysts for the sustainable formation of amide bonds, avoiding the use of hazardous coupling reagents, stoichiometric by-products and waste-intensive molecular sieves (**Scheme 2**).[7]

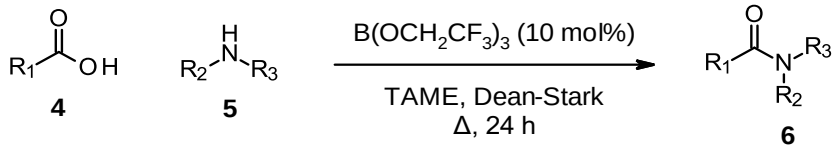

***Scheme 2**. Amidation protocol using a borate ester catalyst.*

Recently, Ingleson and co-workers reported on the novel use of organoboranes as fluoride phase-transfer catalysts for the fluorination of organohalides with commercially available CsF (**Scheme 3**).[8] Remarkably, while boron typically exhibits high fluorophilicity to form very stable B-F bonds, judicious selection of the organoborane **7** allows for a balanced fluoride affinity for the borane to form a fluoroboronate **8** and subsequent transfer of the fluoride to an electrophile **9** to furnish the fluorinated compound **10**. Enantioenriched β-fluoroamines were also possible using oxazaborolane catalysts albeit with low enantioselectivities.

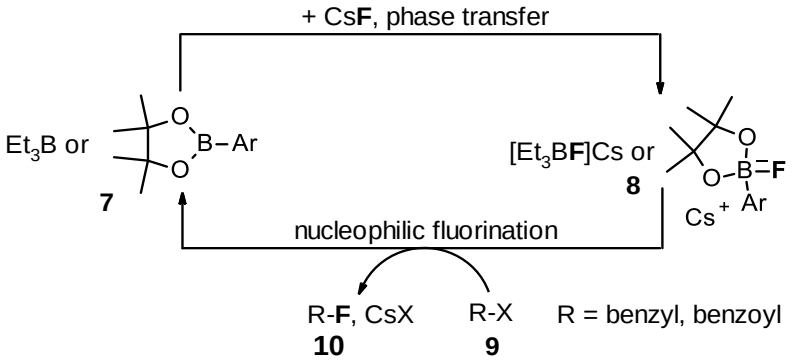

***Scheme 3**. Fluorination using simple boranes as CsF phase transfer catalysts.*

1.3 Hydroboration

Recognised with a Nobel prize in chemistry that was shared with none other than Wittig, Brown first reported the conversion of olefins into organoboranes.[9–11] The organoboranes can be oxidised to the corresponding alcohol with the overall process resulting in the syn addition of a hydrogen and a hydroxyl group across the alkene.

With unsymmetrical alkenes such as **11**, the reaction furnishes the *anti*-Markovnikov product **12**, where the boron adds to the less substituted end of the double bond (**Scheme 4, top**). Alkynes can also undergo hydroboration, such to the addition of catecholborane to alkyne **14** furnishing 1-alkenylboronate **15** (**Scheme 4, bottom**)

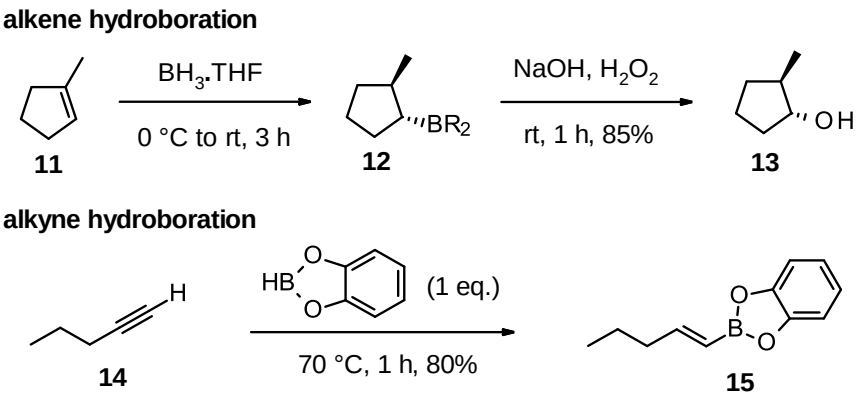

***Scheme 4**. Hydroboration of alkenes and alkynes.*

Alkenyl boronates were also used as coupling partners in the Pd-catalysed reaction with bromide **17**, in the seminal report by Akira Suzuki in 1979 **(Scheme 5**).[12,13] Since then, this reaction, more commonly known as the Suzuki-Miyaura cross-coupling, has led to a significant

advancement in transition-metal catalysed reactions. Whilst this is beyond the scope of this introductory review, the reader will find more details in the following chapter.

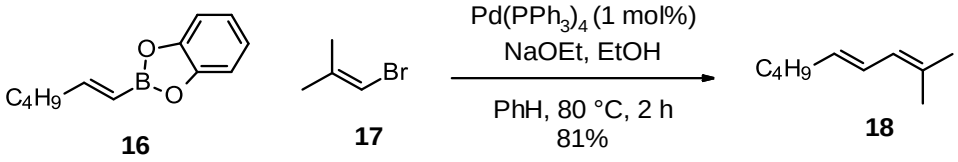

Scheme 5**. Palladium catalysed cross-coupling of alkenylboronate **16** with halide **17.

1.4 Boron-mediated aldol reactions

The Aldol reaction, a cornerstone in organic chemistry, involves the powerful union of carbonyl compounds to form β-hydroxy carbonyl compounds via an enolate intermediate. The enolization of sterically unhindered ketones with lithium amides however leads to poor *E*/*Z* lithium enolate stereoselectivity with a mixture of *syn* and *anti* aldol adducts formed.

Stemming from the pioneering work of Mukaiyama and co-workers in the early 1970s who first utilised boron enolates,[14] the boron-mediated aldol reaction has emerged as a formidable method to form new carbon-carbon bonds with precise stereoselectivity.

The strong association between the enolate geometry and the resultant stereochemistry of the product (with *Z*-enolates yielding *syn* aldol adducts and *E*-enolates yielding *anti* aldol adducts) demonstrates the high stereospecificity of the boron-mediated aldol reaction (**Scheme 6**).[15]

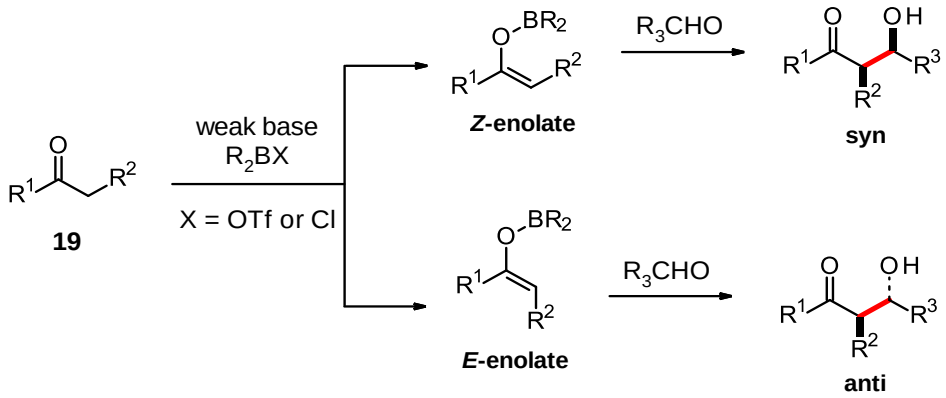

***Scheme 6**. The directed aldol reaction employing boron enolates.*

Brown and colleagues reported controlling stereochemistry of the enolization through careful selection of the boron reagent used.[16] The preferred formation of the *E*-enolate over the *Z*-enolate is favoured by using: R_2BCl instead of R_2BOTf; NEt_3 instead of *i*Pr_2NEt; and (*c*-$Hex)_2B$ over 9-BBN. Conversely, dialkylboron triflates commonly yield *Z*-enolates, displaying

little sensitivity to both the choice of amine and the steric attributes of the alkyl groups associated with the boron reagent (**Scheme 7**).

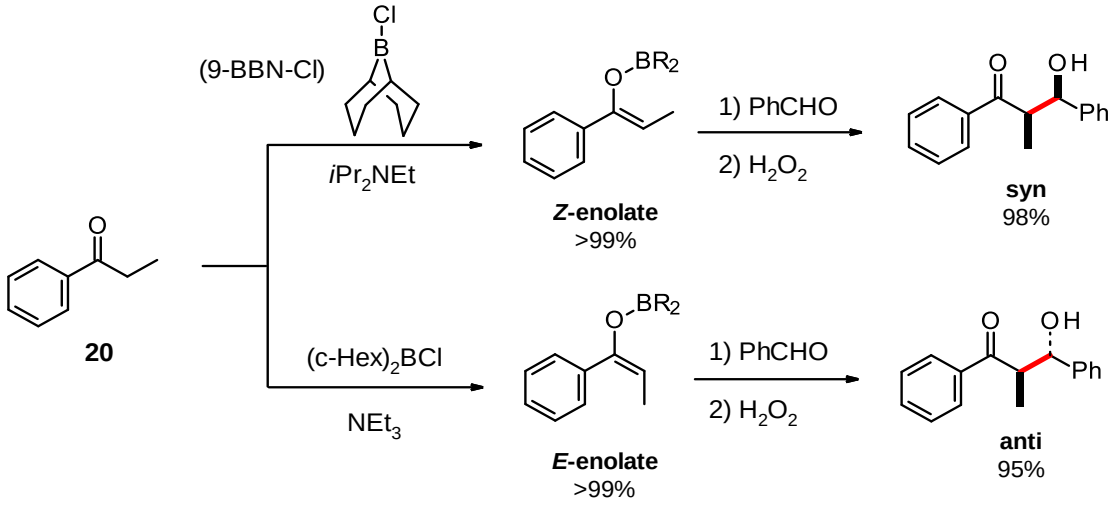

***Scheme 7**. Conversion of propiophenone **20** into E- or Z-enol borinates.*

This stereoselective enolization approach has been successfully employed in the synthesis of complex natural products, such as the precursor **23** of Elaiolide (**Scheme 8**).[17]

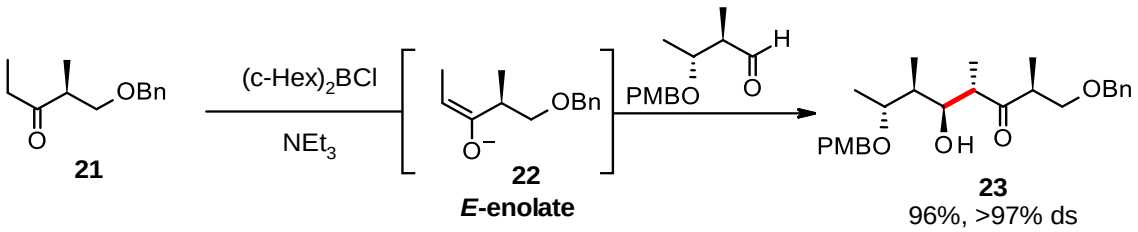

***Scheme 8**. Boron enolate approach used in the total synthesis of Elaiolide.*

1.5 Frustrated Lewis pairs

Boron has also garnered significant attention for its unique ability to form frustrated Lewis pairs (FLPs). In classical Lewis acid-base interactions, a Lewis acid accepts an electron pair from a Lewis base. FLPs however, defy this traditional paradigm by resisting the formation of a stable Lewis acid-base adduct, thereby offering a novel pathway for exploring unconventional reactivity in chemical systems.

While this topic is outside of the scope of this introductory review, the reader is referred to the final chapter of this thesis where this behaviour of boron is discussed in more detail.

1.6 Borohydrides

In contrast to boranes, known for their robust Lewis acid character, borohydrides exhibit a nucleophilic nature. Marking the inception of the first alkali metal borohydride, Schlesinger and Brown documented the synthesis of lithium borohydride in 1940 (**Figure 2**).[18]

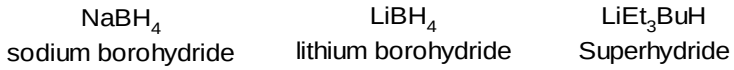

***Figure 2**. Commonly used borohydrides in organic chemistry.*

Sodium borohydride, while less reactive than $LiBH_4$ due to the smaller charge density on sodium compared to lithium, is commonplace within a chemist's toolkit, capable of reducing various functional groups including aldehydes, ketones and acid chlorides.[19]

Additionally, $NaBH_4$ can carry out selective 1,2-reduction of enones such as **24** in combination with $CeCl_3$, referred to as the Luche conditions (**Scheme 3**).[20]

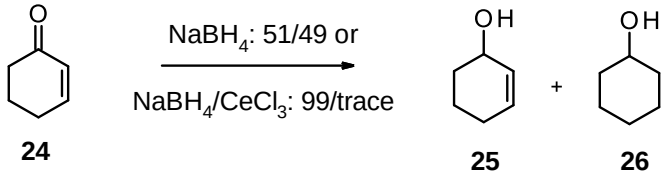

***Scheme 9**. The selective reduction of α,β-unsaturated ketone **24** using the Luche conditions.*

Its more reactive cousin, lithium triethylborohydride (Superhydride), because of the electron-donating alkyl groups, can reduce additional functional groups such as amides and nitriles.

Substituting one hydrogen atom by CN in $NaBH_4$ gives rise to sodium cyanoborohydride whose remaining hydrides have attenuated nucleophilicity. As a result, $NaBH_3CN$ is employed in slightly acidic conditions where it reacts significantly slower with ketones and aldehydes than iminium salts formed *in situ* by reacting a ketone or aldehyde with an amine. This reductive amination process can also be carried out by sodium triacetoxyborohydride which also avoids generation of toxic side-products HCN or NaCN.

1.7 Medicinal applications of boron-containing compounds

Boron has emerged as a compelling player in the field of therapeutics with various boron-containing compounds showing different modes of inhibition against a spectrum of biological targets.

Isolated from Streptomyces antibiotics in 1967, Boromycin marked the inception of boron-containing natural products.[21] Consisting of a complex of boric acid with a tetradentate coordination, it is effective against most Gram-positive bacteria where it disrupts the cytoplasmic membrane and induces the release of potassium ions. Furthermore, Boromycin has demonstrated anti-HIV activity.[22] Other notable boron-containing natural products include the antibiotics borophycin, aplasmomycins and tartrolons, which were extracted from marine bacteria.[23–27]

α-Aminoboronic acids can create dative bonds, due to the empty p-orbital on boron, with nucleophilic amino acid residues, such as serine, commonly located in the active site of proteases. These reversible dative bonds are more robust than non-bonding intermolecular interactions and this interaction is exemplified by the anticancer medication bortezomib (sold as Velcade) (**Figure 3, left**). Bortezomib was the first proteasome inhibitor, gaining FDA approval in 2003, but also holds the accolade for being the first boronic acid-based drug on the market.

The mode of action of bortezomib involves binding reversibly to the active site of a proteasome, where the boronic acid group interacts with the hydroxyl group of a nucleophilic threonine residue (**Figure 3, right**).[28] Inhibiting the proteasome causes a build-up of pro-apoptotic proteins (regulators of cell death processes) in tumorigenic cells while sparing non-cancerous tissue.

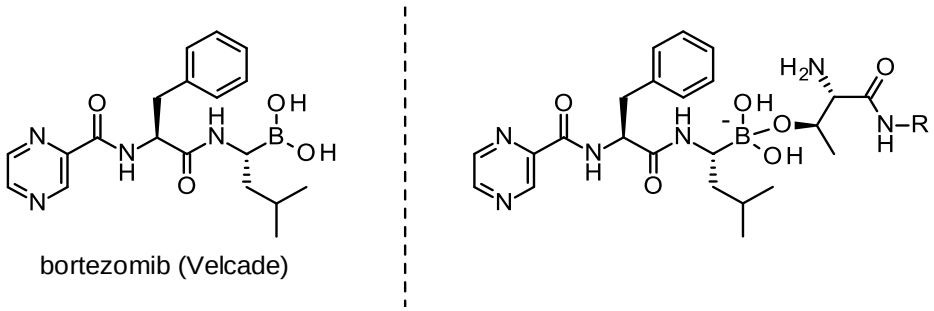

***Figure 3**. The first dipeptidyl boronic-containing approved drug (left), key interaction between bortezomib and a terminal threonine residue of a proteasome (right).*

Ixazomib **27**, a second-generation proteasome inhibitor sold as Ninlaro, demonstrates an enhanced pharmacokinetic profile when contrasted with bortezomib, including a shorter half-life and better distribution in the blood. Ixazomib also has the distinction of being the first oral proteasome inhibitor, approved by the FDA in 2015, for treating multiple myeloma. It is generally given orally in the form of a citrate boronic ester prodrug, which undergoes hydrolysis in the bloodstream to transform into the active boronic acid form (**Figure 4**). Delanzomib **28**, a related boronic acid-based proteasome inhibitor is also given orally.

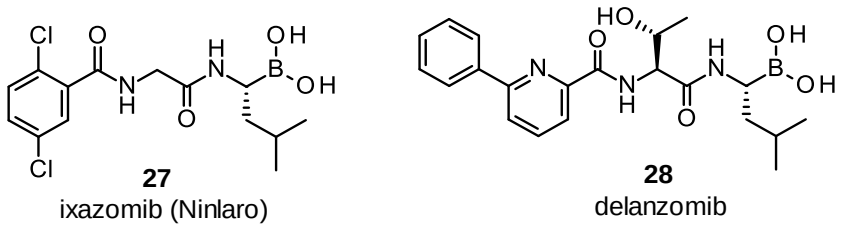

27
ixazomib (Ninlaro)

28
delanzomib

Figure 4*. Structures of ixazomib and delanzomib.*

Tavaborole **29**, sold as Kerydin and approved by the FDA in 2014, is an oxaborole antifungal and is used for treating fungal infection of the toenail. Its mode of action is by disrupting fungal protein synthesis through inhibiting leucyl-tRNA synthetase. Specifically, tavaborole interacts with the cis diol found in the ribose component of the terminal adenosine within leucyl-tRNA **30**, resulting in the inactivation of the essential fungal enzyme, leucyl-tRNA synthetase (**Scheme 10**).[29]

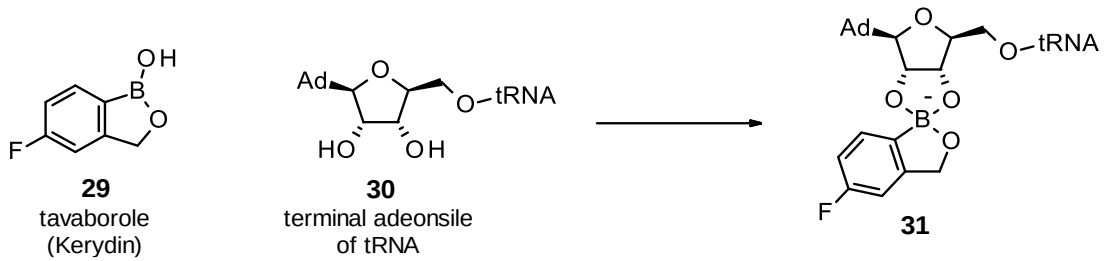

29
tavaborole
(Kerydin)

30
terminal adeonsile
of tRNA

31

Scheme 10*. Mode of action of tavaborole with leucyl-tRNA synthetase.*

Talabostat **32**, a dipeptide boronic acid, acts as a dipeptidyl peptidase (DPP) inhibitor and has demonstrated anti-tumour effects on fibrosarcoma, lymphoma, melanoma, and mastocytoma cell line-derived tumours.[30] The active drug can also undergo cyclisation at physiological pH, attenuating its potency by over 100-fold (**Scheme 11**).[31]

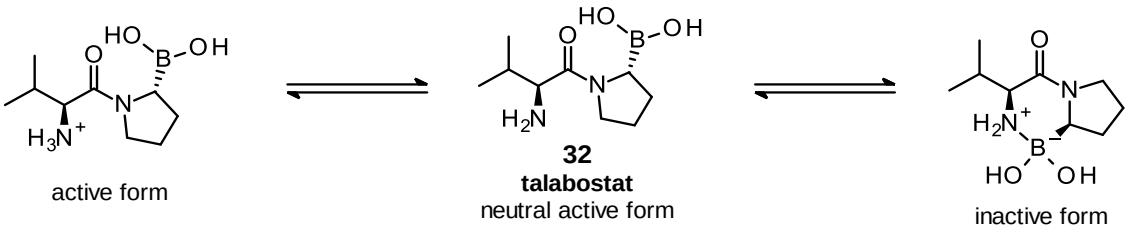

***Scheme 11**. Structure of active talabostat and its inactive cyclised form.*

2 Boron-directed C–H functionalisation

2.1 Introduction

2.1.1 Transition metal-catalysed C–H functionalisation

Reactions that involve transition metal catalysis have played a crucial role in forming C–C/ C–heteroatom bonds since the 1950s with the Co-catalysed C–H functionalisation being the first major milestone in this field.[32] In addition, synthetic approaches for drug discovery tend to rely heavily upon well-established transition metal (TM) catalysed reactions such as Suzuki cross-couplings or Buchwald-Hartwig aminations which are both among the top 20 most used reactions in drug discovery (**Figure 5**).[33]

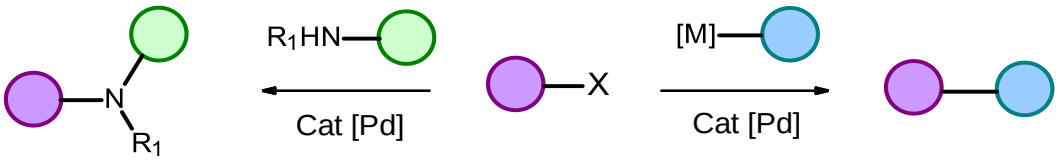

***Figure 5**. Pd-catalysed Suzuki and amination cross-coupling reactions.*

However, incorporating diverse functional groups to create complex building blocks using sustainable strategies remains a key objective. Efforts to achieve this have involved using directed TM-catalysed reactions. These reactions have facilitated the synthesis of highly functionalised molecules whilst also maintaining low atom economy and being environmentally friendly. In this directed approach, a C–H bond is activated after insertion by a TM catalyst and thereafter functionalised leading to a highly site-selective C–H transformation (**Figure 6**).

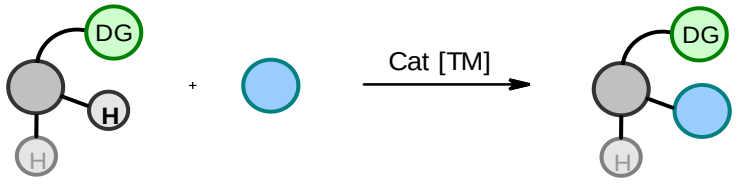

***Figure 6**. Illustration of directed transition-metal catalysed functionalisation of C–H bonds.*

For many organic molecules however, the presence of several C–H bonds which share similar bond dissociation enthalpies can lead to issues in controlling site-selectivity in C–H activation reactions. To overcome the inherent regioselectivity challenges in these processes, several protocols have been developed, whereby a TM is positioned near to the desired C–H bond.

This long-standing challenge of achieving highly selective C–H transformations in this field has been addressed in numerous ways. One strategy involves the use of steric control (**Figure 7a**) to favour specific C–H bond over others in the same region of the molecule. Other methods involve employing motifs such as Lewis basic moieties, to act as a directing group (DGs). (**Figure 7b-d**). These DG motifs can be inherently present in substrates or are exogenous.[34–37]

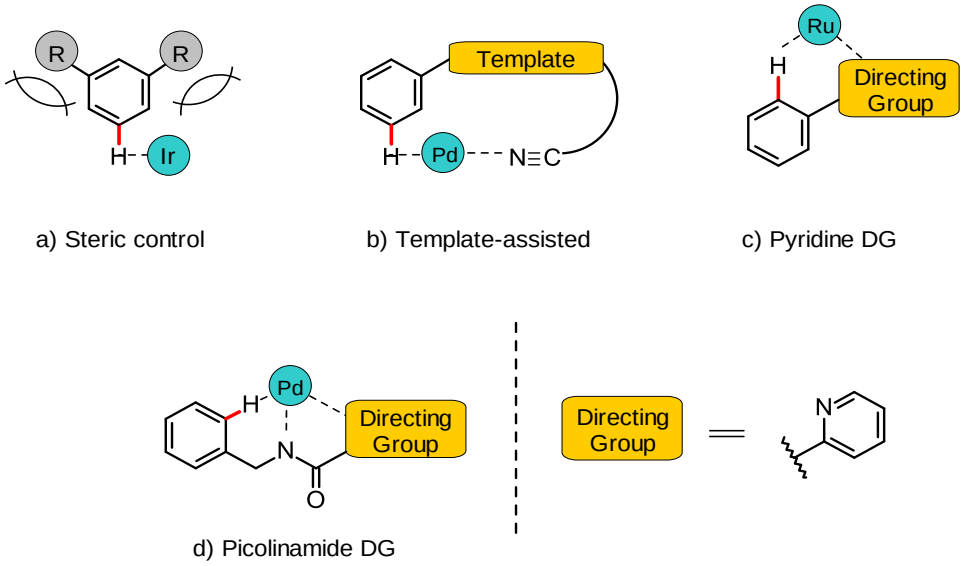

Figure 7. *Some existing strategies for ortho- and meta-directed C(sp^2)–H functionalisation.*

Despite DGs being an attractive method in controlling regioselectivity there are many drawbacks to their use. For instance, many existing DGs often require lengthy syntheses, play no important role in subsequent synthetic steps and can be difficult to install and remove without using harsh conditions.

In the last decade there has been a breakthrough in the use of weakly coordinating DGs and specialised ligands that help promote C–H activation. This has paved the way to functionalising a range of substrates such as carboxylic acids, amines, and alcohols.

It should be noted that the catalytic cycle of these methods, are dependent upon expensive and toxic oxidants such as silver and copper salts in superstoichiometric amounts. This has a huge impact on the atom economy of the reaction and indeed, in addition to being environmentally unfriendly, makes these methods highly undesirable to pursue in the synthesis of pharmaceutical precursors on an industrial scale. Thus, there exists a need for a method that is both sustainable and capable of performing a diverse set of C–H transformations.

This introduction aims to deliver a comprehensive overview of the significant advances made in directed TM-catalysed C–H functionalisation as well as the recent progress in this field. A critical assessment will be given on whether the core challenges of directed C–H functionalisation have been sufficiently met. That is, achieving site-selective functionalisation, with a good functional group tolerance whilst delivering a sustainable reaction.

With the prevalence of cross-coupling reactions such as the Suzuki-Miyaura coupling, it is not unusual to observe that palladium is one of the most used catalysts in TM-directed C–H functionalisation. Thus, methods involving palladium catalysis will be a focal point of this overview. However, functionalisation reactions involving a range of other transition metal catalysts will also be examined.

2.1.2 The early history of directed C–H functionalisation

One of the earliest reports of directed functionalisation was in 1955 by Murahashi and co-workers with work on cobalt catalysed C–H carbonylation (**Scheme 12**).[32] They demonstrated the use of a Schiff base functional group (FG) to recruit and position a cobalt catalyst *ortho* to the imine motif, leading to regioselective *ortho*-C–H functionalisation of **33**. However, the choice of catalyst and reaction conditions were restricted as the reaction failed to proceed using nickel-catalyst systems or with the use of water or alcohol as the solvent.

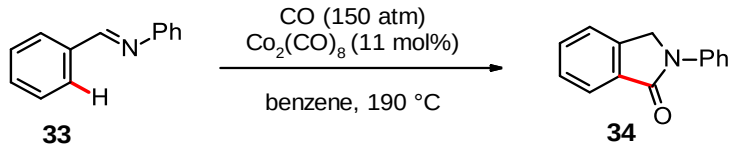

33 **34**

***Scheme 12**. Regioselective Co-catalysed ortho-C–H carbonylation using an imine motif.*

The field was reinvigorated in 1993 by Murai and co-workers who could form a new C–C bond between an aromatic substrate **35** and a terminal alkene **36** using a ruthenium catalyst (**Scheme 13**).[38] Key to achieving high regioselectivity was the use of a ketone DG that coordinates to the ruthenium and positions it at the adjacent *ortho*-C–H bond which could then be cleaved.

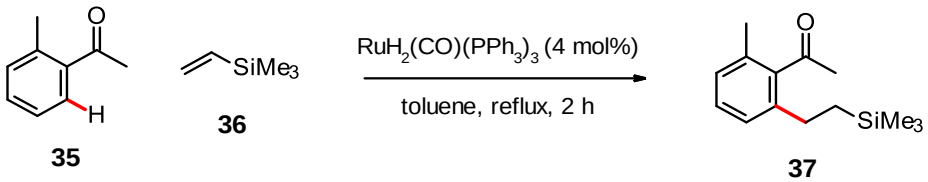

35 **36** **37**

***Scheme 13**. Ru-catalysed C–C bond formation of a terminal alkene and aromatic substrate.*

Notably, the reaction was overall highly efficient with almost quantitative yields of product without resorting to using an excess of one of the starting materials. A postulated mechanism for this functionalisation is shown below (**Scheme 14**).

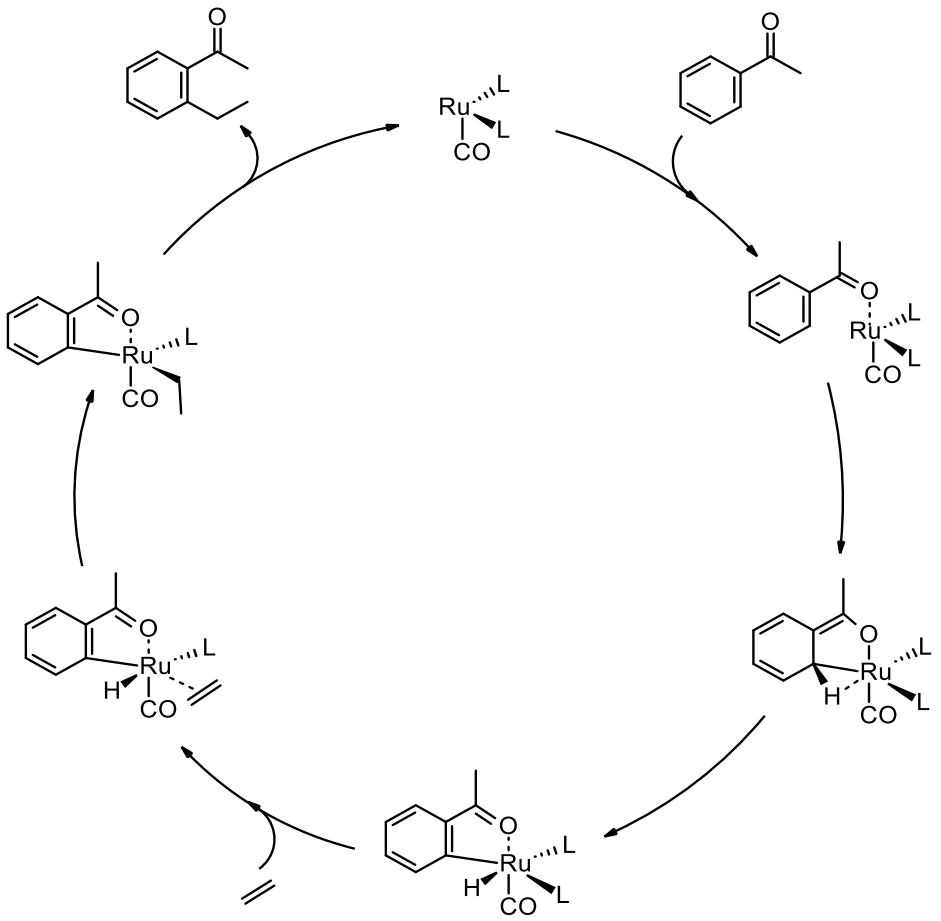

***Scheme 14**. Possible mechanism for the Ru-catalysed alkylation of C(sp²)-H bonds.*

The effect of various substituents on the aromatic substrate was subsequently examined by Murai and co-workers in 1997.[39] With *meta*-substituted acetophenones, two distinct *ortho*-C–H bonds were now available to undergo C–H functionalisation. It was found that the new C–C bond was formed preferentially at the least sterically hindered position (**Scheme 15a**). However, upon coordination of the catalyst to a *meta* substituent the reaction favours the more hindered position. This intriguingly suggests both steric and electronic effects were playing a role in determining regioselectivity (**Scheme 15b**). Moreover, it was proposed that a demethoxylation pathway followed by β-hydride elimination step led to the unexpected product in 10% yield (**Scheme 15c**).

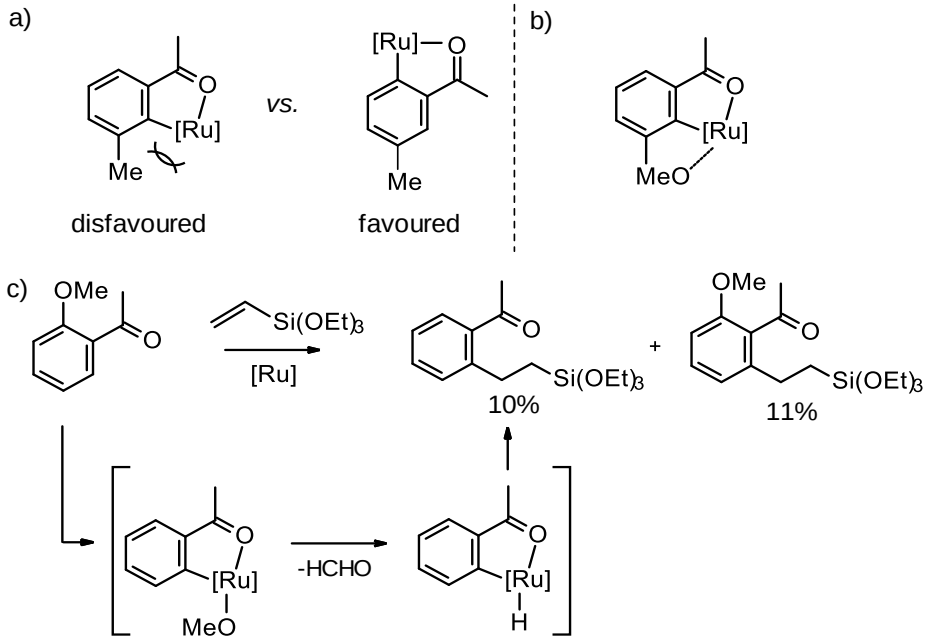

***Scheme 15**. (a) The role of sterics in favouring Ru insertion, (b) meta-substituent coordination leads to Ru insertion at hindered position, (c) proposed pathway of demethoxylation.*

As examined in this seminal work by Murai almost thirty years ago, the issues of functional group tolerance and achieving high regioselectivity proved to be as problematic then, as they are today.

Substituted pyridines such as 2-phenylpyridines can also undergo selective functionalisation at the *ortho* position of the phenyl ring. Here, the sp^2 nitrogen in the pyridine is critical for its ability to coordinate to a transition metal and facilitate selective C–H activation.

One of the earliest uses of a pyridine DG was the *ortho*-alkylation of 2-phenylpyridine **38** by reaction with a terminal alkene using a rhodium catalyst (**Scheme 16**). While highly selective for the mono-alkylated product **39**, the doubly alkylated product was isolated in some cases.[40]

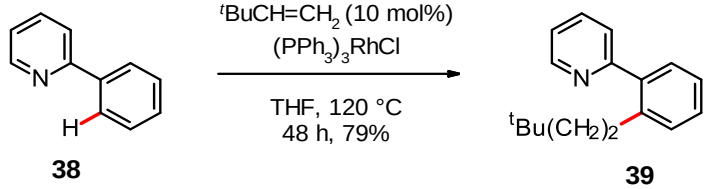

***Scheme 16**. Alkylation of 2-phenylpyridine with a terminal alkene using a rhodium catalyst.*

However, upon modification of the pyridine DG by introducing a methyl group at the 3-position, not only was the reaction yield improved, but it also afforded exclusively the mono-alkylated product **40**. It was postulated that the steric hindrance of the methyl group on DG

disrupted the formation of a second rhodium-hydride complex that leads to the di-alkylated product (**Scheme 17**).

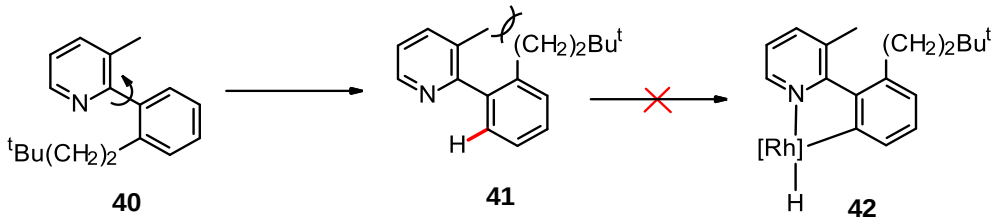

***Scheme 17**. The role of sterics in the failed attempt to form the di-alkylated product.*

The substrate **43** was found to be highly versatile and was also employed by Inoue and co-workers.[41] The arylation of *ortho*-C(sp^2)–H bonds using organostannanes afforded the mono-arylated product **44** selectively with an isolated yield of 78% (**Scheme 18**). Regioselectivity was probed, and reverting to the 2-phenylpyridine substrate **38**, a mixture of mono- and di-arylated products were isolated and in much lower yields, 36% and 18% respectively.

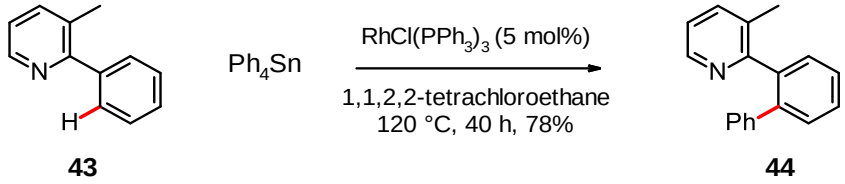

***Scheme 18**. Monoarylation of 3-methyl-2-phenylpyridine with a rhodium catalytic system.*

Inoue and co-workers report on the use of organostannanes substrates marked the start of employing nucleophilic organometallic compounds as cross-coupling partners with aromatic C–H bonds. Aryl boronic acid esters, specifically phenylboronic acid pinacol ester **46** was promptly used as a coupling partner in the ruthenium-catalysed arylation of aromatic compound **45** containing a ketone DG (**Scheme 19**).[42]

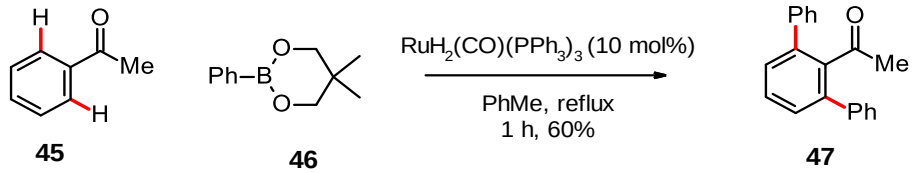

***Scheme 19**. Ruthenium-catalysed C–H functionalisation leading to doubly-arylated product **47**.*

This transformation suffered from poor regioselectivity, delivering the mono- and di-arylated products in 60% and 7% yields, respectively. However, the was addressed by using a bulky

substrate, *tert*-butylphenyl ketone **48**, which afforded only the mono-arylated product **49** in a 95% yield **(Scheme 20**).

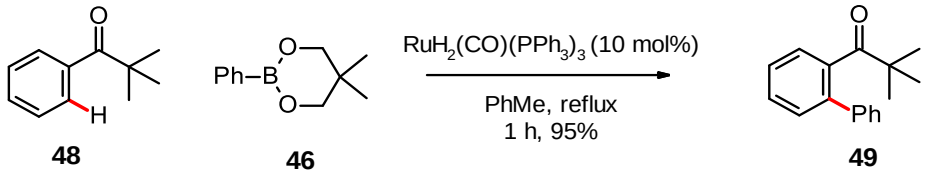

***Scheme 20**. Effect of sterically congested substrates on the regioselectivity of C–H arylation.*

The improvement in regioselectivity can also be rationalised by sterics, specifically the bulky *tert*-butyl motif attached to the ketone DG in **48**, which is seen to further disrupt activation of other C–H bonds. Both electron-withdrawing and electron-donating substituents such as OMe, F and CF_3 were well tolerated, with the yield decreasing slightly to 86% when using *p*-N,N-dimethylaminophenylboronate. The bulky *o*-tolyl- and α-naphthylboronates suffered no detrimental effect on the reactivity, affording the corresponding biaryl compound in a 92% yield in each case.

From the reports above, it was becoming increasingly apparent that with careful selection of a directing motif and if necessary, introducing bulky substituents, regioselectivity could be improved.

With the prevalence of cross-coupling reactions such as the Suzuki-Miyaura coupling, it is not unusual to observe that palladium has become one of the most used catalysts in TM-directed C–H functionalisation.

At the start of the century, there were several reports of Pd systems functionalising both aromatic and aliphatic C–H bonds (**Scheme 21**).[43,44] The DGs in **50** and **52** were employed that could successfully coordinate to palladium demonstrating the potential versatility of using this metal as a catalyst in these processes.

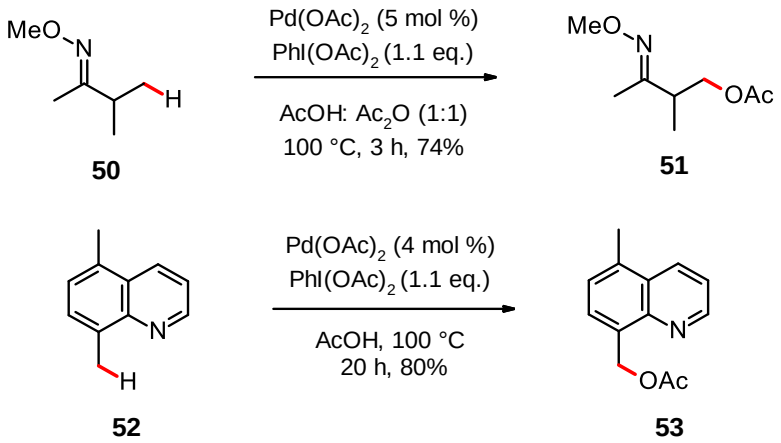

***Scheme 21**. Examples of Pd-catalysed transformations of C(sp^2)-H and C(sp^3)-H bonds.*

With regard to the *ortho*-C–H acetoxylations of the substrates **50** and **52**, both proceed in high yields, and a Pd(II)/Pd(IV) catalytic cycle has been proposed (**Scheme 22**).[43,44] The final step of this cycle involves a C-O bond forming reductive elimination, which typically proceeds via an intramolecular C-X bond elimination from the metal centre[45,46] or external nucleophilic attack in a S_N2-type fashion.[47,48]

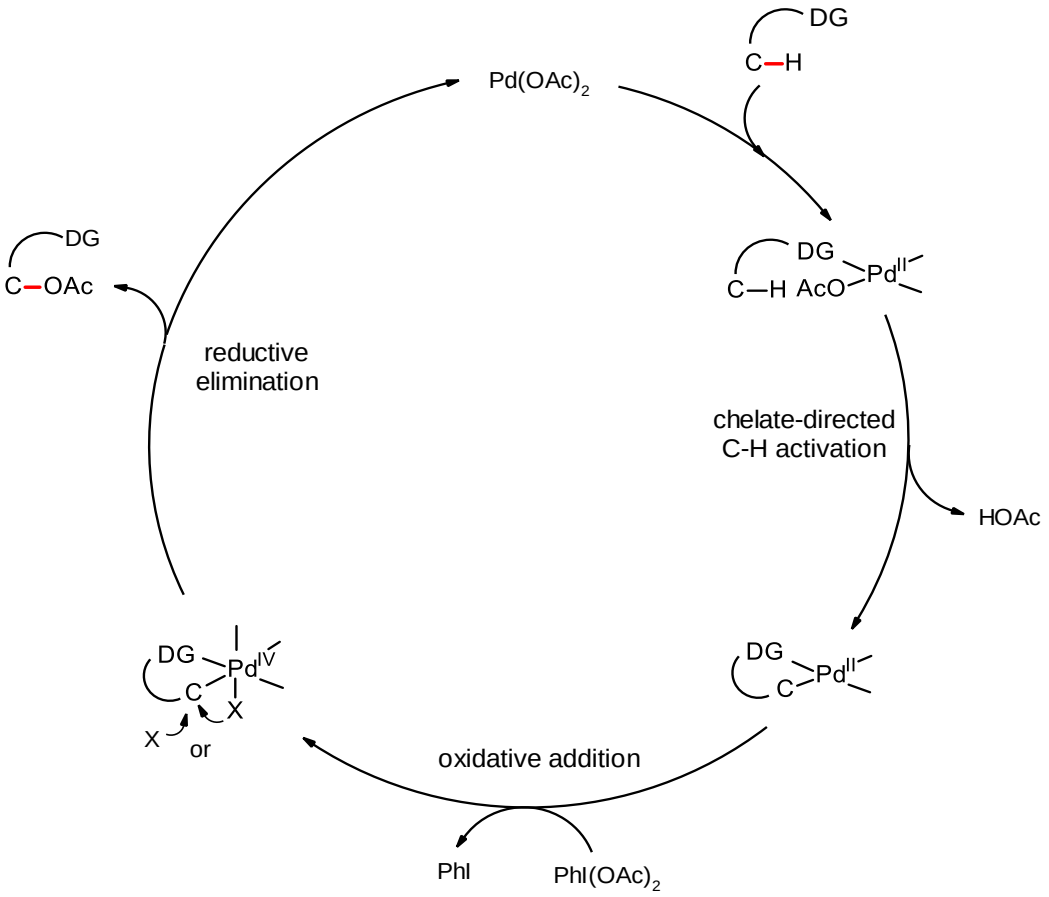

***Scheme 22**. Proposed Pd(II)/Pd(IV) catalytic cycle for ortho-C–H acetoxylation.*

As well as the postulated catalytic cycle above, there have been various mechanisms proposed for the key step of the addition of Pd(II) into a C(sp^2)–H bond. This includes electrophilic palladation[49], oxidative addition[50] and concerted metalation-deprotonation (CMD)[51] (**Figure 8**). However, electrophilic addition and CMD are two of the most referred-to processes (**Scheme 23**).

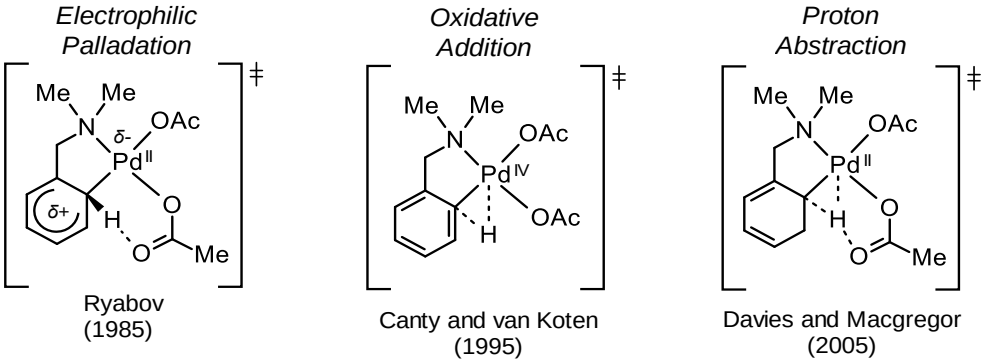

***Figure 8**. Key intermediates in three proposed mechanisms for the addition of Pd(II) into a C(sp^2)-H bond.*

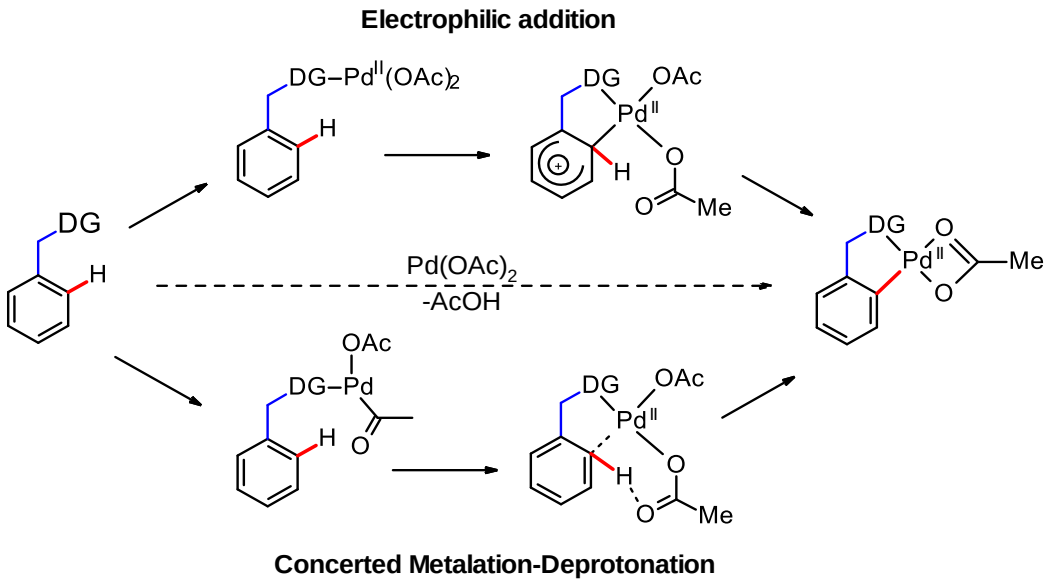

***Scheme 23**. Two most invoked mechanisms for the addition of Pd(II) into C(sp²)-H bonds.*

The electrophilic addition mechanism was postulated in 1985 by Ryabov and co-workers.[49] A nucleophilic attack of the electrophilic Pd(II) centre, that is proximally positioned by the DG group, was proposed. This results in the formation of a Wheland intermediate before the Pd(II) co-ordinates to the π-system of the arene. Subsequent proton transfer between the Wheland intermediate and a bound acetate leads to the cyclopalladated species.

With the CMD pathway, upon coordination of the Pd centre to the DG, the C–H and Pd-OAc bonds are broken while the Pd–H and AcO–H bonds form simultaneously. Unlike electrophilic addition, in the CMD pathway a substantial build-up of charge on the arene is avoided; as such, the reaction rate is less affected by variations in the electronic properties of arene substituents.

Common to many catalytic cycles is the presence of oxidants such as benzoquinone and $Cu(OAc)_2$,[52] as well as silver salts which can be used as halide scavengers.[53] These oxidants, required in a stoichiometric quantity, are a common drawback for many TM-catalysed C–H transformations. Not least because from an environmental perspective it remains a challenge to replace metal-based oxidants with more sustainable alternatives.

Despite this, there are reports of transformations that utilise more sustainable oxidants. For example, Yu and co-workers reported C(sp^2)–H arylation of benzoic acids including **54** using potassium aryltrifluoroborates with air or O_2 as the oxidant (**Scheme 24**).[54]

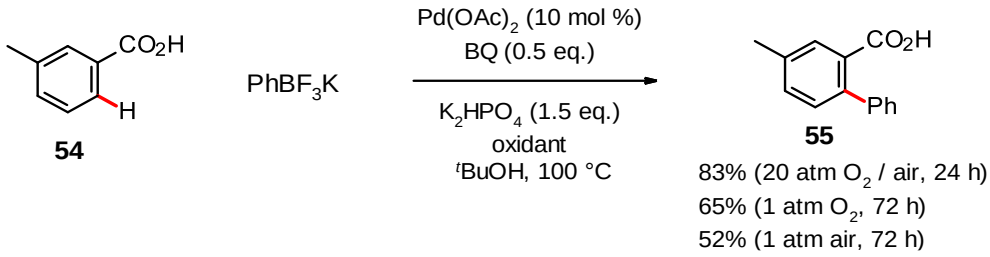

***Scheme 24**. Effect of oxidant on the reaction time and yield of Pd-catalysed arylation of C(sp²)-H with potassium aryltrifluoroborates as coupling partners.*

While high pressures of 20 atm of air or molecular oxygen were necessary to cut the reaction times down to 24 hours, the arylated products including **55** could be obtained in 60-70% yields after 72 hours with just 1 atm of O_2 or air. This method was also found to be compatible with electron-deficient arenes unlike a previous report which was limited to a handful of benzoic acids.[55]

C(sp^2)–H arylation of benzoic acids could also be performed with aryl chlorides as coupling partners, circumventing the use of an external oxidant completely (**Scheme 26**).[56,57]

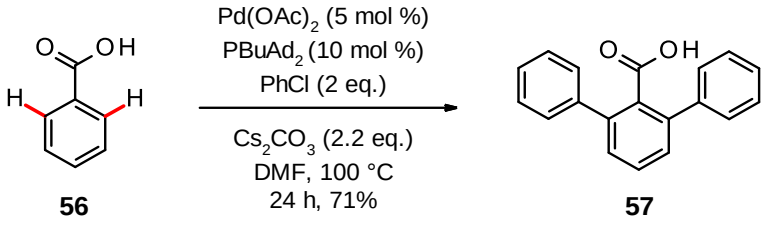

***Scheme 26**. Arylation of C(sp²)-H bonds without requiring an external oxidant.*

A Pd(II)/Pd(0) catalytic cycle was proposed with the mechanism by Macgregor and Echavarren being selected as the most probable for the C–H cleavage step (**Scheme 27**).

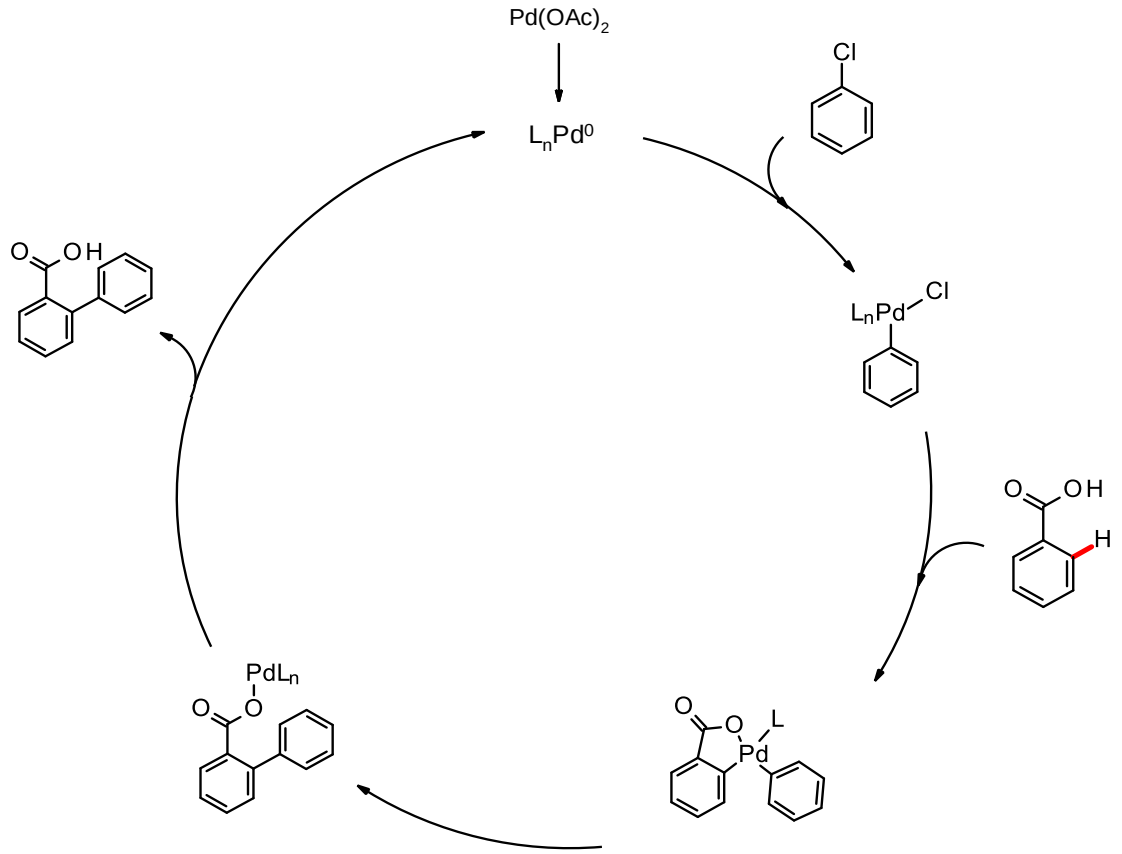

***Scheme 27**. Proposed Pd(II)/Pd(0) mechanism for C(sp²)–H arylation of benzoic acid with chlorobenzene as the coupling partner.*

One of the earliest examples of C(sp^3)–C(sp^3) bond formation in this field could proceed smoothly using an alkylboronic acid coupling partner **59** with either air or Ag_2O as the oxidant (**Scheme 28**).[58] Using *O*-methyl hydroxamic acid motif, present in **58**, which are readily accessible from carboxylic acids also improved the practicality of this reaction. One limitation was that the coupling of C(sp^3)–H bonds could only proceed with sterically hindered 2,2,5,5-tetramethyltetrahydrofuran as the solvent, the use of which likely suppresses the undesired β-hydride elimination pathway.

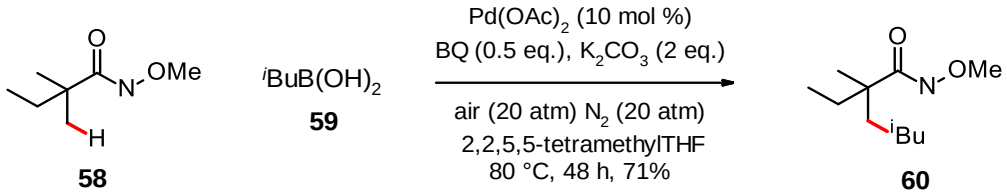

***Scheme 28**. C(sp^3)-C(sp^3) bond formation using a O-methyl hydroxamic acid as the DG.*

By employing the chiral oxazoline **61**, the $Pd(OAc)_2$-catalysed oxygenation of prochiral $C(sp^3)$–H bonds was achieved in a diastereoselective manner (**Scheme 29**).

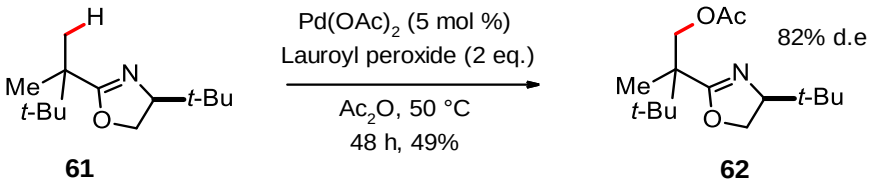

***Scheme 29**. Diastereoselective C(sp³)-H acetoxylation using a chiral oxazoline DG in **61**.*

The use of the inexpensive oxidant lauroyl peroxide in this functionalisation was a cost-effective substitute of $PhI(OAc)_2$. However, it should be brought to the reader's attention that acetic anhydride was a necessary addition. This was postulated to help promote turnover of the catalytic cycle, which was proposed to proceed via a Pd(II)/Pd(IV) system (**Scheme 30**).[59]

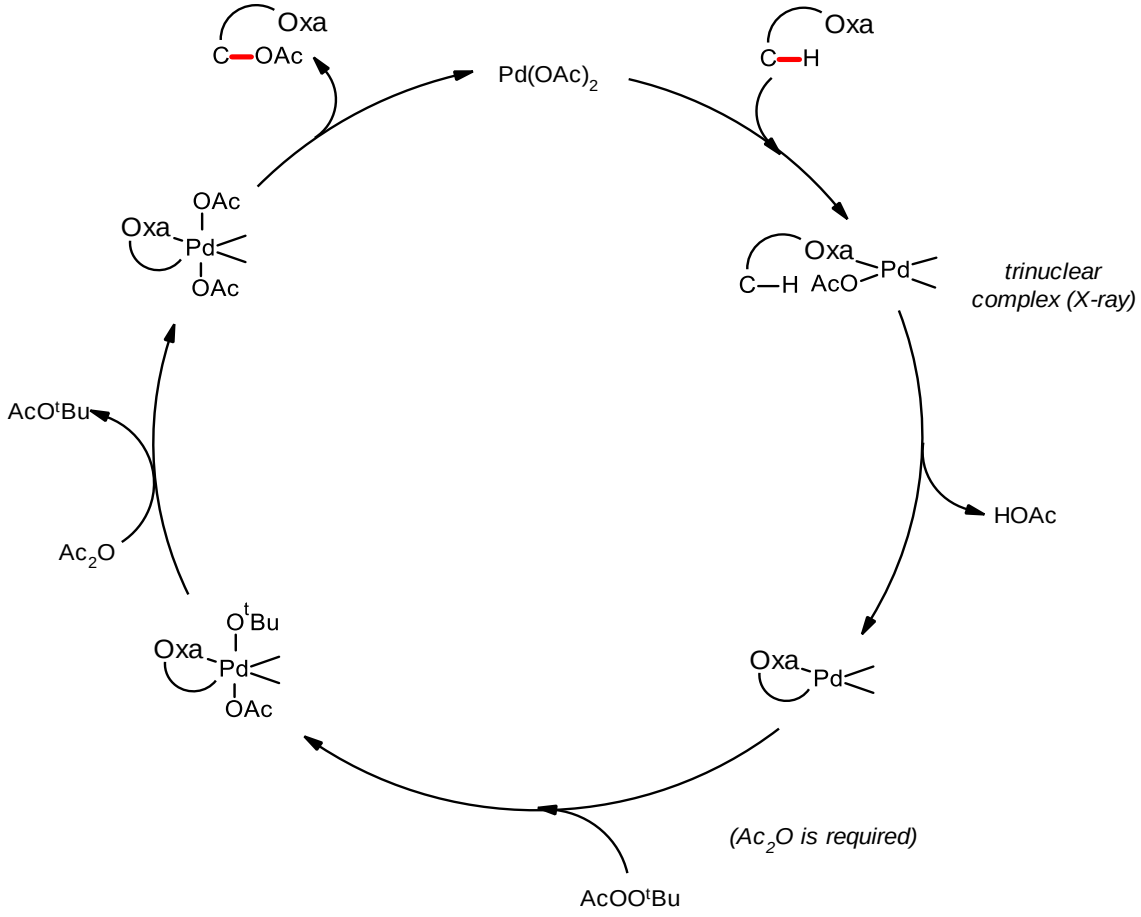

***Scheme 30**. Proposed Pd(II)/Pd(IV) mechanism of C(sp³-H) acetoxylation with a peroxide oxidant.*

By employing CONHOMe as a directing motif in C–H functionalisation improves its synthetic usefulness since the DG can be readily converted to esters,[60] amides[61] or a hydrogen.[61] Thus,

it is highly desirable to incorporate DGs which crucially can be derivatised after the C–H functionalisation step but also can be removed without requiring harsh conditions.

These desired DG characteristics contrast with those of strongly coordinating bidentate amides as exogenous DGs. The first examples of such motifs, 8-aminoquinoline (AQ) and picolinamide (PA), were described in the seminal work of Daugulis in 2005, for the β-C–H arylation of carboxylic acid derivatives **63** and γ-arylation of amine derivatives **66** (**Scheme 31**).[62]

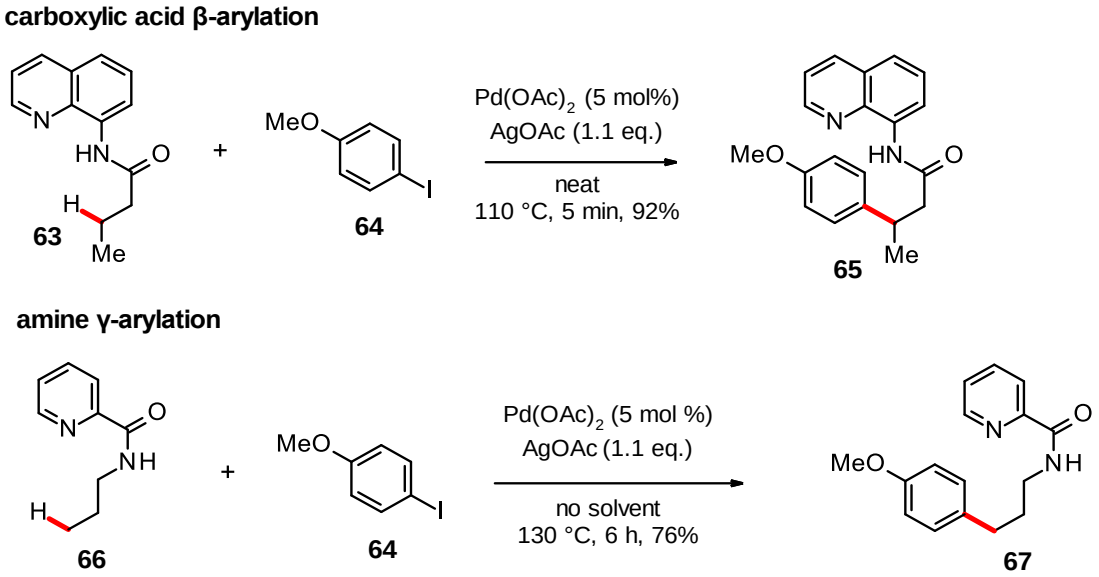

***Scheme 31**. Regioselective Pd-catalysed arylation of β- and γ-C(sp³)-H bonds within carboxylic acid and amine derivatives.*

Whilst other strongly coordinating bidentate amides have also been introduced in the last two decades (**Figure 9**) they too share the same undesirable characteristic. That is, many of these motifs are not an integral part of the substrate and thus require installation and removal steps leading to a protracted synthesis and poor atom economy.[63,64]

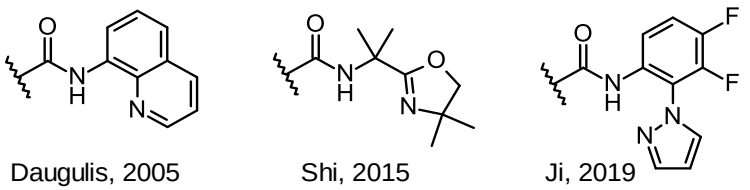

***Figure 9**. Examples of strongly coordinating bidentate amide DGs for C–H functionalisation.*

Removing the AQ or PA DGs can lead to various synthetically useful FGs. For example, PA cleavage can be carried out using acidic and basic conditions to afford the Boc-protected amine

and free amine respectively (**Scheme 32**). However, these forcing conditions are tolerated by simple substrates containing a limited range of functional groups. A procedure developed by Spring and co-workers utilising Zn/HCl for PA cleavage is a milder alternative which exhibits useful functional group tolerance.[65]

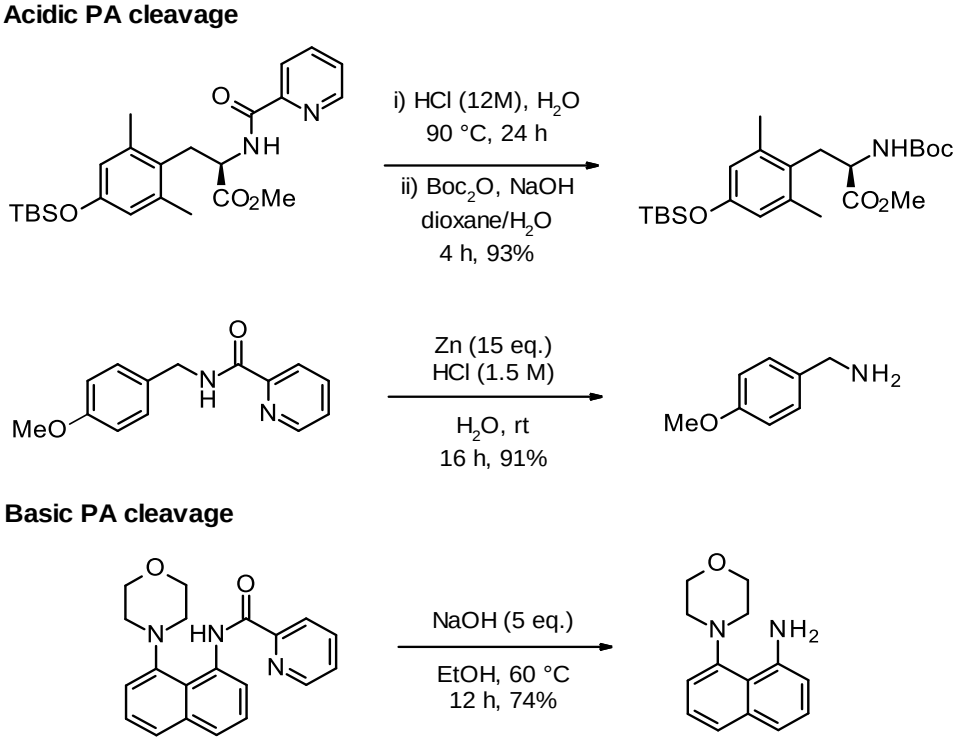

***Scheme 32**. Various removal strategies for the PA directing group.*

Harsh conditions are also typically required when removing the AQ motif. In a bid to overcome these conditions, various strategies for the removal of this DG have been reported leading to a range of different products (**Scheme 33**).[66–70]

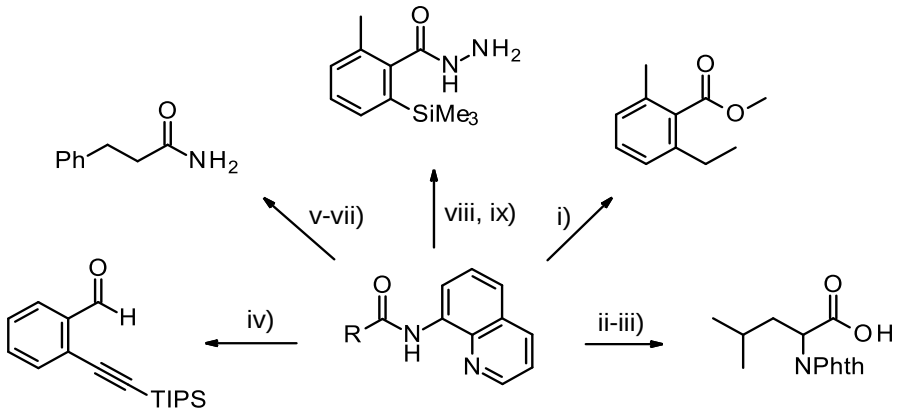

i) $BF_3.H_2O$, MeOH, 100 °C, 48 h, 72%. ii) Boc_2O, DMAP, rt, 24 h. iii) LiOH, H_2O_2, 0°C, 2.5 h, 99%. iv) $Cp_2Zr(H)Cl$, THF, rt, 6 h, 75%. v) O_3, DCM, -78 °C, 10 min. vi) DMS, rt, 2 h. vii) NH_4OH, THF, rt, 24 h, 75%. viii) Boc_2O, DMAP, 80 °C, 30 h. ix) H_2NNH_2, NH_4I, EtOH, 80 °C, μw, 24 h, 71%.

***Scheme 33**. Possible deprotection routes for the AQ directing group.*

Efforts to move away from AQ or PA based DGs has led to focusing on pyridyl-containing motifs. Given the prevalence of pyridines and unsaturated *N*-heterocycles in many bioactive compounds, installation of the pyridine motif into the substrate is avoided.[71] This contrasts with AQ or PA motifs which must be added prior to the C–H functionalisation step, via an amide coupling using a carboxylic acid or amine substrate respectively.

The method itself offers a wide range of highly regioselective transformations. For example, 2-phenylpyridine has been reported to have undergone C(sp^2)–H arylations,[72,73] cyanations,[74] sulfonylations,[75] and decarboxylative acylation transformations.[76] However, unlike the PA or AQ DGs, the derivatisation or removal of the pyridine moiety post-C–H functionalisation is a major challenge. This is because the disassociation between the substrate and DG group requires a strong C–C bond to broken. One route to overcome this is by bridging the substrate and DG with a heteroatom or suitable group that can be modified further.

This was realised by Wu and co-workers[77] who derivatised the functionalised product via activation of the pyridine motif in **68** before cleaving rendering the corresponding phenol **69** (**Scheme 34**).

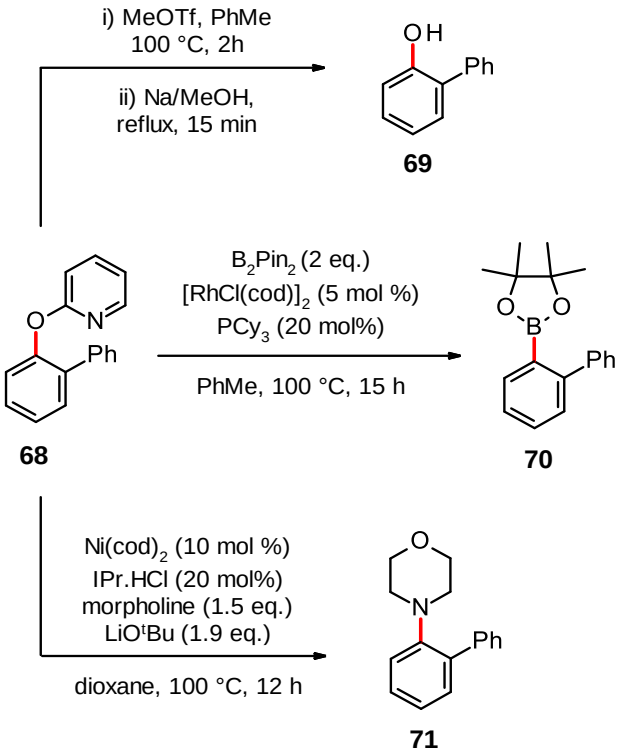

***Scheme 34**. Possible routes for further functionalisation of a pyridyl-tethered DG **68**.*

This work was further explored by Chatani who reported rhodium-catalysed borylative cleavage which involves substitution of the DG with a boronic ester, a highly versatile synthetic handle, leading to **70**.[78] The DG can also be functionalised to furnish amine products such as **71** using a nickel-catalysed amination pathway as developed by Wang and co-workers.[79]

A silicon linked pyridyl directing motif, incorporated into arene **72** was subsequently reported by Gevorgyan and co-workers enabling *ortho*-acyloxylation and *ortho*-halogenation of aromatic substrates (**Scheme 35**).[80,81]

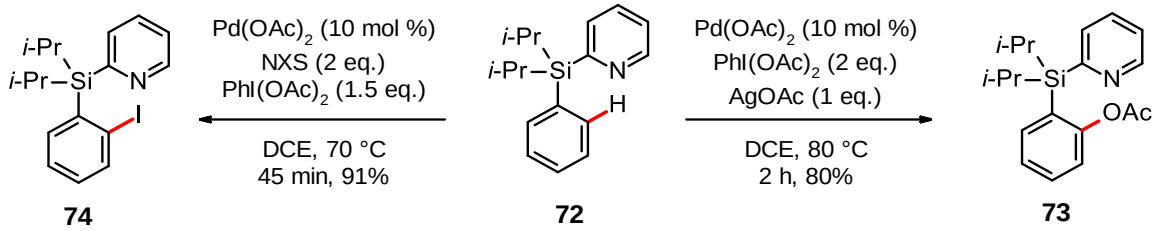

***Scheme 35**. ortho-Acyloxylation and ortho-halogenation of arenes with a silicon linked pyridyl DG.*

Thes silicon linked pyridyl DG, coined PyDipSi, could also be modified leading to a wide range of functional groups after the C–H functionalisation step (**Scheme 36**). Notably, PyDipSi could be cleaved entirely and substituted with a C–H or C-D bond, enabling PyDipSi to serve as a traceless DG.

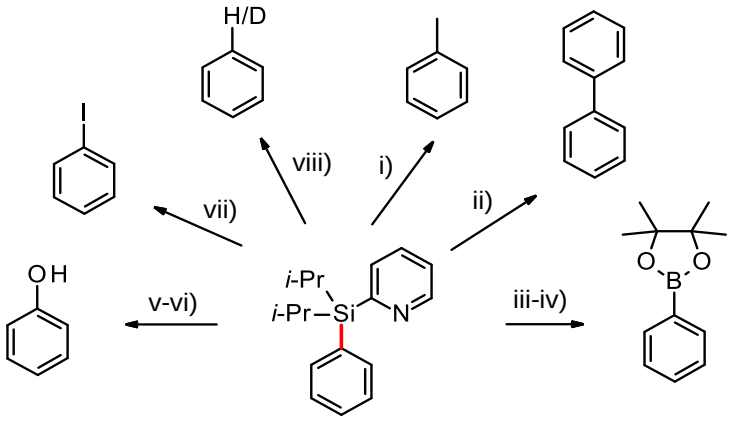

i) Pd cat., ≡R ii) Pd cat., PhI iii) BCl_3, DCM iv) pinacol, NEt_3 v) BCl_3, DCM vi) H_2O_2, NaOH vii) AgF, NIS, THF viii) AgF, MeOH or D_2O/THF.

***Scheme 36**. Possible routes for further functionalisation of the PyDipSi DG.*

Despite the promising characteristics exhibited by PyDipSi, its installation requires the use of the strong organolithium base BuLi. This renders the method unsuitable for base-sensitive functional groups. However, an alternative approach which accommodates a range of different functional groups has been developed using a rhodium-based catalytic system.[81] Indeed, the cross-coupling of hydrosilanes containing a heterocycle motif with aryl halides has been observed using this method.

The above methods of PyDipSi installation require the use of halogenated arenes. Specifically, aryl iodides substrates were preferred over the corresponding bromides and chlorides derivatives which further limits the scope of the substrates used.

Another class of pyridyl-tethered DGs that incorporate a sulfur group, such as **75** have been investigated. Mancheno and Carretero have reported the *ortho*-acetoxylation and *ortho*-alkenylation of these scaffolds respectively (**Scheme 37**).[82,83]

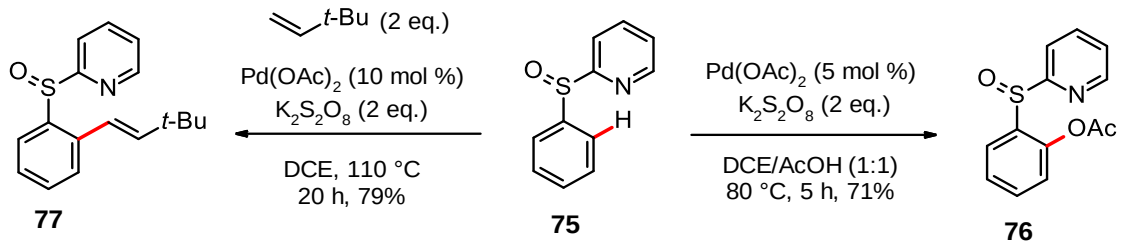

***Scheme 37**. ortho-C–H olefination and acetoxylation directed by a pyridyl tethered motif.*

This directing motif can be cleaved or further functionalised to afford more useful arene derivatives (**Scheme 38**).

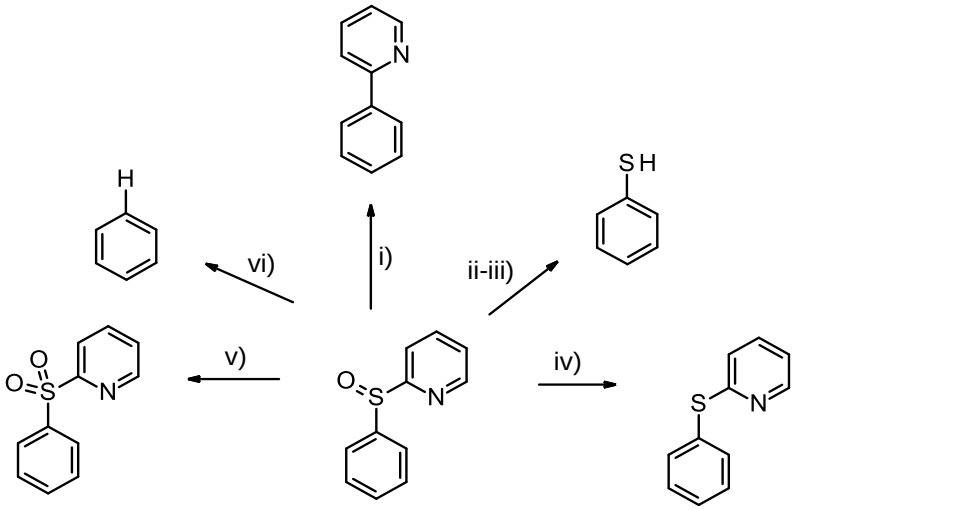

i) EtMgBr ii) Zn, AcOH iii) HCl, MeOH iv) Zn, THF/ aq. NH_4Cl v) mCPBA, DCM vi) Raney Ni, aq. NaOH.

***Scheme 38**. Possible routes for further functionalisation of a pyridyl tethered DG linked to sulphur.*

Mancheno and co-workers' explored a range of sulfur groups attached to a pyridyl motif. They revealed that a sulfoxide tethered DG was both more reactive and selective for the mono-acetoxylated product compared to the corresponding sulfone. This higher selectivity can be rationalised by the coordination of the S atom of the sulfoxide to the Pd metal. A sulfide tether was also examined but was found to be unstable under the reaction conditions.

Both the sulfone and sulfoxide motifs could be cleaved or further functionalised to afford more useful arene derivatives, highlighting the practical use of S-tethered DGs.

2.1.3 Weakly coordinating directing groups

The strong co-ordination observed between DGs such as AQ, PA and pyridyl motifs to a suitable transition metal, enables the C–H activation step to be more favoured. However, the cyclo-metalated species that forms during this step can be detrimental overall to the reaction. This is due to the thermodynamically stable yet less reactive cyclo-metalated intermediate that is formed. As a result, it can be difficult to perform the subsequent functionalisation of these strongly bound metallocycles.[63,64]

In contrast, employing weakly coordinating directing motifs such as ketones, carboxylic acids and alcohols, which are ubiquitous functional groups, is highly desirable. As mentioned at the

start of this review, the seminal work by Murai and co-workers in the early 1990s demonstrated the use of weakly coordinating ketones to achieve regioselective C–H functionalisation.[38]

However, there has since been little progress reported in literature of employing weakly coordinating DGs. This is presumed to be due to the challenge of overcoming the higher activation energy required for the initial C–H activation step in comparison to using strongly coordinating motifs.

Addressing this, Yu and co-workers in 2008 first reported the use of external ligands to accelerate the C–H cleavage step.[63,84] This pioneering work enables a range of molecules containing a variety of functional groups to be employed as weakly coordinating DGs. For example, ketones,[85,86] carboxylic acids,[55,87–90] alcohols,[91–93] nitriles,[94] amides,[95,96] and ethers[97] could now be used in Pd-catalysed C–H functionalisation reactions.

The key differences in the energy profiles of a strongly coordinating and a weakly coordinating DG are highlighted with a theoretical reaction coordinate of a C–H functionalisation reaction (**Figure 10**).[86]

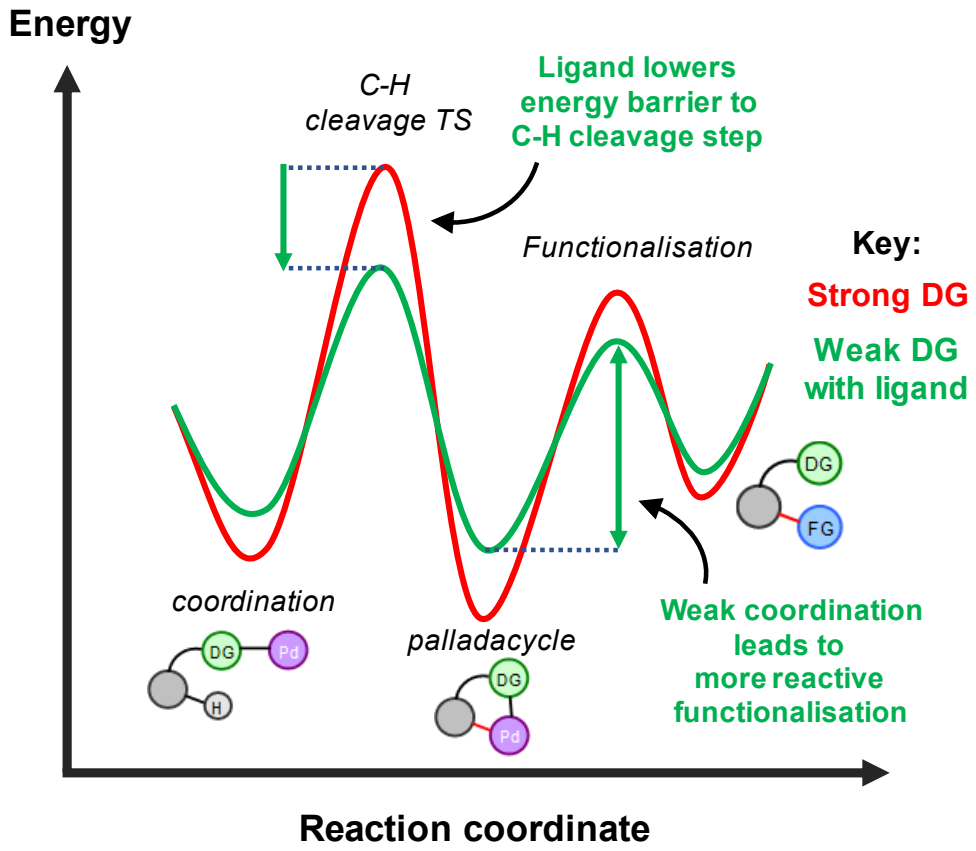

***Figure 10**. Theoretical reaction coordinate profile of a C–H functionalisation reaction with a strongly (red) and weakly coordinating DG (green). Adapted from Yu et al.*

As depicted in **Figure 10**, a weakly coordinating DG in the presence of a ligand leads to a less stable metallacycle. This crucially lowers the energy barrier of the C–H cleavage step and leads to reduced energetics of the functionalisation step. As a result, the substrate is more reactive towards a range of coupling partners compared to a strongly coordinating DG. This helps avoids harsh reaction conditions such as elevated temperatures and strong oxidants.

Yu and co-worker's renaissance of weakly coordinating motifs led to the emergence of mono-protected amino acids (MPAAs) as powerful ligands.[91,98] MPAAs contain several important features which help them accelerate the C–H cleavage step (**Figure 11**). The structure-activity breakdown is such that the *N*-acyl group facilitates deprotonation of the C–H bond; the R_1 group helps with modulating *N*-acyl basicity; the R_2 group is the source of chirality, and the carboxylate assists by binding to the Pd in an X-type manner.[99]

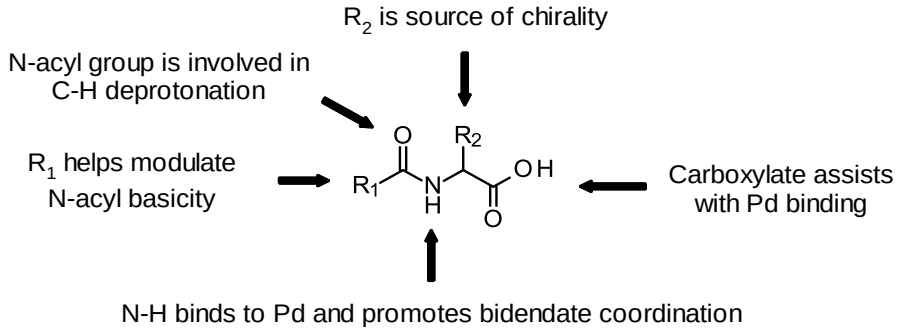

***Figure 11**. Important features of a mono-protected amino acid in C–H functionalisation.*

Insights by Fagnou and others into Pd arene C–H activation by MPAAs, led to a mechanism involving the deprotonation of the C–H bond.[100,101] It was proposed, C–H abstraction was facilitated by the carboxylate and was occurring simultaneously with Pd-C bond formation Fagnoi coined the term 'concerted metalation-deprotonation' (CMD) to describe this cyclic six-membered transition state (**Figure 12, left**).

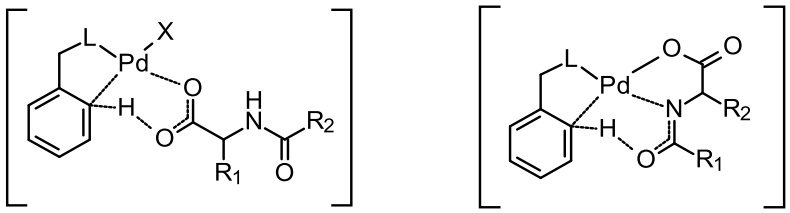

***Figure 12**. Initial monodentate carboxylate CMD hypothesis for C–H cleavage with MPAA ligand (left), Yu's bidentate proposal with an internal acetate (right).*

This initial mechanism hypothesis was expanded further by Yu and co-workers in 2014, who proposed a bidentate MPAA coordination mode which was more energetically favourable.[102] This bidentate MPAA proceeds via the *N*-acyl group acting as an internal base where the transition state maxima was lowered by 4 kcal/mol (**Figure 12, right**).[101]

One of the early uses of MPAAs was the functionalisation of prochiral C–H bonds giving rise to chiral products such as **78** (**Scheme 39**). It was postulated that to deliver high enantioselectivity, coordination of the chiral carboxylate of the MPAA on the metal centre was essential.[84]

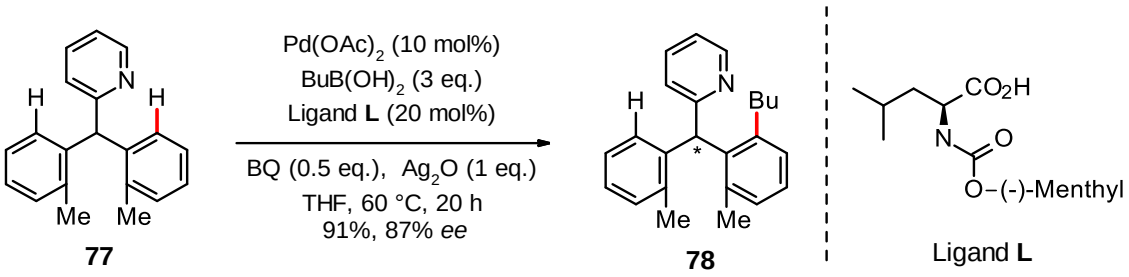

***Scheme 39**. Functionalisation of prochiral bonds with high enantioselectivity with a chiral ligand.*

The improved enantioselectivity achieved using MPAAs called for investigations into their use in facilitating otherwise challenging C–H functionalisations. Electron-deficient phenylacetic acids such as **79** which were poorly reactive towards C-olefination could react smoothly in the presence of the ligand Ac-Ile-OH, with over 99% conversion after 2 h (**Scheme 40**).[103] Replacing the MPAA in this reaction with benzoquinone, conversion dropped to 3% indicating the importance of an amino acid ligand in accelerating C–H olefination.

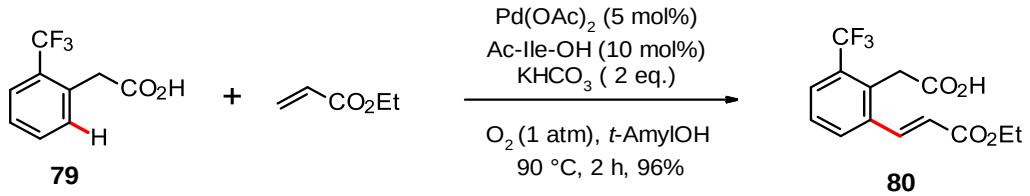

***Scheme 40**. Challenging substrates such as electron-deficient **79** can smoothly undergo C–H olefination in presence of Ac-Ile-OH ligand.*

Yu and co-workers also demonstrated the use of MPAAs to enhance the positional selectivity of Pd-catalysed C–H olefination reactions with phenylacetic acid substrates.[104] For instance, while substrate **81** contains two electronically similar *ortho*-C–H bonds, remarkable positional selectivity could be achieved using the Boc-Ile-OH as the ligand (**Scheme 41**). This boost in selectivity is likely due to the MPAA altering the steric properties around the Pd centre.

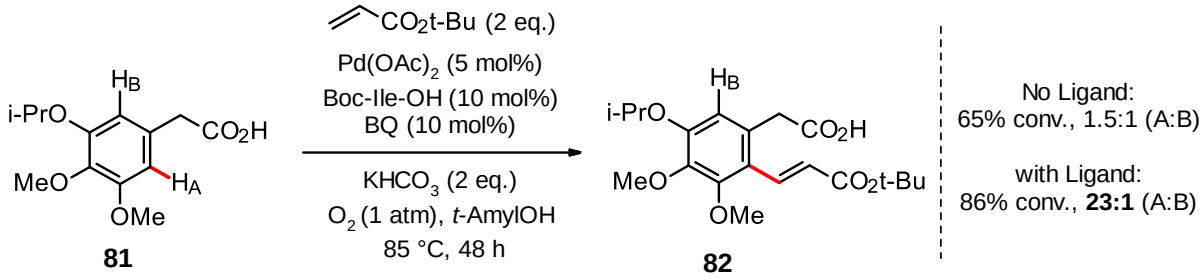

***Scheme 41**. Improved regioselectivity of C–H functionalisation in presence of* a *Boc-Ile-OH ligand.*

Using amino acid ligands also enabled C–H olefination of phenylacetic acid derivative **83** to occur quantitatively even with a reduced catalyst loading (**Scheme 42**).[86] This demonstrates the ability of MPAAs to improve the atom economy of C–H functionalisation reactions.

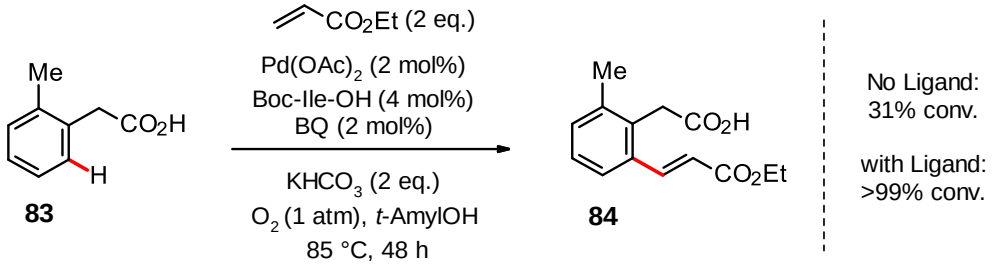

***Scheme 42**. Improved conversion using low loading of Pd catalyst in the presence of a MPAA.*

It is noteworthy to mention that previous C–H functionalisations examined, which typically use the strongly coordinating PA or AQ DGs, proceed via a five-membered cyclometalated intermediate. However, by employing an MPAA ligand, the olefination of **85** proceeded smoothly via the less entropically favoured seven-membered palladocycle. (**Scheme 43**).

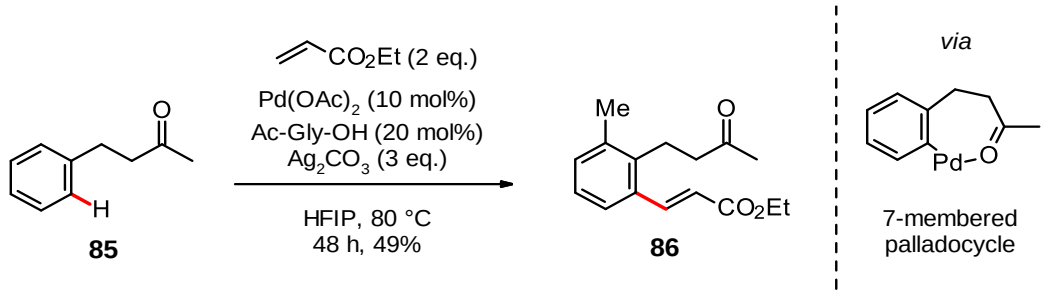

***Scheme 43**. Distal C–H functionalisation with a MPAA and a native ketone acting as a DG.*

However, as detailed by Yu and co-workers, extensive screening of various MPAAs is typically required to find the optimum ligand for different substrates. This illustrates the sensitivity of the mental centre to its steric and electronic environment which can make it difficult to optimise easily. In fact, the screening of different combinations of varying side chains and *N*-protecting groups of the MPAAs can become time-consuming and cost prohibitive. It is crucial that further research into identifying MPAAs that are amenable to a broad range of functionalisations is carried out to be more suitable for use in an industrial level.

2.1.4 Distal C–H functionalisations

Considering the C–H transformations examined above, the functionalisation of *ortho*-C–H bonds in arenes is well-established. For example, when using strongly coordinating motifs

such as a PA or AQ DGs, a double five-membered palladacycle is usually formed in which the *ortho*-C–H bond is activated.

In fact, Daugulis and colleagues successfully identified the reaction intermediate **88**, showcasing its effectiveness in participating in C–H arylation (**Scheme 44**).[105] While efficient arylation usually involves five- and six-membered palladaycles since they are kinetically and thermodynamically the most favoured,[106] a six-membered system may lead to low yields.[107] Thus it will be useful to take into account the ring size of the expected palladacycle intermediate when creating B-linked DGs in this work.

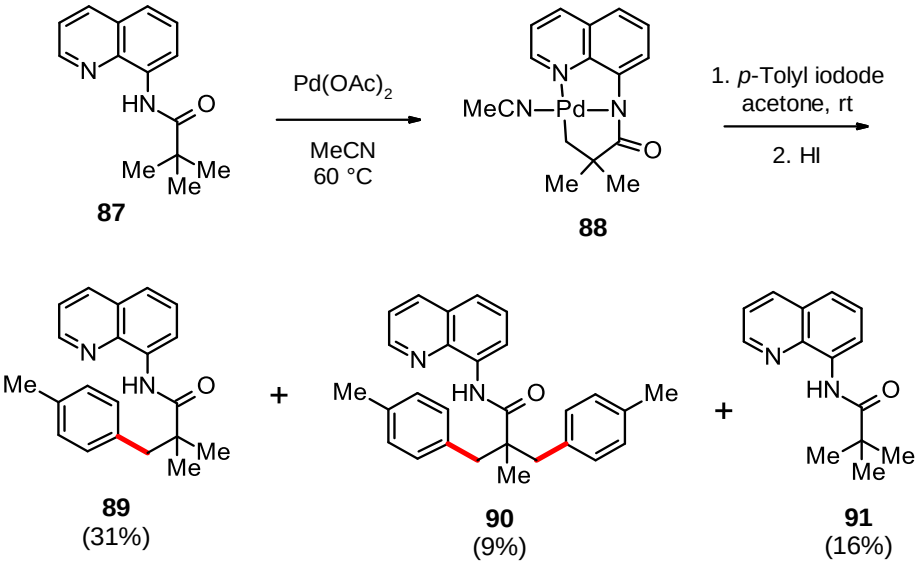

***Scheme 44**. Arylation of isolated palladaycles by Daugulis and co-workers.*

In these systems containing PA or AQ DGs, C–H functionalisation proceeds through a small pre-transition state **92** which leads to *ortho*-C–H activation (**Figure 13**). However, Yu and co-workers have reported the use of a novel U-shaped motif which favours the formation of a larger macrocyclic cyclophase pre-transition state **93**. As a result, C–H activation could be achieved selectively at the *meta*-position via a templated-directed approach.

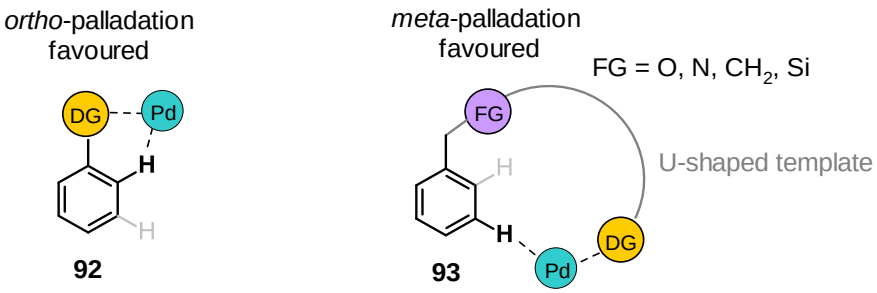

***Figure 13**. Small and large palladaycles leading to either ortho- and meta-CH activation. Illustration adapted from Yu et al.*

Yu and co-workers hypothesised that by using the weakly coordinating nitrile group as the DG, the formation of the smaller *ortho*-palladacycle **92** would be unfavoured.[108,109] The reasoning behind this is two-fold. Firstly, the rigidity of the linear nitrile moiety would lead to increased strain when attempting to form **92**. Secondly, it was anticipated that the nitrile group's weak coordinating nature would result in any potential ring strain formation in the meta-palladacycle **93** being brief, owing to the rapid release of the palladium from the DG.[108] This strategy of using a nitrile led to a range of novel protocols for the *meta*-functionalisation of remote aryl C–H bonds in substrates **94** and **96** (**Scheme 45**).[109,110]

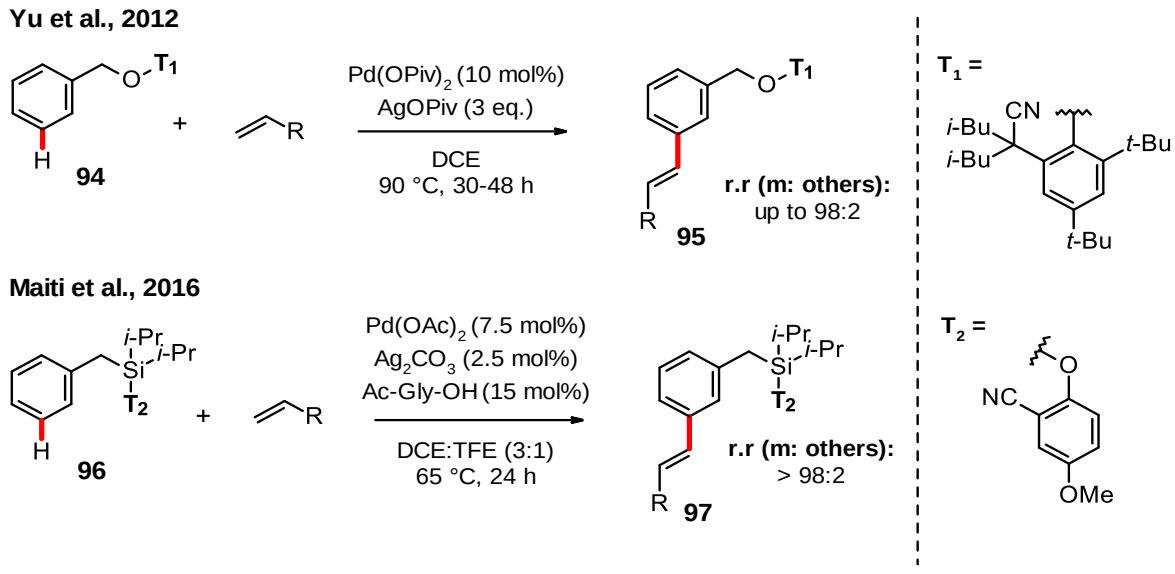

***Scheme 45**. Nitrile template-directed meta-C–H olefination of benzyl substrates **94** and **96**.*

Maiti and co-workers expanded on this further by reporting the highly selective *para*-C–H olefination of arene **98** using a novel D-shaped silyl-biphenyl DG (**Scheme 46**).[111]

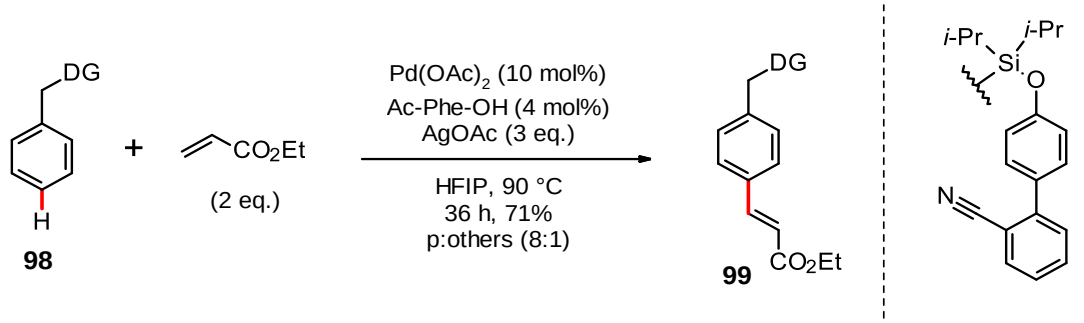

***Scheme 46**. para-C–H functionalisation of arenes using a silyl-biphenyl motif.*

Due to the rigidity of the biphenyl motif and the linearity of the nitrile coordinating group, activation of the *ortho*- and *meta*-C–H bonds are unfavourable owing to the subsequent strained assembly. Moreover, by judicious attachment of two isopropyl groups to the Si centre, it was hypothesised that the Thorpe-Ingold effect was assisting in positioning the metal in close proximity to the *para*-C–H bond. This resulted in the favourable formation of a flexible cyclophane-like 17-membered metallacycle (**Figure 14**).

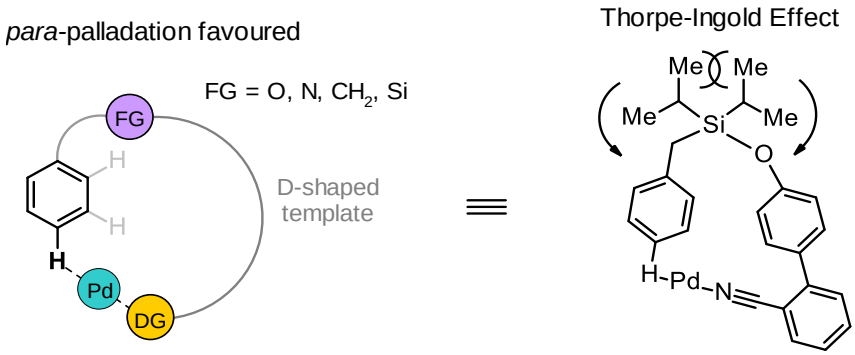

***Figure 14**. Enabling para-C–H functionalisation via use of a D-shaped template.*

Nitrile based DGs such as those described above are also an exogenous motif and so share the same limitations as strongly coordinating AQ and PA motifs. Of particular note are the extra synthetic steps required for the incorporation and removal of the nitrile scaffold which typically leads to a lower overall atom economy.

Nevertheless, although C–H olefination was achieved using a nitrile template, Yu and colleagues observed that the catalyst can coordinate with a reagent due to the inherent weak coordination capability of this nitrile-based DG. This restriction limits the possibilities for additional C–H transformations.[108]

Researchers in the Maiti group addressed this issue by substituting the nitrile DG with a stronger σ-donating pyrimidine motif in 100. This unlocked a range of possible transformations (**Scheme 47**).[112]

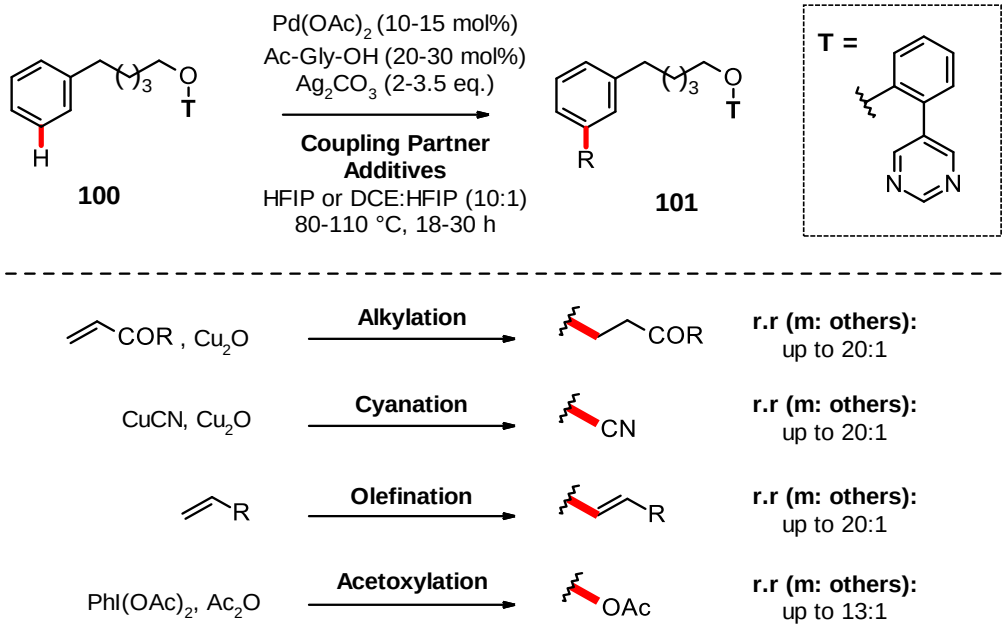

***Scheme 47**. Diverse meta-C–H functionalisation of arenes via a pyrimidine directing motif.*

Examining the C–H functionalisations shown earlier in **Scheme 45**, the linker between the substrate and template is relatively short compared to that in **Scheme 47** above. This aligns with expectations, as a longer tether would lead to a significant entropic penalty due to the creation of a large, organised macrocyclic pre-transition state. However, despite the high entropic cost upon palladacycle formation, Jin and co-workers have reported a selective *meta*-C–H olefination protocol on **102** with long flexible alkyl tethers (**Scheme 48**).[113]

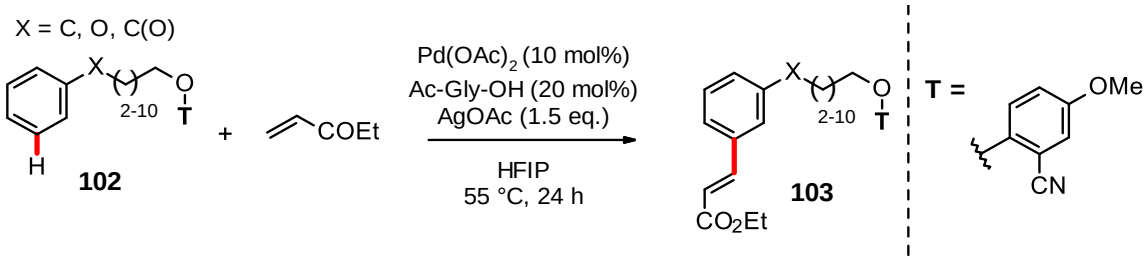

***Scheme 48**. Remote meta-C–H olefination of arenes containing distally tethered templates.*

Jin and co-workers also proposed $PdAg(OAc)_3$ as the active species after conducting DFT computational studies. They justified that the regioselectivity of C–H olefinations in substrates with shorter linkers relies on the angle of the silver-nitrile bond. Here, both *para* and *ortho* functionalisations lead to a bond angle deviating from the preferred 180° linear geometry, thus

making them less favourable. However, in substrates with significantly longer tethers, the crucial factor during the transition state formation shifts to minimising the gauche conformation of the phenyl ether. The *meta* position is preferred over *ortho* and *para* positions due to the unfavourable gauche interactions present in the latter two positions.

2.1.5 Boron-linked DGs for C–H Functionalisation

So far, two approaches for directed C–H functionalisation have been discussed. One approach involves using practical substrates containing native functional groups which avoid the steps of installation and subsequent removal of DG motifs (**Figure 15**, **approach 1**).

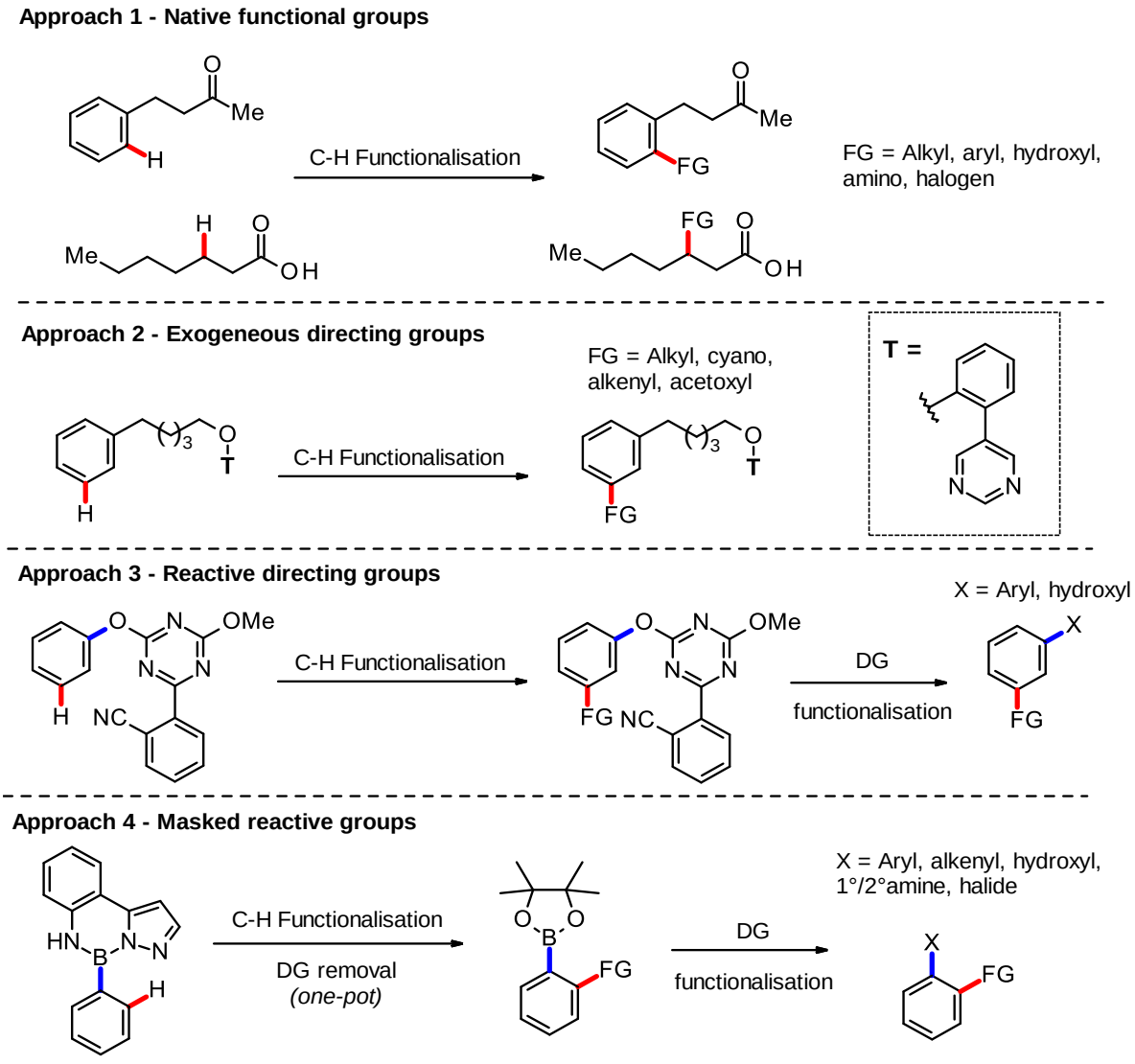

***Figure 15**. Examples of popular approaches to perform C–H functionalisation.*

However, for substrates which do not contain appropriate native functional groups, incorporating exogenous DGs via a tether is a well-established alternative (**Figure 15**,

approach 2). To improve the synthetic usefulness of this method, designing reactive DGs that can undergo post-functionalisation is a valuable tool to synthetic chemists (**Figure 15**, **approach 3**). However, while this methodology is desirable, there are limited DG functionalisations possible and the bespoke DGs used often require lengthy synthetic routes.

An alternative approach makes use of a DG which is linked via a tether to a masked reactive functional group (**Figure 15**, approach **4**). Upon DG removal, the reactivity of the exposed functional group can be exploited leading to a wide range of possible products.

Considering functional groups with masked reactivity, aryl boronic acids are a suitable functional group to use in this last approach. Aryl boronic acids are easy to handle, many are commercially available, and their synthesis can be performed through various pathways (**Scheme 49**).

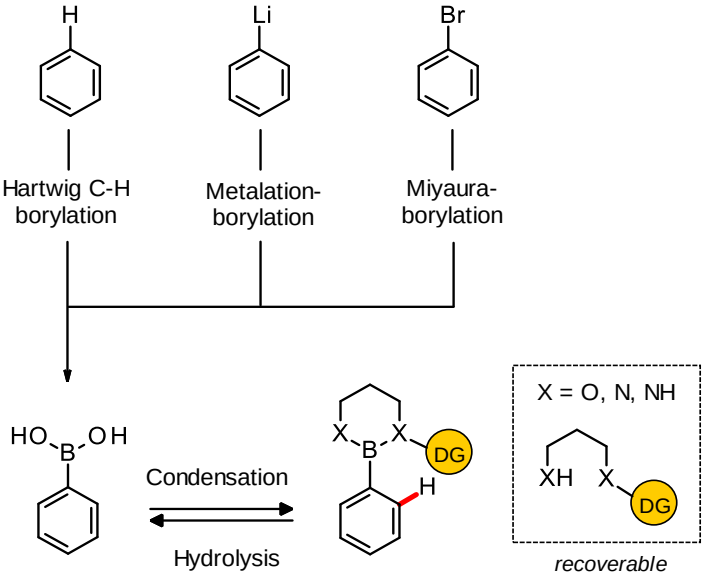

***Scheme 49**. The synthesis and suitability of boronic acids as masked reactive groups.*

Since different boronate esters can be generated by a condensation reaction, a DG tether could potentially be incorporated to form a boron-linked DG. In addition, the DG tether is predicted to be recoverable through a hydrolysis reaction and thus improving the atom-economy of the C–H functionalisation reaction.

To date, there have been few reports in the literature on the use of boron-linked DGs for C–H functionalisation. Suginome and co-workers have designed boron-linked DGs which direct *ortho*-C–H silylation of arylboronic acids.[114,115] These include 2-pyrazol-5-ylaniline (pza) **104**

and anthranilamide (aam) **105** which react with phenylboronic acid in a simple condensation reaction to afford PhB(pza) **107** and Ph(aam) **108** respectively (**Scheme 50**).

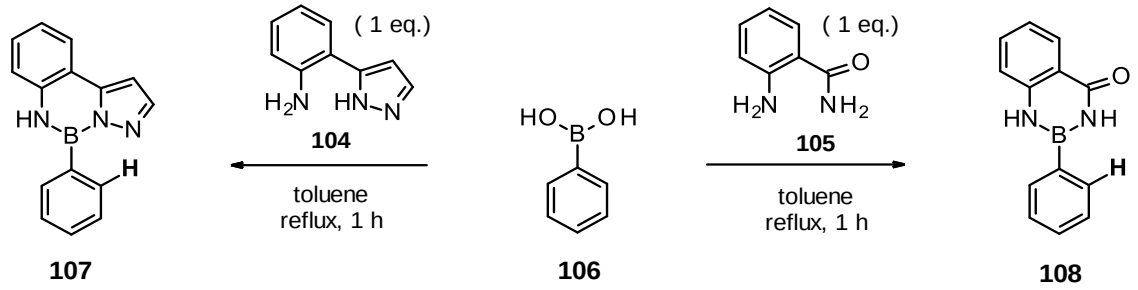

***Scheme 50**. Suginome's DG scaffolds **104** and **105** can direct functionalisation at the ortho-C–H bond of arylboronic acids.*

Moreover, the C–H functionalisation reactions detailed by Suginome involving B(pza) derivatives **109** are primarily limited to C–H silylation and borylation, with a single occurrence of a carbon-carbon bond formation (**Scheme 51**).[116–119]

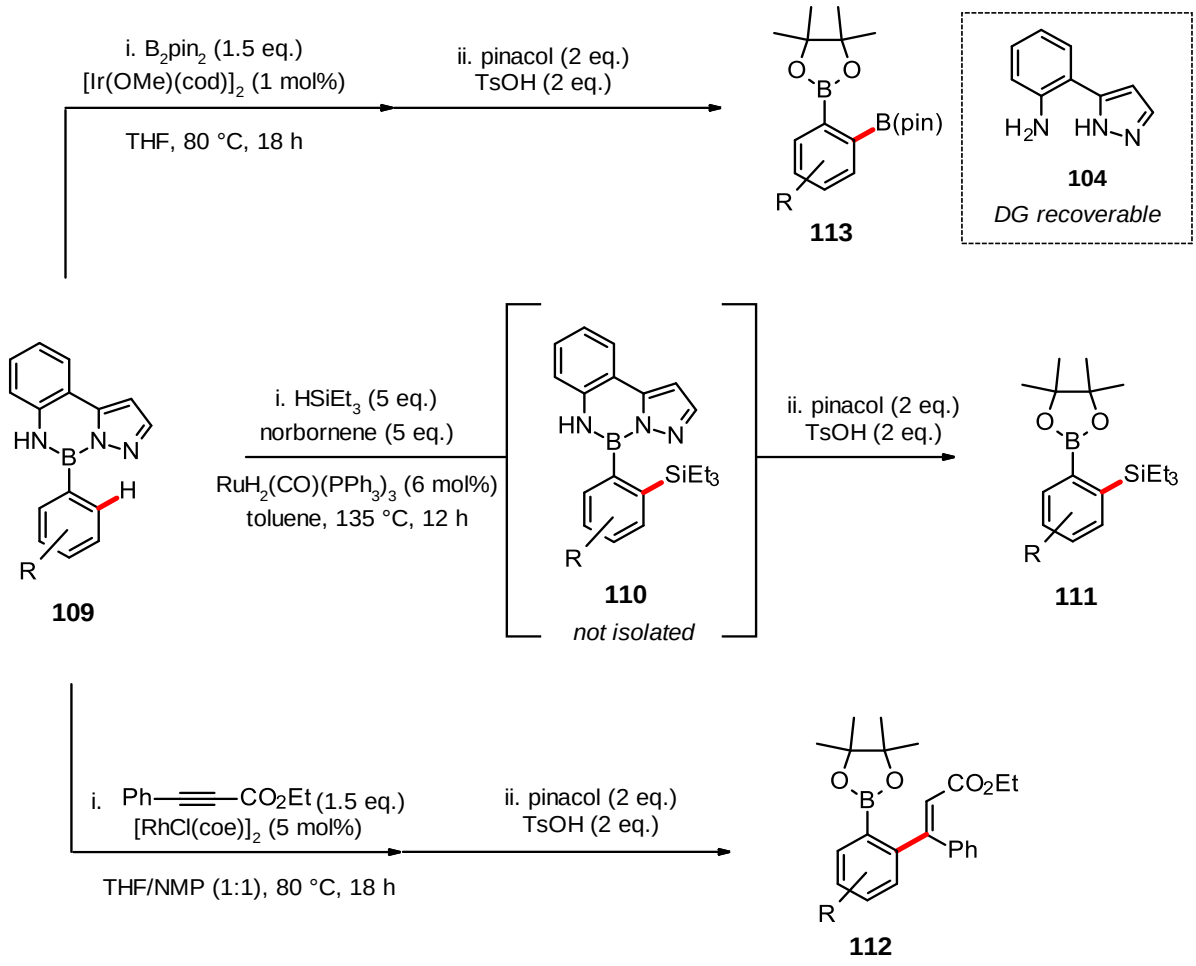

***Scheme 51**. One-pot ortho borylations, silylations and alkenylations on ArB(pza) **109** using iridium, ruthenium, and rhodium catalysts respectively, as developed by Suginome.*

The anthranilamide (AAM) boronate ester **108** undergoes directed *ortho*-C–H silylations, but also exhibits improved stability which prevents transmetallation of B(aam) from occurring due to the delocalised electron density from the anthranilamide ring feeding into the vacant p orbital of the boron atom. As a result, cross coupling of two organoboron species, **114** and an arylboronic acid was possible (**Scheme 52**).[120] Compound **114** was subjected to Suzuki cross-coupling conditions and the resulting product **115** underwent Ru-catalysed *ortho*-selective C-H silylation in a one-pot protocol to furnish **116**.

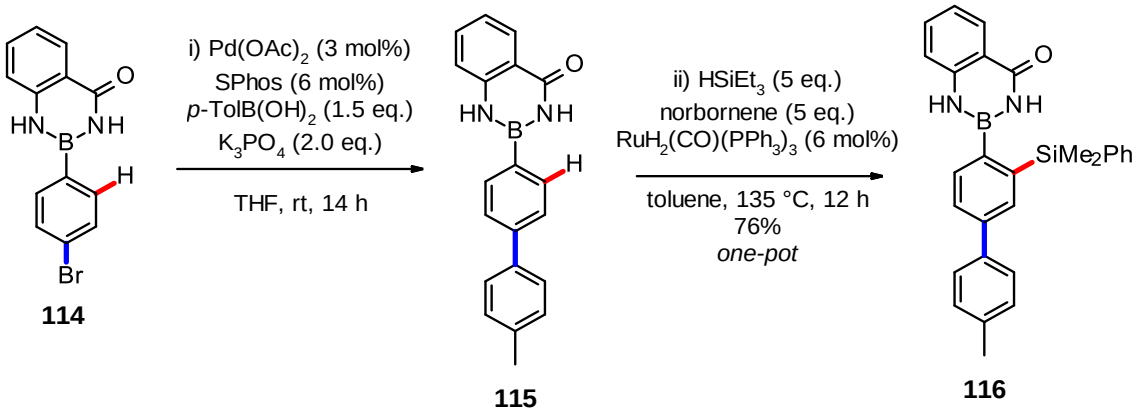

Scheme 52. Boron-linked AAM motif serving as both a protecting and a directing group.

In light of Suginome's work, the advantages of using boron-linked DGs over traditional DGs is apparent. After one-pot *ortho*-functionalisation is performed on substrates such as PhB(pza), recovery of DG **104** is possible using mild conditions. This contrasts with C–H activation that use DGs which are tethered to the substrate via an amide bond. A PA DG requires harsh conditions for its removal such as the use of zinc metal with strong acid[121] or high temperatures[122] in combination with extended reaction times.

Nevertheless, utilising pza **104** comes with certain drawbacks that must be resolved when creating new boron-linked directing groups (DGs). Present limitations involve the instability of ArB(pza) derivatives to silica, making purification through standard chromatography methods impractical. Additionally, given the lengthy three-step synthesis to obtain **104**, there is a pressing need to develop shorter synthetic routes for new boron-linked DGs.

Aryl *N*-methyliminodiacetic acid (MIDA) boronate esters also have the potential to be employed as boron-linked DGs. As these esters suppress B → M transmetalation due to the sp^3-hybridised boron centre, their use can be both dual-purpose, serving not only as a directing group but also as a protecting group under Suzuki-Miyaura coupling conditions (**Scheme 53**).[123]

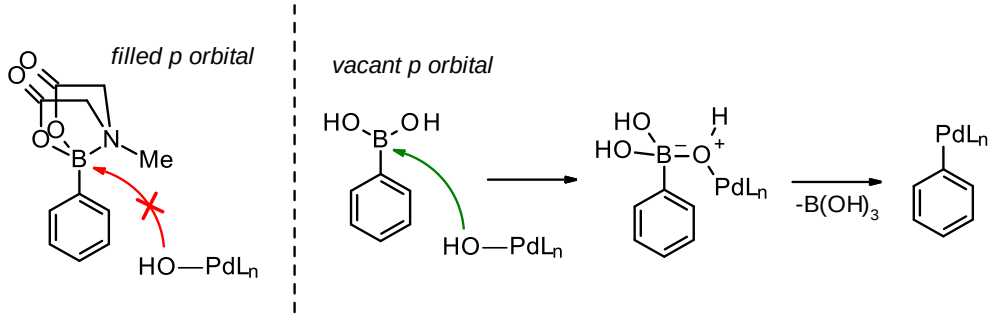

***Scheme 53**. Comparison of transmetalation of phenyl MIDA and phenylboronic acid with palladium, with the former possessing N to B coordination.*

In 2020, Spivey and co-workers reported the *meta*-selective Pd-catalysed C–H functionalisation of arylboronic acid derivatives with a B(MIDA) based DG **118**.[124] The DG could be introduced to an arylboronic acid via a simple condensation reaction (**Scheme 54**).

117 **118**

***Scheme 54**. Condensation reaction of the BMIDA derivative **117** and phenylboronic acid.*

A bespoke *N*-tethered moiety was designed containing a nitrile functional group which enabled C–H functionalisation to occur, including alkenylation, acetoxylation and arylation (**Scheme 55**).

However, poor regioselectivity was obtained using **119,** with a mixture of *meta*- and *para*-functionalised products formed. Also, C–H alkenylation reactions were sensitive to the steric bulk of substituents with reduced yields obtained for arylboronic coupling partners with methyl or methoxy substituents at the *para* position.

Although C–H arylation was achievable, it was accompanied by low reported yields and necessitated very high catalyst loadings (40 mol% of palladium diacetate). This suggests that **119** is not optimal for directed arylation, necessitating the need for more efficient B-linked DGs.

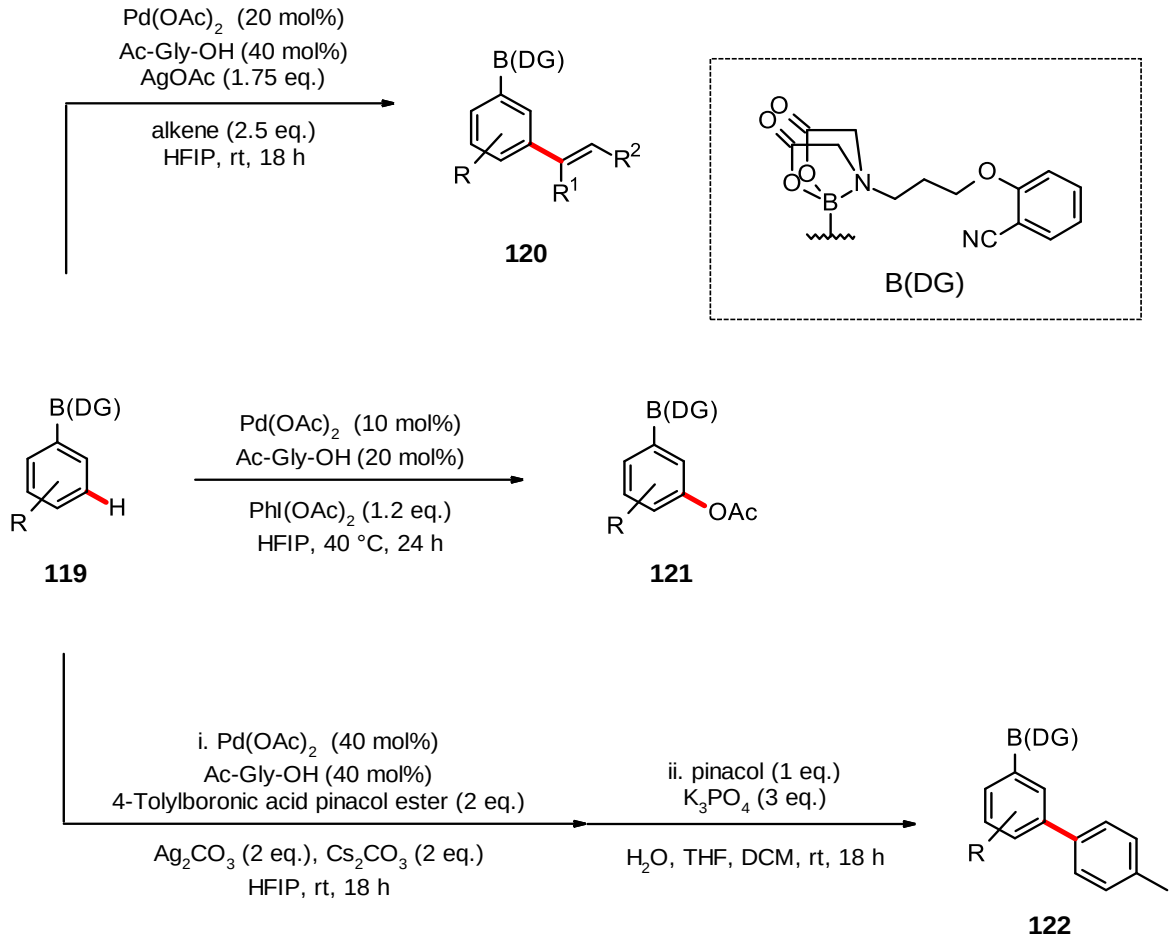

***Scheme 55**. meta-C–H transformations on B-DG scaffold **119** developed by Spivey and co-workers.*

2.2 Project aims

Several boron-linked protecting groups (PGs) have previously been reported, including B(dan), B(mida), B(aam) as well as less-studied boron-containing heterocycles (**Figure 16, top**). We proposed that whilst systems such as B(dan) and B(mida) are compatible with many metal-catalysed transformations, such systems and derivatives thereof may still act as directing groups under appropriate conditions.

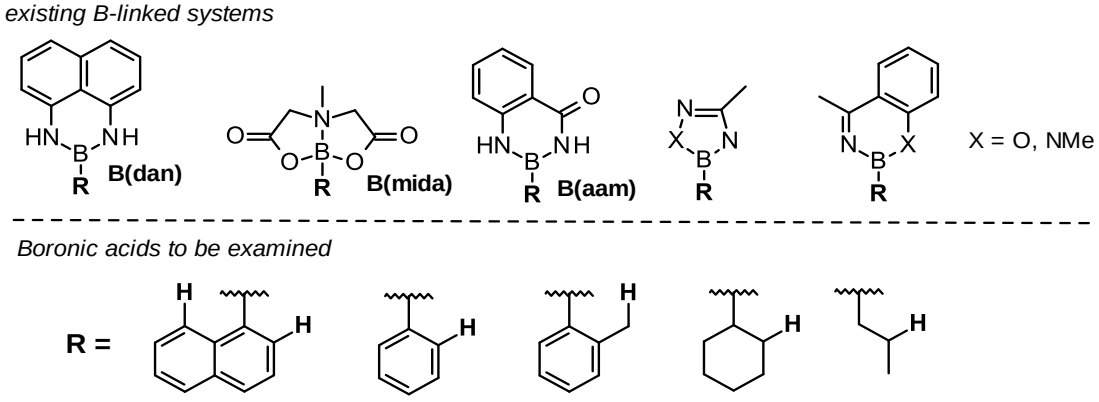

***Figure 16**. (top) Existing B-linked systems, (bottom) selection of substrates to be investigated.*

As B-directed C–H silylation/borylation reactions catalysed by ruthenium are well-established, exploring Ru-catalysed C–H arylation is a priority. This is because at the start of this project (September 2019), there was only a single example of a B-directed reaction in which a carbon-carbon bond is formed.[117] As aryl C–H activation with DGs is well precedented, the design of a range of boron-linked derivatives that incorporate extensively studied directing groups should be straightforward.

Nevertheless, the high rigidity of an aryl system increases the difficulty of reacting the target C(sp^2)–H bond with the metal catalyst once it is coordinated to the DG. Thus, aliphatic systems which offer increased flexibility in the backbone will also be explored, albeit C(sp^3)–H activation can often be more challenging. To serve as a useful compromise, a phenethyl system containing adjacent benzylic, hence more reactive, C–H bonds will be studied in addition to other cyclic and acyclic systems (**Figure 16, bottom**).

The first goal of this project was to investigate if these PGs and derivatives thereof can promote arylation of both C(sp^2)–H and C(sp^3)–H bonds using known Ru or Pd catalysis conditions which use similar coordinating motifs. These potential DGs could coordinate to metal via the nitrogen present in the boron scaffolds, positioning the metal close to the desired C–H bond.

2.3 Results and discussion

2.3.1 Investigation of existing boron-linked groups

The B(dan) system was investigated first as it is readily accessible via a one-step condensation reaction from the boronic acid. Moreover, although recognised for its compatibility in various metal-catalysed reactions as a protective group, this motif might still act as a DG under appropriate conditions.[125] To begin with, several B(dan) derivatives were synthesised using 1,8-diaminonapthalene **123** and the corresponding boronic acids (**Scheme 56**).

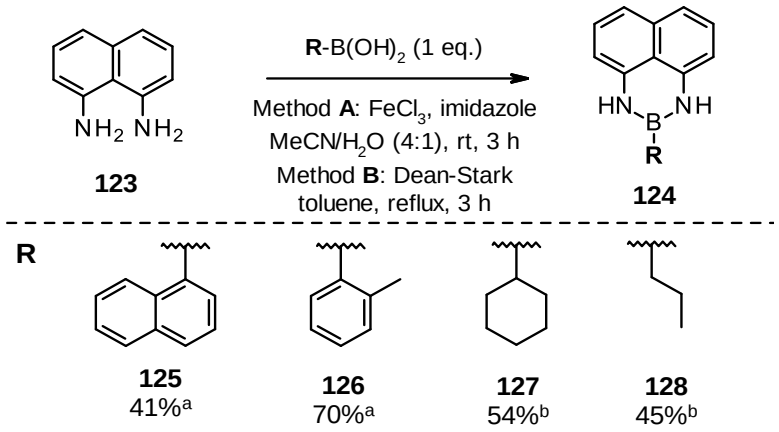

***Scheme 56**. Condensation of 1,8-diaminonapthalene with a range of boronic acids. % Yields shown are of isolated products. [a]Method A. [b]Method B.*

It was hypothesised that deprotonation of the acidic N–H bond in B(dan) could potentially lead to palladium coordination, followed by insertion into the desired C–H bond. This was investigated with substrates **125** – **128** using known palladation conditions[121] including a range of bases (CsOAc, NaOAc, Cs_2CO_3 and CsOPiv) and is illustrated using naphthalene-B(dan) **125** (**Scheme 57**).

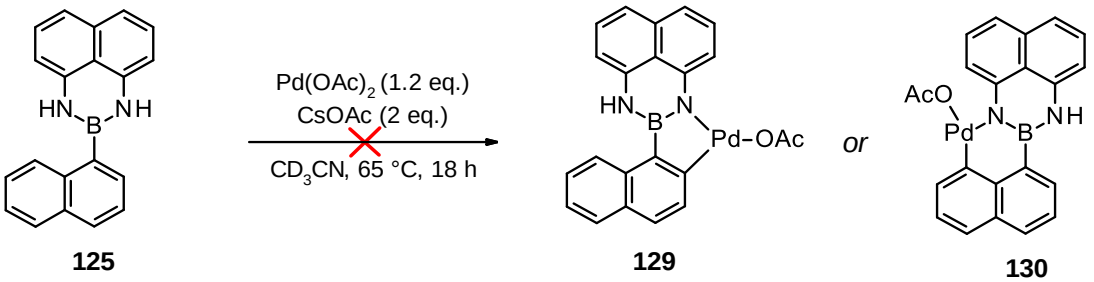

***Scheme 57**. Attempted coordination and C–H insertion of palladium into B(dan) substrate **125**.*

However, efforts to create the corresponding palladacycles from **125** – **128** followed by isolation and characterisation by X-ray crystallography was not successful. NMR analysis of

the reaction with **127** showed loss of the original B(dan) aromatic signals and the appearance of a new proton set (**Figure 17**). However, attempts to isolate this species failed as it reverted to starting material upon work-up, suggesting palladium was attaching only to the acidic NH and not inserting into the nearby C(sp^3)–H bond. A six-membered palladacycle, such as **130** may be more stable but this compound was not observed either. This is likely due to disfavoured geometry between the DG, Pd and the target C–H bond.

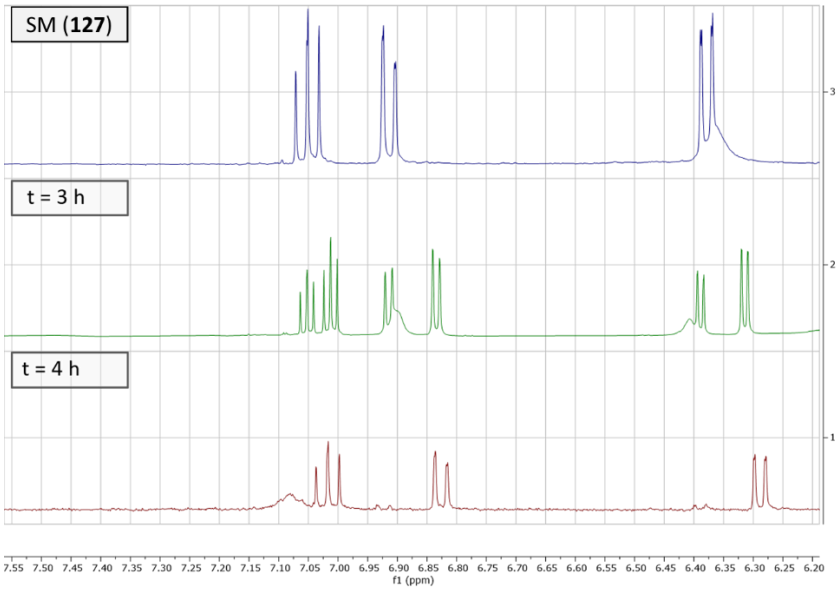

***Figure 17**. NMR overlay showing progress of palladation attempt with B(dan) substrate **127**.*

Subsequently, rather than seeking to isolate palladacycles, our objective shifted towards capturing any potential palladium species formed *in situ* by employing iodine. This process aimed to yield a compound that would be more manageable for isolation and characterisation. This was attempted with **125** and unexpectantly the crude NMR showed that the B(dan) group was cleaved and replaced by an iodine atom. This was confirmed upon purification of the crude reaction mixture which afforded 1-iodonapthalene **131** in 17% yield and none of the iodinated compound **132**, suggesting that C–H palladation did not occur (**Scheme 58**).

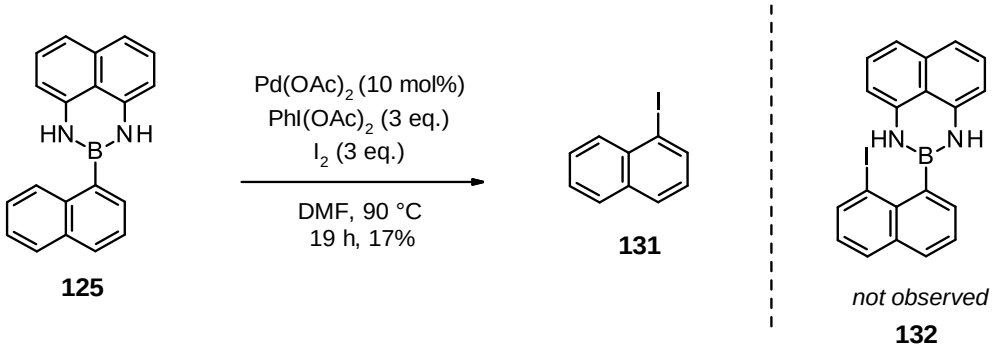

***Scheme 58**. Attempted trapping of a hypothesised palladacycle with iodine.*

Substrate **125** was then subjected to C–H arylation conditions with aryl halides as the coupling partners. Several Pd-catalysed conditions which have been reported for other directed C–H arylations were attempted including the use of additives such as picolinic acid[126] which were reported to regenerate catalytic palladium species, as well as conditions using copper[121] as a co-catalyst. Despite exploring an extensive array of conditions, the anticipated arylated product **133** remained elusive, and instead, unreacted starting material was detected through NMR and TLC analysis (**Scheme 59**).

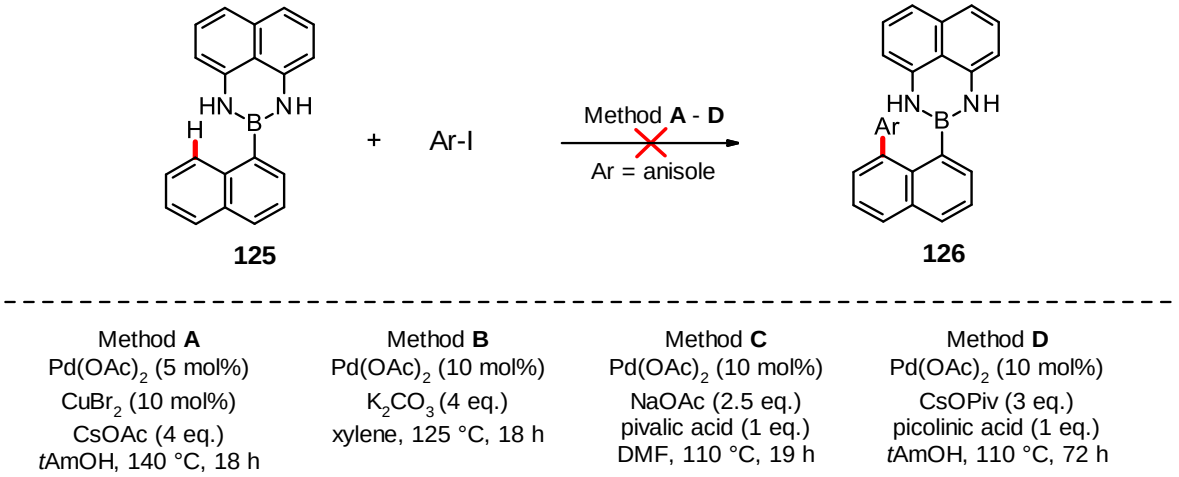

***Scheme 59**. Attempted C–H arylation of B(dan) derivative **125** using known arylation methods.*

Other B(dan) substrates **126** – **128** were also tested against several of the above methods but with the same outcome – no arylated product identified and, in most cases, significant starting material recovered. Due to the consistent lack of desired reactivity of the B(dan) group, a decision was made to pivot attention and explore an already established B-linked DG.

The pza-DG **104** has a proven record in participating as a directing group in C–H functionalisation reactions including silylation[115] but its employment in metal-catalysed

reactions to form new carbon-carbon bonds is limited to alkynes.[117] The objective now was to investigate if this DG can be used for C–H arylation reactions.

Pza-DG **104** was synthesised by a 3-step route in accordance with the procedure laid out by Suginome and co-workers.[115] **104** was subsequently coupled with phenylboronic acid to yield PhB(pza) **107** in high yield after purification (**Scheme 60**).

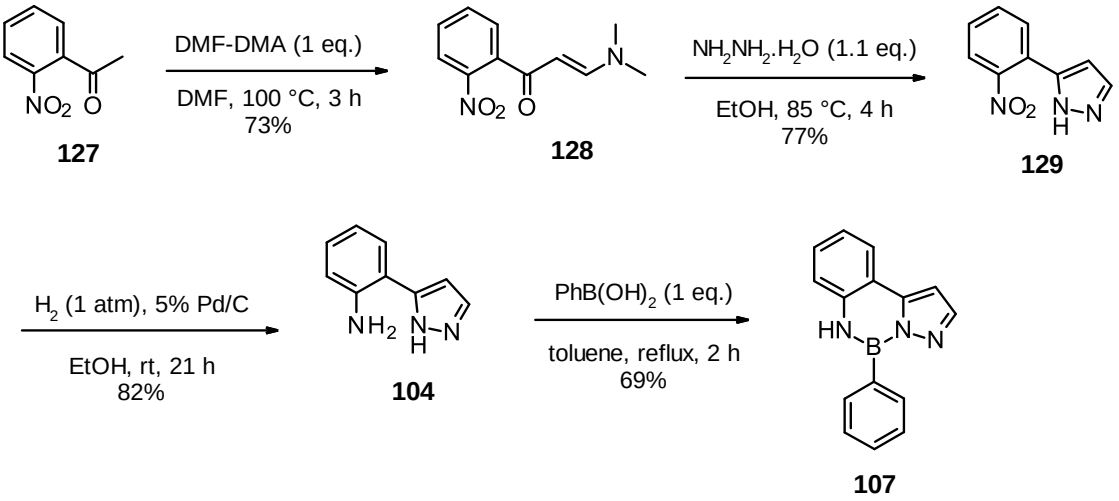

***Scheme 60**. Synthetic route leading to PhB(pza) **107**.*

PhB(pza) **107** was initially subjected to the same palladation conditions as used for B(dan) substrate in **Scheme 57**. However, the expected palladacycle was not observed with TLC and NMR analysis showing that the DG **104** was not present in the crude reaction mixture either.

Next, **107** was tested against the reported C–H silylation procedure, which afforded **18** in a lower amount (<10%) than the literature yield (**Scheme 61**).[115] When the reaction was repeated in the absence of oxygen and water, the yield increased to 26%, highlighting the reaction's high sensitivity.

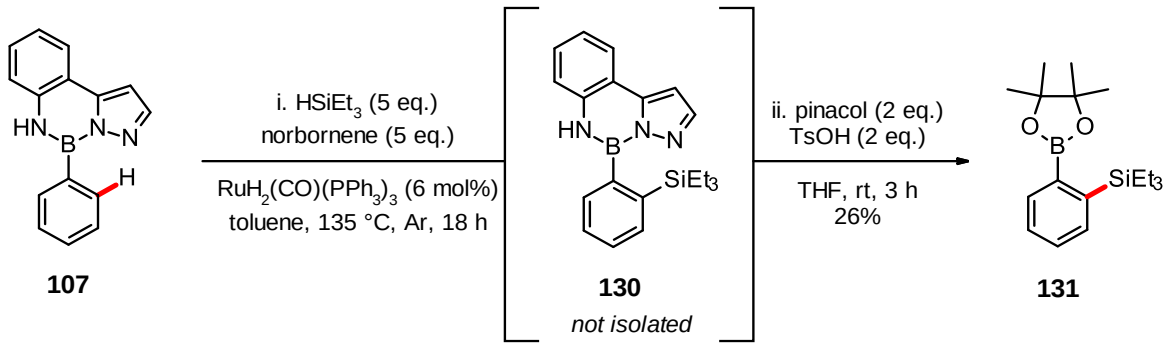

***Scheme 61**. Attempt of a reported C–H functionalisation reaction leading to **131**.*

Ruthenium catalysis has proven effective in facilitating C(sp^2)–H arylation, particularly involving nitrogen-containing heterocycles as the DG, as demonstrated by Ackermann.[36,127] Notably, pyrazole (present in pza-DG **104**) was reported in Ru-catalysed C–H arylation. It was hypothesised that coordinating the nitrogen sp^2 lone pair with a $[RuCl_2(p\text{-cymene})]_2$ catalyst, an aryl group could be introduced at the *ortho* position of ArB(pza) **132** via the proposed ruthenacycle **133** to afford the C–H functionalised product **134** (**Scheme 62**).

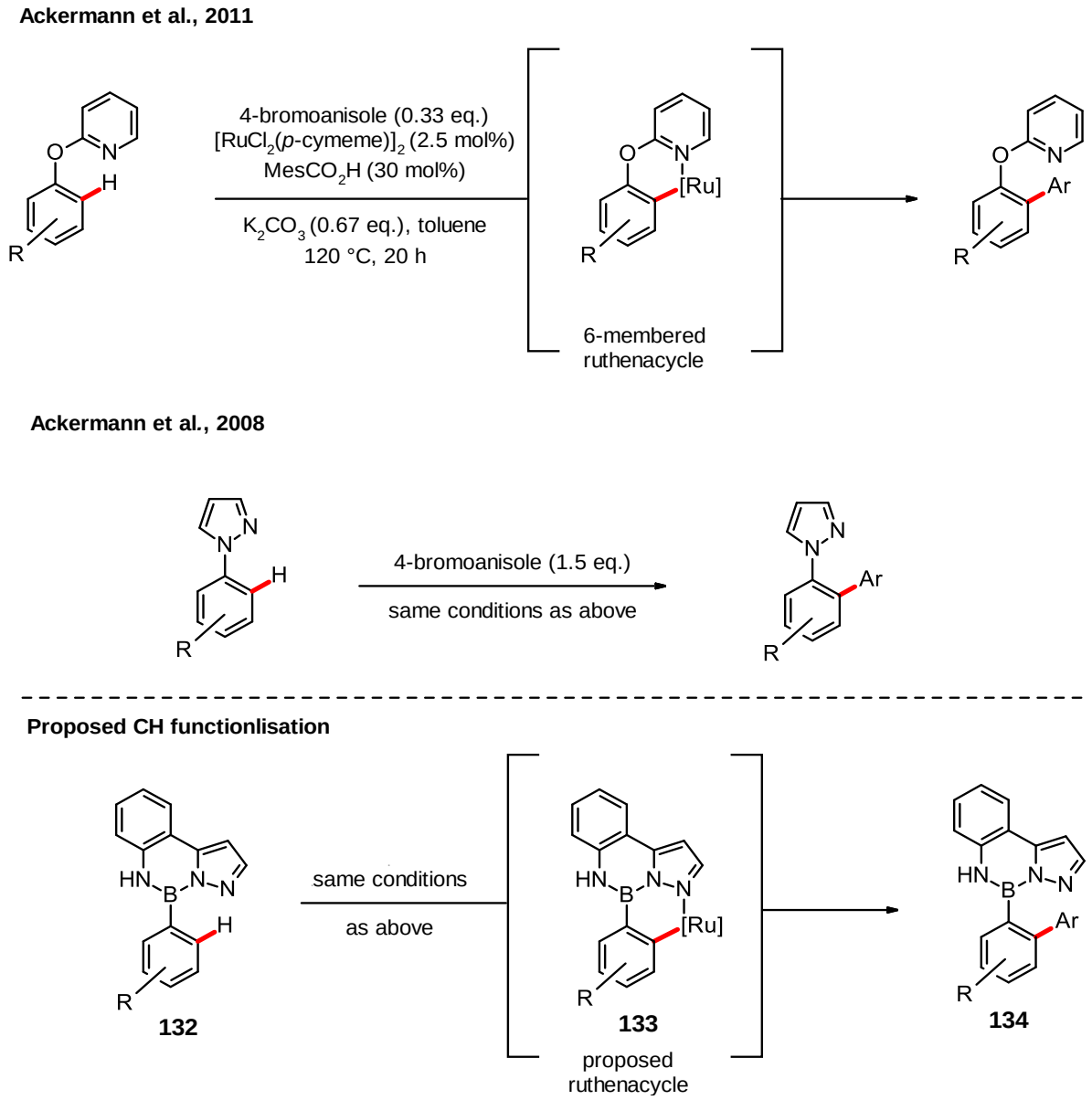

***Scheme 62**. Selected literature ruthenium-catalysed arylations using pyridine and pyrazole as DGs, with Ar = 4-MeOC$_6$H$_4$* and the proposed reaction with **132**.

It was hypothesised that by applying these literature conditions and variations thereof, to the reaction of PhB(pza) **107** with strict exclusion of air and moisture, this would yield **135**

(**Scheme 63**). For ease of isolation and characterisation, potential intermediates were transformed into their respective pinacol esters, such as **136**.

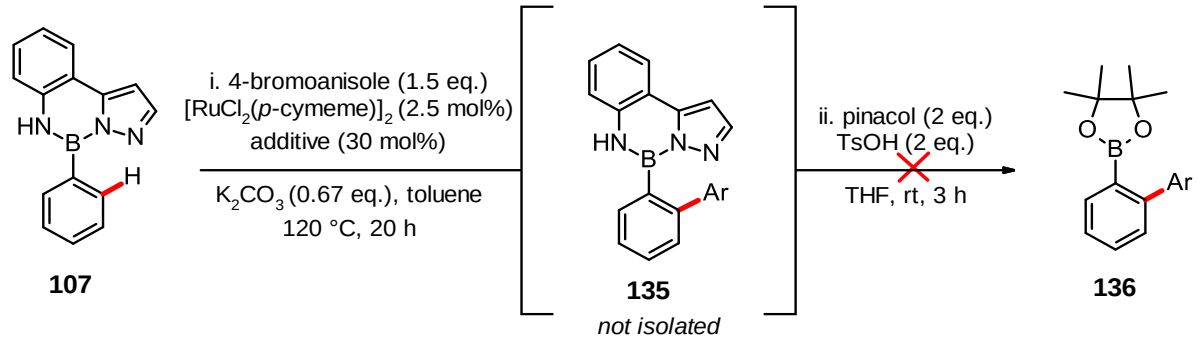

***Scheme 63**. Unsuccessful attempt at C–H functionalisation using ruthenium catalysis with PhB(pza) **107** where Ar = 4-MeOC$_6$H$_4$.*

We explored various additives known for their significance in ruthenium-catalysed C–H activation reactions, including 2,4,6-trimethylbenzoic acid, pivalic acid, Boc-Val-OH, and triphenylphosphine. Despite these efforts, the expected product **136** was not detected. Instead, NMR and TLC analyses revealed unreacted starting material and the presence of cleaved pza **104** in most cases. Pza cleavage likely arises due to coordination of the DG nitrogen atom(s) with the transition metal resulting in a weakened B-N bond.

This lack of reactivity was thought to arise due to the acidic NH motif present in **107**. It is possible that this can result in unwanted metal coordination and thus deactivation of the catalyst. Investigating this further, the nitrogen was replaced by an oxygen atom via reacting commercially available 2-pyrazol-5-ylphenol (pzp) **137** with phenylboronic acid to furnish PhB(pzp) **138** in good yield (**Scheme 64**).

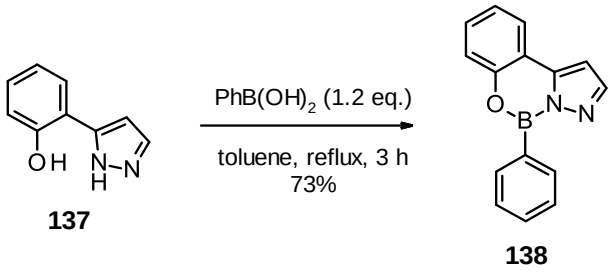

***Scheme 64**. Condensation reaction to yield PhB(pzp) **138**.*

In contrast to PhB(pza) **107**, the stability of PhB(pzp) **138** to silica allowed for purification via flash column chromatography. However, employing silylation and arylation literature conditions involving Pd or Ru catalysis did not yield C–H functionalised products using this

substrate (**Scheme 65**).[115,127] Crude NMR analysis showed unreacted starting material in most cases and in others, decomposition of the starting material with cleaved pzp **137** recovered.

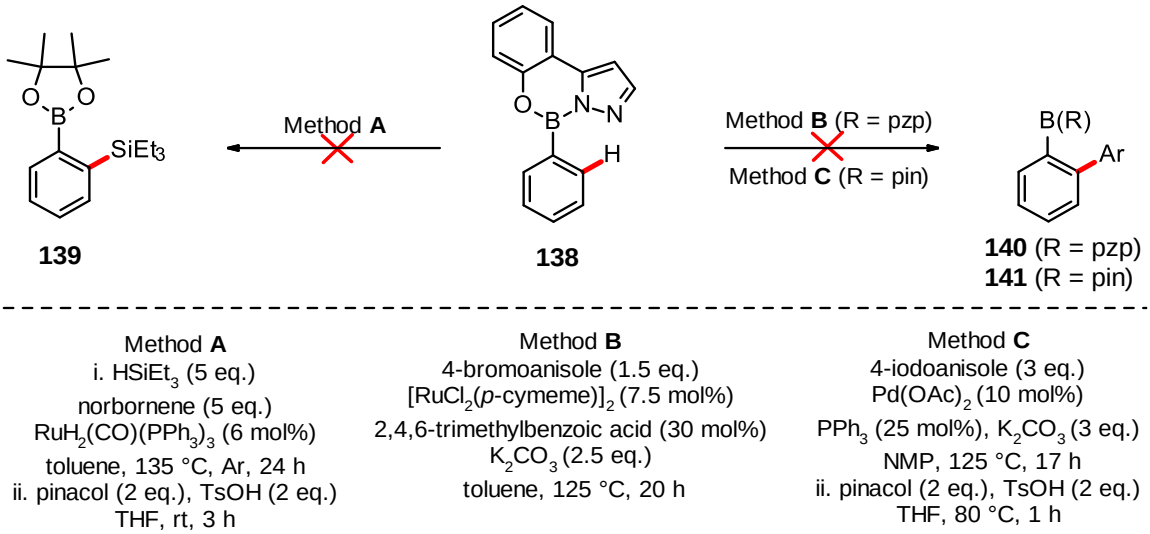

***Scheme 65**. Unsuccessful attempts at C–H silylation and arylation on substrate **138**.*

The complete loss in reactivity for C–H functionalisation observed when altering a single neighbouring heteroatom connected to the boron illustrates the sensitivity of a boron-linked group to act as a DG. Moreover, the stability of existing B-linked groups to hydrolysis can vary significantly from one another (**Figure 18**).[114] Thus, it is imperative that any boron-linked group developed in this work should maintain stability to metal-catalysed reaction conditions while retaining DG ability.

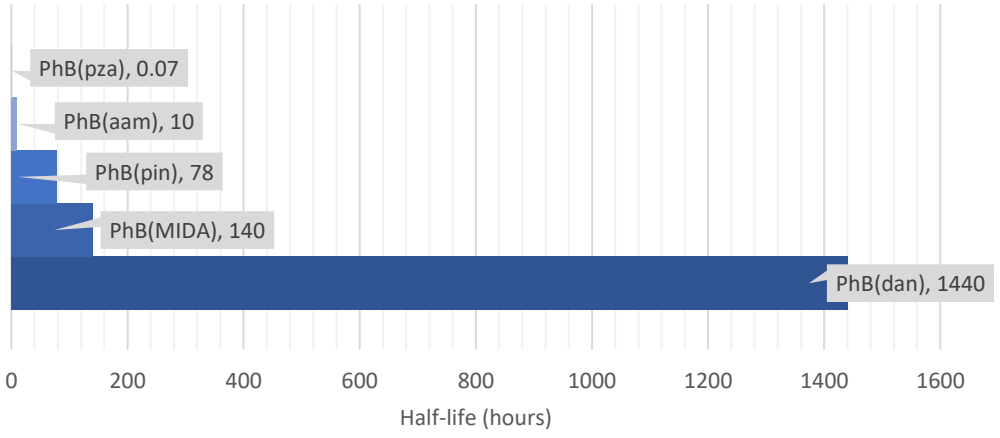

***Figure 18**. Half-lives of phenyl boronates to hydrolysis in DMSO-d_6:D_2O (10:1) at room temperature using NMR spectroscopy, as reported by Suginome et al.*

2.3.2 Designing novel boron-linked groups

After conducting thorough testing of existing B-linked directing groups (DGs) under a range of metal-catalysed C–H functionalization conditions with limited success, a decision was made to shift attention elsewhere. The exploration of structural alterations to the backbone of these boron-linked groups began by employing removable linkers with DGs attached (**Figure 19**).

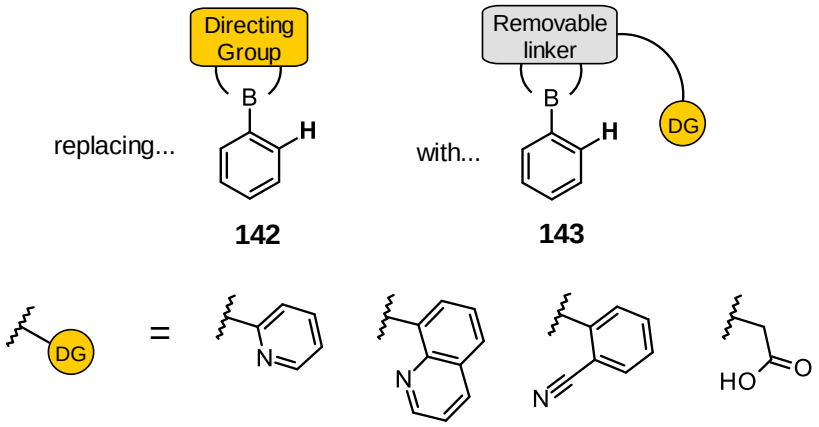

***Figure 19**. Proposed designs for a B-linked DG.*

2.3.2.1 Diazaborole and oxaborole derivatives

This new strategy began with the attempted synthesis of diazaborole and oxaborole derivatives **144c** and **145c** which feature a pyridine moiety connected to a nitrogen atom (**Scheme 66**).

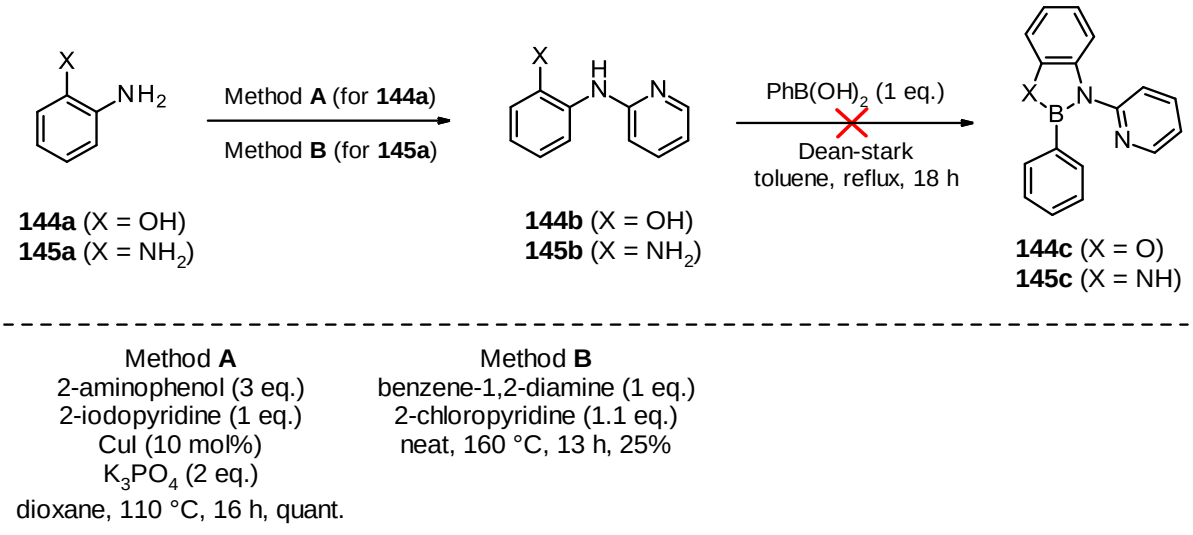

***Scheme 66**. Attempted synthetic route to B-linked substrates **144c** and **145c**.*

The use of a pyridyl motif is well-established for coordinating to a transition metal and bringing it in close proximity to the desired C–H bond to be functionalised. The boron scaffold itself was chosen due to the expected straightforward two-step synthesis route. However, while the incorporation of the pyridyl motif was successful, the final cyclisation step with phenylboronic acid failed to give the desired product with only starting material recovered.

Attempting an alternative strategy, the more reactive $PhBCl_2$ was reacted with **145b**, with ^1H NMR of the crude reaction mixture showing new signals alongside starting material peaks. But subsequent purification via flash column chromatography failed with only **145b** recovered indicating that the species **144c** and **145c** are not stable on silica.

It is likely the instability of these novel diazaborole and oxaborole derivatives is due to the electron withdrawing ability of the pyridyl ring. This leads to a decrease in the π-donating ability of the amine for it to undergo a condensation reaction with a boronic acid.

2.3.2.2 B(MIDA) derivatives

Another strategy investigated involved the derivatisation of a B(MIDA) moiety. This is similar to the work of Spivey and co-workers who recently reported the MIDA-DG **146** (**Figure 20**).[124]

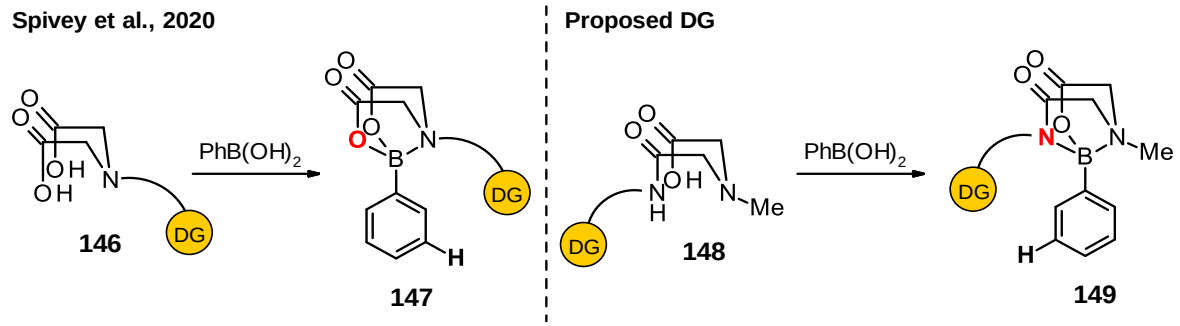

***Figure 20**. Existing DG **146** reported by Spivey and the proposed DG **148**.*

However, we planned for the DG to be attached with different connectivity to the boron, such as **148**. Also, this approach could deliver a more optimised synthetic route to **148** that involves fewer steps than the existing route to **146**.

The synthesis of a derivative **148** began with the cyclisation of MIDA **150** to furnish **151**, followed by ring-opening by the DG-containing amine, 2-picolylamine **152** (**Scheme 67**). However, the final step of condensation with phenylboronic acid failed to furnish **154** and instead unreacted starting material was detected.

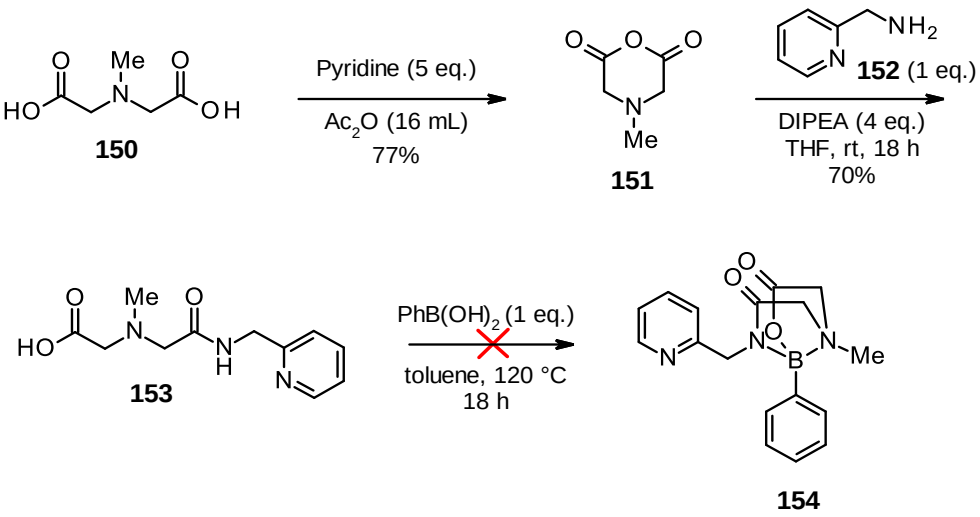

150 **151** **152** **153** **154**

***Scheme 67**. Synthetic route to BMIDA-modified substrate **154**.*

It is probable that 2-picolylamine **152** has attenuated nucleophilicity due to electron-withdrawing effect of the pyridyl group attached to the amino group. As a result, it was unable to undergo a condensation reaction with a boronic acid. At this point, due to the similarity of **46** to that reported by Spivey and co-workers, it was decided to explore other B-DG scaffolds to ensure novelty of this work.

Another class of compounds such as **155** has been detailed in the literature,[128] and upon modification of its backbone could be used in directed functionalisation (**Scheme 68**). Given the recent success of meta-C–H activation with BMIDA derivatives reported by Spivey and co-workers, which exhibit a tetrahedral geometry around the boron atom, there is potential for boronates such as **156** to enable C–H functionalisation. These boronates could offer this capability through structural modifications.

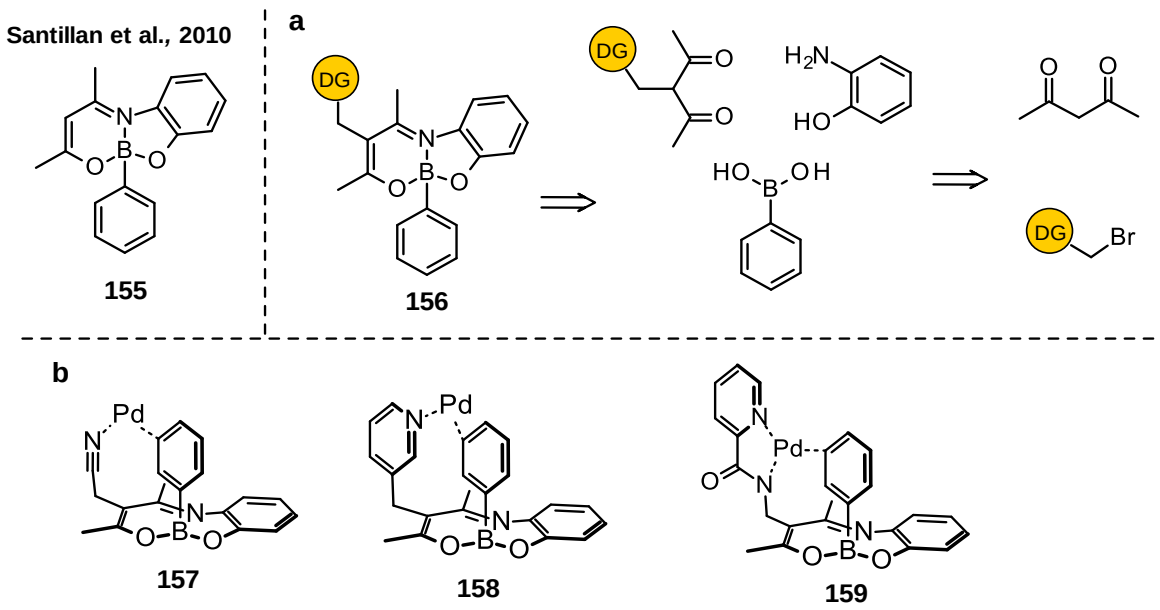

***Scheme 68**. a) Proposed retrosynthetic route to boronate **156**, b) 3D view of hypothesised palladium coordination with three well-established DGs.*

Before work on incorporating DGs into these boron-based scaffolds was started, unmodified **162** was synthesised (**Scheme 69**).

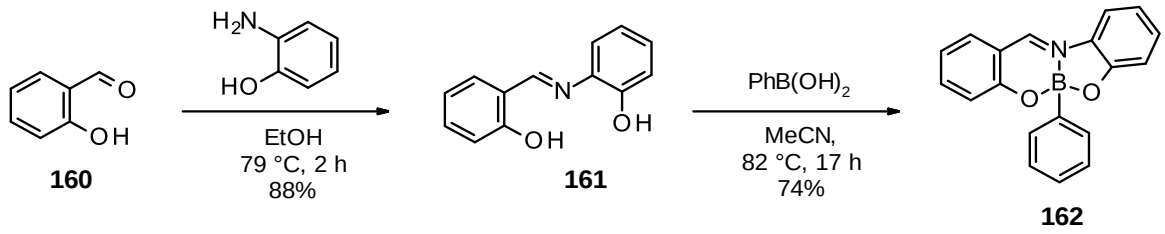

***Scheme 69**. Synthetic route to boron containing scaffold **162**.*

Compound **162** was then then subjected to the most common C–H arylation and olefination reaction conditions to determine its stability (Scheme **70**). Unfortunately, degradation of the starting material was observed with all reaction conditions in varying amounts, with flash column chromatography purification yielding nothing of note. These results suggest that **162** may be unsuitable for C–H functionalisation transformations.

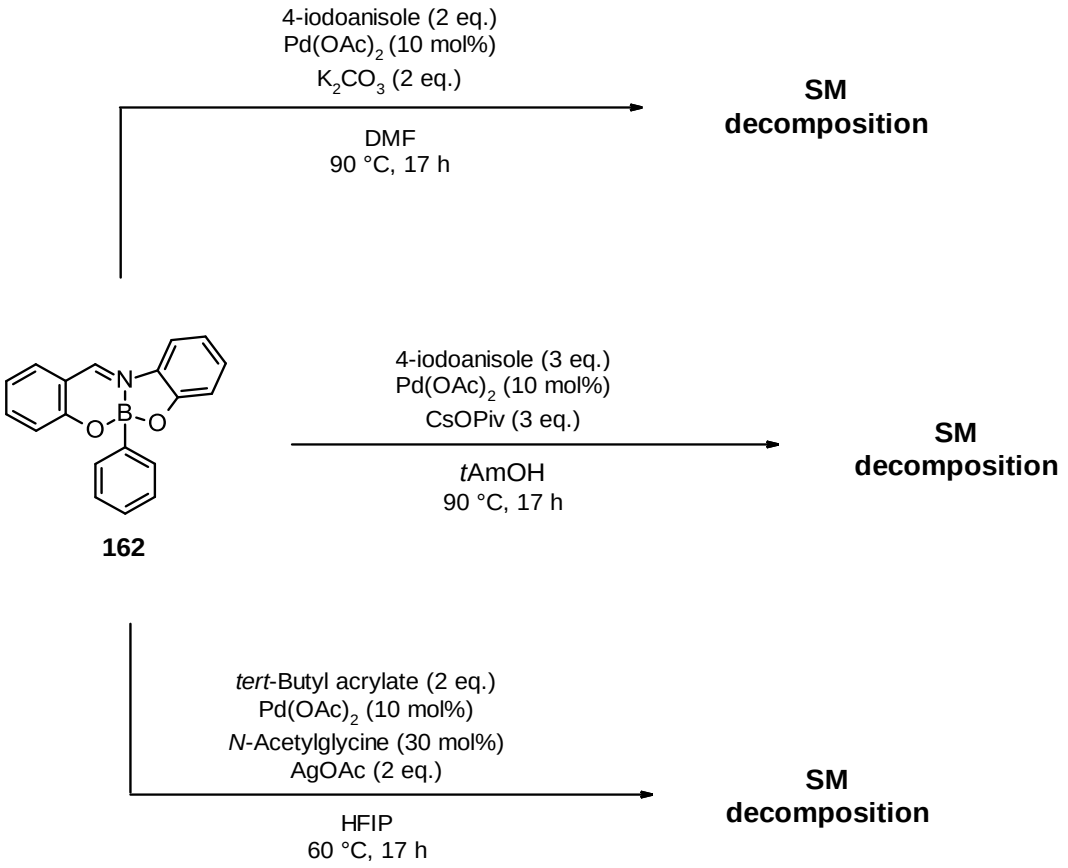

***Scheme 70**. Investigating stability of **162** against common C–H functionalisation conditions.*

Additional analogous scaffolds **163** – **165** were synthesised and subjected to the C–H functionalisation reaction conditions above **(Scheme 71)**. ^{11}B NMR analysis of the reaction mixtures revealed trace amounts of starting material, suggesting the potential cleavage of the phenylboronic acid component via loss of the B–N bond. It is hypothesised that the electron-withdrawing effects from the adjacent aromatic groups is weakening the B–N bond sufficiently enough to result in degradation under reaction conditions.

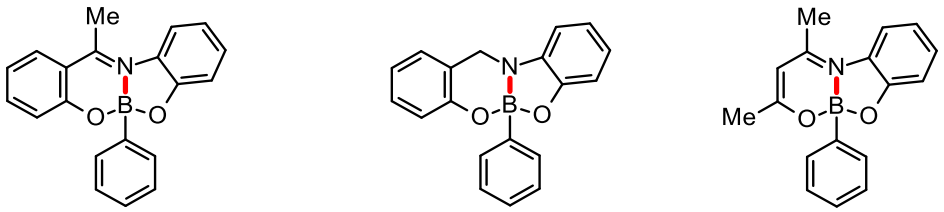

163 **164** **165**

***Scheme 71**. The boron-nitrogen bond is likely weakened in **163**-**165**.*

Hence, an alternative approach is required to mitigate the adverse electronic impact on the B–N bond. One potential method to accomplish this involves substituting the neighbouring sp^2 centres with sp^3 centres and integrating an extended linker to the DG (**Figure 21**).

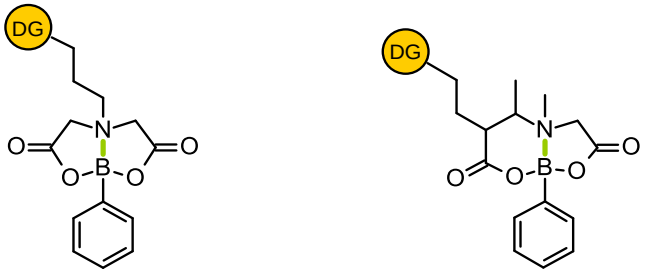

166 **167**

***Figure 21**. Literature B-linked **166** and proposed analogue **167**, where the B-N bond is less likely to be weakened.*

While Spivey *et al*. have recently developed the B-DG **166** with these aspects in mind, the proposed B-DG **167** has the potential to have improved stability due to additional structural features. For instance, the DG linker in **167** is placed at a greater distal position to the nitrogen atom and the *N*-methyl moiety is retained which will help to reduce any negative inductive effects on the B–N bond.

Moreover, the potential conformational changes brought about by Thorpe-Ingold effect[129] from the additional methyl group and by substituting a five-membered ring with a six-membered ring may result in a more favoured transition state intermediate. In fact, other researchers have also utilised Thorpe-Ingold effects to enhance yields in non-boron directed C–H functionalisation reactions.[107,109]

A retrosynthetic analysis of **167** led to a forward route consisting of two alkylations, a reductive amination, a saponification and finally a condensation reaction with a boronic acid (**Scheme 72**).

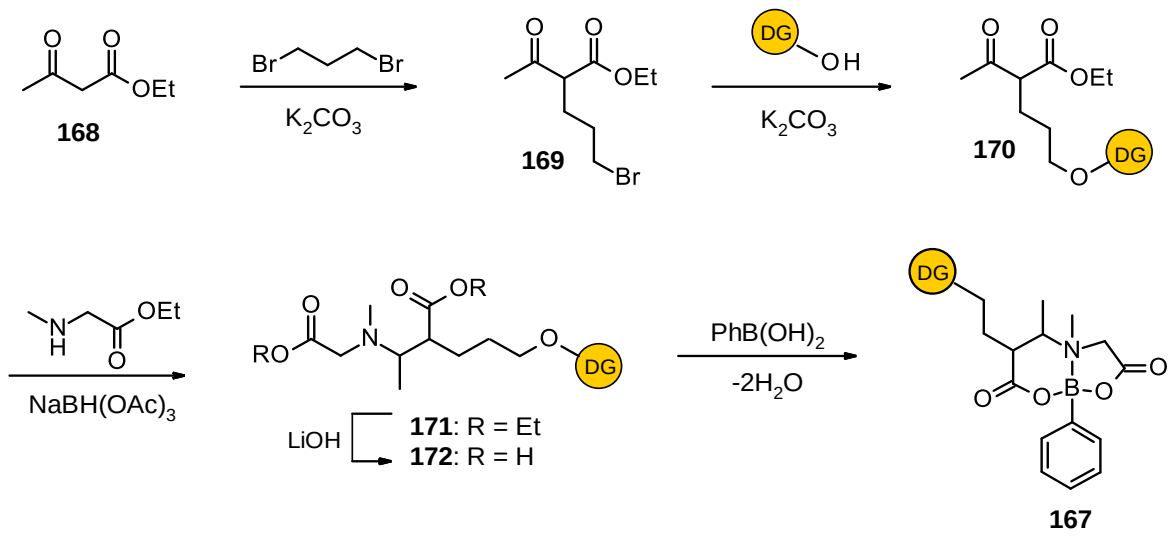

***Scheme 72**. Planned forward route for the synthesis of B-DG **167**.*

Beginning the synthesis, the alkylation of ethyl acetoacetate with 1,3-dibromopropane resulted solely in the unwanted cyclised product **173**. Attempts to prevent this by altering the reaction conditions were unsuccessful, likely because of the minimal energy barrier for intramolecular cyclisation (**Scheme 73**).

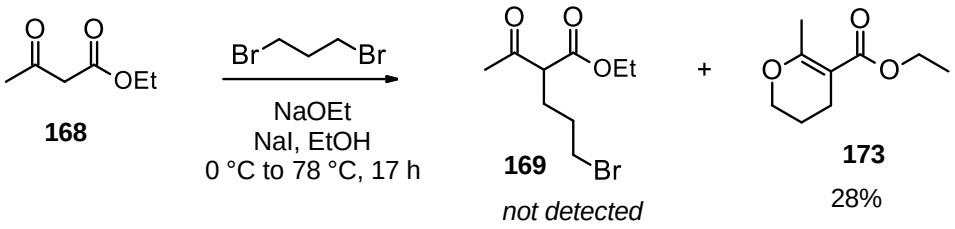

***Scheme 73**. Undesired cyclised side-product **173** was formed during the C-alkylation attempt.*

To avoid any possibility of intramolecular cyclisation occurring during the synthetic route, the boron-based scaffold **176** with no DG motif present was next considered (**Scheme 74**).

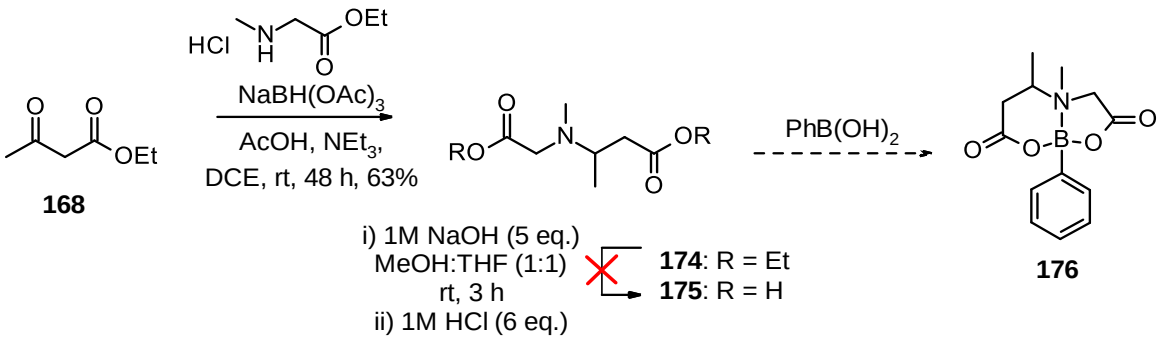

***Scheme 74**. Revised route to boron-scaffold **176** with an unsuccessful saponification step.*

Unfortunately, while the reductive amination was successful in furnishing **174**, the subsequent saponification failed to give the diacid **175**. Despite TLC analysis indicating the reaction was complete, attempts to extract the highly polar compound into the organic layer failed. This was still the case even with varying the acidity of the aqueous layer. This challenge is likely due to the **175** behaving as a zwitterionic species, making its extraction from the aqueous layer difficult.

Another approach was then devised which avoids the use of aqueous work-ups. Here, different variants of the starting material are used – the ethyl groups of the two esters are replaced by *tert*-butyl groups. As a result, TFA in DCM would be able to afford the diacid **72** without further purification, since excess TFA and solvent can be removed by concentrating the sample *in vacuo* and the side products are gaseous isobutylene and carbon dioxide (**Scheme 75**).

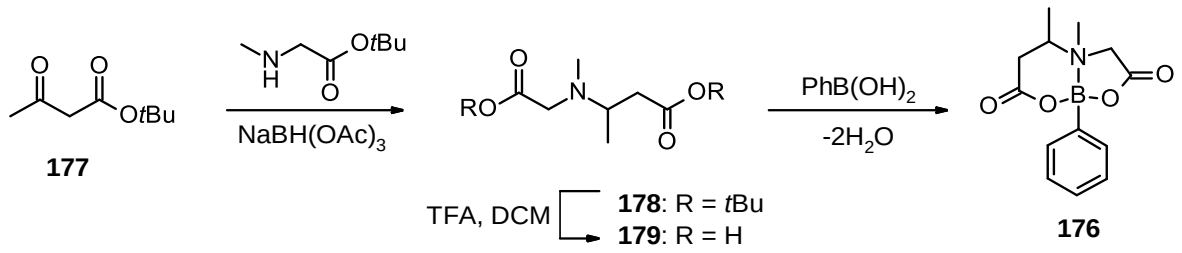

***Scheme 75**. Proposed alternative route to boron-scaffold **176**.*

Even though the synthetic route to **176** is shorter, it does not contain any DG motifs, which will extend the synthetic route when introduced. Since a key objective of this research is to develop a B-DG with a short synthetic route and given the similarity of **176** to the published scaffold **146** from Spivey and co-workers, it was decided to focus on alternative B-DG scaffolds.

2.3.2.3 B(dan) derivatives

Another strategy for a boron-based DG involves the use of a B(dan) moiety with a DG tethered to it, such as **180**. Compound **181** compromised of a diaminobenzene group was also investigated to determine if it can take part in C–H functionalisation reactions (**Figure 22**).

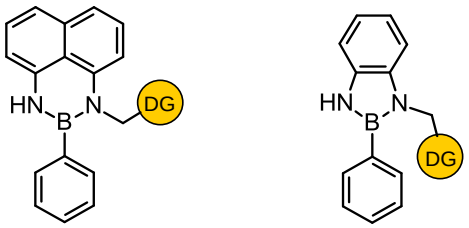

180 **181**

***Figure 7**. B-based scaffolds with DG tethers that can be potentially used in CH functionalisation.*

The forward route in the synthesis of **180** began with the alkylation of 1,8-diaminonapthalene **123** with the benzyl bromide derivative **182** containing a nitrile DG motif (**Scheme 76**).

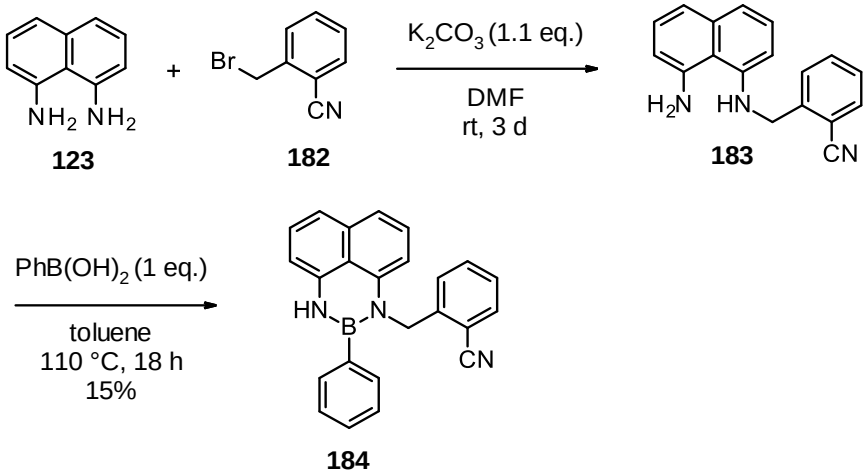

123 **182** **183** **184**

***Scheme 76**. Synthetic route to B-scaffold **184** containing a nitrile DG.*

In an effort to reduce dialkylation, a substantial excess of **123** was employed. However, this approach posed challenges as both **123** and **183** exhibited very similar R_f values on silica TLC, complicating purification via silica gel chromatography. As a result, the desired product couldn't be cleanly separated. Instead, the crude product was directly utilized in the subsequent condensation reaction with phenylboronic acid, yielding **184** in a low yield of 15%.

Since C–H olefination is a transformation that has proven successful in conjunction with a nitrile DG, the next goal was examining this compound against common reaction conditions for this transformation. (**Scheme 77**).

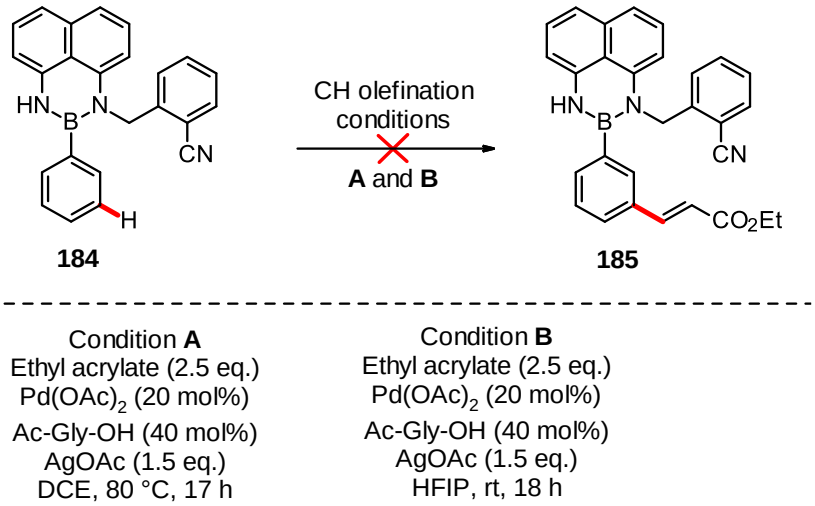

***Scheme 77**. Attempted C–H functionalisation of **184** using typical olefination reaction conditions.*

Both conditions A and B failed to give any indication that C–H activation was occurring, and instead complete decomposition of starting material **184** was observed in both cases. Despite reducing the reaction temperature from 80 °C to room temperature and changing to HFIP as the solvent, a common choice in C–H activation reactions, decomposition persisted. This indicated that a reagent, rather than the temperature, was likely responsible for the degradation.

A similar B(dan) substrate **186** was synthesised in an analogous route to **184** above and subjected to a set of typical C–H arylation reaction conditions (**Scheme 78**). In these reactions C–H functionalisation did not take place, but pleasingly starting material **184** was not decomposing and could tolerate high reaction temperatures. Replacing the base K_2CO_3 with AgOAc, degradation resumed indicating that AgOAc was likely responsible for the decomposition of **184**.

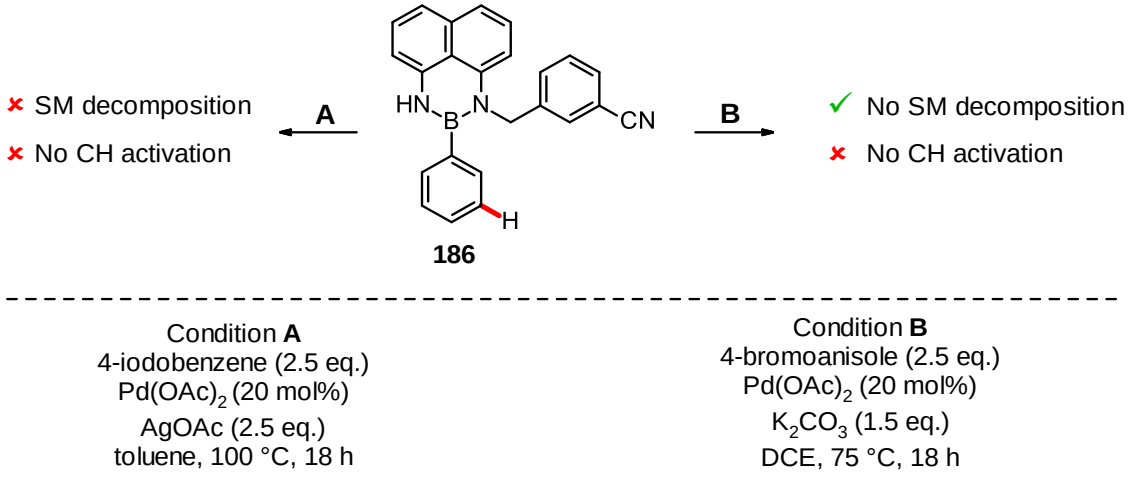

***Scheme 78**. Attempted C–H arylation of B-DG **186** with decomposition observed using AgOAc.*

Studies have indicated that silver can facilitate boron reagent activation and accelerate the trans-metallation step within the catalytic cycle of a Suzuki cross-coupling reaction.[130,131] Therefore it is likely that B → M trans-metalation is not suppressed under these reaction conditions leading to side reactions occurring with the boron atom of the B(dan) motif and the palladium catalyst.

Accounting for the lack of C–H activation being observed, it is possible that the rigidity of the linear nitrile motif disfavours the desired conformation which places the palladium catalyst at the target C–H bond. Thus, the next step would be to install and examine the effect of other commonly used DGs, such as a picolinamide motif.

2.3.2.4 B(dab) derivatives

Beginning this investigation, the 1,8-diaminonapthalene (dan) backbone was replaced with 1,2-diaminobenzene (dab). This action aimed to reduce the overall size of the boryl group and the number of aromatic protons, making the NMR analysis of reaction mixtures more manageable. A general synthetic route to B(dab)-DG **77** was devised with the incorporation of the DG via *N*-alkylation of 2-nitroaniline **187** (**Scheme 79**).

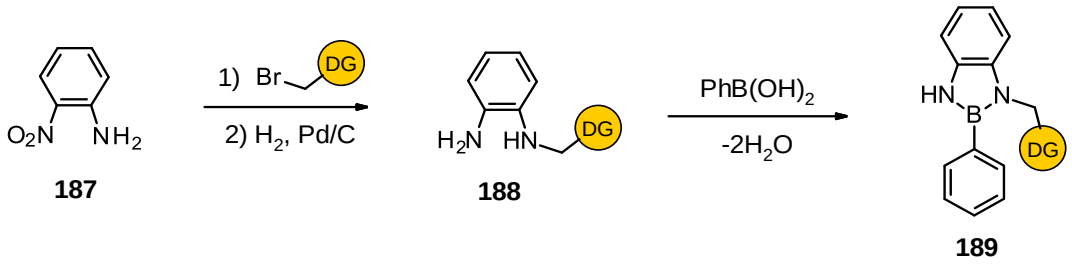

***Scheme 79**. Proposed general synthetic route to B(dab)-DGs **189**.*

Starting from **187** instead of 1,2-diaminobenzene, undesired dialkylation from having two amines in the same molecule could be avoided. Before an aminoquinoline (AQ) or picolinamide (PA) motif could be incorporated into B(dab) backbone, the corresponding alkylating agents **192** and **193** were first synthesised (**Scheme 80**).

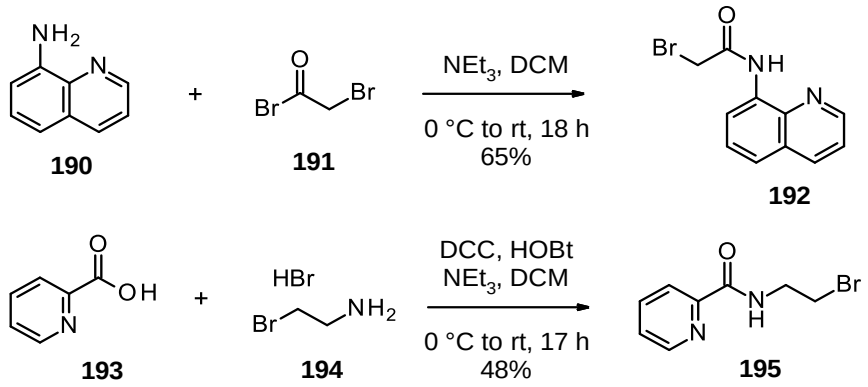

***Scheme 80**. Synthesis of alkylating reagents AQ **192** and PA **195**.*

However, upon attempting to react 2-nitroaniline **187** with **195** no alkylation was observed (**Scheme 81**). Upon further analysis after purification of the crude material, there was complete consumption of **195** and instead of alkylation leading to **197**, intramolecular cyclisation was occurring to furnish **196**. Decreasing the reaction temperature and employing the electron-rich 4,5-dimethyl-2-nitroaniline **198** to enhance amine nucleophilicity led to an identical outcome, with isolation of side-product **196**.

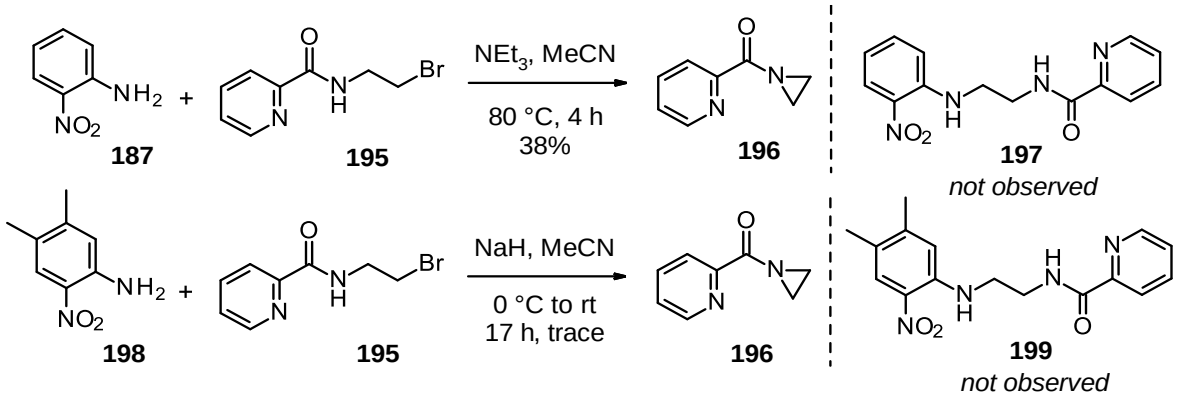

***Scheme 81**. Unexpected cyclisation of alkylating agent **195**.*

Similarly, trying to incorporate the AQ DG via alkylating agent **192**, also failed to furnish the desired product **201** (**Scheme 82**). Using K_2CO_3 at 65 °C in THF resulted in unreacted starting material **187** and **192**. The inclusion of NaI as an additive, a shift in solvent to DMF and increasing the temperature to 90 °C led to the complete consumption of the alkylating agent, converting it into the side-product **200** instead of participating in the *N*-alkylation of **187**.

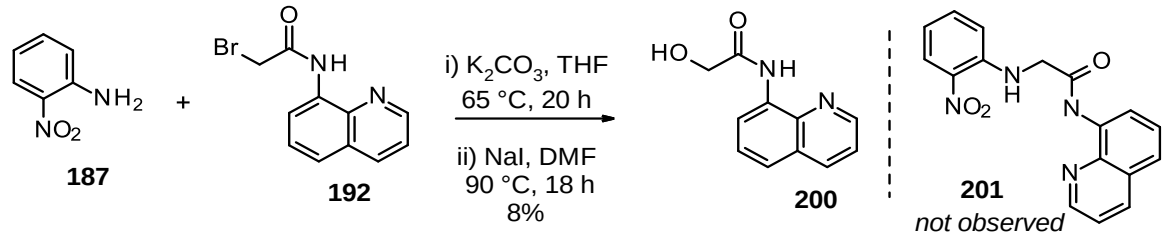

***Scheme 82**. Unexpected transformation of alkylating agent **192**.*

It was now apparent that another method to insert an AQ or PA DG to furnish B(dab)-DG **77** was needed. Instead of an S_N2 *N*-alkylation, a S_NAr strategy was formulated. The AQ based DG was introduced by reacting 1-fluoro-2-nitrobenzene **202** with the corresponding nucleophilic amine **203** (**Scheme 83**).

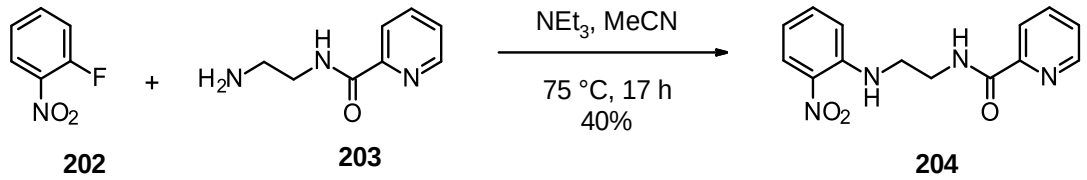

***Scheme 83**. S_NAr approach used to form N-alkylated compound **204**.*

Pleasingly, the desired product **204** was delivered in a moderate yield, where the yield could be higher still as the reaction partner **203** was not completely pure. Utilising the more reactive 1-fluoro-2-nitrobenzene **202** instead of 1-chloro-2-nitrobenzene allowed for a lower reaction temperature to be used. Furthermore, substituting the lower-boiling solvent MeCN for DMF simplified the subsequent work-up procedure.

The following hydrogenation of the nitro group furnished the corresponding amine **205** in quantitative yield (**Scheme 84**). With **205** in hand, boronic acids could successfully be incorporated via a condensation reaction to furnish B-DG scaffolds **206** and **207** in moderate yields.

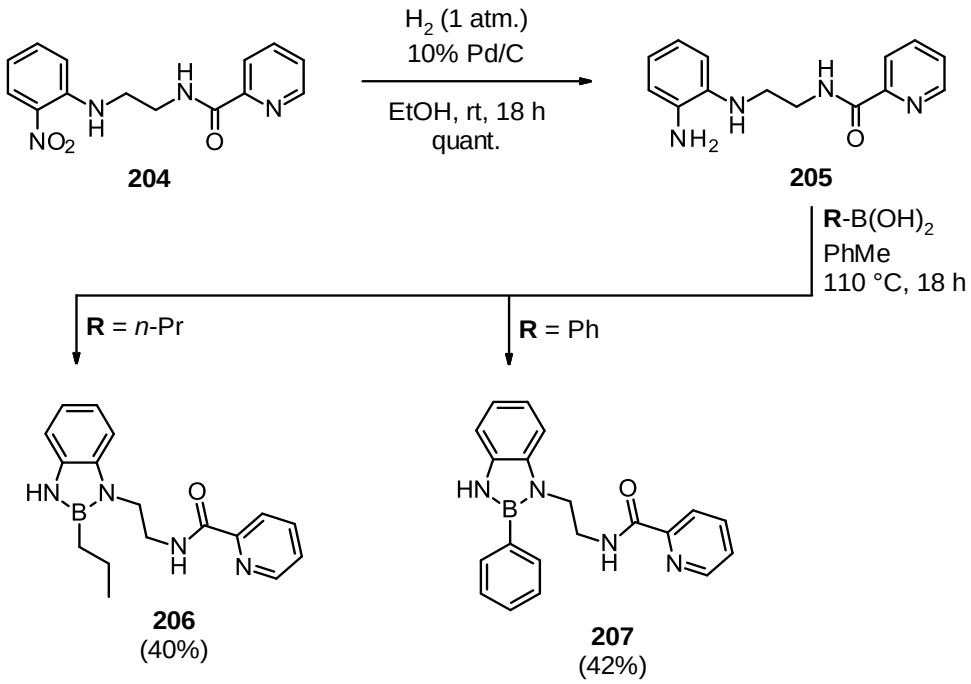

***Scheme 84**. Hydrogenation of **205** and subsequent condensation with corresponding boronic acids leading to B-DG scaffolds **206** and **207**.*

With considerable attention previously given to C(sp^2)–H functionalisation, it was important to also examine functionalising C(sp^3)–H bonds. The aliphatic substrate in scaffold **206** is inherently more flexible compared to the aromatic derivative **207** due to the presence of C(sp^3)–H bonds.

Therefore, the aliphatic substrate might assume a more favourable orientation in order for the DG to place the transition metal at a desired C–H bond. However, unlike scaffold **207**, there is a possibility of acquiring beta-hydride elimination side products with **206**.

Investigating C(sp^3)–H functionalisation further, scaffold **206** was subjected to C–H arylation conditions that were developed by co-workers in our laboratory (**Scheme 84**). These conditions were chosen due to their success in functionalising C(sp^3)–H bonds with the same DG, a picolinamide motif. In addition, this method avoided the use of silver salts which were increasingly found to be incompatible to the boron-based scaffolds examined in this work.

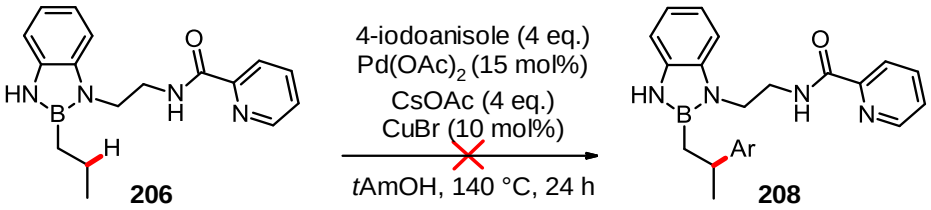

***Scheme 84**. Unsuccessful attempt at C–H arylation of scaffold **206** using silver-free methods.*

However, with both scaffolds a complex crude mixture was obtained rendering NMR analysis difficult. Attempts at purification of the crude mixtures were unsuccessful, with aryl iodide starting material recovered but interestingly none of the corresponding starting material was recovered, indicating degradation pathways were at play. In the interest of time, focus was switched to another promising scaffold which showed improved reaction stability.

2.3.2.5 Boronate ester derivatives

Boronate esters are valuable motifs in synthetic chemistry due to their masked reactivity and stability under a range of reaction conditions. It was envisaged that this dual functionality could be exploited by incorporating a DG into the boronate moiety to enable C–H functionalisation and then be modified to furnish a doubly functionalised product.

The boron scaffolds investigated in this chapter so far exhibit poor stability to typical C–H functionalisation conditions, such as HFIP, AgOAc and elevated temperatures. However, it was expected this would not be the case for a boronate-ester scaffold considering reports of arylBPin substrate **209** tolerating C–H olefination conditions without degradation (**Scheme 85**).[132]

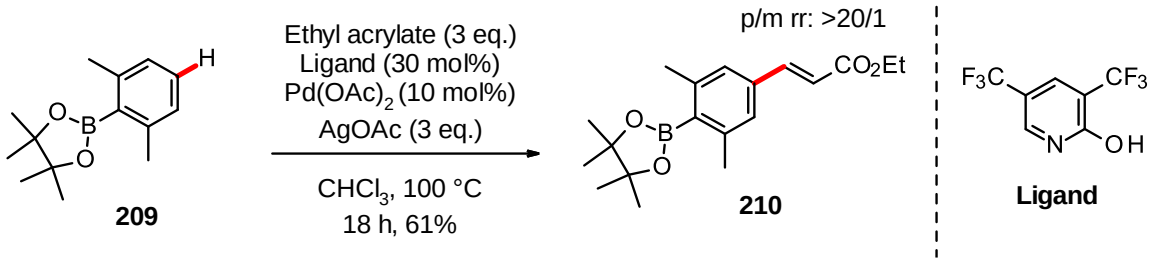

***Scheme 85**. Stability of Bpin group to C–H olefination conditions reported by Wang.*

Since a boronate ester could have a different ring size and with various DG attachment points possible, careful positioning of the DG could lead to a highly regioselective C–H functionalisation method (**Figure 23**).

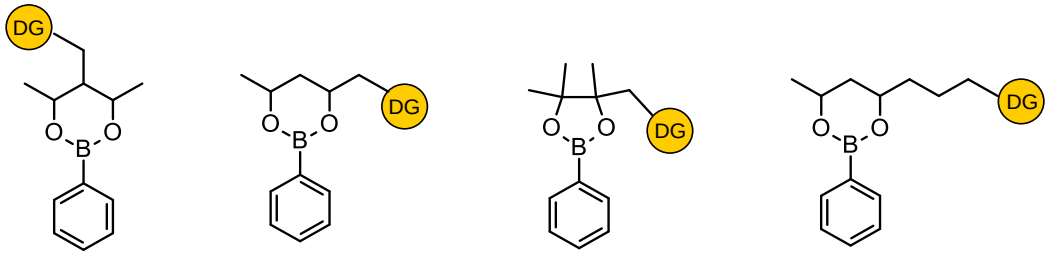

***Figure 23**. Possible DG attachment points for various boronate ester scaffolds.*

To confirm the stability of the six-membered boronate ester **213** against typical C–H olefination conditions, it was first prepared by the condensation of diol **212** with phenylboronic acid (**Scheme 32**).

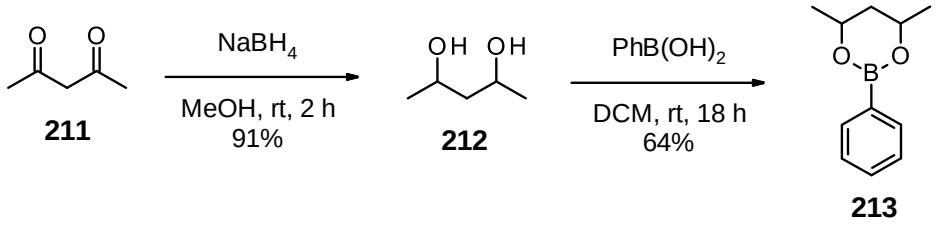

***Scheme 86**. Synthetic route to a boronate ester scaffold **213** containing no DG motifs.*

This scaffold was then subjected to typical C–H olefination conditions which revealed the sensitivity towards different solvents (**Scheme 87**). While $CHCl_3$ was tolerated well with little degradation observed, the use of HFIP as the solvent resulted in the formation of the oxidative Heck product with no starting material recoverable.

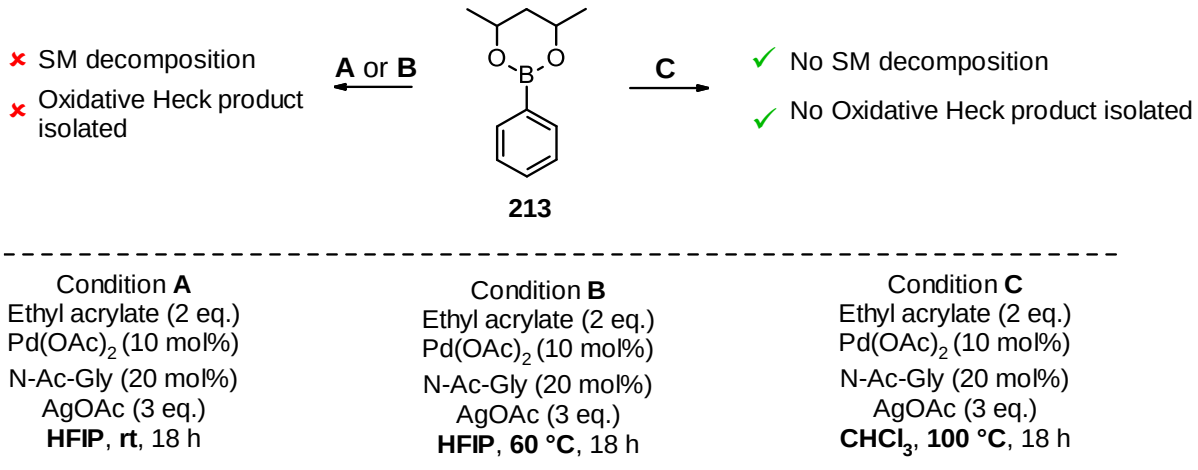

***Scheme 87**. Effect of solvent on the stability of **213** towards typical C–H olefination conditions.*

While **213** was reactive towards an oxidative Heck pathway, it was apparent that a change of solvent was crucial in restoring stability of the scaffold to C–H olefination conditions. Thus,

with careful selection of solvent and with a suitable DG group incorporated into **213**, this will likely lead to improved stability and regioselective C–H functionalisation. Moreover, judicious choice of base for the alkylation of **211** can lead to two distinct boron-based scaffolds (Scheme **88**).

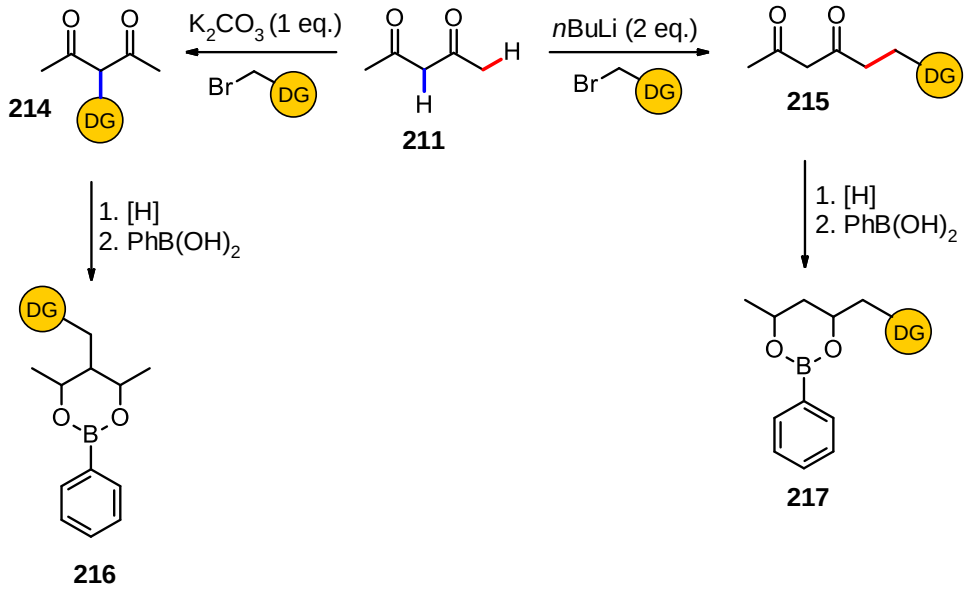

***Scheme 88**. Proposed synthetic route to two boronate ester based scaffolds.*

Implementing this approach, scaffold **216** was synthesised through a three-step route involving C-alkylation of acetylacetone to place the DG motif at the terminal position (**Scheme 89**).

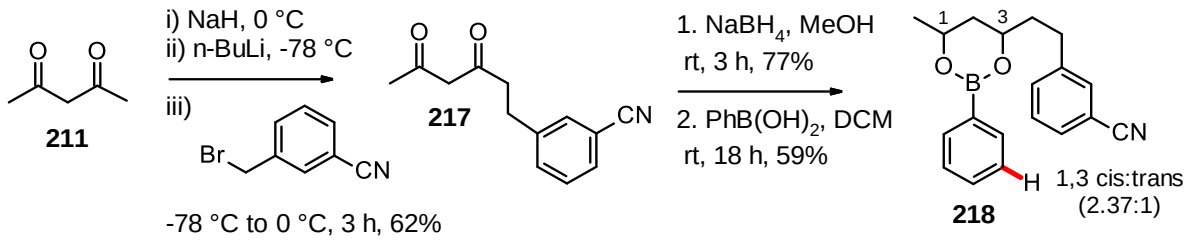

***Scheme 89**. Synthetic route to B-DG scaffold **218**.*

Not unexpectedly, subjecting **218** to C–H olefination condition B from **Scheme 87** above, the mono-olefin Heck product was the major product. However, like scaffold **213**, moderate stability to C–H olefination condition C was retained with **218** but with no desired C–H functionalisation observed. Various other solvents were also investigated including fluorobenzene and DCE, each resulting in the same outcome of unreacted starting material along with trace amounts of the oxidative Heck product **219** (**Scheme 90**).

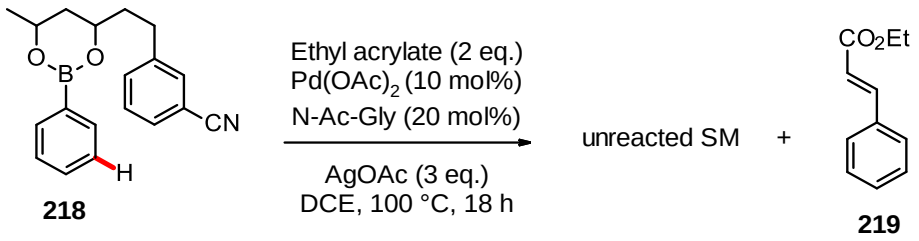

***Scheme 90**. Subjecting scaffold **218** to C–H olefination conditions led to oxidative Heck product.*

Confirming the incompatibility of HFIP as a solvent for C–H functionalisation, condition A from **Scheme 87** above showed almost complete conversion to the oxidative Heck product. A binary mixture of solvents (DCE with 5 eq. of HFIP) led to improved stability of scaffold **218**, but unfortunately desired C–H olefination was not detected.

Due to the instability of scaffolds **213** and **218** towards HFIP, the lack of reactivity towards C–H olefination and the report by Spivey for the C–H olefination of a B(MIDA)-based DG described above, we decided to focus on more novel C–H functionalisation methods.

Maiti and co-workers could facilitate C(sp^2)–H allylation using internal alkenes without resorting to HFIP and determined MeCN as the optimal solvent for this transformation (**Scheme 91**).[133] This solvent is also compatible with our boronate ester derived scaffolds, and so this reaction was next investigated.

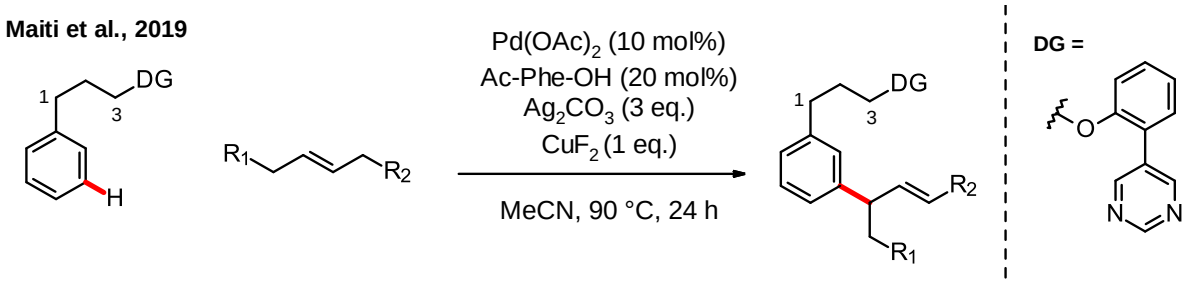

***Scheme 91**. meta-C–H allylation of arenes using a pyrimidine-based DG reported by Maiti et al.*

While the allylation conditions reported by Maiti were optimised for a pyrimidine-based DG and a copper fluoride additive, it would nevertheless be useful to ascertain the stability of scaffold **218** to these conditions (**Scheme 92**).

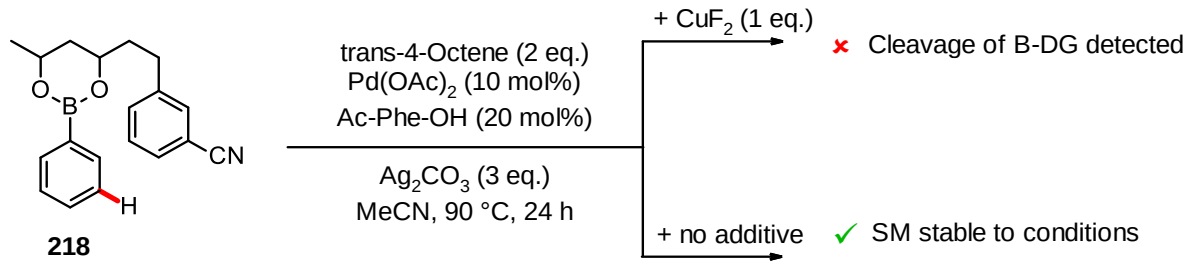

***Scheme 92**. Investigating stability of scaffold **218** against C–H allylation conditions.*

Interestingly, analysis via TLC and ^{1}H NMR showed with the addition of copper fluoride, scaffold **218** was significantly less stable to the C–H allylation conditions. However, with the absence of this additive, the scaffold was found to be significantly more stable. To further investigate this scaffold's suitability to TM-catalysed reactions, a C–H alkynylation reaction developed by the Maiti group was examined (**Scheme 94, top**).[134]

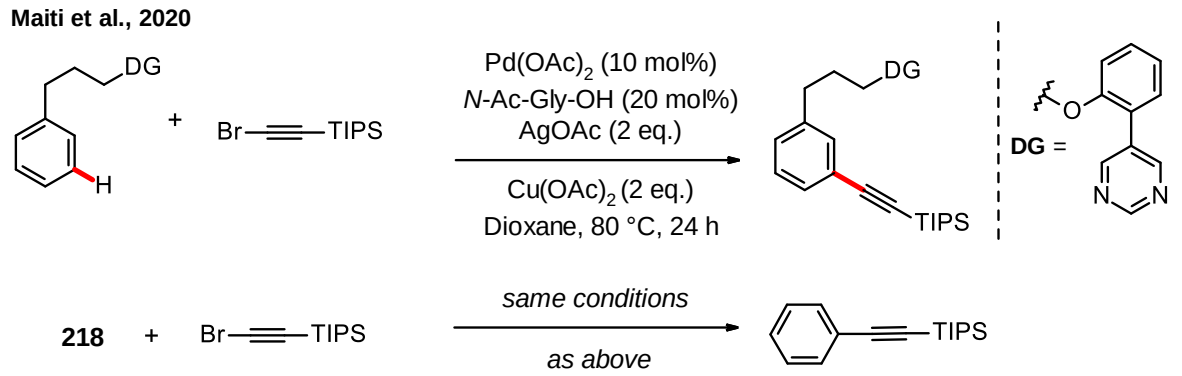

***Scheme 94**. Literature alkynylation (top) and functionalisation attempt with B-DG scaffold **218** (bottom).*

Surprisingly, use of scaffold **218** resulted entirely in a Suzuki pathway to give *ipso*-C-B functionalisation with complete consumption of the starting material (**Scheme 94, bottom**). This highlights the intricate balance between boron-scaffold stability and reactivity, where more forceful conditions required for common C–H functionalisation reactions leads to unwanted side-reactions taking place at the boron centre.

2.3.2.6 B(aam) derivatives

Mindful of the stability concerns of previously examined scaffolds, we moved towards investigating anthranilamide (aam) derivatives tethered to well-established DGs (**Figure 24**). While less stable than B(dan) and B(MIDA) scaffolds, B(aam) exhibit high stability compared to the previously examined B(pza) DG and so could be a viable boron-based scaffold.

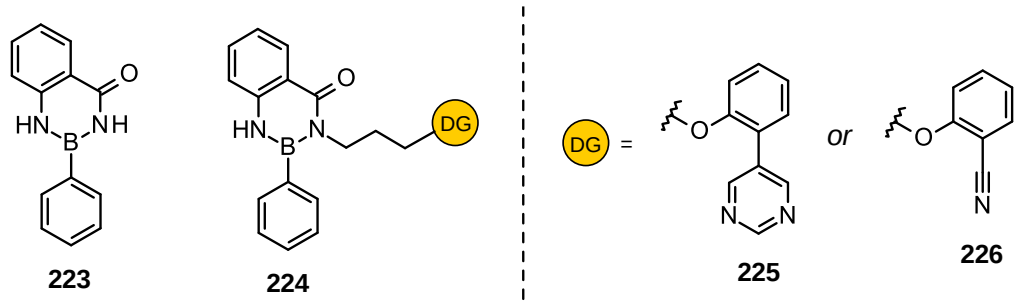

***Figure 24**. PhB(aam) scaffold **223** and derivatives **224** incorporating DG groups.*

Synthesis of scaffold **225** began with attaching a methylene tether to the pyrimidine DG (**Scheme 95**). Subsequent ring-opening of isatoic anhydride by the free amine tethered DG followed by condensation with phenylboronic acid afforded **225**, albeit in a low yield of 10%.

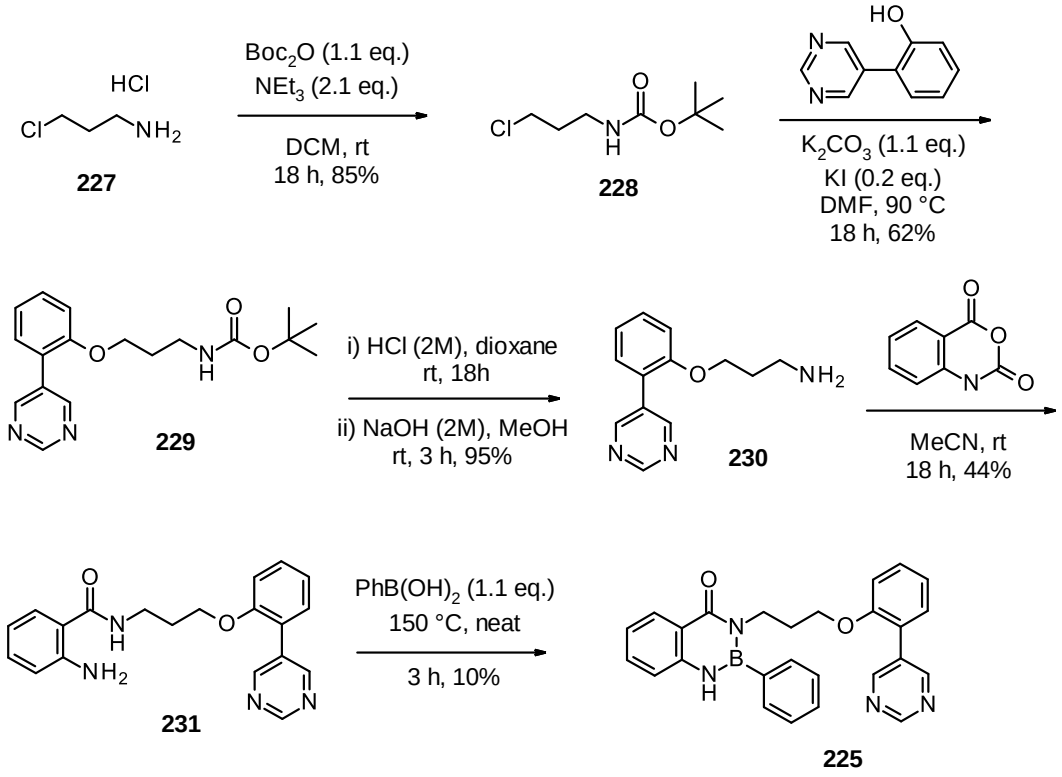

***Scheme 95**. Route to PhB(aam) scaffold **225** tethered to a pyrimidine DG.*

Forceful conditions were required in the final condensation step and the low yield obtained was likely due to the sterics associated with the long DG tether. Deleterious electronic effects of an alkylated amide undergoing condensation compared to a primary amine cannot be discounted either. This effect is highlighted by Suginome and co-workers in their synthesis of methylated B(aam) analogues **233** and **234** (**Figure 25**).[114]

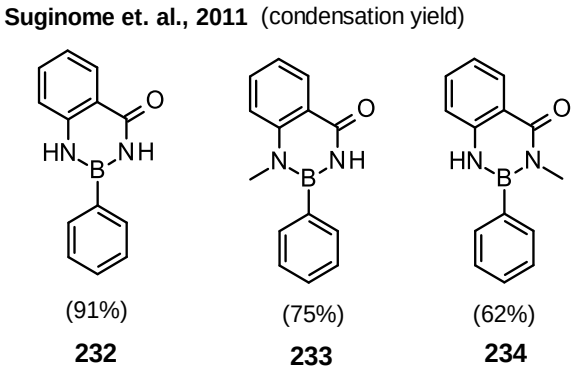

***Figure 25**. Decrease in condensation yields for methylated analogues of B(aam).*

With the B-DG scaffold **225** in hand, attempts were made to carry out C–H allylation and C–H alkynylation using conditions previously examined (**Scheme 96**). In both cases, C–H functionalisation was not detected and instead degradation of the starting material was observed.

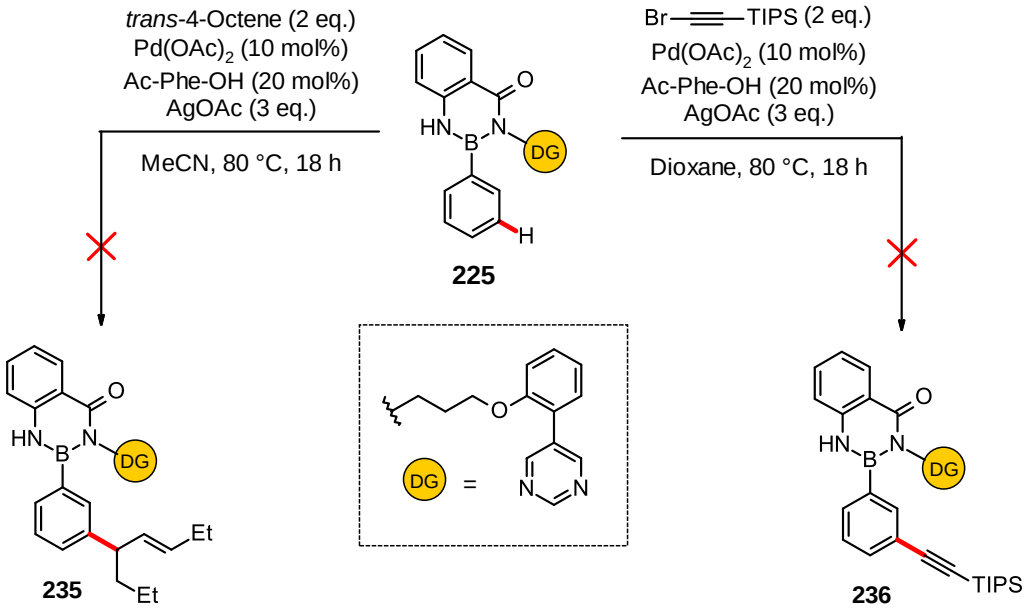

***Scheme 96**. Unsuccessful attempts at C–H allylation and alkynylation of scaffold **225**.*

The use of a similar scaffold **237** in which the nitrogen atom attached to the boron group was replaced with an oxygen atom was next examined (**Figure 26**). It was envisaged this modification would reduce any unwanted coordination of metal catalyst to the secondary amine due to the increased electronegativity of an oxygen atom compared to a nitrogen atom. This may explain the lack of C–H functionalisation observed with scaffold **225**.

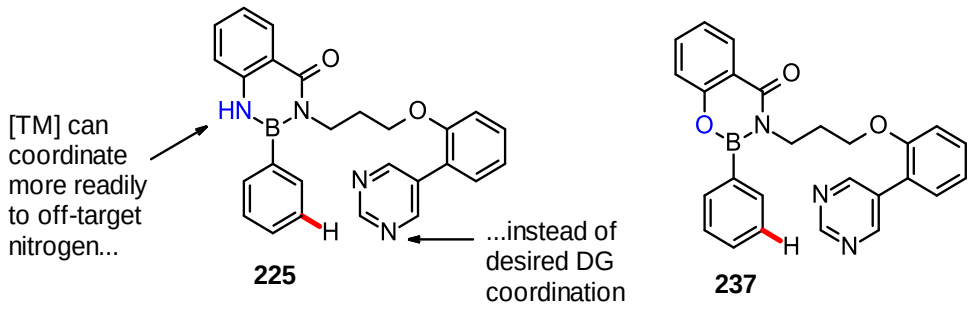

***Figure 26**. Design of analogue of scaffold **237** with modification of boron-heteroatom connectivity.*

However, the final step in the synthesis leading to modified analogue **237** was unsuccessful, even with a high reaction temperature (**Scheme 97**). The failure of the condensation step likely occurred due to the oxygen atom's lower reactivity due to its increased electronegativity, which was the characteristic we initially sought.

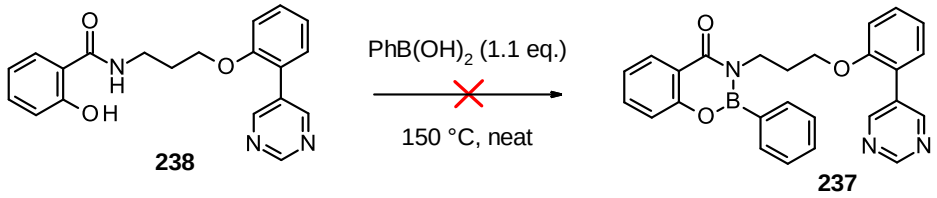

***Scheme 97**. Unsuccessful attempt of synthesis of scaffold **237** by a condensation reaction.*

With the precedence of performing C(sp^2)–H olefination and C(sp^2)–H arylation using a nitrile-based DG, it was decided to examine the boron-based scaffold **238**. Subjecting this scaffold to two C–H functionalisation conditions, hydrolysis of the B-DG group was observed as the major component of the reaction mixture instead of the desired products **240** or **241** (**Scheme 98**).

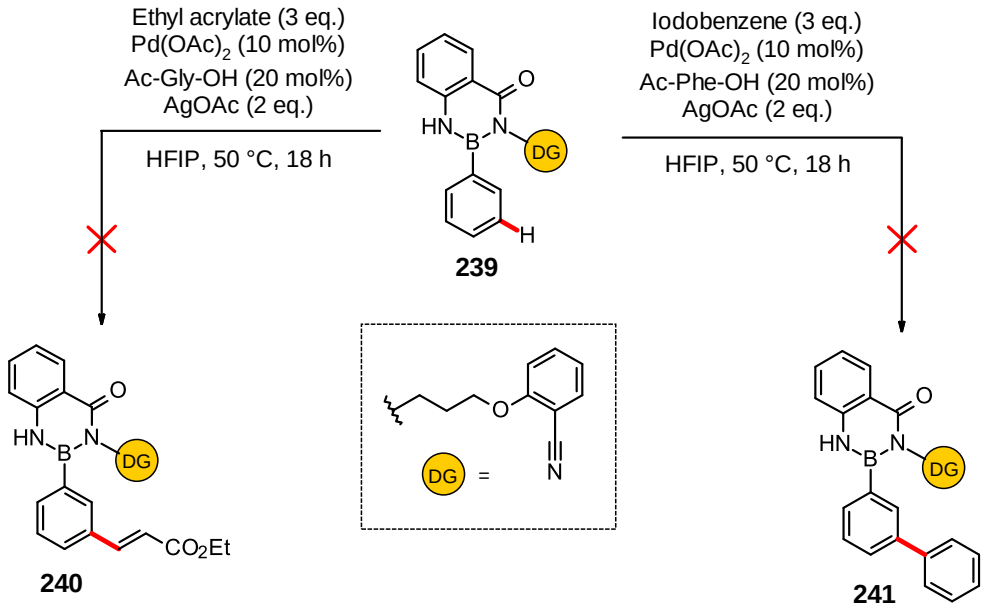

***Scheme 98**. Unsuccessful attempts at C–H olefination and arylation of scaffold **239**.*

While TLC and NMR analysis methods were commonly employed for analysing crude reaction mixtures in this chapter, their use was limited due to complex proton signals and instability to silica gel TLC for many boron-DG scaffolds. In addition, the use of HPLC/LCMS techniques was avoided as boron scaffolds such as **225** or **239** were not stable to typical HPLC conditions.

Instead, to quantify and monitor reaction progress, the less common technique of supercritical fluid chromatography (SFC) was chosen. This is a HPLC technique in which supercritical fluid is used to replace the liquid mobile phase. Crucially, the supercritical fluid chosen was carbon dioxide which the boron scaffold **239** is stable to.

Pleasingly, for the C–H olefination of **239**, the expected product mass (blue trace) was observed at 1 hour (**Figure 27**). However, over time breakdown of the starting material **239** (red trace) to its precursor **243** (green trace) and the mono-C–H functionalised product was observed. Analysing the reaction mixture further, the side product was proposed to be compound **242**, with its mass in agreement with the detected mass.

The presence of side product **242** suggests that instead of C–H olefination occurring on the desired benzene ring, functionalisation was taking pace on the anthranilamide ring followed by arene cleavage.

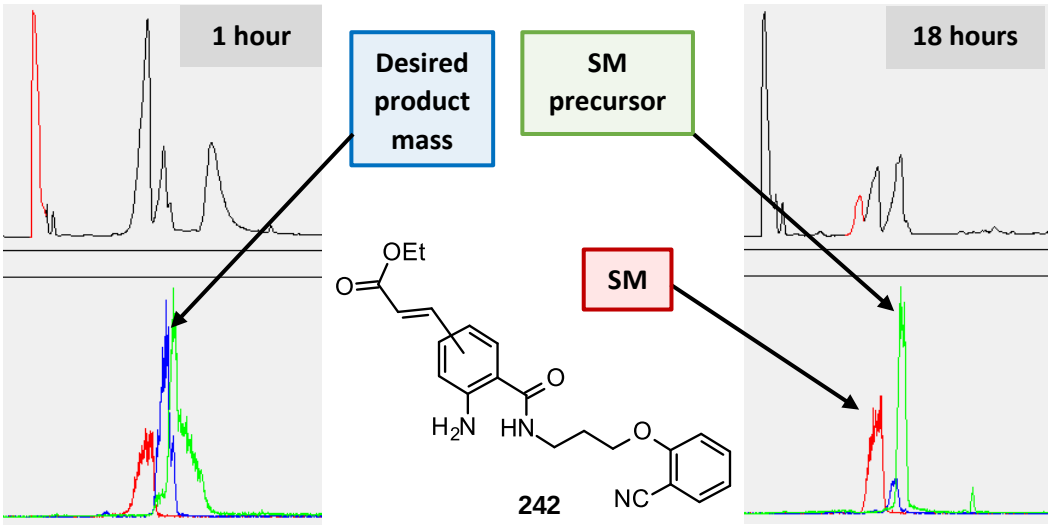

***Figure 27**. UV trace and ion selective chromatograph of C–H olefination attempt with **239** at 1 h and 18 h. Side-product **242** which corresponded to a detected mass is shown in the centre.*

Subjecting C–H arylation conditions to the same scaffold, SFC analysis painted a similar picture (**Figure 28**). While the desired product mass was detected (blue trace), the generated product was degrading as the reaction progressed. In addition, starting material **239** (red trace) was also breaking down to its precursor **243** (green trace).

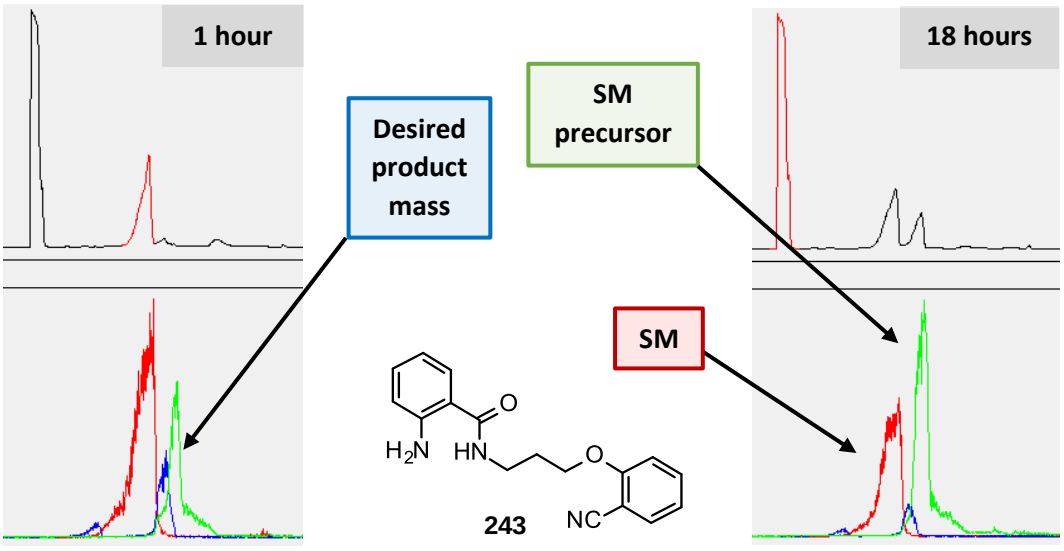

***Figure 28**. UV trace and ion selective chromatograph of C–H arylation attempt with **239** at 1 h and 18 h. The detected cleaved SM adduct **243** is shown in the centre.*

In both C–H functionalisation attempts, while C–H functionalisation could be detected, the desired product's subsequent degradation, in addition to SM cleavage, renders scaffold **239**

incompatible in this work. Thus, a different approach to the design of B-DG scaffolds is necessary.

2.3.3 Non-covalent interactions for B-directed functionalisation

With the established instability of covalently attached DGs to a boron-based scaffold, then a non-covalent approach using hydrogen bonding interactions for example, may provide the desired reactivity while maintaining scaffold stability.

Non-covalent directed functionalisation has been reported for many reactions, including by Phipps and co-workers with their work on ion-pair controlled and hydrogen-bonding assisted meta-selective borylation (**Scheme 99**).[135,136]

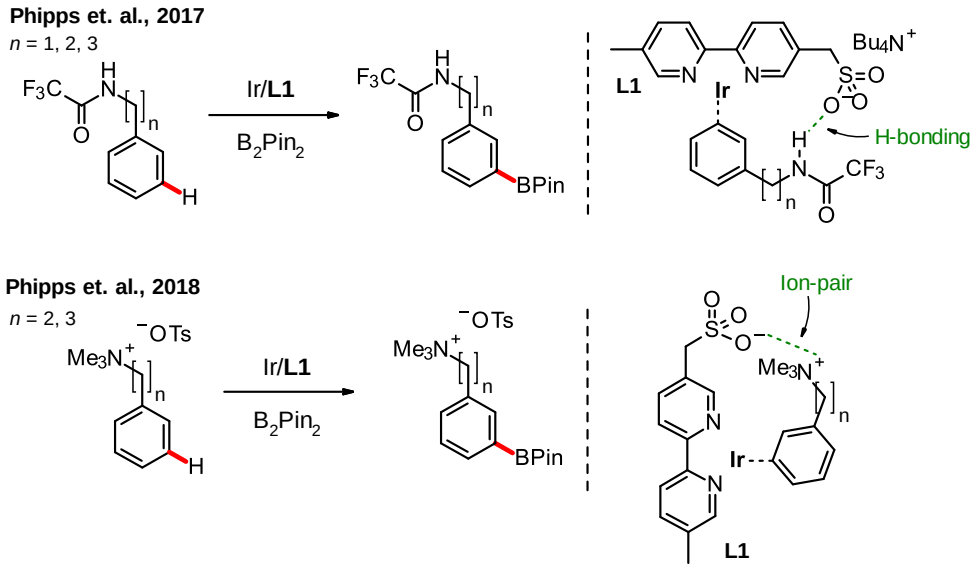

***Scheme 99**. top: Hydrogen bonding assisted meta-C–H borylation, bottom: Ion-pair assisted meta-C–H borylation.*

It was postulated that the B(dan) motif would be a suitable substrate for hydrogen bonding due to the presence of a N–H bond acting as a hydrogen bond donor. To investigate further, the ligand **L1** was first synthesised via a two-step process involving a radical bromination (**Scheme 100**).

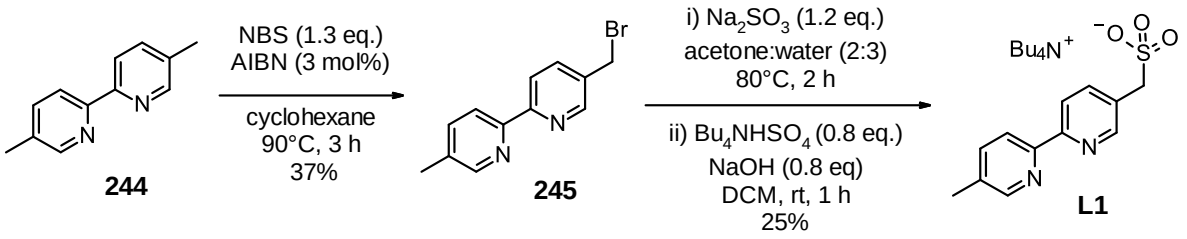

***Scheme 100**. Synthetic route to ligand **L1** involved in H-bonding directed C–H*

Subjecting the previously examined PhB(dan) scaffold **126** to the conditions reported by Phipps and co-workers, an unexpected adduct was observed (**Scheme 101**). Instead of the desired C–H functionalisation leading to **246**, a short-lived complex was formed which was identified as the N-BPin species **247** which reverted to **126** on standing.

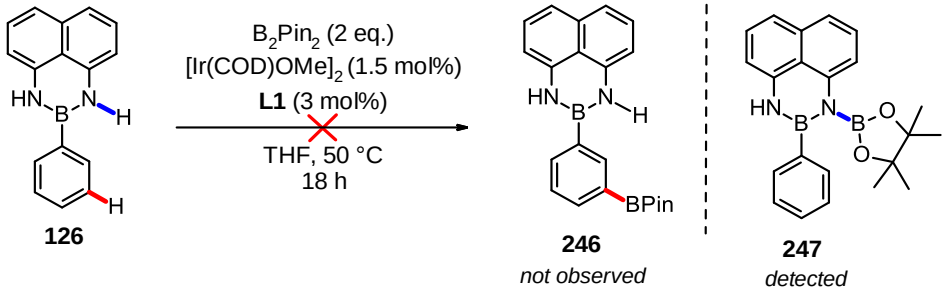

***Scheme 101**. Attempt at H-bonding assisted C–H borylation with PhB(dan) scaffold **126**.*

While it is likely this result is due to the NH being more reactive than a C–H bond, it is possible also that the high rigidity of the B(dan) motif results in a suboptimal positioning of the DG ligand upon H-bonding interaction. This contrasts with the flexible methylene linker present in substrates reported by Phipps and co-workers mentioned earlier (**Scheme 99**). To examine this further, scaffolds such as those with different three-dimensional structures were considered.

Scaffold **249** was synthesised from a high-yielding condensation reaction of **248** and phenylboronic acid (**Scheme 102**). It was postulated that the boronamide motif could provide the desired hydrogen bond donor role required to participate in H-bonding with ligand **L1**.

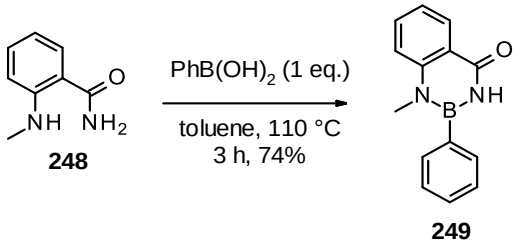

***Scheme 102**. Synthesis of N-methylated PhB(aam) scaffold **249**.*

With scaffold **249** in hand, it was subjected to conditions reported by Phipps and co-workers as well as a control experiment where the ligand 4,4′-di-*tert*-butyl-2,2′-dipyridyl (dtbpy) was used instead of **L1** (**Scheme 103**). Due to the instability of the scaffold to silica, NMR and SFC HPLC techniques were used to analyse reaction mixture. Examining the control experiment, analysis showed unreacted starting material which was expected since no H-bonding interactions should be possible between the dtbpy ligand and the scaffold.

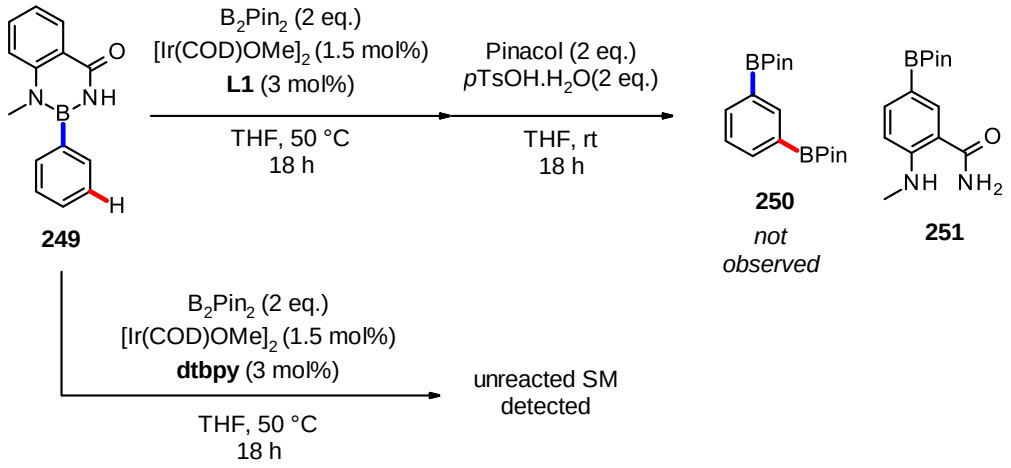

***Scheme 103**. H-bonding assisted C–H borylation attempt with scaffold **249**.*

However, in a subsequent experiment where **L1** was used as the ligand, NMR analysis showed the presence of new aromatic proton signals in addition to unreacted starting material. Due the instability of scaffold **249** to silica, standard flash column chromatography was unsuitable and instead the anthranilamide protecting group was exchanged for pinacol to generate silica-stable compounds that could be purified and identified more easily.

Interestingly, instead of the desired di-borylated product **250**, only the adduct **251** was found. It is possible that ligand **L1** and scaffold **249** did successfully undergo H-bonding interactions but with incorrect ligand orientation leading to positioning the iridium metal in proximity of the undesired anthranilamide ring.

To compare the effectiveness of the two hydrogen bond donor motifs, the amine-borane and amide groups, scaffold **253** was next synthesised via a one-step condensation reaction from **252** (**Scheme 104**).

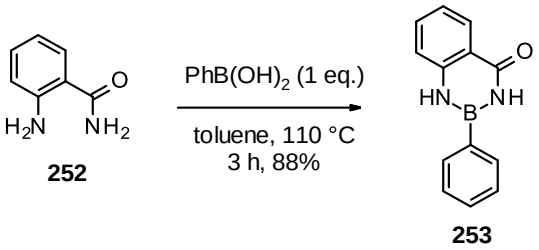

***Scheme 104**. Synthesis of PhB(aam) scaffold **253**.*

With scaffold **253** in hand, it was then subjected to two conditions, varying the ligand used (**Scheme 105**). In the presence of ligand **L1** which can participate in H-bonding, a complex reaction mixture was observed by NMR analysis. However, no noticeable amount of directed C–H borylation was detected and instead borylated starting material **254** was isolated in trace amounts.

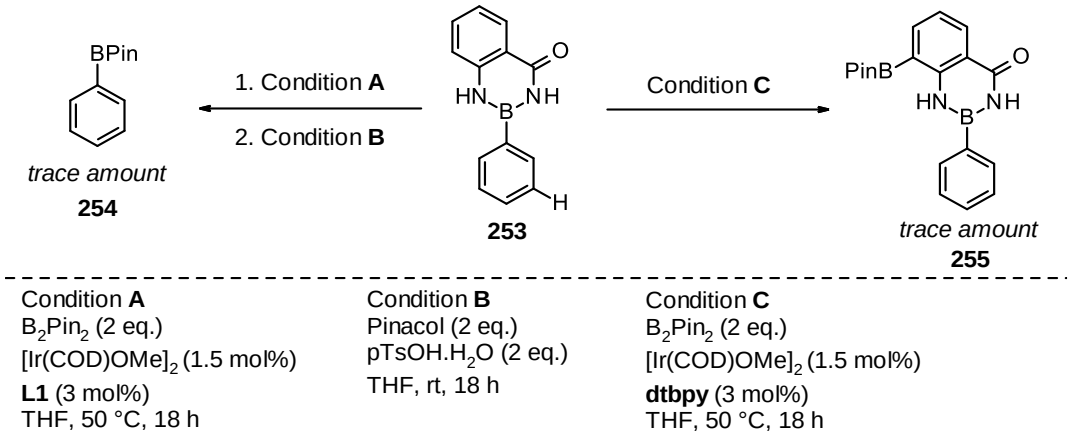

***Scheme 105**. H-bonding assisted C–H borylation attempt with scaffold **253**.*

This was surprising as the corresponding borylated adduct to **251** was not found even with the presence of the amide H-bonding motif in **253**. It is thus possible that the amide group was disfavoured in participating in H-bonding interactions compared to the amine-borane motif.

However, if H-bonding was occurring between the amine-borane motif in **253** and **L1**, there was no indication of successful positioning of the iridium catalyst at a C(sp^2)–H bond in the molecule since only **254** was isolated. This is indicative of a geometry mismatch between the amine-borane motif and the bipyridine DG of **L1** during any H-bonding interactions that may have occurred.

Interestingly, replacing the ligand used from **L1** to dtbpy, C–H borylation was observed albeit at the undesired anthranilamide ring. As scaffold **253** was stable to silica, no post-functionalisation was necessary and so **255** could be isolated directly.

In the absence of H-bonding interactions, it is probable that the iridium catalyst preferentially coordinates with the primary amine-borane motif over the amide group. This would bring the catalyst in closer proximity to the C–H bond of the undesired benzamide ring. Thus, it is not unexpected that the undesired anthranilamide ring was functionalised leading to the formation of **255**.

With the lack of desired reactivity observed with the tricoordinate boron-based scaffolds above, it was decided to move focus and examine tetracoordinate boronates. The B(mida) derivative **256** containing a secondary amine instead of a *N*-methylated motif was then investigated. The free N–H bond in **256** was hypothesised to undergo H-bonding interactions with the sulfonate group of the bipyridine ligand as depicted in intermediate **257** (**Scheme 106**).

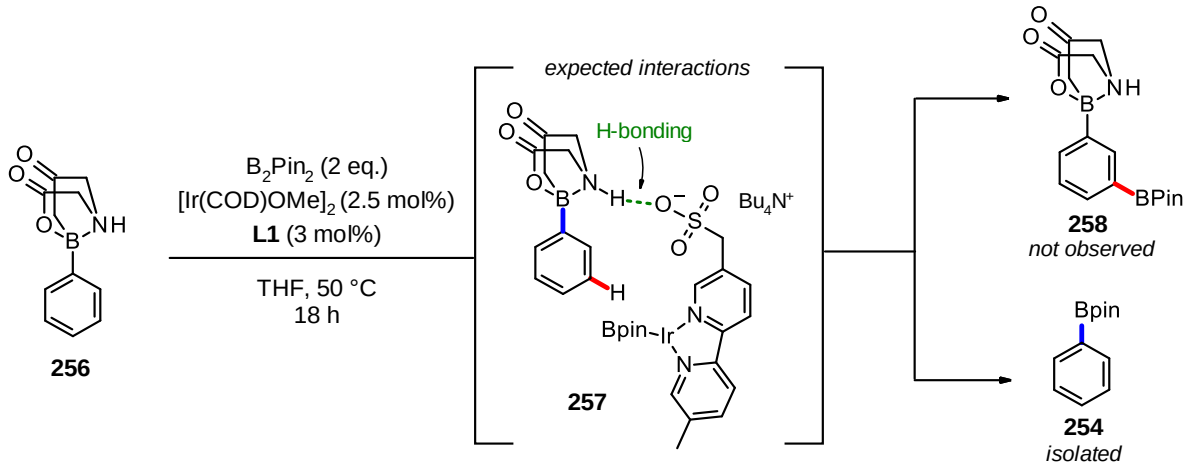

***Scheme 106**. Attempt at H-bonding assisted C–H borylation with PhB(mida) scaffold **256**.*

However, instead of pathways leading to desired C–H functionalisation like **258** or N-BPin complex formation such as **247** as seen previously with B(dan) scaffold **126**, *ipso*-C–H borylation was instead likely occurring. This was unexpected as it was theorised that the B(mida) motif would be stable to these reaction conditions due to the tetracoordinate connectivity of boron.

With the various boron scaffolds investigated containing at least one suitable hydrogen bond donor group, C–H functionalisation on the desired aromatic system could not be achieved. While the scaffolds investigated for non-covalent interactions were generally quite stable to H-bonding directed conditions, C–H functionalisation took place on the DG motif rather than the substrate. This is ripe for further investigation into the use of boron-scaffolds containing tethered DGs for regioselective remote H-bonding directed borylation.

2.3.4 Conclusions and future work

In this chapter, we investigated the use of boron-based scaffolds in carrying out regioselective C–H functionalisation reactions. This work involved examining existing boron protecting groups, such as B(dan) and B(mida) motifs as well as novel boron-based DGs.

Our extensive functionalisation attempts suggest that there is a sensitive balance between stability and desired reactivity of these scaffolds. In many cases, the scaffolds were found to be unstable to common C–H functionalisation conditions, in particular HFIP and/or silver salts. Investigating alternative conditions which were more amenable to these scaffolds led to the opposite effect, where the scaffold was unreactive towards C–H functionalisation.

Regardless of the sensitive reactivity and stability of the scaffolds, pleasingly SFC HPLC analysis confirmed C–H olefination and C–H arylation was successfully taking place with some scaffolds. However, SFC analysis also confirmed the rapid degradation of products and starting material which limited the practicality of the examined boron-based scaffolds.

The emergence of a report by Spivey and co-workers into the use of a B(MIDA) tethered DG to perform various C(sp^2)–H functionalisations, led us to focus our efforts away from covalently attached tethered DGs.

Investigating the non-covalent directed C–H borylation using hydrogen-bonding interactions, these scaffolds had greatly improved stability although the observed reactivity was not as desired. Specifically, C–H functionalisation took place on the unwanted aromatic ring of the boron scaffold rather than the aryl substrate. Further work would be required to develop a bespoke boron scaffold and/or ligands which will likely require a protracted synthesis route.

One avenue that is unexplored in this work is the use of a radical directed approach to perform regioselective C–H functionalisation with boron-based scaffolds. This would likely involve a radical translocation pathway similar to that seen with Hofmann and Löffler/Freytag.[137–139]

However, at this point, despite tireless efforts to develop a method for B-directed C–H functionalisation, it was decided to focus our attention elsewhere. Specifically, on other novel reactions involving the use of boron in order to broaden the scope of the thesis and to make a more effective use of the remaining research time.

3 Novel uses of halomethyl boronates

3.1 Introduction to frustrated Lewis pairs (FLPs)

In 1923, Lewis categorised molecules that accept electron pairs as acids and those that donate electrons pairs as bases.[140] According to this principle, when a Lewis basic phosphine and a Lewis acidic borane combine, they are expected to form a 'classical' P–B Lewis adduct. While this principle has come to be a key axiom of chemistry,[140–142] certain limitations such as geometric restrictions or the presence of bulky substituents can hinder the formation of this bonding interaction.

One of the first encounters of a system that deviated from Lewis' axiom was in 1942 by Brown and co-workers when examining the interaction of pyridines with simple boranes. They attributed steric hindrance to the observation that while lutidine formed a stable Lewis adduct with BF_3, it did not react with BMe_3 (**Scheme 107**).[143,144] Brown and co-workers did not investigate this further.

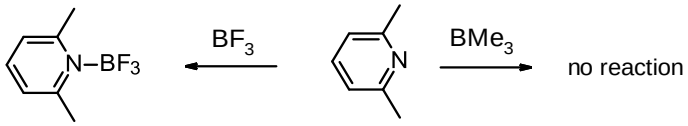

***Scheme 107**. Attempts at reacting lutidine with BMe_3 and BF_3.*

More recently, the Stephan group investigated systems that incorporated both Lewis acid and Lewis base groups with the key distinction of being sterically prevented from undergoing classical adduct formation.[145] This led to the synthesis of zwitterion **259** which upon heating to 150 °C led to the expulsion of H_2 (**Scheme 108**).

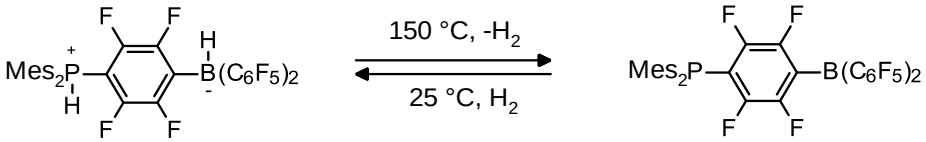

259 **260**

***Scheme 108**. Activation of H_2 with **260**.*

On the other hand, under contrasting conditions, the introduction of H_2 to **260** at only 25 °C triggered the rapid regeneration of **259**, symbolising the first non-transition-metal system that both releases and takes up H_2. A year after these findings, Stefan coined the term 'frustrated Lewis pair' or 'FLP' to denote the frustrating dative bond formation in such systems.

When the formation of such a Lewis-adduct is hindered, either through steric interactions or restricted geometry, this unquenched reactivity can be used to activate a variety of chemical bonds.

Due to the extensive scope of FLP chemistry, this introductory review will focus solely on FLP systems containing boron as the Lewis acid.

3.1.1 Hydrogenation of unsaturated molecules

The capacity of FLPs to trigger H_2 activation under ambient conditions presents a distinctive opportunity for transition-metal free catalytic hydrogenation of unsaturated substrates. A year later after introducing the concept of FLPs, in 2007, Stephan and co-workers reported the first example of metal-free catalytic imine hydrogenation with the phosphonium borate **3** as the catalyst (**Scheme 109**).[146]

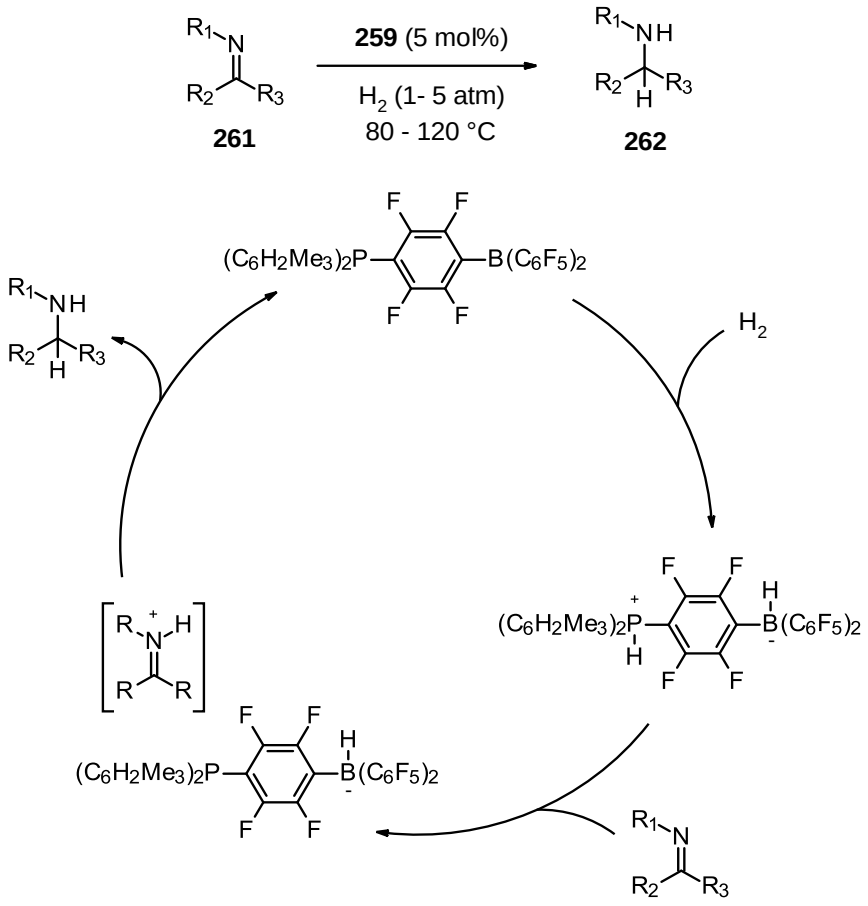

***Scheme 109**. Metal-free FLP catalysed hydrogenation of imines.*

Catalytic hydrogenation of electron-rich olefins was developed by Paradies and co-workers using intermolecular FLPs consisting of $B(C_6F_5)_3$ and $P(C_6F_5)Ph_2$ (**Scheme 110**).[147] This metal-

free hydrogenation is hypothesised to proceed via protonation of the olefin by the H_2 activated product **265** to form carbenium species **266**. This species then abstracts the hydride from **267** to furnish alkane **264**.

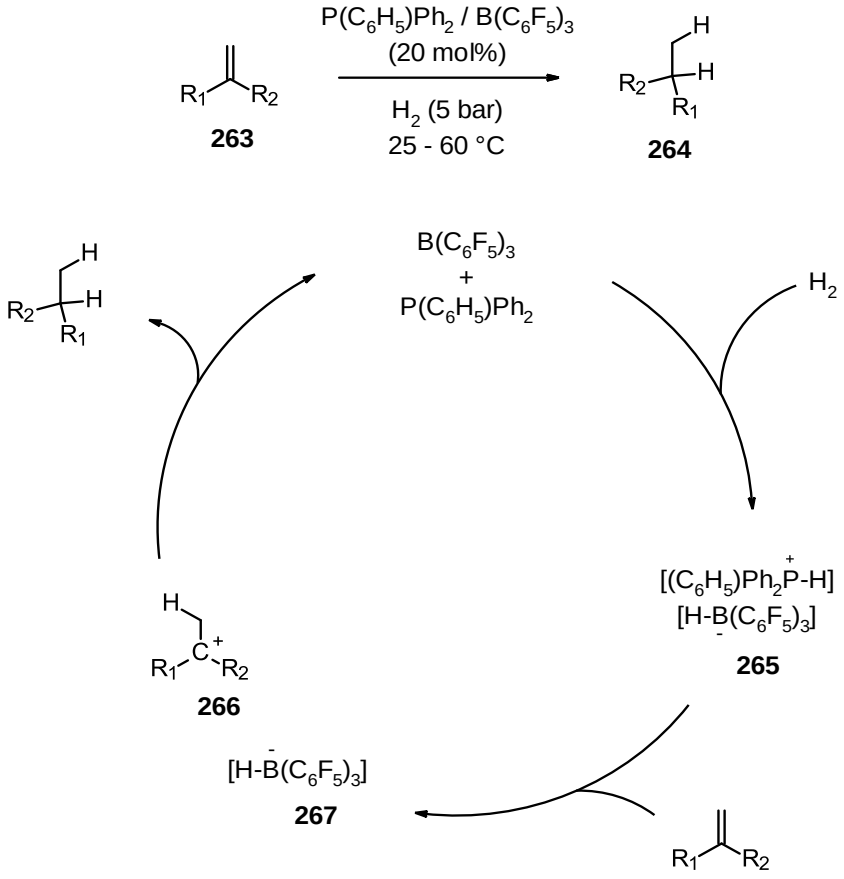

***Scheme 110**. Metal-free FLP catalysed hydrogenation of olefins.*

3.1.2 Asymmetric hydrogenation

The utilisation of FLPs has been applied to asymmetric hydrogenation, a significant area in asymmetric synthesis,[148] through the development of chiral FLP catalysts. In 2008, Klankermayer and colleagues presented the first instance of asymmetric hydrogenation using chiral borane **270** derived from α-pinene as the catalyst, furnishing amine **269** from imine **268** with low enantioselectivity (13% *ee*) (**Scheme 111**).[149]

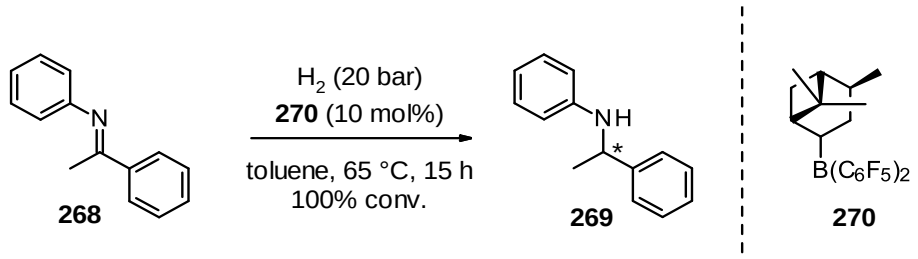

***Scheme 111**. Asymmetric reduction of imine **268** using chiral borane **270**.*

With the low stability of Lewis acid **270** a major drawback in the route above, the same group employed chiral borane **273** derived from camphor, leading to a highly enantioselective process (**Scheme 112**).[150]

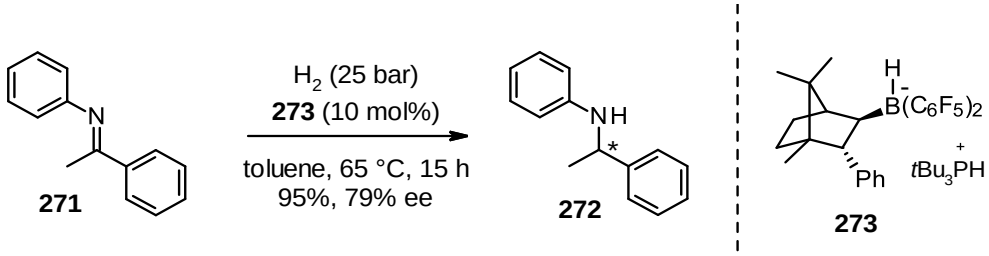

***Scheme 112**. Asymmetric reduction of imine **271** using chiral FLP salt **273**.*

Despite advancements in the FLP-catalysed asymmetric hydrogenation of imines, the development of readily accessible chiral FLP catalysts presented a challenge that Du and colleagues effectively resolved. Their approach involved performing hydroboration on binaphthyl based chiral **276** containing two terminal olefins with $HB(C_6F_5)_2$, allowing the *in-situ* generation of enantiomerically pure borane catalysts, with up to 89% *ee* obtained (**Scheme 113**).[151] This method offers an advantage over other catalysts such as **273**, which requires purification through recrystallisation from a mixture of stereoisomers.

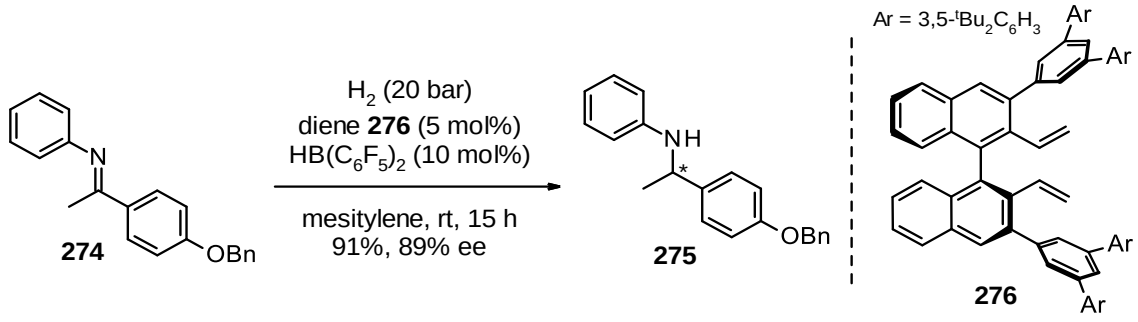

***Scheme 113**. Asymmetric reduction of imine **274** using a binaphthyl-based chiral borane generated in situ.*

Based on binaphthyl scaffolds like above, but with the key distinction of using an intramolecular FLP, Repo and co-workers developed a catalyst that could reduce enamines with extremely high asymmetric induction (**Scheme 114**).[152] However, one drawback of this approach is that the synthesis of catalyst **279** requires a four step route, unlike the simpler *in-situ* generation of the borane catalyst as described previously in **Scheme 113**.

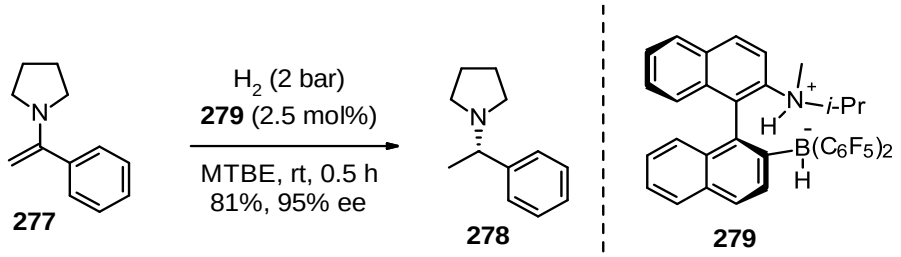

***Scheme 114**. Asymmetric reduction of enamine **277** using chiral FLP **279**.*

Other than the intramolecular FLP shown above in **Scheme 114**, the aforementioned examples primarily focus on the use of chiral boron Lewis acids but chiral Lewis base-derived FLPs are less established. However, in the last few years, Du and co-workers have reported a novel FLP system combining the chiral oxazoline Lewis base **282** with an achiral boron Lewis acid for the highly asymmetric reduction of ketones and enones (**Scheme 115**).[153]

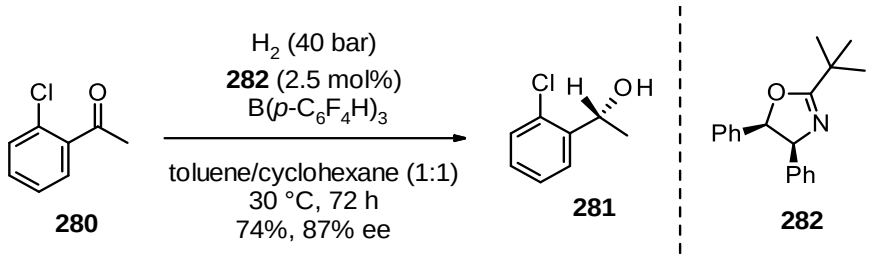

***Scheme 115**. Asymmetric reduction of ketone **280** using a chiral-base based FLP.*

3.1.3 Hydrogenation of carbon dioxide

Carbon dioxide, a prominent greenhouse gas, contributes to the escalating global temperatures and poses a significant threat to our planet's atmosphere.[154,155] Converting CO_2 into useful chemical compounds presents a potential solution to this issue, however the conversion of CO_2 is a challenging undertaking due to its high thermodynamic and kinetic stability.

While there have been reports of transition metal catalysts capable of modifying carbon dioxide, utilising more abundant and less costly FLPs would be a sustainable alternative. Stephan, Erker and co-workers were the first with their report on reversible binding of CO_2 under mild conditions to form a novel carbonic acid derivative (**Scheme 116**).[156]

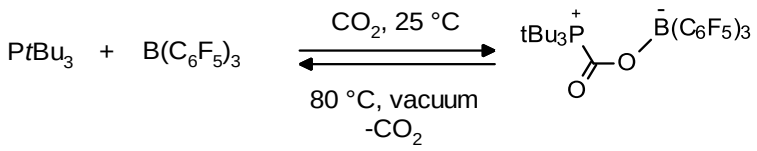

***Scheme 116**. Reversible uptake and release of CO_2 by an intermolecular FLP.*

A year later, Piers and co-workers developed a method for transforming CO_2 to methane using a TMP and $B(C_6F_5)_3$ FLP system with triethylsilane as the reductant.[157] However, this method suffers from limited turnovers. In addition, the CO_2 hydrogenation method reported by O'Hare and co-workers requires stoichiometric amounts of TMP/$B(C_6F_5)_3$,[158] extended reaction times (6 days) and temperatures of 160 °C.

Addressing these issues, an intramolecular FLP system devised by Stephan, Fontaine, and co-workers enabled hydrogenation of CO_2 to occur under the mild conditions of ambient temperature, leading to a mixture of reduction products **284**–**286** (**Scheme 117**).[159]

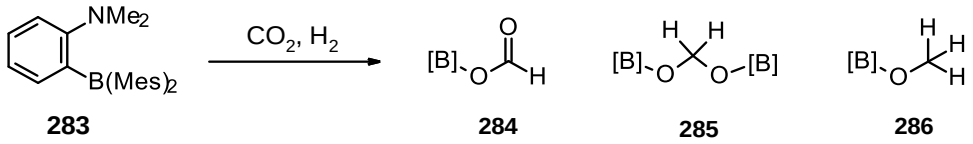

283 **284** **285** **286**

***Scheme 117**. Hydrogenation of carbon dioxide with **283** leading to a mixture of reduction products.*

3.1.4 C–H Functionalisation with FLPs

Apart from FLPs' applications in hydrogenation, catalytic C–H functionalisation stands out as another notable area for FLP catalysts. This breakthrough was first reported by Fontaine and co-workers, who could achieve transition metal-free C–H borylation of heteroarenes using low cost and abundant organoboranes, such as **289** (**Scheme 118**).[160]

In the proposed catalytic cycle, the C–H activation step occurs at the most nucleophilic carbon, leading to zwitterionic intermediate **290** which then expels H_2 generating **291**. This subsequently reacts with HBPin to afford the borylated product **288** and regenerates the FLP catalyst. One drawback of this intramolecular FLP process is the substrate scope is limited to electron-rich heteroarenes, with the presence of electron-withdrawing substituents leading to complete inhibition of the reaction.

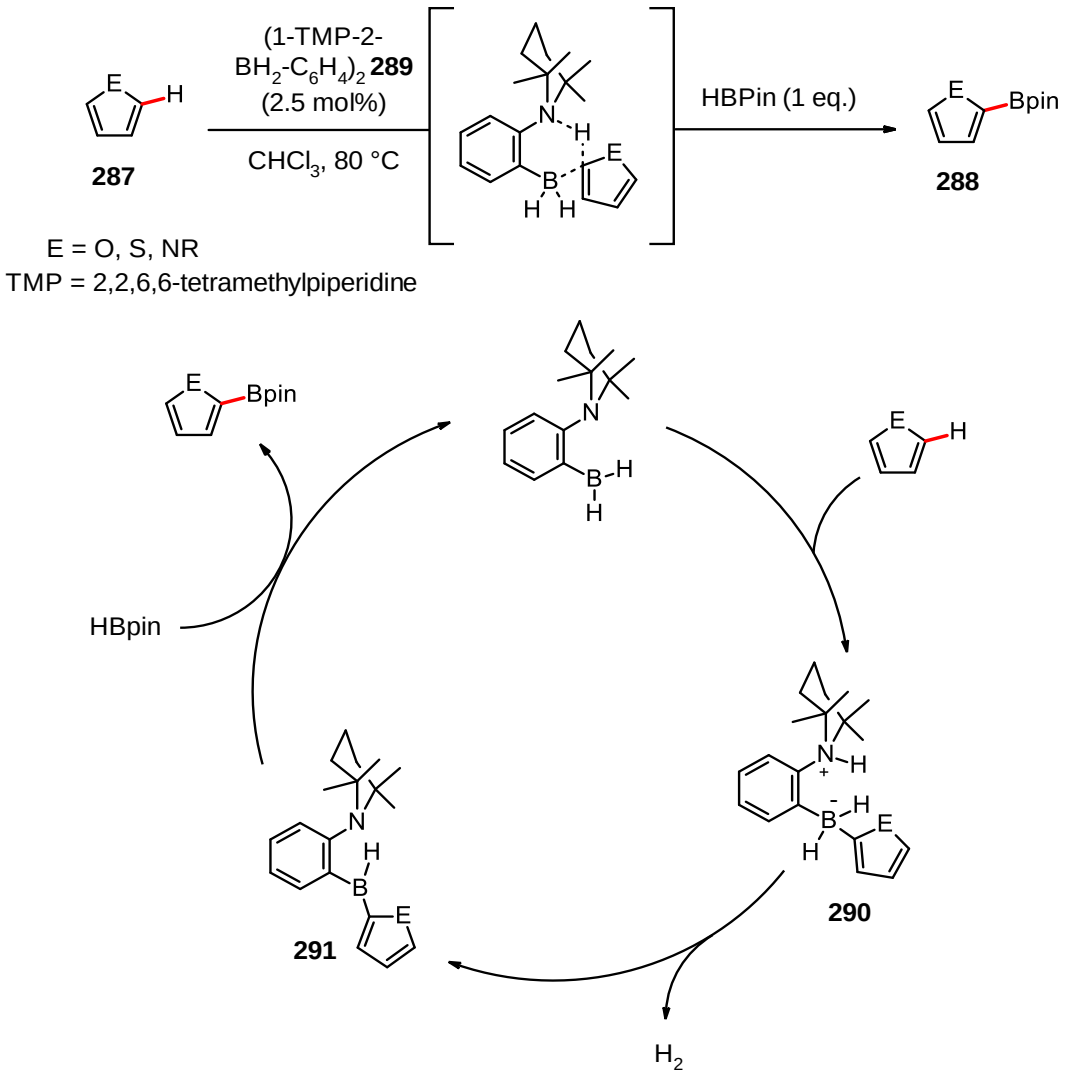

***Scheme 118**. C–H borylation of heteroarenes using transition metal-free FLP catalysis.*

Apart from aryl C–H bond functionalistion, Wasa and co-workers have documented a FLP-catalysed asymmetric Mannich reaction furnishing **294** using chiral borane **295** (**Scheme 119**).[161] The naphthyl-based scaffold employed was similar to that used by Du and co-workers in their work on imine hydrogenation in **Scheme 113**, however Wasa and co-workers elected not to generate the chiral borane *in situ*.

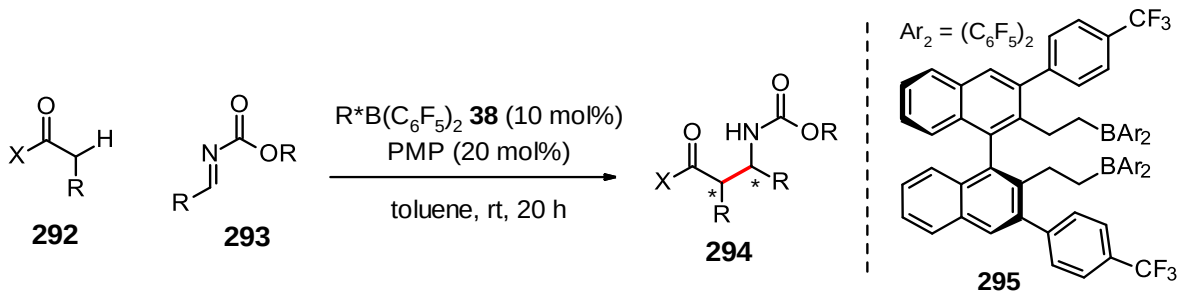

***Scheme 119**. Mannich-type reaction catalysed by a FLP complex of **295** and PMP.*

In conclusion, boron-based frustrated Lewis pairs (FLPs) have emerged as promising catalysts in various chemical transformations, showcasing their potential in activating inert bonds and facilitating novel reactivity with high stereoselectivity. Their ability to engage in diverse reactions while using abundant and relatively inexpensive materials highlights their significance in sustainable chemistry.

Despite their advancements and promising applications, further exploration of FLPs is crucial for harnessing their full potential. Continued research into boron-based FLPs is poised to offer innovative solutions for challenging chemical transformations including the activation of small molecules that are currently considered inert to chemical modification.

3.2 Project aims

The primary aim of this project was to optimise the novel use of halomethylboronate reagents to form boron-centred spiro compounds. Termed diazaboroles, these compounds such as **298**, were recently discovered in our group (**Scheme 120**).[162]

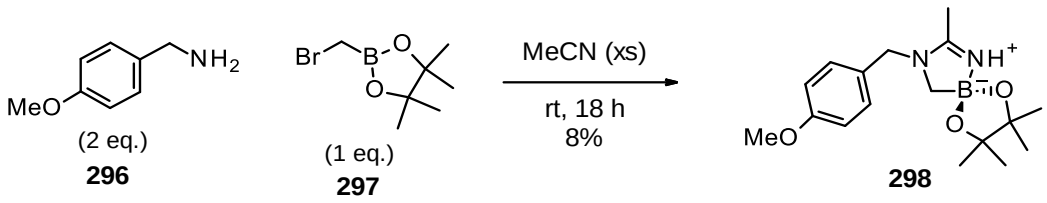

***Scheme 120**. Diazaborole **298**, discovered by Dr Matt Cross during his PhD studies.*

Once this goal was met, different vectors of functional group attachment would be explored to improve the substrate scope of this novel reaction. In addition, the use of halomethylboronates in the mono-*N*-methylation of primary amines, also previously reported in the group, was studied to improve the yield of the reaction. The main objective was to obtain total conversion of the starting material to overcome the low methylation yields observed.

3.3 Related boron-centred spiro compounds

Despite their rarity, literature records exist of other boron-centred spiro compounds that possess a similar structure to **298**. For instance, in 1992, Biedrzycka and co-workers detailed a series of aliphatic and benzylic boronate esters with the aim of assessing their potential as ligands for affinity chromatography (**Scheme 121**).[163]

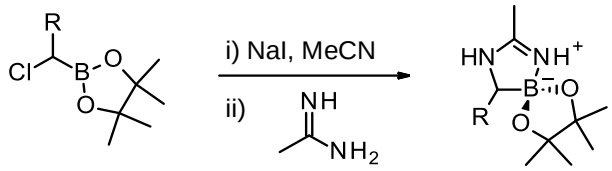

***Scheme 121**. Synthesis of diazaboroles as described by Biedrzycki and co-workers.*

In a more recent study, Nizioł and co-workers altered the nucleoside deoxycytidine to produce a diazaborole compound characterized by an intramolecular N-B coordination between the pyrimidinone and boron that takes place subsequent to α-aminoboronate formation (**Scheme 122**).[164]

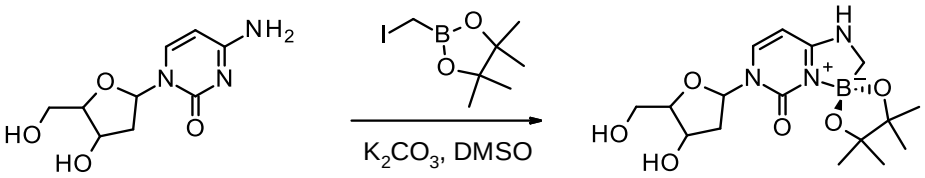

***Scheme 122**. Incorporation of diazaborole motif via modification of deoxycytidine.*

In the last year, Oba and co-workers have reported a similar spiro compound but where the BPin ester is replaced with a BF_2 group (**Scheme 123**).[165] This compound was noted to have potential applications in medicinal chemistry due its peptidomimetic structure.

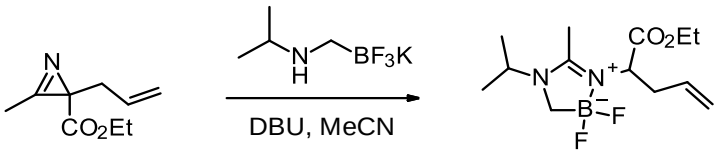

***Scheme 123**. Synthesis of a peptide-like boron-containing molecule by Oba and co-workers.*

Also in 2022, Houston and co-workers described the amidination of 2-aminophenylboronic acid with various nitriles (**Scheme 124**).[166] Using a perfluoropinacol protecting group was postulated to increase the Lewis acidity of the resultant boronate ester leading to efficient activation of a nitrile under mild conditions.

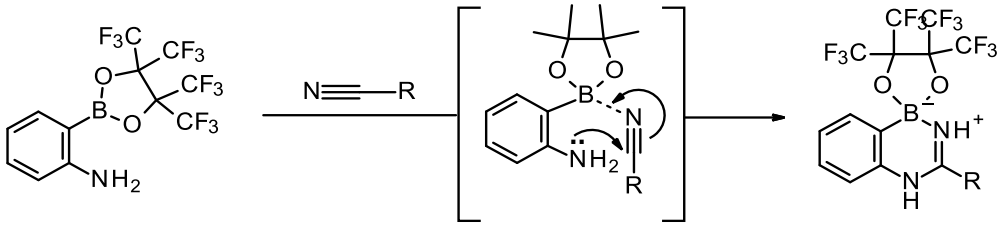

***Scheme 124**. Amidination of 2-aminophenylboronic acid by Houston and co-workers.*

Tang and co-workers reported the synthesis of chiral α-amino tertiary boronic esters via the rhodium-catalysed asymmetric hydroboration of α-arylenamides (**Scheme 125**).[167] These were confirmed by X-ray crystallography to undergo coordination between the boron atom and carbonyl group to furnish compounds similar to those of this work.

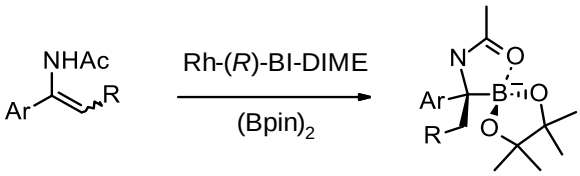

***Scheme 125**. Synthesis of chiral α-amino tertiary boronate esters by Tang and co-workers.*

3.4 Results and discussion

3.4.1 Activation of nitriles via halomethyl boronates

Herein, we report the novel activation of nitriles using a halomethylboronate reagent acting as a frustrated Lewis pair to form boron-centred spiro compounds **(Scheme 126**). As these diazaboroles are comprised of three components; an amine, a boron reagent, and a nitrile, this enables the possibility for a high degree of diversification to generate highly functionalised compounds such as **299**.

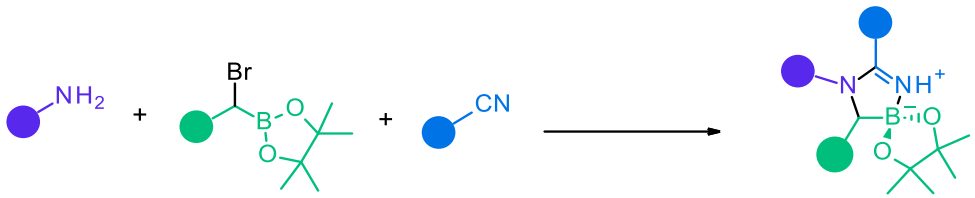

299

***Scheme 126**. Three-component reaction to form highly functionalised diazaboroles **299**.*

The proposed mechanism of diazaborole formation first involves coordination of primary amine **300** to the boron of the boronate reagent **301** to form amine-borate complex **302** (**Scheme 127**). Upon the displacement of bromide from **302** this leads to α-aminoboronate **304** which acts as a frustrated Lewis pair where a nitrile molecule can "quench" leading to diazaborole **306** after a hydrogen transfer process from **305**.

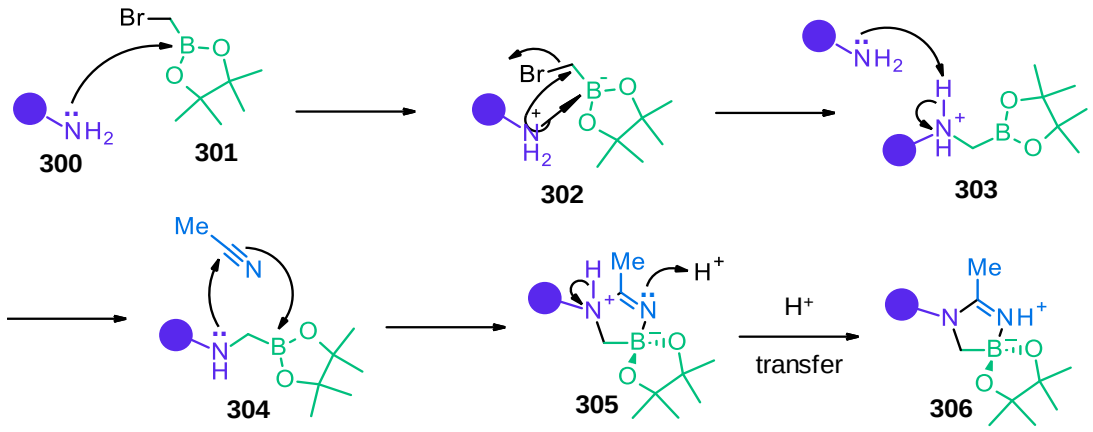

***Scheme 127**. Proposed mechanism for the synthesis of diazaboroles.*

However, the reported yield of this reaction was poor, and the substrate scope was limited (**Figure 29**). Thus, the key objective in this work was optimising the diazaborole synthesis. Once a high-yielding procedure was established, the next task would involve exploring the substrate scope.

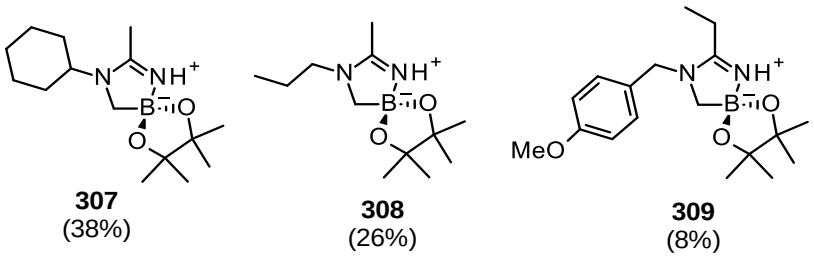

307
(38%)

308
(26%)

309
(8%)

***Figure 29**. Selected diazaborole products **307**-**309** synthesised by Dr Matt Cross, with isolated yields showed in parenthesis.*

3.4.1.1 Improving diazaborole yields

To become familiar with the procedure and relevant techniques, work began by repeating the conditions established in our group for the synthesis of diazaborole **308** from *n*-propylamine **310**, boronate **297** and excess acetonitrile (**Scheme 128**). With purification by silica gel chromatography possible, and well-resolved on TLC, product **308** could be isolated with high purity in 22% yield. This was in close agreement with the yield previously reported within our group (26%).

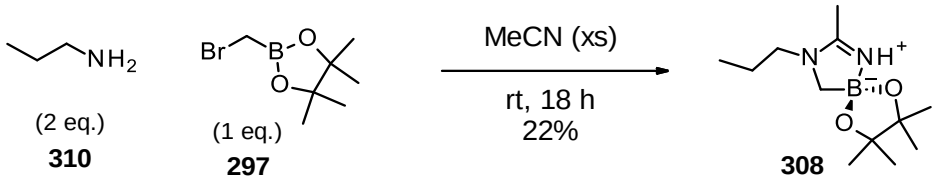

***Scheme 128**. Repeating existing method within our group for the synthesis of diazaborole **308**.*

It is possible that the additional equivalent of starting material, while neutralising the HBr salt formed, it can also hinder the desired pathway. It was hypothesised that the additional amine can coordinate to **304** above in scheme **127** and so prevent it from acting as a frustrated Lewis pair in the activation of a nitrile molecule, leading to a lower diazaborole yield.

Investigating an alternative route to diazaborole **308**, which involved the use of *n*-BuLi and a single equivalent of the amine coupling partner was next examined (**Scheme 129**). However, the desired diazaborole **308** was not observed and only side product **311** was isolated.

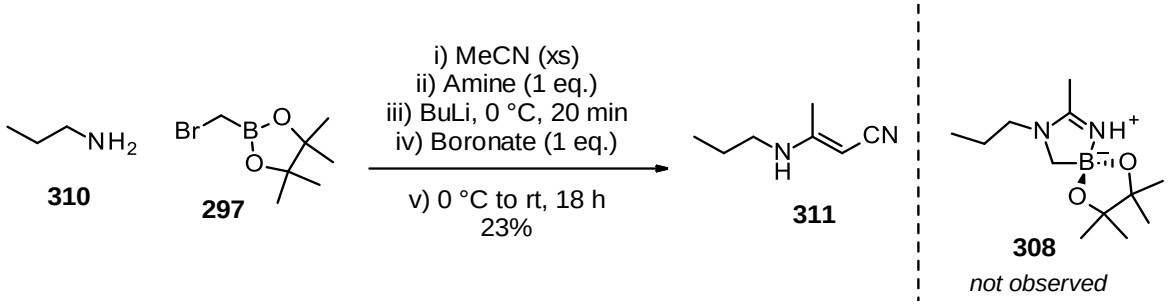

***Scheme 129**. Unexpected formation of side product **311** instead of diazaborole **308**.*

To confirm the reliability of this reaction, it was repeated in the presence of a cyclohexylamine amine coupling partner (**Scheme 130**). Not surprisingly, only adduct **313** was found.

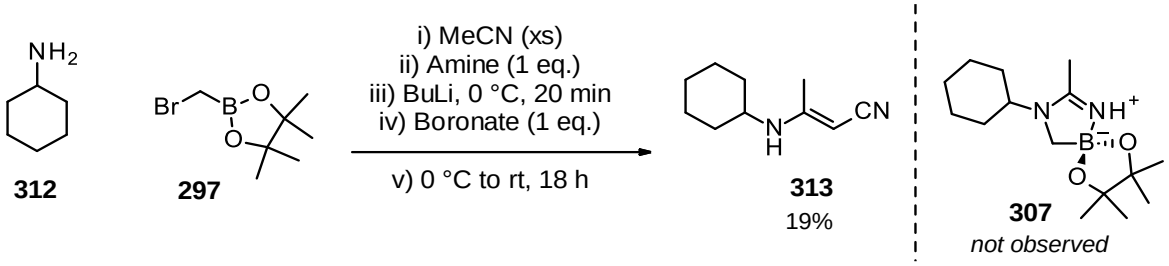

***Scheme 130**. Unexpected formation of side product **313** instead of diazaborole **307**.*

On closer inspection of the order of reagent addition, it was realised that the addition of acetonitrile and amine followed by *n*BuLi likely resulted in the deprotonation of acetonitrile rather than the amine. To prevent this from occurring, the reaction solvent should be switched

to THF and acetonitrile added as the last reagent. Alternatively, a less acidic nitrile could be used, such as benzonitrile.

The unexpected products **311** and **313** were also formed in similar yields when repeating the reactions above but in the absence of the halomethylboronate reagent which led to proposing a self-condensation mechanism based on the Thorpe reaction (**Scheme 131**).[168]

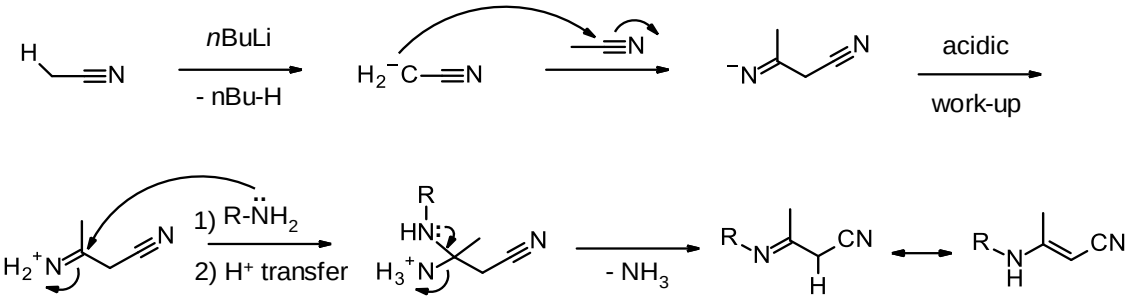

***Scheme 131**. Proposed mechanism for the formation of side products **311** and **313**.*

Moving away from organolithium bases, a screen of additives including non-nucleophilic bases was carried out (**Table 1**). With triethylamine, the isolated yield was significantly lower, suggesting NEt_3 was more successful in coordinating with the boronate compared to the cyclohexylamine substrate. With the inorganic base lithium *tert*-butoxide only a trace amount of diazaborole was isolated, likely due to hydrolysis of the BPin ester. The use of a proton sponge was ineffective with no desired diazaborole found. Propylene oxide was also screened since it should not participate in undesired coordination with the boron of the halomethyl boronate. Instead, this should undergo ring-opening by S_N2 attack of the bromide ion, thereby aiding its sequestration. However, its use was unsuccessful with no diazaborole isolated.

***Table 1**. Additive screen for the formation of diazaborole **307**.*

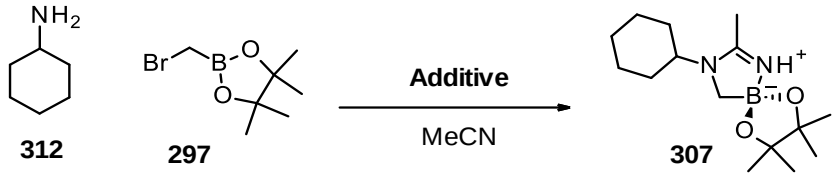

312 **297** **307**

Entry	Additive	Isolated yield (%)
1	Triethylamine	10
2	Lithium *tert*-butoxide	trace
3	Proton sponge	0
4	Propylene oxide	0

Reaction conditions: $BrCH_2BPin$ (1 mmol, 1 eq.), cyclohexylamine (1.05 eq.), base (1 eq.), MeCN (2 mL), rt, 18 h.

With the additive screen not yielding any encouraging results, we moved on to examining another important parameter, the reaction temperature. This parameter was of particular interest since upon addition of halomethyl boronate reagent, the temperature of the reaction increased.

This led to a hypothesis that cooling the reaction mixture would slow down undesirable pathways and so result in a higher yield of diazaborole **308**. To investigate this, four conditions were examined where the reaction time and temperature were varied while keeping the amine substrate the same (**Table 2**).

***Table 2**. Temperature screen for the formation of diazaborole **308**.*

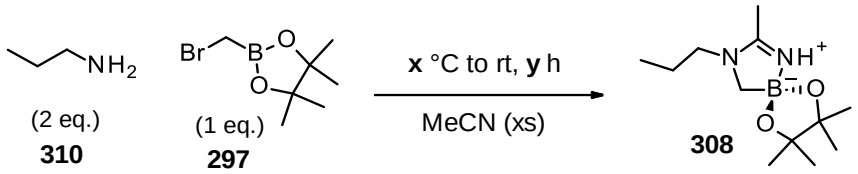

Entry	Temperature (**x** °C)	Reaction time (**y** h)	Isolated yield (%)
1[a]	rt	18	26
2	-30	18	21
3	0	18	30
4[b]	0	66	**64**

[a]Control experiment; previously reported by Dr Matt Cross. [b]Reaction left to stir over the weekend.

Due to acetonitrile being used as both a reaction partner and solvent, the lowest temperature investigated was –30 °C to prevent the solvent from freezing. However, no improvement in yield was observed (entry 2). Lowering the initial reaction set-up temperature to 0 °C, a slight increase in yield was observed compared to the control experiment (entry 3).

Given that a lower reaction temperature might require a longer reaction time, the experiment was repeated but with extended reaction time of 3 days (entry 4). Pleasingly, the isolated yield of the diazaborole product was 64%, a yield significantly higher than any previously reported.

Rationalising this, it should be noted that upon adding the boronate reagent to the amine reaction mixture, a white precipitate is generated within seconds in an exothermic reaction. This white precipitate is likely to be the amine-borate complex **302** from Scheme **127** above. Also, given that the white precipitate develops rapidly with or without cooling, this suggests that the initial N–B coordination leading to **302** is very fast.

However, the initial cooling is likely preventing deleterious side reactions from occurring such as the formation of possible side product **319** (**Scheme 132**). The subsequent heating is likely helping to dissociate N–B bonds in complexes such as **316** and promote the nitrile trapping with the FLP **317**. While we can expect N–B coordination to be fast and reversible at almost all temperatures, from an entropic standpoint, dissociation will become more favourable at higher temperatures.

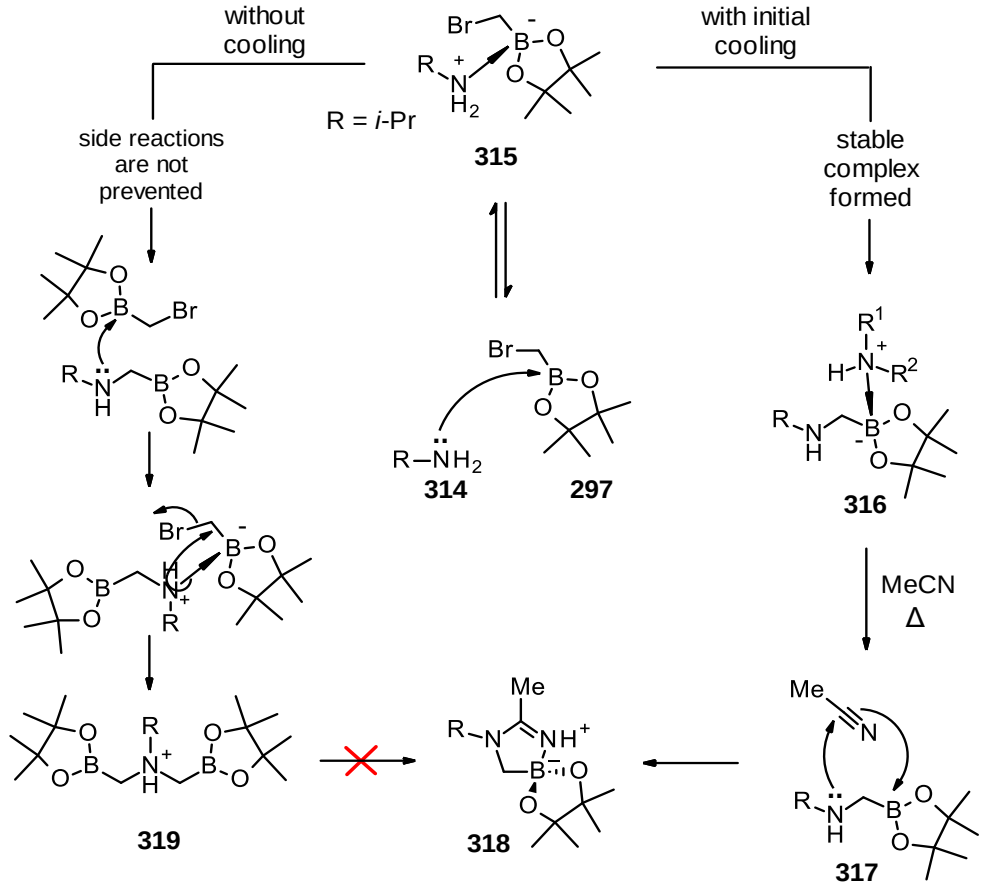

***Scheme 132**. Rationalising the effect of cooling and heating on diazaborole formation.*

With extended reaction times required so far to achieve high yields, the next aim was to lower the reaction time without negatively impacting the diazaborole yield. It was hypothesised that a dual cooling-heating approach would be most effective. This method would involve initially cooling the reaction mixture to minimise unwanted pathways from dominating, followed by heating overnight to ensure for a faster rate of diazaborole formation. Gratifyingly, with a choice of 65 °C for the heating temperature and a more reasonable reaction time of 18 h, diazaborole **321** was isolated in a high yield (**Scheme 133**).

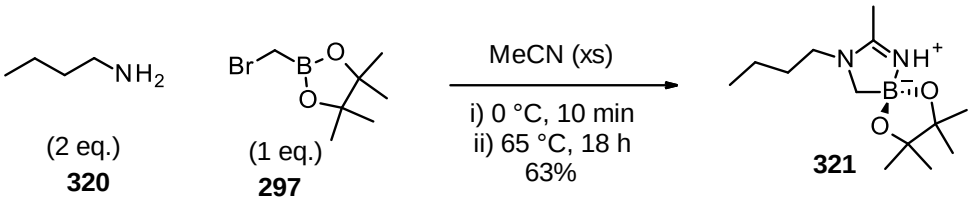

***Scheme 133**. Synthesis of diazaborole **321** with high yield via a dual heating-cooling method.*

3.4.1.2 Diazaborole substrate scope

With an improved procedure in hand, the amine scope of diazaborole products was next investigated (**Scheme 134**). Straight-chain and cyclic aliphatic amines including cyclohexylamine and n-butylamine were well-tolerated, delivering **307** and **321** in 66% and 63% yield respectively. In addition, aromatic amines, such as *p*-anisidine had sufficient nucleophilic character to react to furnish **322** in 61% yield. Moderate success was also achieved with benzylamine and phenethylamine coupling partners, affording analogues **324** and **325** in 39% and 54% yield respectively. While a respectable yield of 39% was achieved for the glycine *tert*-butyl ester compound **327**, this was not the case for the acetal derivative **326** with only 13% isolated yield.

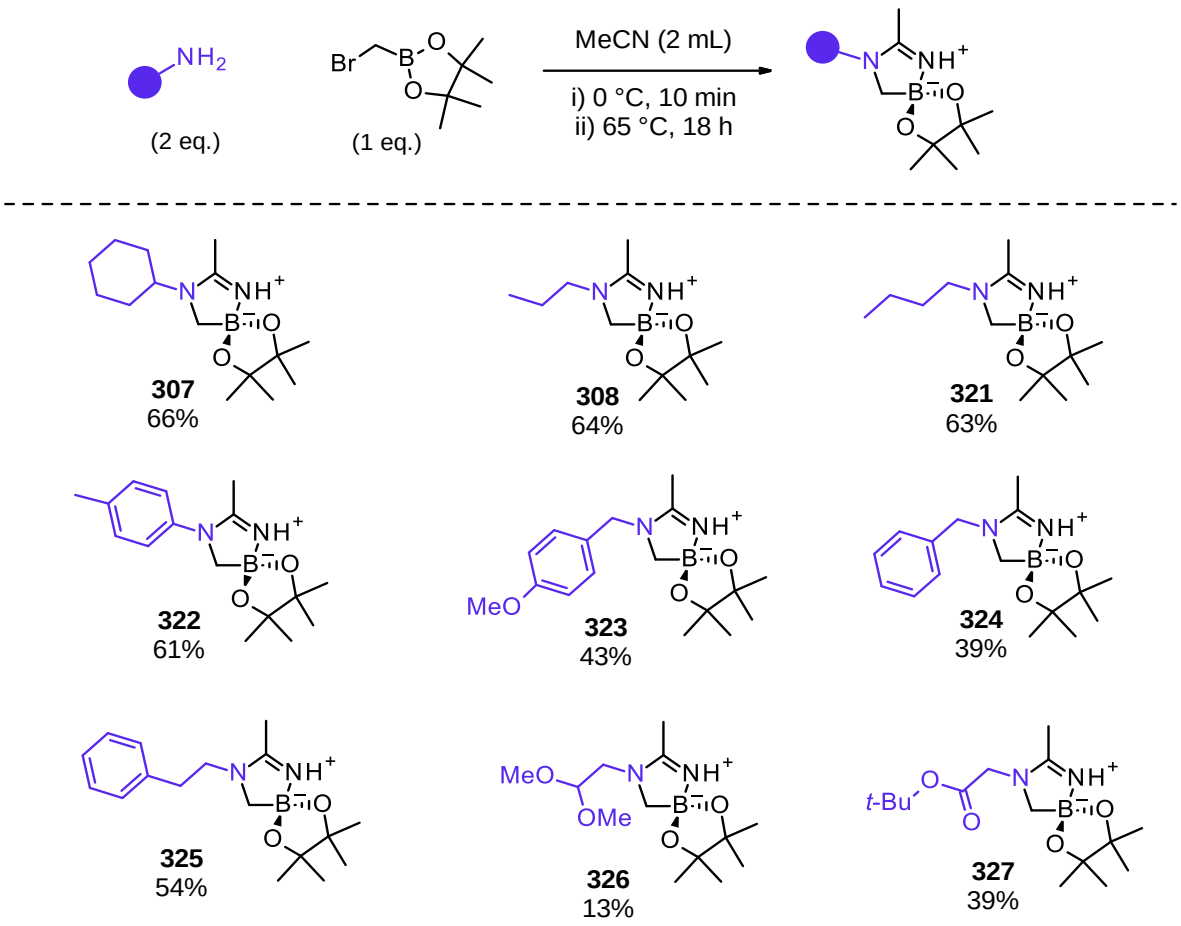

***Scheme 134**. Amine scope of diazaborole analogues. % Yields shown are of isolated products.*

Next, the nitrile scope of this reaction was investigated with six equivalents of the nitrile source alongside THF as the solvent (**Scheme 135**). Examining propionitrile, a slightly lower yield was observed with the resulting diazaborole **328** compared to the analogous acetonitrile-derived compound **321**.

Increasing the steric hindrance of the nitrile used, isobutyronitrile furnished **329** in significantly lower yields. When the same reaction was attempted with pivalonitrile as the nitrile source, diazaborole **330** was not detected. This result is not surprising given the highly sterically crowded nature of the nitrile carbon in pivalonitrile which hinders nucleophilic attack of the C-N π* orbital. As a result, nitrile activation is prevented.

N-Boc protected nitrile was well-tolerated, furnishing diazaborole **331** in moderate yield, which opens opportunities for further functionalisation upon cleavage of the Boc group. Benzonitrile was less favoured however, with a low yield of 16% for the corresponding diazaborole **332**. This is likely due to the increased crowded nature of the nitrile carbon in benzonitrile.

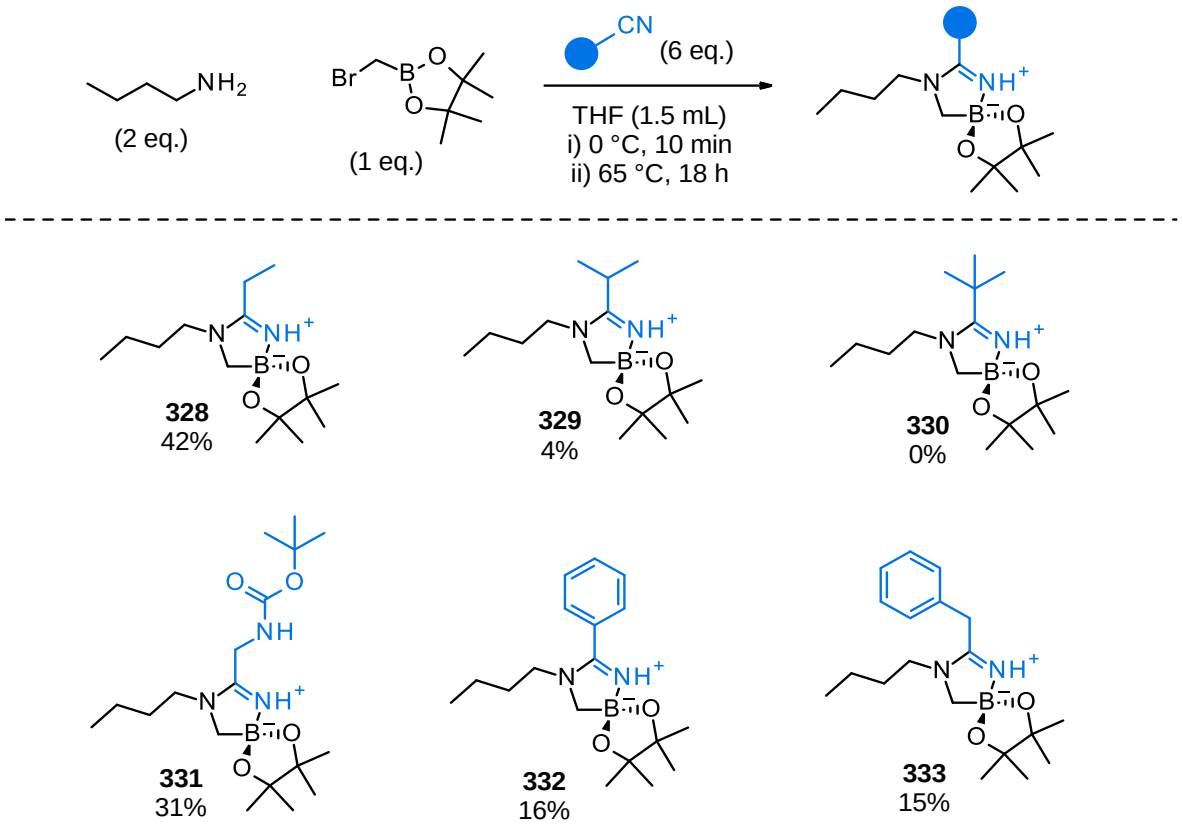

***Scheme 135**. Nitrile scope of diazaborole analogues. % Yields shown are of isolated products.*

So far in this work, the boron component of this reaction was fixed as the bromomethyl boronate ester **297**. The chloromethyl boronate ester analogue was also investigated and was found to provide comparable yields but due to commercial availability, the bromomethyl derivative was used. Substituted derivatives, which can be generated via the Matteson homologation reaction, were next considered to install a third vector in the diazaborole compounds (**Scheme 136**).

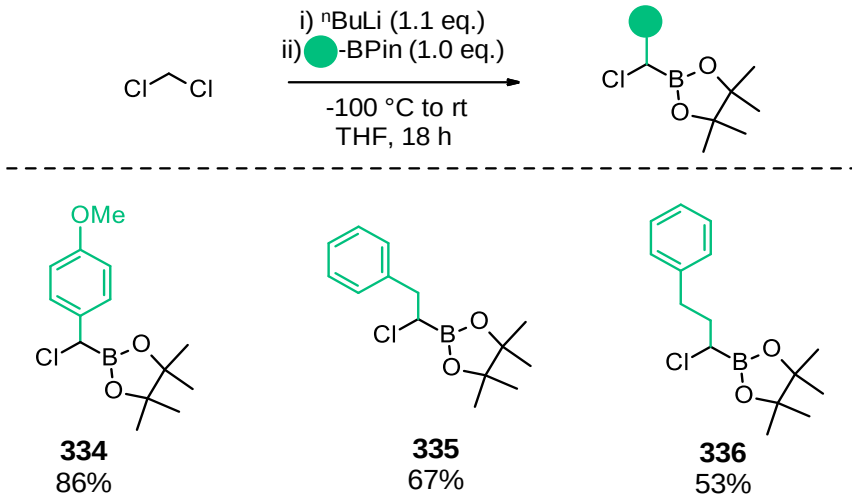

***Scheme 136**. Formation of substituted halomethyl boronates **334**-**336** via the Matteson reaction.*

Additionally, the di-methyl substituted halomethyl boronate **338** was generated by a radical bromination reaction whilst the mono-substituted analogue **339** was prepared by a colleague in the group (**Scheme 137**).

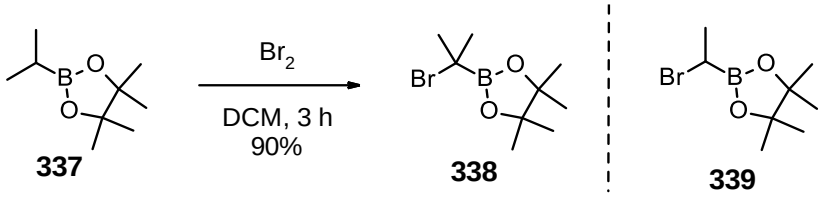

***Scheme 137**. Synthesis of di-substituted halomethyl boronate **338**.*

With a range of substituted halomethyl boronates in hand, these were then examined via reacting with acetonitrile and a set of amines (**Scheme 138**). Pleasingly, reacting the mono-substituted halomethyl boronate **339** with aliphatic amines furnished products **340** and **341** in the highest yields of diazaboroles to date with over 70% isolated yield.

This boost in yield likely arises from Thorpe-Ingold effects accelerating ring closure between the boronate and nitrile. Intrigued whether Thorpe Ingold Effects would further accelerate the reaction with the di-methyl substituted halomethyl boronate **338**, the resulting compound **342** was formed in 23% yield. This was a three-fold decrease in yield compared to diazaborole **341**. It is probable that the high steric hindrance of boronate **338** to nucleophilic attack significantly offsets the favourable Thorpe-Ingold effects on diazaborole formation.

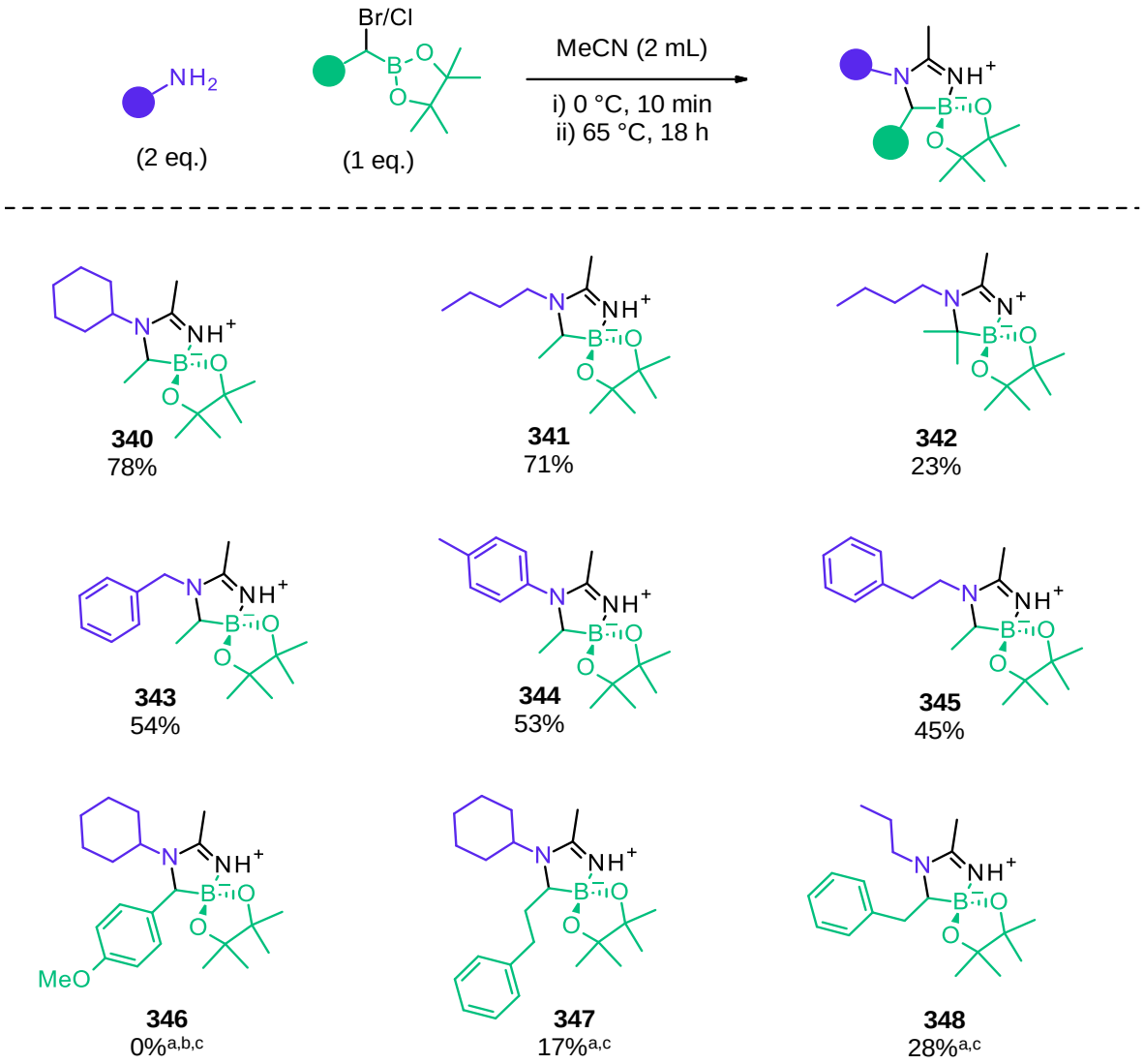

***Scheme 138**. Mixed scope of diazaborole analogues. % Yields shown are of isolated products.*
[a]Previously reported reaction conditions used: rt, 18 h. [b]Only p-Anisaldehyde isolated instead.
[c]The substituted chloromethyl boronate was used instead of a bromomethyl derivative.

Reacting boronate **339** with benzylamine and aniline coupling partners, the yields of the corresponding products **343** and **344** were similar to the diazaboroles derived from the unsubstituted boronate **297**.

With chloromethyl boronate **334**, the corresponding diazaborole **346** was not detected. Instead, only *p*-anisaldehyde was isolated. It is likely that **346** is prone to oxidation at the α-position and this is exacerbated by the presence of the benzylic group adjacent to the boron atom. To validate this hypothesis, two analogues **347** and **348**, were devised with varying methylene spacers present between the aromatic group and the diazaborole ring system. Gratifyingly, boronates **335** and **336** could deliver the corresponding diazaboroles in moderate yields. The

use of benzylic halomethyl boronates to furnish compounds such as **346** are likely to be more compatible to form diazaboroles with the strict exclusion of oxygen.

3.4.1.3 Hydrolysis of diazaboroles

It should be noted that in a few cases, co-elution of the diazaborole product with a small amount of pinacol was detected after the purification step. This is likely due to extended exposure to silica during flash column chromatography causing hydrolysis of the Bpin group. In addition, this effect could be enhanced through electronic effects imparted by the nitrile and amine groups on the diazaborole. The resulting hydrolysis phenomenon could also be playing a role in the low yields observed for this reaction.

To investigate further, an attempt was made to fully hydrolyse diazaborole **321** in the presence of D_2O and isolate the resulting hydrolysed product **349** (**Scheme 139, top**). It became quickly apparent that an equilibrium was being formed with a 1:1 ratio of starting material **321** to cleaved product **349** observed at 18 h, with no noticeable change at 36 h, 48 h or with heating at 50 °C for extended periods.

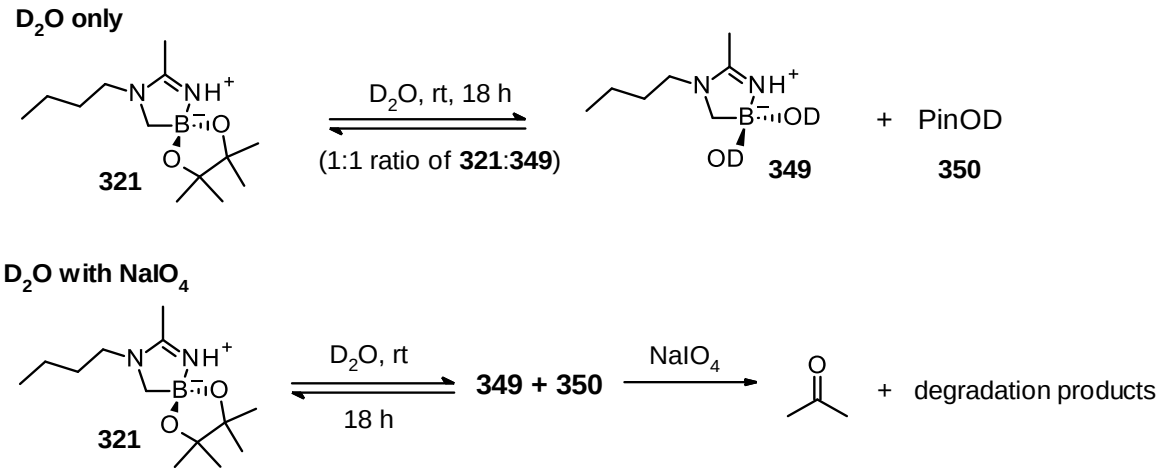

***Scheme 139**. Attempts at hydrolysis of diazaborole **321** using D_2O only (top) and with sodium periodate (bottom).*

To force the equilibrium towards complete hydrolysis, sodium periodate was added to cleave the diol by-product PinOD **350** which generates acetone that serves in a spectator role (**Scheme 139, bottom**). However, while complete consumption of PinOD and diazaborole **321** was observed, the NMR spectrum was much more complex with the presence of multiple new proton signals and a reduced amount of hydrolysed product **349**. This is indicative of its degradation by sodium periodate through oxidation pathways. In the interest of time, further work into the synthesis of the hydrolysed analogue was not carried out.

3.4.1.4 Expanding diazaborole ring size

So far, only five-membered diazaboroles were investigated due to the commercial availability of halomethylboronates. Investigating diazaboroles of larger ring sizes would provide useful insights into ring size effects on reaction yields and any changes to stability of these compounds.

To begin, several routes were attempted to prepare 1,2-bromoethylBPin **351**, with one extra methylene compared to the halomethylboronates used so far in this work. One method investigated involved reacting *in-situ* prepared halomethyllithium species with **297**, however this returned only starting material (**Scheme 140**). One possible problem in this route is that lithium halogen exchange may be occurring on **297** leading to a side product which would be stabilised by delocalisation of the electron density into the empty p orbital on boron. An attempt at HBr addition to a vinylboronate also delivered the same undesired result.

Matteson-type route

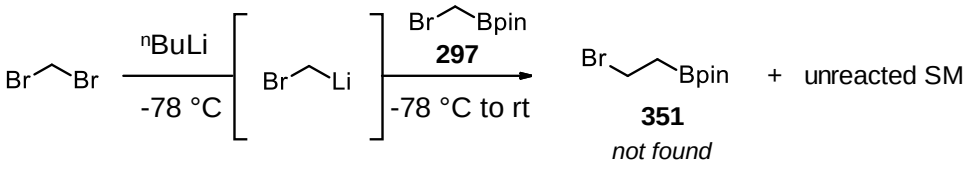

Hydrobromination route

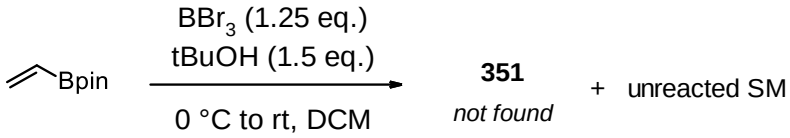

***Scheme 140**. Attempted routes to 1,2-bromoethylBpin **351**.*

Intriguingly, Watson and co-workers recently explored routes to **351**, however their attempts were also unsuccessful in affording the desired product. Their attempts included a radical borylation route (**Scheme 141a**), hydrobromination of vinylBpin by addition of HBr (**Scheme 141b**) and hydroboration with HBpin (**Scheme 141c**).

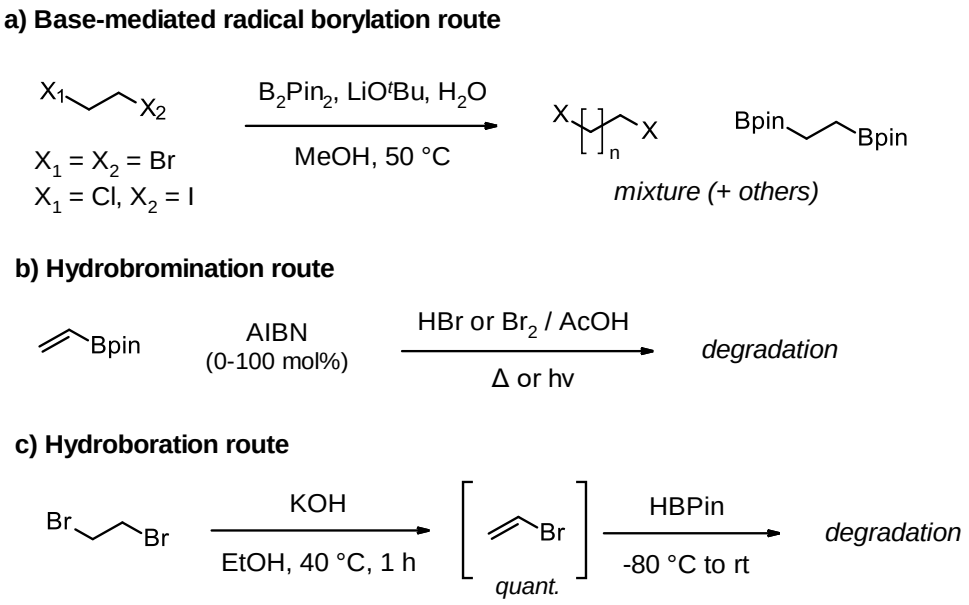

Scheme 141*. Unsuccessful attempts to 1,2-bromoethylBpin* ***1*** *by Watson and co-workers.*

With extensive work into the preparation of **351** not yielding successful results, it was decided to focus on the synthesis of seven-membered diazaboroles. Pleasingly, the corresponding boronate **352**, was synthesised within the group following a procedure by Thomas and co-workers. Reacting **352** using our standard diazaborole conditions with *n*-butylamine and acetonitrile, interestingly rather than the expected diazaborole **353**, the side product **354** was observed instead (**Scheme 142**). It is likely the higher entropic penalty associated with the formation of **85** compared to the smaller five-membered compound **86** is the deciding factor in the outcome of this reaction.

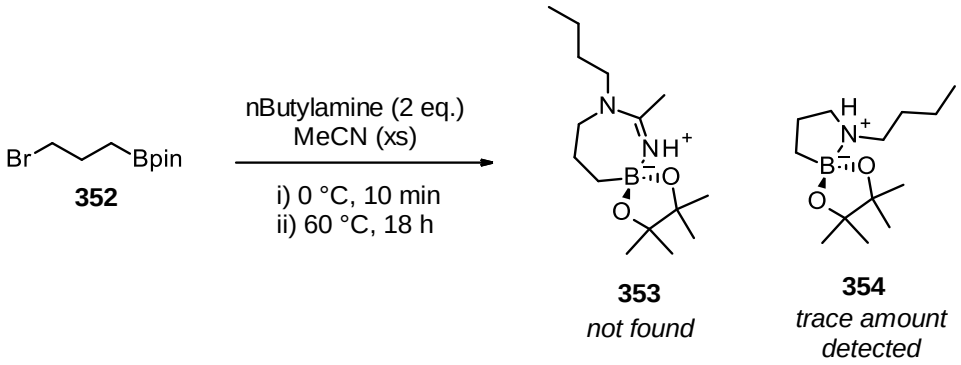

Scheme 142*. Attempted synthesis of seven-membered diazaborole* ***353*** *led to the formation of side-product* ***354*** *instead.*

3.4.2 Mono-*N*-alkylation of primary amines via halomethyl boronates

3.4.2.1 Previous work in group

In addition to the use of halomethyl boronates **357** to generate highly functionalised diazaborole compounds, unpublished work in our group has shown they can deliver a –CH_2BPin onto cysteine (**Scheme 143**).

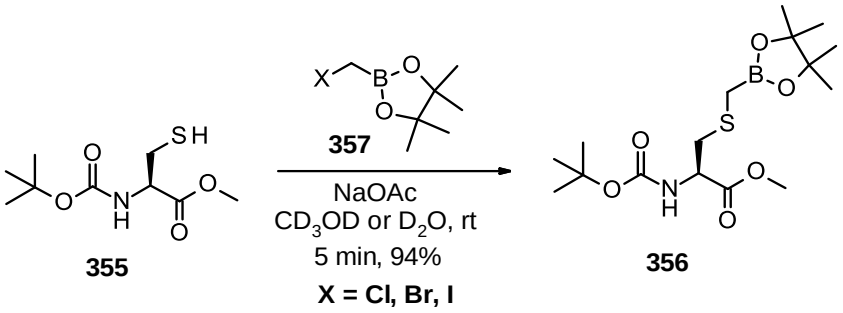

***Scheme 143**. The rapid reaction of a cysteine with an halomethyl boronate ester **357**.*

Previous unpublished work in our group has demonstrated that halomethyl boronates, in a similar manner to cysteine modification, can assist in the monomethylation of primary amines. This is an attractive transformation since other methods such as reductive amination can be challenging to control for the mono-*N*-methylation of primary amines.

In this reaction, it is proposed that first the primary amine **357** coordinates to the boron reagent leading to **358** followed by displacement of the bromide to furnish HBr and α-aminoboronate **359** (**Scheme 144**). The HBr can be sequestered by either an additional equivalent of starting amine or in the presence of a non-nucleophilic base. Species **359** is expected to be unstable and rearranges to the N–BPin intermediate **360**, where ideally the reaction should halt and hence avoid over-alkylation. Following an aqueous work-up, this should hydrolyse the N–BPin intermediate **360** to afford the mono-*N*-methylated amine **361**.

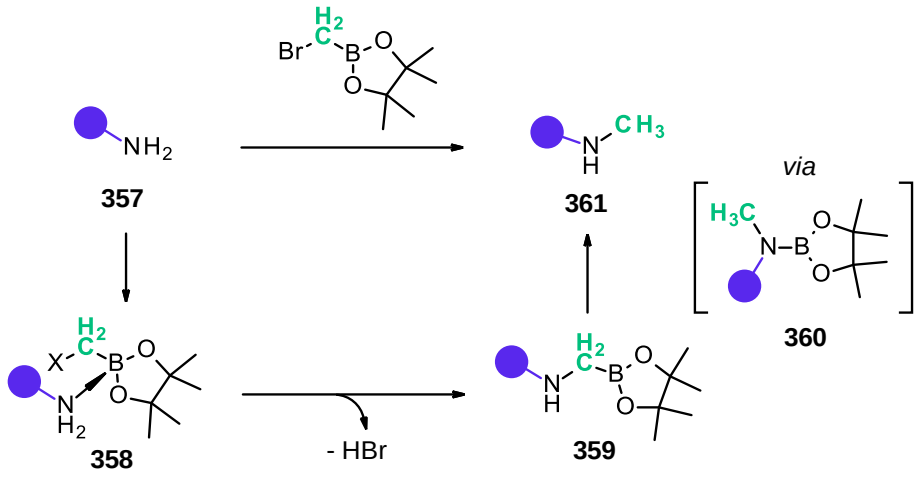

***Scheme 144**. Proposed mechanism for mono-N-methylation of primary amines with halomethyl boronate esters.*

A report by Dong and co-workers on the synthesis of tertiary aminoboronates, via the so-called aza-Matteson reaction, also introduces methylene into N-B bonds (**Scheme 145**).

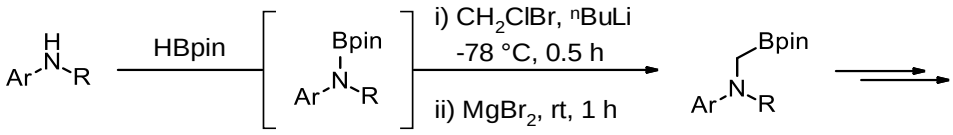

***Scheme 145**. The aza-Matteson reaction as reported by Dong and co-workers.*

A major limitation of the previous work conducted in the group was that the *N*-methylation reaction did not achieve full conversion of the primary amine starting material. This was of a major limitation since the starting amine and product amine have similar R_f values and are difficult to separate by conventional purification methods.

3.4.2.2 Optimisation strategies for the mono-*N*-methylation reaction

In previous work, the non-nucleophilic base *N,N,N',N'*-tetramethylguanidine (TMG) was found to offer the most promising yield of the methylated amine **362** (**Scheme 146**).

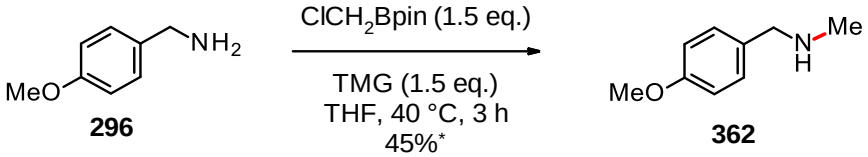

***Scheme 146**. The most promising result obtained from previous co-worker in the group.*
% Yield determined by ^{1}H NMR spectroscopy and **362 was not isolated as pure sample.*

Encouraged by the development of an optimised synthesis route to diazaboroles earlier in this chapter, we envisaged that a similar method could be applied to the monomethylation reaction. By implementing reaction conditions of initial cooling followed by heating at elevated temperatures, it was hoped that a similar improvement in yield would be achieved. However, repeating the above reaction in **Scheme 146** but now with a dual cooling-heating approach, an improvement in yield was not realised with only similar yields obtained instead.

Moving on from considering the temperature of the reaction, it is possible that complete conversion could be achieved by further investigating the base component. Examining any effects arising from using TMG, the stoichiometry of the TMG base was increased from 1.5 equivalents to 3 equivalents in a reaction involving cyclohexylamine **(Scheme 147**).

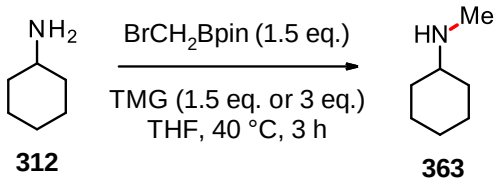

***Scheme 147**. Investigating the effects of TMG on the mono-N-methylation of cyclohexylamine.*

Since an authentic sample of product **363** was at hand, analysis of the crude mixture by ^{1}H NMR was carried out since TLC was not a viable option due to high polarity and similar R_f values of **312** and **363**. ^{1}H NMR analysis showed a more complex reaction mixture with 3 equivalents of TMG and a decrease in the product yield. It is likely that TMG undergoes deleterious interactions with the halomethyl boronate preventing desired primary amine-boronate coordination events such as the formation of intermediate **359** (**Scheme 144**). It should also be noted that ^{1}H NMR analysis of reaction mixtures involving halomethyl boronates was not as straightforward as initially expected. Complex spectra were obtained which is likely due to various interactions taking place between the amine motif of the starting material and the product with a halomethyl boronate.

To avoid unwanted TMG-boronate interactions, TMG was replaced with the inorganic base LiO^{t}Bu. In addition, the same dual cool-heating approach used for the diazaborole synthesis was employed (**Scheme 148**). Pleasingly, ^{1}H NMR of the crude mixture showed complete consumption of starting material **364** but the mono-methylated product **365** was isolated in a rather low yield of 30%.

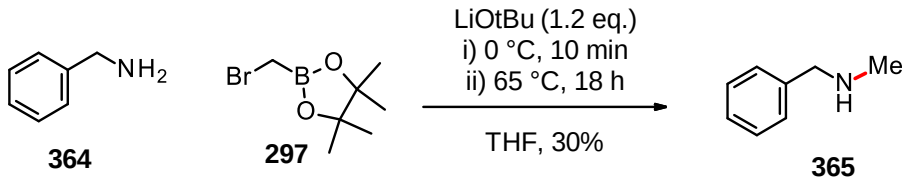

***Scheme 148**. N-methylation attempt of benzylamine with boronate **297** and LiOtBu.*

It is possible that the *N*-alkylated product **365** was being washed out into the aqueous layer during the work up step. To prevent this from occurring, a one-pot *N*-alkylation and *N*-Boc protection step was implemented. Additionally, the reaction was quenched with a small amount of water to ensure rearrangement of the corresponding intermediate **360** (**Scheme 144**) to **365**, before the *N*-Boc protection step (**Scheme 149**).

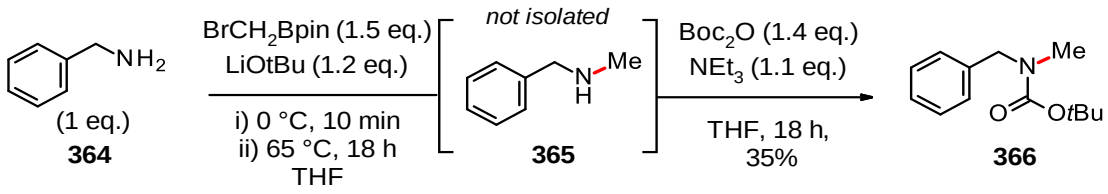

***Scheme 149**. One pot N-methylation and N-Boc protection of benzylamine.*

With the *N*-Boc derivative of starting material **364** not found, this one-pot procedure however furnished **366** in a similar yield to that of **Scheme 148**. This indicates that side reactions involving the starting material **364** were the dominant forces at play leading to low product yields. Examining the aqueous layer from the work-up step, staining with ninhydrin confirmed the presence of amine-containing material and ^{1}H NMR analysis showed aromatic proton signals. This led to the hypothesis that adducts were forming during the reaction. These boronate complexes were difficult to break apart during an aqueous work-up and a possible structure is shown below (**Scheme 150**).

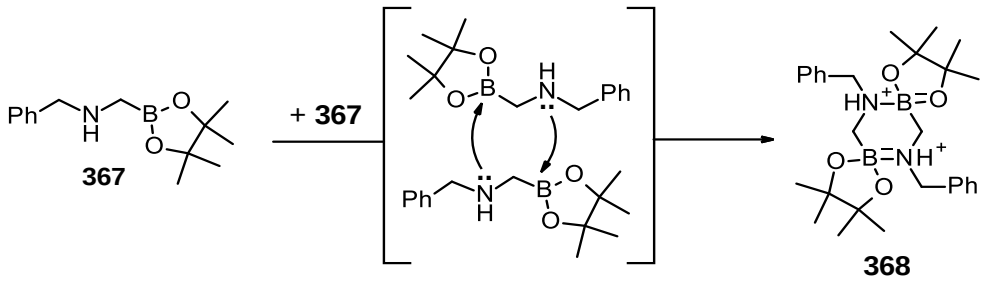

***Scheme 150**. Possible structure of a boronate complex formed during the N-methylation attempt of benzylamine.*

Referring to the diazaborole work discussed earlier in this chapter, it is likely that the presence of a 'quench' reagent, in this case a nitrile, in combination with heating, helps nitrile trapping to occur with the dissociation of boronate complexes like **368**. However, in the absence of a nitrile, as is the case for the *N*-methylation of amines with halomethyl boronates, these adducts persist.

In an attempt to cleave boronate complexes such as the postulated adduct **368**, several conditions were examined. Strongly acidic and basic work-up conditions, using HCl and NaOH respectively, had no desirable effect since low alkylated product yields were observed in both cases. Similarly, the use of TBAF and aqueous ammonia were unsuccessful in breaking apart the complexes.

One possible route to circumvent this is the use of halomethyl boronates that can undergo protodeboronation more readily. As uncovered earlier in this work, diazaboroles with benzylic boron groups are unstable and undergo C-B oxidation. Thus, it is likely that benzene-substituted α-halomethyl boronates can undergo protodeboronation before the formation of amine-boronate complexes can take place. While this hypothesis is ripe for further investigation, due to limited research time remaining this was not explored further.

3.5 Conclusions and future work

The primary aim of this work was to establish an optimised method for the synthesis of novel diazaboroles. This objective was successfully met, with a high-yielding method developed using a dual cooling-heating approach.

Confirming the optimised method for high-yielding diazaboroles, a selection of compounds previously reported in our group were re-synthesised using this method (**Figure 30**). Pleasingly, in many cases a minimum doubling of yield was observed and notably the method previously used to generate **59** in trace amounts was now improved to 39% isolated yield.

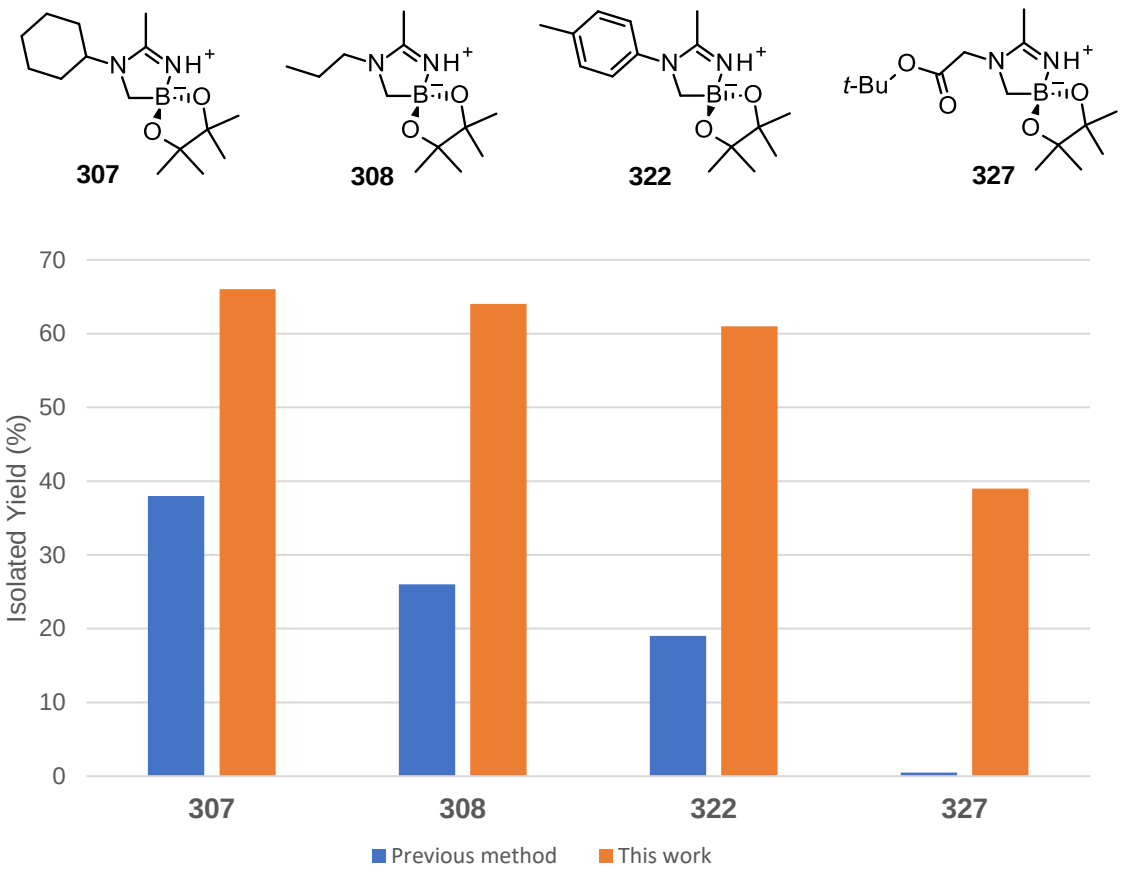

***Figure 30**. Yield comparisons of diazaboroles synthesised through previously reported method and the improved approach of this work.*

The diazaborole scope was extensive, with three different vectors of functionalisation explored via the amine, the nitrile and the halomethyl boronate components. However, further investigation into the level of amine nucleophilicity required for this reaction to proceed would be useful via testing deactivated aniline **369** and 2-aminopyridine **370** (**Figure 31**). The opportunity to deliver bioactive drug-like compounds with the inclusion of chirality such as by incorporating amide **371** and the chiral amine **372** would be valuable in expanding the diazaborole scope.

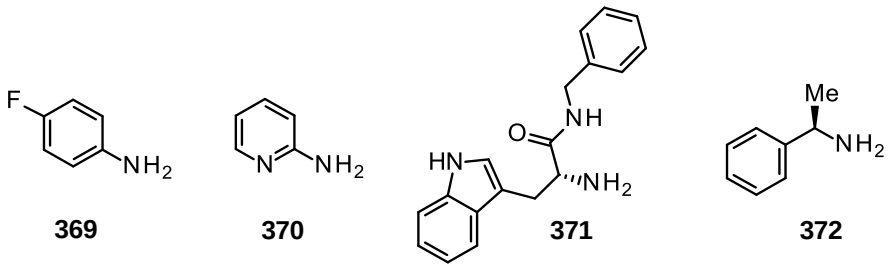

***Figure 31**. Potential coupling partners to further expand substrate scope of diazaboroles.*

With regards to the nitrile coupling partner, while various nitriles were examined in this work, it is possible that analogous molecules such as isothiocyanates or isocyanates can be activated by halomethyl boronates in a similar fashion (**Scheme 151**).

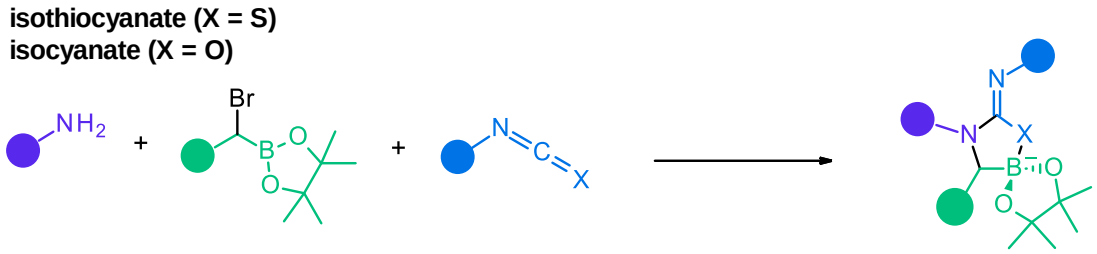

***Scheme 151**. Possible activation of isothiocyanate and carbon dioxide.*

This approach appears feasible based on the findings of Hou and co-workers, which involve the activation of carbon dioxide via an α-borylalkylamido copper species acting as an FLP to furnish **373** (**Scheme 152**).[169] A metal-free approach would be a highly attractive transformation and is ripe for future research into.

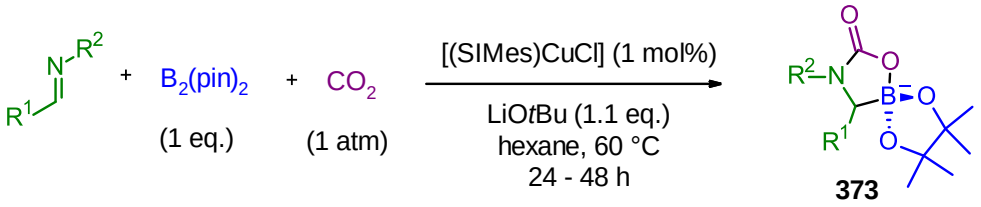

***Scheme 152**. Functionalisation of imines through CO_2 activation by intramolecular N/B Lewis*

With these diazaboroles in hand, their synthetic usefulness can be further expanded by converting the Bpin group to a BF_2 motif, another functionalisable handle. In addition, due to three vectors for functionalisation possibles, diazaboroles can be used for structure activity relationships, further improving their pharmaceutical attractiveness.

While successful in optimising the synthesis of diazaboroles, developing an improved method for the mono-*N*-methylation of primary amines using halomethyl boronates proved more elusive. It was found that a majority of the amine starting material was being sequestered to likely form amine-boronate complexes as the reaction progressed. While various work-up conditions were investigated to break apart these adducts, these attempts were not successful.

4 Experimentals

4.1 Techniques

All reagents and solvents were purchased from Sigma Aldrich, Fisher Scientific or Fluorochem and used as supplied unless otherwise stated. Solvents were degassed by sparging with argon for at least 15 minutes. All catalytic reactions were carried out with dry, degassed solvents and under argon atmosphere using oven-dried or flame-dried glassware unless specified.

All reactions were monitored by TLC or 1H NMR. TLC plates used were pre-coated with silica gel 60 F_{254} on aluminium (Merck KGaA). The spotted TLCs were visualised by UV light at 254 nm or 365 nm, or with an appropriate stain. Column chromatography purification was performed using a Biotage Isolera flash purification system with either Buchi FlashPure, Biotage SNAP or GraceResolv flash cartridges prepacked with silica gel (40-60 μm).

^{1}H NMR and ^{13}C NMR spectra were recorded at 400, 500, 600 or 700 MHz (for ^{1}H) and 100, 125, 150 or 175 MHz (for ^{13}C) on a Bruker AMX400, AMX500, AMX600 or AMX700 spectrometer respectively at ambient temperature, unless otherwise indicated. ^{11}B NMR was recorded at 160 or 225 MHz on a Bruker AMX500 or AMX700 spectrometer respectively. Deuterated solvents used for NMR spectroscopy were $CDCl_3$, CD_3CN, $(CD_3)_2CO$ or CD_2Cl_2 as stated in the spectrum.

Peaks are assigned as singlet (s), doublet (d), triplet (t), quartet (q), quintet (qn), sextet (sext), multiplet (m), broad (br) or combinations thereof. Chemical shifts, δ, are reported in parts per million (ppm) and compared against residual solvent signals: $CDCl_3$ (δ = 7.26 ppm, s), CD_3CN (δ = 1.94 ppm, qn) or CD_2Cl_2 (δ = 2.50 ppm, qn) as the internal standard. Coupling constants (J) are quoted in Hertz (Hz) to one decimal place.

Mass spectrometry was performed on a Waters VG70 SE spectrometer (ES+, CI, ES- modes). Infra-red spectra were obtained using a Perkin-Elmer Spectrum 100 FTIR Spectrometer operating in ATR mode; all frequencies reported in reciprocal centimetres (cm^{-1}). Melting points were measured with a Gallenkamp heating block and unless otherwise stated were recorded with an amorphous solid. Reactions performed above the solvent boiling point were carried out in a Radley Quick-Thread Glass Reaction Tube (24 × 150 mm).

4.2 General Procedures

General Procedure A: Synthesis of diazaborinane using iron catalysis and water[170]

To a solution of boronic acid (1 eq.) in MeCN (0. 25 M) was added, sequentially, a solution of $FeCl_3$ (5 mol%) in H_2O (0.05 M), imidazole (3 eq.) and 1,8-diaminonapthalene (1 eq.). The resulting mixture was stirred at room temperature for 3 h. The reaction was then diluted with H_2O (10 mL) and extracted with EtOAc (3 × 20 mL). The combined organic extracts were dried over $MgSO_4$ and concentrated *in vacuo*. The resultant crude residue was then purified by flash column chromatography to afford the corresponding product.

General Procedure B: Synthesis of diazaborinane using a Dean-Stark trap[171]

To a solution of 1,8-diaminonapthalene (1 eq.) in toluene (0.04 M) was added the boronic acid (1 eq.) in one portion. The round-bottom flask was equipped with a Dean-Stark trap, and the solution was stirred at reflux at 110 °C for 3 h. The reaction mixture was cooled to rt, concentrated *in vacuo* and the resultant crude residue was purified by flash column chromatography to afford the corresponding product.

General Procedure C: Synthesis of diazaborole

To a vial cooled to 0 °C, amine (2 mmol, 2 eq.) and nitrile (2 mL if acetonitrile, otherwise 6 eq. used) was added followed by $BrCH_2Bpin$ or BrCHR'Bpin (1 mmol, 1 eq.). The reaction mixture was stirred for a further 15 minutes at 0 °C and then transferred to an oil bath and heated at 65 °C for 18 h. The reaction mixture was allowed to cool to room temperature, diluted with sat. aq. $NaHCO_3$ (20 mL), extracted with DCM (3 × 20 mL) and washed with brine (20 mL). The combined organic extracts were dried over $MgSO_4$, filtered and concentrated *in vacuo*. The resultant crude residue was then purified by flash column chromatography to afford the corresponding product.

4.3 Characterisation data

4.3.1 Boron-directed C–H functionalisation

1-(2,3-Dihydro-1H-naphtho[1,8-de]-1,3,2-diazaborinyl)naphthalene, 125

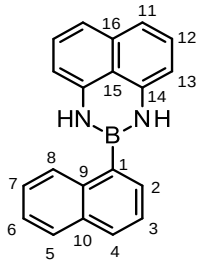

Following general procedure **A**, using naphthalene-1-boronic acid (340 mg, 1.98 mmol). Purification by flash column chromatography (cyclohexane/EtOAc = 10:1) afforded compound **125** (241 mg, 41%) as a grey solid. The spectral data were in accordance with those reported in the literature.[172]

^{1}H NMR (400 MHz, $CDCl_3$): δ 8.23 – 8.16 (m, 1H, H-8), 7.94 – 7.87 (m, 2H, H-4 and H-5), 7.70 (dd, *J* = 6.8, 1.2 Hz, 1H, H-2), 7.56 – 7.48 (m, 3H, H-3, H-6 and H-7), 7.17 (dd, *J* = 8.3, 7.2 Hz, 2H, H-12), 7.10 (dd, *J* = 8.3, 1.0 Hz, 2H, H-11), 6.39 (dd, *J* = 7.2, 1.1 Hz, 2H, H-13), 6.02 (br s, 2H, NH).

^{13}C NMR (101 MHz, $CDCl_3$): δ 141.2 (C-14), 136.5 (C-16), 135.5 (C-9), 133.4 (C-10), 130.8 (C-2), 129.6 (C-4), 128.9 (C-5), 128.0 (C-8), 127.8 (C-12), 126.4 (C-7), 126.0 (C-6), 125.5 (C-3), 120.1 (C-15), 118.1 (C-11), 106.1 (C-13). Note: the boron-bound carbon (C-1) was not detected, presumably due to quadrupolar relaxation.

^{11}B NMR (225 MHz, $CDCl_3$): δ 31.0.

HRMS (ESI): $C_{20}H_{16}BN_2$ [M+H$^+$]: calculated 295.1401, found 295.1396.

IR ν_{max} (neat/cm^{-1}): 3421 (N–H), 3402 (N–H), 3053 (aryl C–H), 1510 (aryl C=C)

m.p. 141-143 °C

2-Methyl-1-(2,3-dihydro-1H-naphtho[1,8-de]-1,3,2-diazaborinyl)benzene, 126

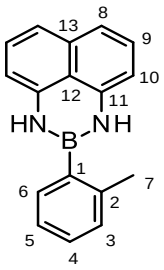

Following **general procedure A**, using 2-methylbenzeneboronic acid (150 mg, 1.10 mmol). Purification by flash column chromatography (petroleum ether/EtOAc = 10:1) afforded compound **126** (200 mg, 70%) as a grey solid. The spectral data were in accordance with those reported in the literature.[173]

^{1}H NMR (700 MHz, $CDCl_3$): δ 7.46 (dd, *J* = 7.5, 1.5 Hz, 1H, H-6), 7.33 (td, *J* = 7.5, 1.5 Hz, 1H, H-4), 7.25 – 7.23 (m, 2H, H-3 and H-5), 7.15 (dd, *J* = 8.5, 7.2 Hz, 2H, H-9), 7.07 (dd, *J* = 8.5, 1.1 Hz, 2H, H-8), 6.36 (dd, *J* = 7.2, 1.1 Hz, 2H, H-10), 5.83 (s, 2H, NH), 2.51 (s, 3H, H-7).

^{13}C NMR (176 MHz, $CDCl_3$): δ 141.2 (C-11), 140.8 (C-2), 136.5 (C-13), 132.4 (C-6), 129.8 (C-3), 129.4 (C-4), 127.8 (C-9), 125.4 (C-5), 119.9 (C-12), 118.0 (C-8), 106.0 (C-10), 22.5 (C-7). Note: the boron-bound carbon (C-1) was not detected, presumably due to quadrupolar relaxation.

^{11}B NMR (225 MHz, CD_3CN): δ 30.8.

HRMS (ESI): $C_{17}H_{16}BN_2$ [$M+H^+$]: calculated 259.1401, found 259.1396.

IR ν_{max} (neat/cm^{-1}): 3421 (N–H), 3406 (N–H), 3052 (aryl C–H), 1597 (aryl C=C).

m.p. 89-91 °C.

1-(2,3-Dihydro-1H-naphtho[1,8-de]-1,3,2-diazaborinyl)-cyclohexane, 127

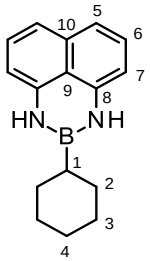

Following general procedure **B**, using cyclohexylboronic acid (400 mg, 3.13 mmol). Purification by flash column chromatography (cyclohexane/EtOAc = 10:1) afforded compound **127** (418 mg, 54%) as a light-yellow oil.

^{1}H NMR (700 MHz, $CDCl_3$): δ 7.09 (dd, *J* = 8.3, 7.3 Hz, 2H, H-6), 6.99 (dd, *J* = 8.3, 1.0 Hz, 2H, H-5), 6.29 (dd, *J* = 7.3, 1.0 Hz, 2H, H-7), 5.59 (br s, 2H, NH), 1.81 – 1.68 (m, 5H, H-2', H-3' and H-4'), 1.36–1.18 (m, 5H, H-2'', H-3'' and H-4''), 0.97 (tt, *J* =11.8, 3.1 Hz, 1H, H-1).

^{13}C NMR (176 MHz, $CDCl_3$): δ 141.4 (C-8), 136.5 (C-10), 127.7 (C-6), 119.8 (C-9), 117.5 (C-5), 105.6 (C-7), 29.0 (C-2), 27.6 (C-3), 26.9 (C-4). Note: the boron-bound carbon (C-1) was not detected, presumably due to quadrupolar relaxation.

^{11}B NMR (225 MHz, CD_3CN): δ 32.9.

HRMS (ESI): $C_{16}H_{20}BN_2$ [M+H$^+$]: calculated 251.1714, found 251.1706.

IR ν_{max} (neat/cm^{-1}): 3418 (N–H), 3406 (N–H), 3055 (aryl C–H), 2914 (alkyl C–H), 2843 (alkyl C–H), 1595 (aryl C=C).

1-(2,3-Dihydro-1H-naphtho[1,8-de]-1,3,2-diazaborinyl)-*n*-propane, 128

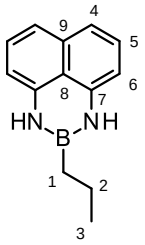

Following general procedure **B**, using *n*-propylboronic acid (175 mg, 1.99 mmol). Purification by flash column chromatography (petroleum ether/EtOAc = 10:1) afforded compound **128** (188 mg, 45%) as a light-yellow oil.

^{1}H NMR (400 MHz, $CDCl_3$): δ 7.10 (t, *J* = 7.7 Hz, 2H, H-5), 7.00 (d, *J* = 7.7, 1.0 Hz, 2H, H-4), 6.30 (dd, *J* = 7.7, 1.0 Hz, 2H, H-6), 5.61 (br s, 2H, NH), 1.48 (sext, *J* = 7.4 Hz, 2H, H-2), 1.00 (t, *J* = 7.4 Hz, 3H, H-3), 0.87 (t, *J* = 7.4 Hz, 2H, H-1).

^{13}C NMR (176 MHz, $CDCl_3$): δ 141.4 (C-7), 136.5 (C-9), 127.7 (C-5), 119.7 (C-8), 117.5 (C-4), 105.5 (C-6), 18.3 (C-2), 17.2 (C-3). Note: the boron-bound carbon (C-1) was not detected, presumably due to quadrupolar relaxation.

^{11}B NMR (225 MHz, $CDCl_3$): δ 32.0.

HRMS (ESI): $C_{13}H_{16}BN_2$ [M+H$^+$]: calculated 211.1401, found 211.1398.

IR ν_{max} (neat/cm^{-1}): 3402 (N–H), 3051 (aryl C–H), 2953 (alkyl C–H), 2924 (alkyl C–H), 2866 (alkyl C–H), 1595 (aryl C=C).

1-Iodonaphthalene, 131

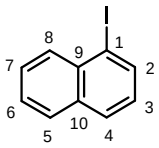

A mixture of compound **125** (37 mg, 0.13 mmol, 1 eq.), $Pd(OAc)_2$ (3 mg, 0.01 mmol, 0.1 eq.), $PhI(OAc)_2$ (122 mg, 0.38 mmol, 3 eq.) and I_2 (96 mg, 0.38 mmol, 3 eq.) in DMF (2 mL) was sealed under air in a 20 mL screw-capped glass tube and heated at 90 °C for 18 h. The reaction mixture was cooled, diluted with EtOAc then filtered through a pad of Celite® and the resulting filtrate concentrated *in vacuo*. Purification by flash column chromatography (petroleum ether/EtOAc = 95:5) afforded compound **131** (9 mg, 0.02 mmol, 17%) as a light-yellow oil. The spectral data were in accordance with those reported in the literature.[174]

^{1}H NMR (700 MHz, $CDCl_3$): δ 8.13 – 8.06 (m, 2H, H-2 and H-8), 7.84 (d, *J* = 7.7 Hz, 1H, H-4), 7.78 (dd, *J* = 8.1, 1.4 Hz, 1H, H-5), 7.58 (ddd, *J* = 8.4, 6.8, 1.3 Hz, 1H, H-7), 7.53 (ddd, *J* = 8.1, 6.8, 1.3 Hz, 1H, H-6), 7.19 (t, *J* = 7.7 Hz, 1H, H-3).

^{13}C NMR (176 MHz, $CDCl_3$): δ 137.6 (C-2), 134.5 (C-9), 134.3 (C-10), 132.3 (C-8), 129.1 (C-4), 128.7 (C-5), 127.8 (C-7), 127.0 (C3-), 126.9 (C-6), 99.7 (C-1).

IR ν_{max} (neat/cm^{-1}): 3051 (aryl C–H), 1557 (aryl C=C), 1498 (aryl C=C).

(*E*)-3-(Dimethylamino)-1-(2-nitrophenyl)prop-2-en-1-one, 128

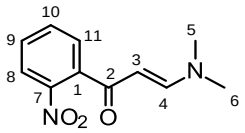

A solution of 2′-nitroacetophenone (1.49 g, 1.21 mL, 8.99 mmol, 1 eq.) and *N*,*N*-dimethylformamide dimethyl acetal (1.07 g, 1.2 mL, 8.99 mmol, 1 eq.) in DMF (4 mL) was heated at 100 °C for 3 h. The mixture was then cooled, concentrated *in vacuo* and purification by flash column chromatography (cyclohexane/EtOAc = 2:8) afforded compound **128** (1.44 g, 73%) as a yellow solid. The spectral data were in accordance with those reported in the literature.[175]

^{1}H NMR (400 MHz, $CDCl_3$): δ 7.96 (d, *J* = 8.1 Hz, 1H, H-8), 7.64 – 7.59 (m, 2H, H-4 and H-10), 7.55 – 7.42 (m, 2H, H-9, H-11), 5.27 (d, *J* = 12.6 Hz, 1H, H-3), 3.10 (br s, 3H, H-5/H-6), 2.86 (s, 3H, H-5/H-6).

^{13}C NMR (176 MHz, $CDCl_3$): δ 189.0 (br s, C-2), 154.9 (br s, C-4), 147.4 (C-7), 138.8 (br s, C-1), 133.2 (C-10), 129.5 (C-11), 129.0 (C-9), 124.4 (-C8), 94.0 (br s, C-3), 45.3 (C-5), 37.4 (C-6).

HRMS (ESI): $C_{11}H_{13}N_2O_3$ [M+H$^+$]: calculated 221.0921, found 221.0919.

IR ν_{max} (neat/cm^{-1}): 3057 (aryl C–H), 3030 (alkene C–H), 2884 (alkyl C–H), 2808 (alkyl C–H), 1638 (C=O), 1577 (aryl C=C), 1541 (alkene C=C), 1518 (N-O).

m.p. 135-137 °C.

5-(2-Nitrophenyl)-1*H*-pyrazole, 129

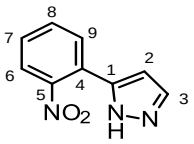

A solution of compound **128** (700 mg, 3.19 mmol, 1 eq.) and hydrazine monohydrate (64%, 266 µL, 5.49 mmol, 1.1 eq.) in EtOH (10 mL) was stirred at reflux at 79 °C for 4 h. The mixture was then cooled, concentrated *in vacuo* and purification by flash column chromatography (cyclohexane/EtOAc = 7:3) afforded compound **129** (464 mg, 77%) as an orange solid. The spectral data were in accordance with those reported in the literature.[176]

^{1}H NMR (400 MHz, $CDCl_3$): δ 11.21 (br s, 1, NH), 7.72 (dd, *J* = 3.6, 1.4 Hz, 1H, H-6), 7.70 (dd, *J* = 3.4, 1.4 Hz, 1H, H-9), 7.62 (d, *J* = 2.4 Hz, 1H, H-3), 7.59 (td, *J* = 7.6, 1.3 Hz, 1H, H-8), 7.47 (td, *J* = 7.6, 1.5 Hz, 1H, H-7), 6.50 (d, *J* = 2.4 Hz, 1H, H-2).

^{13}C NMR (176 MHz, $CDCl_3$): δ 149.3 (C-5), 146.4 (C-1), 132.0 (C-8), 131.0 (C-9), 130.8 (C-3), 128.8 (C-7), 127.0 (C-4), 123.7 (C-6), 104.9 (C-2).

HRMS (ESI): $C_9H_8N_3O_2$ [M+H$^+$]: calculated 190.0611, found 190.0611.

IR ν_{max} (neat/cm^{-1}): 3283 (N–H), 3146 (aryl C–H), 3129 (aryl C–H), 1520 (N-O), 1504 (aryl C=C).

m.p. 81-83 °C.

2-(1*H*-Pyrazol-5-yl)aniline, 104

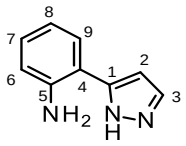

A mixture of compound **129** (464 mg, 2.45 mmol, 1 eq.) and 5% Pd/C (99 mg) in EtOH (15 mL) was degassed by evacuation and backfilling with Ar thrice. A balloon of H_2 was then attached, and the round-bottom flask evacuated and back-filled with H_2 thrice before stirring at room temperature for 21 h. The mixture was then filtered through a pad of Celite® and the filtrate concentrated *in vacuo* to afford compound **104** (320 mg, 82%) as a grey solid. This was used in the next step without further purification. The spectral data were in accordance with those reported in the literature.[176]

^{1}H NMR (700 MHz, DMSO-d_6): δ 12.85 (s, 1H, NH), 7.78 (d, *J* = 2.4 Hz, 1H, H-3), 7.49 (d, *J* = 7.4 Hz, 1H, H-9), 6.98 (t, *J* = 7.4 Hz, 1H, H-7), 6.72 (d, *J* = 7.4 Hz, 1H, H-6), 6.68 (d, *J* = 2.4 Hz, 1H, H-2), 6.56 (t, *J* = 7.4 Hz, 1H, H-8), 6.30 (s, 2H, NH_2).

^{13}C NMR (176 MHz, DMSO-d_6): δ 151.4 (C-1), 145.7 (C-5), 128.9 (C-3), 127.8 (two coinciding peaks; C-7 and C-9), 115.5 (C-6), 115.4 (C-8), 115.3 (C-4), 102.1 (C-2).

HRMS (ESI): $C_9H_{10}N_3$ [M+H$^+$]: calculated 160.0869, found 160.0869.

IR ν_{max} (neat/cm^{-1}): 3406 (N–H), 3262 (N–H), 3136 (aryl C–H), 1607 (aryl C=C).

m.p. 120-122 °C.

5-Phenyl-6*H*-pyrazolo[1,5-c][1,3,2]benzodiazaborinine, 107

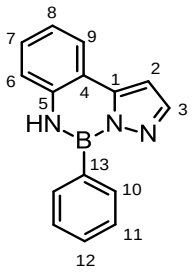

Compound **104** (398 mg, 3.27 mmol, 1 eq.) and phenylboronic acid (520 mg, 3.27 mmol, 1 eq.) were dissolved in toluene (5 mL) and the resulting solution was added to a round-bottom flask equipped with a Dean-Stark trap. The solution was stirred at reflux at 110 °C for 3 h. The reaction mixture was then cooled, concentrated *in vacuo* and purification by Kugelrohr distillation (225 °C, 1–10 mmHg) afforded compound **107** (549 mg, 67%) as a white solid. The spectral data were in accordance with those reported in the literature.[115]

^{1}H NMR (700 MHz, $CDCl_3$): δ 8.31 – 8.24 (m, 2H, H-10), 8.13 (d, *J* = 1.8 Hz, 1H, H-3), 7.96 (d, *J* = 7.2 Hz, 1H, H-9), 7.55 – 7.51 (m, 3H, H-11 and H-12), 7.42 (t, *J* = 7.6 Hz, 1H, H-7), 7.27 – 7.23 (m, 2H, H-6 and H-8), 7.17 (br s, 1H, NH), 6.97 (d, *J* = 1.8 Hz, 1H, H-2).

^{13}C NMR (176 MHz, $CDCl_3$): δ 146.0 (C-3), 145.3 (C-1), 136.6 (C-5), 134.5 (C-10), 130.9 (C-12), 129.1 (C-7), 128.3 (C-11), 125.1 (C-9), 122.5 (C-8), 117.8 (C-6), 117.2 (C-4), 100.3 (C-2). Note: the boron-bound carbon (C-13) was not detected, presumably due to quadrupolar relaxation.

^{11}B NMR (225 MHz, $CDCl_3$): δ 29.3.

HRMS (ESI): $C_{15}H_{13}BN_3$ [M+H$^+$]: calculated 246.1197, found 246.1025.

IR ν_{max} (neat/cm^{-1}): 3416 (N–H), 3314 (aryl C–H), 1620 (aryl C=C).

m.p. 123-125 °C.

Triethyl-[2-(4,4,5,5-tetramethyl-1,3,2-dioxaborolan-2-yl)phenyl]silane, 131

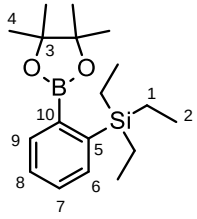

A mixture of compound **107** (61 mg, 0.25 mmol, 1 eq.), $RuH_2(CO)(PPh_3)_3$ (13.8 mg, 0.02 mmol, 0.06 eq.), norbornene (118 mg, 1.25 mmol, 5 eq.) and triethylsilane (145 mg, 200 µL, 1.25 mmol, 5 eq.) in degassed toluene (0.13 mL) was heated at 135 °C for 18 h. The resultant mixture was cooled, and pinacol (59 mg, 0.50 mmol, 2 eq.), *p*-toluenesulfonic acid monohydrate (95 mg, 0.50 mmol, 2 eq.) and THF (1 mL) were added, whereupon the mixture was stirred at room temperature for 3 h. The reaction mixture was diluted with EtOAc, filtered through a pad of Florisil® and the filtrate was concentrated *in vacuo*. Purification by flash column chromatography (cyclohexane/EtOAc = 95:5) afforded compound **131** (15 mg, 26%) as a colourless oil.

^{1}H NMR (700 MHz, $CDCl_3$): δ 7.89 (dd, *J* = 7.4, 1.5 Hz, 1H, H-9), 7.56 (dd, *J* = 7.4, 1.3 Hz, 1H, H-6), 7.38 (td, *J* = 7.4, 1.5 Hz, 1H, H-7), 7.33 (td, *J* = 7.4, 1.3 Hz, 1H, H-8), 1.35 (s, 12H, H-4), 0.93 – 0.91 (m, 15H, H-1 and H-2).

^{13}C NMR (176 MHz, $CDCl_3$): δ 143.8 (C-5), 136.2 (C-9), 135.5 (C-6), 129.6 (C-7), 127.7 (C-8), 83.8 (C-3), 25.0 (C-4), 7.9 (C-2), 4.4 (C-1). Note: the boron-bound carbon (C-10) was not detected, presumably due to quadrupolar relaxation.

^{11}B NMR (225 MHz, $CDCl_3$): δ 31.9.

5-Phenylpyrazolo[1,5-c][1,3,2]benzoxazaborinine, 138

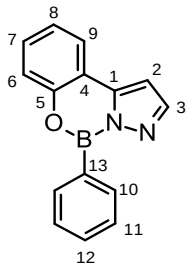

To a solution of 2-(1*H*-Pyrazol-5-yl)phenol (400 mg, 2.50 mmol, 1 eq.) in toluene (10 mL) was added phenylboronic acid (365 mg, 3.00 mmol, 1.2 eq.) in one portion. The round-bottom flask was equipped with a Dean-Stark trap, and the solution was stirred at reflux at 110 °C for 3 h. The reaction mixture was then cooled and concentrated *in vacuo*. Purification by flash column chromatography (cyclohexane/EtOAc = 8:2) afforded compound **138** (451 mg, 73%) as a white solid. The spectral data were in accordance with those reported in the literature.[117]

^{1}H NMR (700 MHz, $CDCl_3$): δ 8.27 (d, *J* = 2.5 Hz, 1H, H-3), 7.58 (dd, *J* = 7.5, 1.7 Hz, 1H, H-9), 7.25 (ddd, *J* = 8.3, 7.5, 1.7 Hz, 1H, H-7), 7.00 (dd, *J* = 8.3, 1.1 Hz, 1H, H-6), 6.92 (td, *J* = 7.5, 1.1 Hz, 1H, H-8), 6.87 (t, *J* = 7.6 Hz, 1H, H-12), 6.80 (d, *J* = 2.5 Hz, 1H, H-2), 6.76 (t, *J* = 7.6 Hz, 2H, H-11), 6.70 – 6.67 (d, *J* = 7.6 Hz, 2H, H-10).

^{13}C NMR (176 MHz, $CDCl_3$): δ 153.8 (C-5), 143.5 (C-1), 134.7 (C-3), 131.9 (C-7), 130.9 (C-10), 127.0 (C-12), 126.9 (C-11), 125.4 (C-9), 120.2 (C-8), 119.8 (C-6), 115.8 (C-4), 101.3 (C-2). Note: the boron-bound carbon (C-13) was not detected, presumably due to quadrupolar relaxation.

^{11}B NMR (225 MHz, $CDCl_3$): δ 3.4.

HRMS (ESI): $C_{15}H_{12}BN_2O$ [M+H$^+$]: calculated 247.1037, found 247.1039.

IR ν_{max} (neat/cm^{-1}): 3134 (aryl C–H), 3119 (aryl C–H), 3071 (aryl C–H), 3009 (aryl C–H), 1614 (aryl C=C).

m.p. > 250 °C

2-(2-Pyridylamino)phenol, 144b

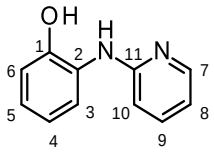

2-Aminophenol (327 mg, 3.00 mmol, 3 eq.), copper(I) iodide (19 mg, 0.10 mmol, 0.1 eq.) and K_3PO_4 (425 mg, 2.00 mmol, 2 eq.) was added to screw-cap glass tube. The tube was then evacuated and back-filled with Ar thrice. Under a flow of Ar, 2-iodopyridine (205 mg, 106 µL, 1.00 mmol, 1 eq.) was added followed by 1,4-dioxane (2 mL) and the resultant mixture was heated at 110 °C for 16 h. The mixture was then cooled, and EtOAc (10 mL) and H_2O (1 mL) were added to the reaction mixture and stirred for 5 min. The organic layer was separated, and the aqueous layer further extracted with EtOAc (2 × 30 mL). The combined organic extracts were dried over $MgSO_4$ and concentrated *in vacuo*. Purification by flash column chromatography (cyclohexane/EtOAc = 3:1) afforded compound **145b** (232 mg, quantitative yield) as a dark red oil. The spectral data were in accordance with those reported in the literature.[177]

^{1}H NMR (700 MHz, $CDCl_3$): δ 8.07 (dd, *J* = 5.8, 1.8 Hz, 1H, H-7), 7.52 (ddd, *J* = 8.4, 7.2, 1.9 Hz, 1H, H-9), 7.09 – 7.04 (m, 2H, H-5 and H-6), 6.95 (ddd, *J* = 7.9, 1.3, 0.6 Hz, 1H, H-3), 6.83 (ddd, *J* = 7.9, 6.1, 2.6 Hz, 1H, H-4), 6.73 – 6.67 (m, 2H, H-8 and H-10), 6.35 (br s, 1H, NH).

^{13}C NMR (176 MHz, $CDCl_3$): δ 156.4 (C-11), 149.6 (C-1), 146.2 (C-7), 139.0 (C-9), 129.4 (C-2), 125.8 (C-5), 122.4 (C-3), 120.2 (C-4), 120.1 (C-6), 114.3 (C-8), 110.8 (C-10).

HRMS (ESI): $C_{11}H_{11}N_2O$ [M+H$^+$]: calculated 187.0866, found 187.0866.

IR ν_{max} (neat/cm^{-1}): 3306 (O-H), 3229 (N–H), 3198 (aryl C–H), 3103 (aryl C–H), 1628 (aryl C=C).

***N*[1]-(Pyridin-2-yl)benzene-1,2-diamine, 145b**

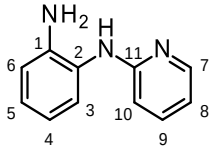

Benzene-1,2-diamine (540 mg, 5.0 mmol, 1 eq.) was added to 2-chloropyridine (624 mg, 520 µL, 5.5 mmol, 1.1 eq.) and the resulting mixture was heated at 160 °C for 13 h. The mixture was cooled, and acetone (10 mL) and H_2O (10 mL) were added to fully dissolve the reaction mixture. The pH value of the resulting solution was adjusted to 10 by adding Na_2CO_3 portion-wise. The mixture was then extracted with EtOAc (3 × 30 mL) and the combined organic extracts were washed with brine (30 mL), dried over $MgSO_4$ and concentrated *in vacuo*. Purification by flash column chromatography (cyclohexane/EtOAc = 2:8) afforded compound **145b** (233 mg, 25%) as a light brown solid. The spectral data were in accordance with those reported in the literature.[178]

^{1}H NMR (700 MHz, $CDCl_3$): δ 8.13 (d, *J* = 5.1 Hz, 1H, H-7), 7.46 (ddd, *J* = 8.6, 7.2, 1.9 Hz, 1H, H-9), 7.18 (dd, *J* = 7.6, 1.5 Hz, 1H, H-3), 7.09 (td, *J* = 7.6, 1.5 Hz, 1H, H-5), 6.82 (dd, *J* = 7.6, 1.5 Hz, 1H, H-6), 6.77 (td, *J* = 7.6, 1.5 Hz, 1H, H-4), 6.70 (dd, *J* = 7.2, 5.1 Hz, 1H, H-8), 6.50 (br s, 1H, NH), 6.45 (d, *J* = 8.6 Hz, 1H, H-10), 3.75 (br s, 2H, NH_2).

^{13}C NMR (176 MHz, $CDCl_3$): δ 157.5 (C-11), 147.3 (C-7), 143.2 (C-1), 138.6 (C-9), 127.6 (C-5), 127.2 (C-3), 125.4 (C-2), 119.1 (C-4), 116.4 (C-6), 114.5 (C-8), 107.8 (C-10).

HRMS (ESI): $C_{11}H_{12}N_3$ [M+H$^+$]: calculated 186.1026, found 186.1026.

IR ν_{max} (neat/cm^{-1}): 3478 (N–H), 3383 (N–H), 3090 (aryl C–H), 3003 (aryl C–H), 1622 (N–H), 1583 (aryl C=C).

2-[[(2-Hydroxyphenyl)imino]methyl]phenol, 161

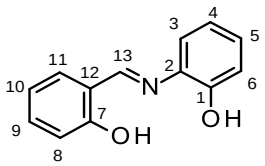

A mixture of 2-aminophenol (4.50 g, 0.04 mol, 1 eq.) and 2-hydroxybenzaldehyde (5.04 g, 4.30 mL, 0.04 mol, 1 eq.) in EtOH (30 mL) was stirred at reflux at 79 °C for 2 h. The resulting red mixture was then cooled to rt and concentrated *in vacuo* to two thirds the volume and then cooled in an ice bath. The solid obtained was filtered and washed with ice-cold EtOH (3 × 10 mL) to afford compound **161** (7.70 g, 88%) as a crystalline red solid.

^{1}H NMR (700 MHz, DMSO-d_6): δ 13.77 (br s, 1H, OH), 9.73 (br s, 1H, OH), 8.96 (s, 1H, H-13), 7.61 (dd, *J* = 7.6, 1.8 Hz, 1H, H-11), 7.38 (ddd, *J* = 8.3, 7.3, 1.7 Hz, 1H, H-9), 7.35 (dd, *J* = 8.1, 1.6 Hz, 1H, H-3), 7.12 (ddd, *J* = 8.1, 7.3, 1.6 Hz, 1H, H-5), 6.98 – 6.92 (m, 3H, H-6, H-8 and H-10), 6.88 (td, *J* = 8.1, 1.4 Hz, 1H, H-4).

^{13}C NMR (176 MHz, DMSO-d_6): δ 161.7 (C-13), 160.7 (C-7), 151.1 (C-1), 135.0 (C-2), 132.8 (C-9), 132.3 (C-11), 128.0 (C-5), 119.6 (two coinciding peaks; C-3 and C-4), 119.5 (C-12), 118.7 (C-10), 116.7 (C-8), 116.5 (C-6).

HRMS (ESI): $C_{13}H_{12}NO_2$ [M+H$^+$]: calculated 214.0862, found 214.0862.

IR ν_{max} (neat/cm^{-1}): 3045 (aryl C–H), 3024 (aryl C–H), 3012 (aryl C–H), 1626 (C=N). 1604 (aryl C=C).

m.p. 185-187 °C.

2-Phenyl-benzo[d]benzo[h]-6-aza-1,3-dioxa-2-boracyclonon-6-ene, 162

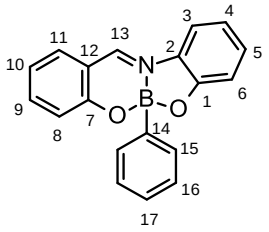

A mixture of compound **161** (470 mg, 2.20 mmol, 1 eq.) and phenylboronic acid (269 mg, 2.20 mmol, 1 eq.) in MeCN (10 mL) was heated at 82 °C for 17 h. The resulting orange solution was then cooled to rt, concentrated *in vacuo* followed by recrystallisation from $CHCl_3$/*N*–*H*exane (1:1) to afford compound **162** (488 mg, 74%) as orange plates.

^{1}H NMR (700 MHz, $CDCl_3$): δ 8.32 (s, 1H, H-13), 7.55 (ddd, *J* = 8.4, 7.9, 1.7 Hz, 1H, H-9), 7.44 (ddd, *J* = 7.9, 1.4, 0.5 Hz, 1H, H-3), 7.38 (dd, *J* = 7.2, 1.7 Hz, 1H, H-11), 7.36 – 7.31 (m, 3H, H-5 and H-15), 7.22 (ddt, *J* = 8.4, 1.2, 0.5 Hz, 1H, H-8), 7.19 – 7.15 (m, 1H, H-17), 7.15 – 7.12 (m, 2H, H-16), 7.11 (dd, *J* = 8.1, 1.2 Hz, 1H, H-6), 6.94 (ddd, *J* = 7.9, 7.2, 1.1 Hz, 1H, H-10), 6.91 (td, *J* = 7.9, 1.1 Hz, 1H, H-4).

^{13}C NMR (176 MHz, $CDCl_3$): δ 158.9 (C-1), 157.7 (C-7), 148.7 (C-13), 138.1 (C-9), 132.5 (C-5), 131.5 (C-11), 131.4 (C-15), 130.7 (C-2), 128.0 (C-17), 127.6 (C-16), 120.5 (two coinciding peaks; C-8 and C-10), 119.5 (C-4), 119.4 (C-12), 115.4 (C-6), 115.2 (C-3). Note: the boron-bound carbon (C-14) was not detected, presumably due to quadrupolar relaxation.

^{11}B NMR (225 MHz, $CDCl_3$): δ 8.4.

HRMS (ESI): $C_{19}H_{15}BNO_2$ [M+H$^+$]: calculated 300.1190, found 300.1189.

IR ν_{max} (neat/cm^{-1}): 3046 (aryl C–H), 3024 (aryl C–H), 2970 (alkyl C–H), 1625 (C=N).

m.p. 201-203 °C.

2-(1-(2-Hydroxyphenyl)ethylideneamino)phenol, 163a

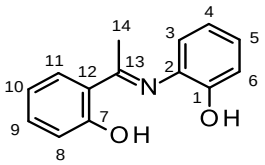

A mixture of 2-aminophenol (1.64 g, 0.02 mol, 1 eq.) and 2′-hydroxyacetophenone (2.05 g, 1.81 mL, 0.02 mol, 1 eq.) in EtOH/toluene (2:1, 25/13 mL) was stirred at 79 °C for 22 h. After cooling to rt, the solid was filtered off and washed with ice-cold EtOH (3 × 10 mL) to afford compound **163a** (570 mg, 17 %) as a yellow solid.

^{1}H NMR (700 MHz, $CDCl_3$): δ 14.33 (br s, 1H, OH), 7.65 (dd, *J* = 8.0, 1.6 Hz, 1H, H-11), 7.39 (ddd, *J* = 8.3, 7.2, 1.7 Hz, 1H, H-9), 7.13 (ddd, *J* = 8.1, 7.6, 1.6 Hz, 1H, H-5), 7.00 – 7.03 (m, 2H, H-6 and H-8), 6.95 (td, *J* = 7.6, 1.4 Hz, 1H, H-4), 6.91 (ddd, *J* = 8.0, 7.2, 1.3 Hz, 1H, H-10), 6.81 (dd, *J* = 7.6, 1.6 Hz, 1H, H-3), 5.20 (br s, 1H, OH), 2.40 (s, 3H, H-14).

^{13}C NMR (176 MHz, $CDCl_3$): δ 175.6 (C-13), 162.1 (C-7), 147.5 (C-1), 133.9 (C-2), 133.8 (C-9), 129.3 (C-11), 126.9 (C-5), 122.1 (C-3), 120.8 (C-4), 119.8 (C-12), 118.6 (C-10), 118.5 (C-8), 116.2 (C-6), 17.7 (C-14).

HRMS (ESI): $C_{14}H_{14}NO_2$ [M+H$^+$]: calculated 228.1019, found 228.1018.

IR ν_{max} (neat/cm^{-1}): 3342 (O-H), 3061 (aryl C–H), 3007 (aryl C–H), 1601 (C=N), 1578 (aryl C=C), 1364 (O-H).

m.p. 204-206 °C.

2-Phenyl-benzo[d]benzo[h]-6-aza-1,3-dioxa-2-bora-6-methylcyclonon-6-ene, 163

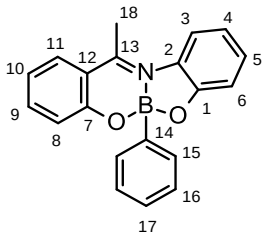

A mixture of compound **163a** (350 mg, 1.54 mmol, 1 eq.) and phenylboronic acid (188 mg, 1.54 mmol, 1 eq.) in MeCN (8 mL) was heated at 82 °C for 17 h. The resulting yellow solution was then cooled to rt, concentrated *in vacuo* followed by recrystallisation from chloroform/ *n*–Hexane (3:1) to afford compound **163** (414 mg, 86%) as a yellow crystalline solid.

^{1}H NMR (700 MHz, $CDCl_3$): δ 7.59 – 7.52 (m, 2H, H-9 and H-11), 7.51 (dd, *J* = 8.0, 1.4 Hz, 1H, H-3), 7.34 (td, *J* = 8.0, 1.3 Hz, 1H, H-5), 7.28 – 7.25 (m, 2H, H-15), 7.23 (dd, *J* = 8.3 Hz, 1H, H-8), 7.15 – 7.08 (m, 3H, H-6, H-16 and H-17), 6.95 (ddd, *J* = 8.2, 7.2, 1.2 Hz, 1H, H-10), 6.91 (td, *J* = 8.0, 1.3 Hz, 1H, H-4), 2.77 (s, 3H, H-18).

^{13}C NMR (176 MHz, $CDCl_3$): δ 161.3 (C-13), 159.5 (C-1), 157.2 (C-7), 137.2 (C-9), 131.8 (C-5), 131.7 (C-2), 131.5 (C-15), 128.8 (C-11), 127.7 (C-17), 127.4 (C-16), 121.6 (C-12), 120.8 (C-8), 120.3 (C-3), 120.2 (C-10), 118.9 (C-4), 115.1 (C-6), 18.3 (C-18). Note: the boron-bound carbon (C-14) was not detected, presumably due to quadrupolar relaxation.

^{11}B NMR (225 MHz, $CDCl_3$): δ 8.1.

HRMS (ESI): $C_{20}H_{17}BNO_2$ [M+H$^+$]: calculated 314.1347, found 314.1345.

IR ν_{max} (neat/cm^{-1}): 3067 (aryl C–H), 3043 (aryl C–H), 3026 (aryl C–H), 2922 (alkyl C–H), 1614 (aryl C=C).

m.p. 209-210 °C.

2-[[(2-Hydroxyphenyl)amino]methyl]phenol, 164a

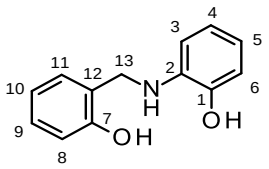

To a flame-dried round-bottom flask was added compound **161** (500 mg, 2.34 mmol, 1 eq) in DCM (5 mL) and AcOH (0.5 mL) before cooling to 0 °C with an ice-bath. To this cold solution was added $NaBH_3CN$ (265 mg, 4.22 mmol, 1.8 eq) and stirring was continued for 4 h at rt. The reaction mixture was then diluted with H_2O (5 mL) and extracted with $CHCl_3$ (3 × 30 mL). The combined organic extracts were washed with brine (30 mL) and concentrated *in vacuo*. Purification by flash column chromatography (cyclohexane/EtOAc = 1:1) afforded compound **164a** (238 mg, 47%) as a white solid.

^{1}H NMR (700 MHz, $CDCl_3$): δ 7.22 (ddd, *J* = 8.1, 7.4, 1.7 Hz, 1H, H-9), 7.16 (ddd, *J* = 7.5, 1.7, 0.9 Hz, 1H, H-11), 6.92 – 6.85 (m, 4H, H-3, H-4, H-8 and H-10), 6.79 (td, *J* = 7.5, 1.6 Hz, 1H, H-5), 6.76 (dd, *J* = 7.5, 1.6 Hz, 1H, H-6), 4.42 (s, 2H, H-13).

^{13}C NMR (176 MHz, $CDCl_3$): δ 156.9 (C-7), 145.0 (C-1), 135.7 (C-2), 129.3 (C-9), 128.8 (C-11), 123.1 (C-12), 121.8 (C-4), 121.1 (C-5), 120.2 (C-10), 116.8 (C-8), 115.7 (C-3), 114.9 (C-6), 49.0 (C13).

HRMS (ESI): $C_{13}H_{14}NO_2$ $[M+H^+]$: calculated 216.1019, found 216.1011.

IR ν_{max} (neat/cm^{-1}): 3485 (O-H), 3056 (N–H), 3045 (aryl C–H), 2963 (alkyl C–H), 2891 (alkyl C–H), 1608 (aryl C=C).

m.p. 101-102 °C.

2-Phenyl-benzo[d]-benzo[h]-6-aza-1,3-dioxa-2-boracyclononene, 164

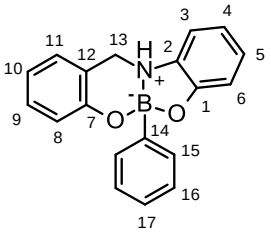

A mixture of compound **164a** (225 mg, 1.05 mmol, 1 eq.) and phenylboronic acid (127 mg, 1.05 mmol, 1 eq.) in MeCN (5 mL) was heated at 82 °C for 17 h. The reaction mixture was then cooled to rt, concentrated *in vacuo* followed by recrystallisation from $CHCl_3$/MeOH to afford compound **120** (252 mg, 80%) as a light brown crystalline solid.

^{1}H NMR (700 MHz, $CDCl_3$): δ 7.68 – 7.63 (m, 2H, H-15), 7.34 – 7.28 (m, 3H, H-16 and H-17), 7.23 (td, *J* = 8.1, 1.6 Hz, 1H, H-9), 7.15 – 7.10 (m, 2H, H-3 and H-5), 7.02 (dd, *J* = 8.1, 1.2 Hz, 1H, H-8), 6.91 (dt, *J* = 7.3, 1.2 Hz, 1H, H-11), 6.82 – 6.76 (m, 2H, H-6 and H-10), 6.73 (td, *J* = 7.7, 1.2 Hz, 1H, H-4), 5.78 (br s, 1H, NH), 4.56 (dd, *J* = 13.1, 4.0 Hz, 1H, H-13'), 4.08 (dd, *J* = 13.1, 2.2 Hz, 1H, H-13'').

^{13}C NMR (176 MHz, $CDCl_3$): δ 159.5 (C1), 156.9 (C-7), 131.8 (C-15), 130.9 (C-5), 130.7 (C-9), 128.5 (C-17), 128.3 (C-11), 128.2 (C-16), 127.5 (C-2), 120.8 (C-10), 120.7 (C-3), 120.2 (C-12), 120.0 (C-8), 118.7 (C-4), 113.9 (C-6), 50.5 (C-13). Note: the boron-bound carbon (C-14) was not detected, presumably due to quadrupolar relaxation.

^{11}B NMR (225 MHz, $CDCl_3$): δ 9.2.

LRMS (ESI): $C_{19}H_{17}BNO_2$ [M+H$^+$]: calculated 302.13, found 216.07; likely fragment **164a**.

IR ν_{max} (neat/cm^{-1}): 3165 (N–H), 3050 (aryl C–H), 2918 (alkyl C–H), 2850 (alkyl C–H), 1600 (aryl C=C).

m.p. 216-218 °C.

8,10-Dimethyl-6-phenyl-5,7-dioxa-11-aza-6-bora-benzocyclononene, 165

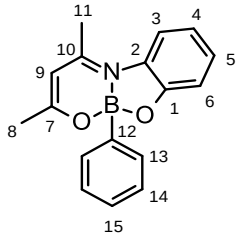

A mixture of 2-aminophenol (358 mg, 3.28 mmol, 1 eq.), phenylboronic acid (400 mg, 3.28 mmol, 1 eq.) and acetylacetone (328 mg, 337 µL, 3.28 mmol, 1 eq.) in toluene (15 mL) was added to a round-bottom flask equipped with a Dean-Stark trap and heated at 85 °C for 18 h. The reaction mixture was then cooled to rt and concentrated *in vacuo* to afford compound **165** (186 mg, 21%) as a yellow oil. This was used in the next step without further purification.

^{1}H NMR (700 MHz, $CDCl_3$): δ 7.35 – 7.31 (m, 3H, H-3 and H-13), 7.22 – 7.18 (m, 4H; H-5, H-14 and H-15), 7.03 (dd, *J* = 8.1, 1.2 Hz, 1H, H-6), 6.83 (td, *J* = 7.8, 1.2 Hz, 1H, H-4), 5.55 (s, 1H, H-9), 2.44 (s, 3H, H-11), 2.22 (s, 3H, H-8).

^{13}C NMR (176 MHz, $CDCl_3$): δ 173.3 (C-7), 161.2 (C-10), 156.8 (C-1), 132.5 (C-2), 131.0 (C-13), 128.9 (C-5), 127.8 (C-15), 127.5 (C-14), 118.7 (C-4), 118.0 (C-3), 114.2 (C-6), 103.6 (C-9), 23.0 (C-8), 21.3 (C-11). Note: the boron-bound carbon (C-12) was not detected, presumably due to quadrupolar relaxation.

^{11}B NMR (225 MHz, $CDCl_3$): δ 8.3.

HRMS (ESI): $C_{17}H_{17}BNO_2$ [M+H$^+$]: calculated 278.1347, found 278.1346.

IR ν_{max} (neat/cm^{-1}): 3067 (aryl C–H), 3007 (aryl C–H), 2959 (alkyl C–H), 2918 (alkyl C–H), 1625 (C=N), 1600 (aryl C=C).

m.p. 163-165 °C.

Ethyl 6-methyl-3,4-dihydro-2H-pyran-5-carboxylate, 173

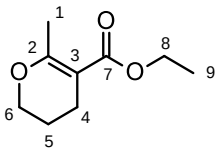

To a solution of sodium ethoxide (21% solution in EtOH, 7.40 mL, 0.02 mol, 1 eq.) in EtOH (50 mL) cooled to 0 °C, was added ethyl acetoacetate (2.5 mL, 0.02 mol, 1 eq.) dropwise followed by NaI (20 mg) and 1,3-dibromopropane (4.0 g, 2.01 mL, 0.02 mol, 1 eq.). The resulting clear orange solution was heated to reflux at 80 °C for 18 h. The cloudy orange reaction mixture was allowed to cool to rt and then concentrated in vacuo. The resulting residue was then diluted with H_2O (10 mL) and extracted with Et_2O (3 × 30 mL). The combined organic extracts were dried over $MgSO_4$, filtered and concentrated *in vacuo*. The resultant crude residue was then purified by flash column chromatography to afford **173** (778 mg, 28%) as a colourless oil.

^{1}H NMR (700 MHz, $CDCl_3$): δ 4.12 (q, *J* = 7.1 Hz, 2H, H-8), 3.98 (t, *J* = 6.0 Hz, 2H, H-6), 2.27 (td, *J* = 6.5, 1.6 Hz, 2H, H-4), 2.19 (br t, *J* = 2.1 Hz, 3H, H-1), 1.82 – 1.77 (m, 2H, H-5), 1.24 (t, *J* = 7.1 Hz, 3H, H-9).

^{13}C NMR (176 MHz, $CDCl_3$): δ 168.8 (C-7), 164.9 (C-2), 101.5 (C-3), 66.8 (C-6), 59.6 (C-8), 21.8 (C-5), 21.5 (C-4), 20.4 (C-1), 14.5 (C-9).

HRMS (ESI): $C_9H_{15}O_3$ [M+H$^+$]: calculated 171.1016, found 171.1016.

IR ν_{max} (neat/cm^{-1}): 2978 (alkyl C–H), 2951 (alkyl C–H), 2882 (alkyl C–H), 2859 (alkyl C–H), 1701 (C=O).

Ethyl 3-[(2-ethoxy-2-oxo-ethyl)-methyl-amino]butanoate, 174

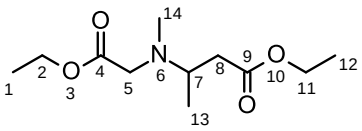

To a solution of ethyl acetoacetate (278 µL, 2.20 mmol, 1 eq.) in DCE (10 mL) cooled to 0 °C, was added sarcosine ethyl ester hydrochloride (405 mg, 2.64 mmol, 1.2 eq.), triethylamine (429 µL, 3.08 mmol, 1.4 eq.) and acetic acid (251 µL, 4.40 mmol, 2 eq.). The resulting suspension stirred at 0 °C for a further 15 mins before adding $NaBH(OAc)_3$ (932 mg, 4.40 mmol, 2 eq.) and then stirred at rt for 2 days. The resulting reaction mixture was then quenched with sat. aq. $NaHCO_3$ (15 mL) and extracted with DCM (3 × 30 mL). The combined organic extracts were dried over $MgSO_4$, filtered and concentrated *in vacuo*. The resultant crude residue was then purified by flash column chromatography to afford **174** (318 mg, 63%) as a light-yellow oil.

^{1}H NMR (700 MHz, $CDCl_3$): δ 4.14 (q, *J* = 7.1 Hz, 2H, H-2), 4.10 (q, *J* = 7.2 Hz, 2H, H-11), 3.27 – 3.22 (m, 1H, H-7), 3.20 (d, *J* = 3.7 Hz, 2H, H-5), 2.54 (dd, *J* = 14.5, 5.5 Hz, 1H, H-8'), 2.31 (s, 3H, H-14), 2.19 (dd, *J* = 14.5, 8.6 Hz, 1H, H-8''), 1.23 (t, *J* = 7.1 Hz, 3H, H-1), 1.22 (t, *J* = 7.2 Hz, 3H, H-12), 1.04 (d, *J* = 6.7 Hz, 3H, H-13).

^{13}C NMR (176 MHz, $CDCl_3$): δ 172.4 (C-9), 171.4 (C-4), 60.7 (C-2), 60.5 (C-11), 55.8 (C-7), 55.2 (C-5), 38.5 (C-8), 37.9 (C-14), 15.7 (C-13), 14.3 (two coinciding peaks, C-1 and C-12).

HRMS (ESI): $C_{11}H_{22}N_1O_4$ $[M+H]^+$: calculated 232.1543, found 232.1535.

IR ν_{max} (neat/cm^{-1}): 2970 (alkyl C–H), 2941 (alkyl C–H), 2876 (alkyl C–H), 1730, (C=O), 1229 (C–N), 1179 (C–O).

1-Amino-8-(2-cyanobenzylamino)naphthalene, 183

1-(2-Cyanobenzyl)-2-phenyl-2,3-dihydro-1H-naphtho[1,8-de][1,3,2]diazaborinine, 184

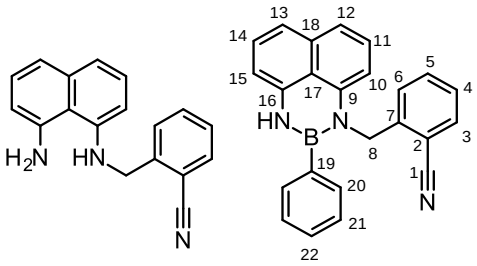

To a solution of 1,8-diaminonaphthalene (403 mg, 2.55 mmol, 1 eq.) in DMF (12 mL) was added K_2CO_3 (388 mg, 2.81 mmol, 1.1 eq.) and 2-cyanobenzyl bromide (500 mg, 2.55 mmol, 1 eq.). The resulting dark red mixture was stirred at rt over three days. The reaction mixture was then diluted with EtOAc (30 mL) and washed with saturated aqueous $NaHCO_3$ (20 mL) and then with brine (20 mL). The organic layer was then dried over $MgSO_4$ and then concentrated *in vacuo* using toluene to form an azeotropic mixture to aid in the removal of DMF. An attempt at purification by flash column chromatography (cyclohexane/EtOAc = 8:2) afforded a crude amount (233 mg) containing compound **183** along with other inseparable side products. This was then used directly in the successor reaction.

A solution of impure compound **183** (233 mg, 0.85 mmol, 1 eq.) and phenylboronic acid (104 mg, 0.85 mmol, 1 eq.) in toluene (9 mL) was stirred at reflux at 110 °C for 19 h. The reaction mixture was then cooled to rt, concentrated *in vacuo* and dry-loaded onto silica. Purification by flash column chromatography (cyclohexane/EtOAc = 9:1) afforded compound **184** (45 mg, 15%) as a white solid.

^{1}H NMR (500 MHz, $CDCl_3$): δ 7.69 (d, *J* = 7.6 Hz, 1H, H-3), 7.54 (d, *J* = 7.9 Hz, 1H, H-6), 7.51 (t, *J* = 7.9 Hz, 1H, H-5), 7.45 (d, *J* = 7.1 Hz, 2H, H-20), 7.43 – 7.31 (m, 4H, H-4, H-21 and H-22), 7.21 (t, *J* = 7.7 Hz, 1H, H-14), 7.16 – 7.11 (m, 2H, H-12 and H-13), 7.08 (t, *J* = 7.9 Hz, 1H, H-11), 6.47 (d, *J* = 7.7 Hz, 1H, H-15), 6.09 (d, *J* = 7.9 Hz, 1H, H-10), 6.06 (br s, 1H, NH), 4.97 (s, 2H, H-8).

^{13}C NMR (151 MHz, $CDCl_3$): δ 142.8 (C-7), 141.5 (C-9), 140.0 (C-16), 136.3 (C-18), 133.4 (two coinciding peaks, C-3 and C-5), 131.8 (C-20), 129.6 (C-22), 128.5 (C-21), 127.6 (three coinciding peaks, C-4, C-11 and C-14), 126.5 (C-6), 120.5 (C-17), 119.1 (C-12), 118.4 (C-13), 117.2 (C-1), 110.9 (C-2), 106.5 (C-15), 106.0 (C-10), 49.4 (C-8). Note: the boron-bound carbon (C-19) was not detected, presumably due to quadrupolar relaxation.

^{11}B NMR (160 MHz, $CDCl_3$): δ 31.7.

HRMS (ESI): $C_{24}H_{19}BN_3$ [M+H^+]: calculated 360.1667, found 360.1664.

IR ν_{max} (neat/cm^{-1}): 3374 (N–H), 3080 (aryl C–H), 3026 (aryl C–H), 2970 (alkyl C–H), 2943 (alkyl C–H), 2226 (nitrile C≡N), 1740, 1587 (aryl C=C).

m.p. 231-233 °C.

1-amino-8-(3-cyanobenzylamino)naphthalene, 186a

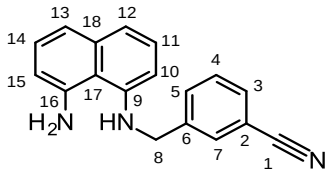

To a solution of 1,8-diaminonaphthalene (403 mg, 2.55 mmol, 1 eq.) in DMF (12 mL) was added K_2CO_3 (388 mg, 2.81 mmol, 1.1 eq.) and 3-cyanobenzyl bromide (500 mg, 2.55 mmol, 1 eq.). The resulting dark red mixture was stirred at rt for 24 h. The reaction mixture was then diluted with EtOAc (30 mL) and washed with saturated aqueous $NaHCO_3$ (20 mL) and then with brine (20 mL). The organic layer was then dried over $MgSO_4$ and then concentrated *in vacuo* using toluene to form an azeotropic mixture to aid in the removal of DMF. The resulting residue was dry-loaded onto silica and purification by flash column chromatography (cyclohexane/EtOAc = 9:1) afforded compound **186a** (131 mg, 19%) as a red oil. An impure fraction was also isolated (369 mg).

^{1}H NMR (600 MHz, $CDCl_3$): δ 7.70 (s, 1H, H-7), 7.63 (d, *J* = 7.8 Hz, 1H, H-5), 7.56 (d, *J* = 7.8 Hz, 1H, H-3), 7.44 (t, *J* = 7.8 Hz, 1H, H-4), 7.31 (dd, *J* = 7.7, 1.2 Hz, 1H, H-13), 7.21 (t, *J* = 7.7 Hz, 1H, H-14), 7.20 – 7.17 (m, 2H, H-11 and H-12), 6.71 (dd, *J* = 7.7, 1.2 Hz, 1H, H-15), 6.37 (dd, *J* = 5.0, 3.7 Hz, 1H, H-10), 5.15 (br s, 3H; NH_2 and NH), 4.39 (s, 2H, H-8).

^{13}C NMR (151 MHz, $CDCl_3$): δ 145.8 (C-9), 143.1 (C-16), 141.0 (C-6), 137.0 (C-18), 132.0 (C-5), 131.1 (two coinciding peaks; C-3 and C-7), 129.6 (C-4), 126.6 (C-14), 126.2 (C-11), 121.5 (C-13), 119.1 (C-1), 119.0 (C-12), 117.4 (C-17), 114.3 (C-15), 112.8 (C-2), 106.6 (C-10), 48.5 (C-8).

HRMS (ESI): $C_{18}H_{16}N_3$ [M+H$^+$]: calculated 274.1339, found 274.1336.

IR ν_{max} (neat/cm^{-1}): 3350 (N–H), 3025 (aryl C–H), 2950 (alkyl C–H), 2225 (nitrile C≡N), 1750 1625 (aryl C=C).

1-(3-cyanobenzyl)-2-phenyl-2,3-dihydro-1H-naphtho[1,8-de][1,3,2]diazaborinine, 186

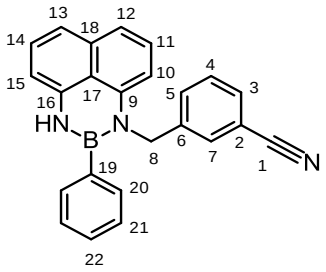

A solution of compound **186a** (131 mg, 0.48 mmol, 1 eq.) and phenylboronic acid (58 mg mg, 0.48 mmol, 1 eq.) in toluene (5 mL) was stirred at reflux at 110 °C for 17 h. Instead of a typical Dean-Stark apparatus being used, a modified dropping funnel was used to eliminate water as described in the literature.[179] The reaction mixture was then cooled to rt, concentrated *in vacuo* and dry-loaded onto silica. Purification by flash column chromatography (cyclohexane/EtOAc = 9:1) afforded compound **186** (40 mg, 23%) as a white solid.

^{1}H NMR (700 MHz, $CDCl_3$): δ 7.61 (s, 1H, H-7), 7.57 (ddd, *J* = 7.9, 2.0, 1.1 Hz, 1H, H-5), 7.54 (dt, *J* = 7.6, 1.4 Hz, 1H, H-3), 7.48 – 7.46 (m, 2H, H-20), 7.44 – 7.40 (m, 2H, H-4 and H-22), 7.38 – 7.35 (m, 2H, H-21), 7.22 (dd, *J* = 8.3, 7.3 Hz, 1H, H-14), 7.16 (dd, *J* = 8.3, 1.1 Hz, 1H, H-13), 7.14 (d, *J* = 7.8 Hz, 1H, H-12), 7.08 (t, *J* = 7.8 Hz, 1H, H-11), 6.48 (dd, *J* = 7.3, 1.1 Hz, 1H, H-15), 6.13 (d, *J* = 7.8 Hz, 1H, H-10), 6.08 (br s, 1H, NH), 4.80 (s, 2H, H-8).

^{13}C NMR (151 MHz, $CDCl_3$): δ 141.6 (C-9), 140.5 (C-6), 140.1 (C-16), 136.4 (C-18), 131.8 (C-20), 130.9 (C-5), 130.7 (C-3), 129.8 (two coinciding peaks; C-4 and C-22), 129.6 (C-7), 128.5 (C-21), 127.6 (two coinciding peaks; C-11 and C-14), 120.6 (C-17), 119.2 (C-12), 119.0 (C-1), 118.4 (C-13), 113.0 (C-2), 106.5 (C-15), 106.1 (C-10), 50.3 (C-8). Note: the boron-bound carbon (C-19) was not detected, presumably due to quadrupolar relaxation.

^{11}B NMR (225 MHz, $CDCl_3$): δ 31.5.

HRMS (ESI): $C_{24}H_{19}BN_3$ [M+H$^+$]: calculated 360.1667, found 360.1666.

IR ν_{max} (neat/cm^{-1}): 3358 (N–H), 3057 (aryl C–H), 2971 (alkyl C–H), 2926 (alkyl C–H), 2235 (nitrile C≡N), 1738, 1626 (aryl C=C).

m.p. 130-132 °C.

2-Bromo-*N*-(quinolin-8-yl)acetamide, 192

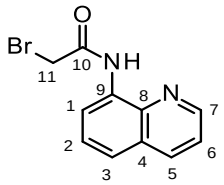

To a suspension of 8-aminoquinoline (1.40 g, 9.71 mmol, 1 eq.) in anhydrous DCM (50 mL), was added triethylamine (983 mg, 1.35 mL, 9.71 mmol, 1 eq.) under an argon atmosphere and the mixture cooled to 0 °C. Bromoacetyl bromide (2.16 g, 931 µL, 0.01 mol, 1.1 eq.) was dissolved in anhydrous DCM (20 mL) before being added to the cooled solution dropwise over 30 minutes. The reaction mixture was allowed to warm to rt and stirred for 19 h. The reaction mixture was then quenched with 0.3 M HCl (50 mL, 15 mmol) and the resulting layers were separated, and the organic layer was dried over $MgSO_4$ and concentrated *in vacuo.* Purification by flash column chromatography (cyclohexane/EtOAc = 8:2) afforded compound **192** (1.60 g, 62%) as a yellow solid.

^{1}H NMR (500 MHz, $CDCl_3$): δ 10.74 (br s, 1H, NH), 8.86 (dd, *J* = 4.1, 1.3 Hz, 1H, H-7), 8.74 (dd, *J* = 5.9, 3.1 Hz, 1H, H-1), 8.18 (d, *J* = 8.3 Hz, 1H, H-5), 7.58 – 7.53 (m, 2H, H-2 and H-3), 7.48 (dd, *J* = 8.3, 4.1 Hz, 1H, H-6), 4.15 (s, 2H, H-11).

^{13}C NMR (151 MHz, $CDCl_3$): δ 164.3 (C-10), 148.6 (C-7), 138.5 (C-8), 136.8 (C-5), 133.8 (C-9), 128.1 (C-4), 127.4 (C-2), 122.7 (C-3), 121.9 (C-6), 117.0 (C-1), 29.9 (C-11).

HRMS (ESI): $C_{11}H_{10}BrN_2O$ [$M+H^+$]: calculated 264.9971, found 264.9972.

IR ν_{max} (neat/cm^{-1}): 3306 (N–H), 3044 (aryl C–H), 2994 (alkyl C–H), 2943 (alkyl C–H), 1691 (C=O), 1586 (aryl C=C).

m.p. > 250 °C.

***N*-(2-bromoethyl)pyridine-2-carboxamide, 195**

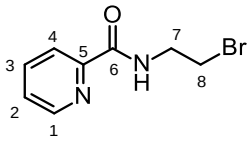

DCC (3.69 g, 0.02 mol, 1.1 eq.) and HOBt.hydrate (2.41 g, 0.02 mol, 1.1 eq.) were added to a mixture of picolinic acid (2.00 g, 0.02 mol, 1 eq.) in MeCN (25 mL) and the reaction mixture was stirred at 0 °C for 1 h. Then, triethylamine (2.49 mL, 0.02 mol, 1.1 eq.) and 2-Bromoethylamine hydrobromide (3.56 g, 0.02 mol, 1 eq.) as added to the reaction mixture and the resulting solution was stirred at rt for 17 h. The mixture was then cooled to 0 °C in order to precipitate the DCU by-product which was then collected by Büchner filtration. The filtrate was concentrated *in vacuo* and the residue was diluted with H_2O (15 mL) and then extracted with DCM (3 × 40 mL). The combined organic extracts were then dried over $MgSO_4$ and concentrated *in vacuo*. Purification by flash column chromatography (cyclohexane/EtOAc = 8:2) afforded compound **195** (1.80 g, 48%) as a white solid.

^{1}H NMR (500 MHz, $CDCl_3$): δ 8.57 (dd, *J* = 4.8, 1.7 Hz, 1H, H-1), 8.43 (br s, 1H, NH), 8.18 (d, *J* = 7.7 Hz, 1H, H-4), 7.85 (td, *J* = 7.7, 1.7 Hz, 1H, H-3), 7.44 (dd, *J* = 7.7, 4.8 Hz, 1H; H-2), 3.90 (q, *J* = 6.0 Hz, 2H, H-7), 3.58 (t, *J* = 6.0 Hz, 2H, H-8).

^{13}C NMR (125 MHz, $CDCl_3$): δ 164.6 (C-6), 149.6 (C-5), 148.3 (C-1), 137.5 (C-3), 126.5 (C-2), 122.4 (C-4), 41.3 (C-7), 32.0 (C-8).

HRMS (ESI): $C_8H_{10}BrN_2O$ [$M+H^+$]: calculated 228.9971, found 228.9971.

IR ν_{max} (neat/cm^{-1}): 3345 (N–H), 3067 (aryl C–H), 2970 (alkyl C–H), 2940 (alkyl C–H), 1660 (C=O), 663 (C-Br).

m.p. 68-69 °C.

Aziridin-1-yl(2-pyridyl)methanone, 196

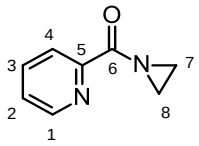

To a solution of **195** (299 mg, 1.30 mmol, 1 eq.) and 2-nitroaniline (180 mg, 1.30 mmol, 1 eq.) in MeCN (6 mL), was added dry triethylamine (264 mg, 361 µL, 2.61 mmol, 2 eq.). The resulting mixture was stirred at 80 °C for 4 h. The reaction mixture was then cooled to rt and concentrated *in vacuo* before dry-loading onto silica. Purification by flash column chromatography (DCM/MeOH = 95:5) afforded compound **196** (73 mg, 38%) as an off-white solid.

^{1}H NMR (500 MHz, $CDCl_3$): δ 8.69 (dd, *J* = 4.9, 1.6 Hz, 1H, H-1), 8.03 (dd, *J* = 8.0, 1.1 Hz, 1H, H-4), 7.77 (t, *J* = 8.0 Hz, 1H, H-3), 7.40 – 7.36 (m, 1H, H-2), 4.52 (t, *J* = 9.9 Hz, 2H; H-8), 4.12 (t, *J* = 9.9 Hz, 2H, H-7).

^{13}C NMR (125 MHz, $CDCl_3$): δ 164.0 (C-6), 149.8 (C-1), 146.9 (C-5), 136.7 (C-3), 125.6 (C-2), 123.9 (C-4), 68.3 (C-8), 55.2 (C-7).

HRMS (ESI): $C_8H_9N_2O$ [$M+H^+$]: calculated 149.0709, found 149.0712.

IR ν_{max} (neat/cm^{-1}): 3061 (aryl C–H), 2970 (alkyl C–H), 2906 (alkyl C–H), 2880 (alkyl C–H), 1641 (C=O),

m.p. 54-55 °C.

2-Hydroxy-*N*-(154uinoline-8-yl)acetamide, 200

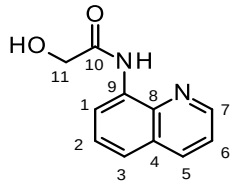

To a solution of **192** (298 mg, 1.12 mmol, 1 eq.) and 2-nitroaniline (155 mg, 1.12 mmol, 1 eq.) in dry THF (7 mL), was added K_2CO_3 (217 mg, 1.57 mmol, 1.4 eq.) and the resulting mixture was stirred at reflux at 65 °C for 20 h. With both starting material unreacted, the reaction mixture was concentrated *in vacuo* to remove THF. Then dry DMF (7 mL), Sodium iodide (168 mg, 1.12 mmol, 1 eq.) and additional K_2CO_3 (155 mg, 1.12 mmol, 1 eq.) were added and the resulting suspension was heated at 80 °C for 18 h. The reaction mixture was then concentrated *in vacuo* and dry-loaded onto silica. Purification by flash column chromatography (cyclohexane/EtOAc = 1:1) afforded compound **200** (18 mg, 8%) as an off-white solid.

^{1}H NMR (500 MHz, $CDCl_3$): δ 10.52 (br s, 1H, NH), 8.84 (dd, *J* = 4.2, 1.7 Hz, 1H, H-7), 8.79 (dd, *J* = 6.2, 2.8 Hz, 1H, H-1), 8.18 (dd, *J* = 8.3, 1.7 Hz, 1H, H-5), 7.58 – 7.53 (m, 2H, H-2 and H-3), 7.47 (dd, *J* = 8.3, 4.2 Hz, 1H, H-6), 4.42 (d, *J* = 3.3 Hz, 2H, H-11), 2.83 (br s, 1H, OH).

^{13}C NMR (176 MHz, $CDCl_3$): δ 170.0 (C-10), 148.6 (C-7), 138.7 (C-8), 136.5 (C-5), 133.8 (C-9), 128.2 (C-4), 127.4 (C-2), 122.3 (C-3), 121.9 (C-6), 116.9 (C-1), 63.1 (C-11).

HRMS (ESI): $C_{11}H_{11}N_2O_2$ [M+H$^+$]: calculated 203.0815, found 203.0813.

IR ν_{max} (neat/cm^{-1}): 3316 (N–H), 3215 (O-H), 3042 (aryl C–H), 2928 (alkyl C–H), 1651, (C=O),

m.p. 174-177 °C.

***N*-(2-Picolinoyl)-1,2-diaminoethane, 203**

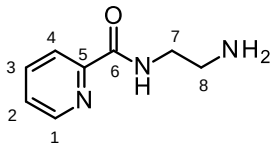

To an oven-dried flask cooled to 0 °C was added picolinic acid (1.60 g, 0.01 mol, 1 eq.) in dry DMF (20 mL). 1,1′-Carbonyldiimidazole (2.32 g, 0.01 mol, 1.1 eq.) was then added under an argon atmosphere and the resulting mixture was allowed to warm to rt. After 2 h, this solution was transferred to a dropping funnel and then added dropwise over 1 h to a solution of ethylenediamine (1.60 g, 1.78 mL, 0.03 mol, 2.05 eq.) in dry DMF. The resulting mixture was stirred at rt for 15 h. The reaction mixture was then concentrated *in vacuo* and dry-loaded onto silica. Purification by flash column chromatography (DCM + 10% MeOH + 1% NEt_3 / MeOH = 95:5) afforded compound **203** (1.66 g, 77%) as a light-yellow oil.

^{1}H NMR (700 MHz, $CDCl_3$): δ 8.45 (ddd, *J* = 4.8, 1.8, 1.0 Hz, 1H, H-1), 8.32 (br s, 1H, NH), 8.10 (dt, *J* = 7.7, 1.1 Hz, 1H, H-4), 7.75 (td, *J* = 7.7, 1.7 Hz, 1H, H-3), 7.33 (ddd, *J* = 7.7, 4.8, 1.3 Hz, 1H, H-2), 3.45 (q, *J* = 6.1 Hz, 2H, H-7), 2.87 (t, *J* = 6.1 Hz, 2H, H-8), 1.73 (br s, 2H, NH_2).

^{13}C NMR (176 MHz, $CDCl_3$): δ 164.8 (C-6), 149.9 (C-5), 148.2 (C-1), 137.4 (C-3), 126.3 (C-2), 122.3 (C-4), 42.4 (C-7), 41.7 (C-8).

HRMS (ESI): $C_8H_{12}N_3O$ [$M+H^+$]: calculated 166.0975, found 166.0976.

IR ν_{max} (neat/cm^{-1}): 3370 (N–H), 3310 (N–H), 3057 (aryl C–H), 2970 (alkyl C–H), 2930 (alkyl C–H), 1661 (C=O).

***N*-[2-(2-Nitroanilino)ethyl]pyridine-2-carboxamide, 204**

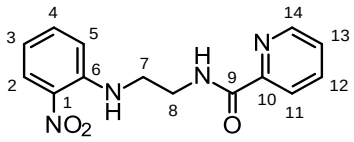

To a solution of **203** (1.33 g, 8.02 mmol, 1 eq.) and 1-fluoro-2-nitrobenzene (1.13 g, 846 µL, 8.02 mmol, 1 eq.) in MeCN (30 mL) was added triethylamine (1.62 g, 2.22 mL, 0.02 mol, 2 eq.). The resulting solution was heated at 75 °C for 17 h. The reaction mixture was then cooled to rt, concentrated *in vacuo* and dry-loaded onto silica. Purification by flash column chromatography (cyclohexane/EtOAc = 1:1) afforded compound **204** (926 mg, 40%) as a bright orange solid.

^{1}H NMR (700 MHz, $CDCl_3$): δ 8.53 (ddd, *J* = 4.7, 1.7, 0.9 Hz, 1H, H-14), 8.36 (br t, *J* = 6.4 Hz, 1H, C(O)NH), 8.25 (t, *J* = 6.4 Hz, 1H, NH), 8.21 (dt, *J* = 7.8, 1.1 Hz, 1H, H-11), 8.17 (dd, *J* = 8.6, 1.6 Hz, 1H, H-2), 7.86 (td, *J* = 7.8, 1.7 Hz, 1H, H-12), 7.47 – 7.42 (m, 2H, H-4 and H-13), 7.03 (dd, *J* = 8.7, 1.2 Hz, 1H, H-5), 6.66 (ddd, *J* = 8.6, 6.9, 1.2 Hz, 1H, H-3), 3.78 (q, *J* = 6.4 Hz, 2H, H-8), 3.63 (q, *J* = 6.4 Hz, 2H, H-7).

^{13}C NMR (176 MHz, $CDCl_3$): δ 165.3 (C-9), 149.5 (C-10), 148.3 (C-14), 145.4 (C-6), 137.6 (C-12), 136.6 (C-4), 132.4 (C-1), 127.1 (C-2), 126.6 (C-13), 122.4 (C-11), 115.9 (C-3), 113.9 (C-5), 42.6 (C-7), 38.6 (C-8).

HRMS (ESI): $C_{14}H_{15}N_4O_3$ [M+H$^+$]: calculated 287.1139, found 287.1139.

IR ν_{max} (neat/cm^{-1}): 3372 (N–H), 3055 (aryl C–H), 2941 (alkyl C–H), 1673 (C=O), 1503 (N–O).

m.p. 125-126 °C.

***N*-[2-(2-Aminoanilino)ethyl]pyridine-2-carboxamide, 205**

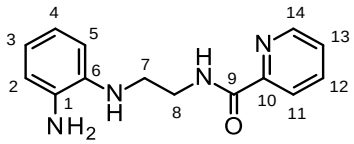

A mixture of compound **204** (620 mg, 2.17 mmol, 1 eq.) and 10% Pd/C (115 mg) in EtOH (10 mL) was degassed by evacuation and backfilling with Ar thrice. A balloon of H_2 was then attached, and the round-bottom flask evacuated and back-filled with H_2 thrice before stirring at room temperature for 18 h. The mixture was filtered through a pad of Celite® and the filtrate concentrated *in vacuo* to afford compound **205** (740 mg, quantitative yield) as a dark brown oil. This was used in the next step without further purification.

^{1}H NMR (700 MHz, $CDCl_3$): δ 8.52 (ddd, *J* = 4.7, 1.8, 0.9 Hz, 1H, H-14), 8.38 (br s, 1H, NH), 8.20 (dt, *J* = 7.6, 1.1 Hz, 1H, H-11), 7.83 (td, *J* = 7.6, 1.7 Hz, 1H, H-12), 7.41 (ddd, *J* = 7.6, 4.7, 1.3 Hz, 1H, H-13), 6.81 (ddd, *J* = 7.8, 7.1, 1.7 Hz, 1H, H-4), 6.72 – 6.66 (m, 3H, H-2, H-3, H-5), 3.77 (q, *J* = 6.0 Hz, 2H, H-8), 3.39 (t, *J* = 6.0 Hz, 2H, H-7), 3.39 (br s, 3H, NH and NH_2).

^{13}C NMR (176 MHz, $CDCl_3$): δ 165.3 (C-9), 149.9 (C-10), 148.2 (C-14), 137.5 (C-12), 137.3 (C-6), 134.6 (C-1), 126.4 (C-13), 122.4 (C-11), 120.7 (C-4), 119.0 (C-3), 116.5 (C-2), 111.8 (C-5), 44.6 (C-7), 39.3 (C-8).

HRMS (ESI): $C_{14}H_{17}N_4O$ [$M+H^+$]: calculated 257.1397, found 257.1396.

IR ν_{max} (neat/cm^{-1}): 3443 (N–H), 3395 (N–H), 3364 (N–H), 3059 (aryl C–H), 2971 (alkyl C–H), 2938 (alkyl C–H), 1650 (C=O).

***N*-[2-(2-Propyl-1H-1,3,2-benzodiazaborol-3-yl)ethyl]pyridine-2-carboxamide, 206**

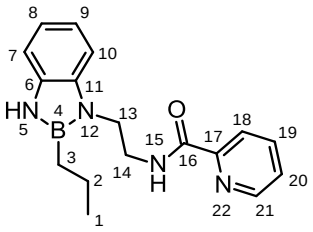

To a solution of **205** (135 mg, 0.53 mmol, 1 eq.) in toluene (5 mL) was added *n*-propylboronic acid (46 mg, 0.53 mmol, 1 eq.) in one portion. The round-bottom flask was equipped with a Dean-Stark trap, and the solution was stirred at reflux at 110 °C for 18 h. The reaction mixture was cooled to rt, concentrated *in vacuo* and the resultant crude residue was directly purified by flash column chromatography to afford compound **206** (65 mg, 40%) as a colourless oil.

^{1}H NMR (700 MHz, $CDCl_3$): δ 8.49 (ddd, *J* = 4.7, 1.6, 0.9 Hz, 1H, H-21), 8.24 – 8.20 (m, 2H, H-15 and H-18), 7.84 (td, *J* = 7.7, 1.7 Hz, 1H, H-19), 7.41 (ddd, *J* = 7.7, 4.7, 1.2 Hz, 1H, H-20), 7.13 (d, *J* = 7.6 Hz, 1H, H-10), 7.03 (dd, J = 7.6, 1.0 Hz, 1H, H-7), 6.97 (td, *J* = 7.6, 1.3 Hz, 1H, H-9), 6.93 (td, *J* = 7.6, 1.2 Hz, 1H, H-8), 6.39 (br s, 1H, H-5), 3.97 (t, *J* = 6.4 Hz, 2H, H-13), 3.76 (q, *J* = 6.4 Hz, 2H, H-14), 1.51 (sext, *J* = 7.4 Hz, 2H, H-2), 1.14 (t, *J* = 7.4 Hz, 2H, H-3), 0.90 (t, *J* = 7.4 Hz, 3H, H-1).

^{13}C NMR (126 MHz, $CDCl_3$): δ 164.7 (C-16), 149.9 (C-17), 148.2 (C-21), 137.4 (C-19), 137.3 (C-11), 136.3 (C-6), 126.3 (C-20), 122.3 (C-18), 118.9 (two coinciding peaks, C-8 and C-9), 110.6 (C-7), 108.5 (C-10), 42.4 (C-13), 39.3 (C-14), 19.3 (C-2), 17.3 (C-1). Note: the boron-bound carbon (C-3) was not detected, presumably due to quadrupolar relaxation.

^{11}B NMR (225 MHz, $CDCl_3$): δ 31.7.

HRMS (ESI): $C_{17}H_{22}BN_4O$ $[M+H]^+$: calculated 309.1881, found 309.1877.

IR ν_{max} (neat/cm^{-1}): 3380 (N-H), 3058 (aryl C-H), 2956 (alkyl C-H), 2919 (alkyl C-H), 2851 (alkyl C-H), 1740 (C=O).

***N*-[2-(2-phenyl-1H-1,3,2-benzodiazaborol-3-yl)ethyl]pyridine-2-carboxamide, 207**

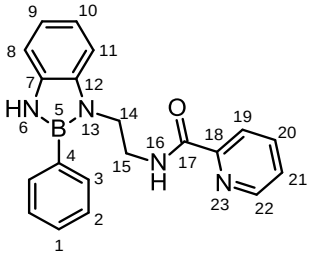

To a vial containing **205** (20 mg, 0.0.08 mmol, 1 eq.) in toluene (2 mL) was added phenylboronic acid (7 mg, 0.08 mmol, 1 eq.). The vial was then sealed with a PTFE cap, and the solution stirred at reflux at 110 °C for 18 h. The reaction mixture was allowed to cool to rt then concentrated *in vacuo* and the resultant crude residue was directly purified by flash column chromatography to afford compound **207** (10 mg, 42%) as a colourless oil.

^{1}H NMR (700 MHz, $CDCl_3$): δ 8.46 (d, *J* = 4.8 Hz, 1H, H-22), 8.17 (br s, 1H, H-16), 8.11 (d, *J* = 7.7 Hz, 1H, H-19), 7.81 (td, *J* = 7.7, 1.4 Hz, 1H, H-20), 7.64 (d, *J* = 7.5 Hz, 2H, H-3), 7.39 (dd, *J* = 7.7, 4.8 Hz, 1H, H-21), 7.34 – 7.29 (m, 4H, (1H, H-1), (2H, H-2), (1H, H-8)), 7.14 (d, *J* = 7.4 Hz, 1H, H-11), 7.06 (t, *J* = 7.4 Hz, 1H, H-10), 7.02 (t, *J* = 7.4 Hz, 1H, H-9), 6.69 (br s, 1H, H-6), 4.18 (t, *J* = 6.7 Hz, 2H, H-14), 3.82 (q, *J* = 6.7 Hz, 2H, H-15).

^{13}C NMR (126 MHz, $CDCl_3$): δ 164.7 (C-17), 149.7 (C-18), 148.0 (C-22), 137.5 (C-12), 137.4 (C-20), 136.0 (C-7), 133.5 (C-3), 129.2 (C-1), 128.1 (C-2), 126.2 (C-21), 122.2 (C-19), 119.7 (C-9), 119.5 (C-10), 111.2 (C-11), 109.5 (C-8), 42.6 (C-14), 39.4 (C-15). Note: the boron-bound carbon (C-4) was not detected, presumably due to quadrupolar relaxation.

^{11}B NMR (225 MHz, $CDCl_3$): δ 29.3.

HRMS (ESI): $C_{20}H_{20}BN_4O$ $[M+H]^+$: calculated 343.1725, found 343.1720.

IR ν_{max} (neat/cm^{-1}): 3350 (N-H), 3053 (aryl C-H), 2956 (alkyl C-H), 2922 (alkyl C-H), 2851 (alkyl C-H), 1738 (C=O).

3-[2-(6-Methyl-2-phenyl-1,3,2-dioxaborinan-4-yl)ethyl]benzonitrile, 218

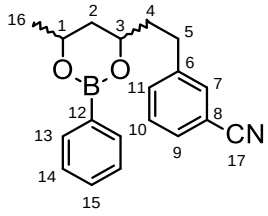

1,3-cis:1,3-trans (2.37:1)

To a stirred solution of diol (464 mg, 2.12 mmol, 1 eq.) in DCM (5 mL), was added a solution of phenylboronic acid (284 mg, 2.33 mmol, 1.1 eq.) in DCM (5 mL) followed by oven-dried molecular sieves (500 mg). The resulting suspension was stirred at rt for 18 h. The reaction mixture was then filtered, concentrated *in vacuo* and the resultant crude residue was directly purified by flash column chromatography to afford **218** (380 mg, 59%) as a pale-yellow oil.

^{1}H NMR (700 MHz, $CDCl_3$): **(1, 3-cis)** δ 7.85 – 7.81 (m, 2H, H-13), 7.57 – 7.55 (m, 1H, H-7), 7.52 – 7.50 (m, 2H, H-9, H-11), 7.45 – 7.42 (m, 1H, H-15), 7.41 (t, J = 7.7 Hz, 1H, H-10), 7.39– 7.35 (m, 2H, H-14), 4.26 (dqd, J = 12.5, 6.2, 2.7 Hz, 1H, H-1_{axial}), 4.08 (dddd, J = 11.3, 8.5, 4.1, 2.9, 1H, H-3_{axial}), 3.00 (dd, J = 9.1, 5.3 Hz, 1H, H-5'), 2.94 – 2.85 (m, 1H, H-5''), 1.97 (dt, J = 13.8, 2.7 Hz, 1H, H-2'), 1.93 – 1.87 (m, 1H, H-4'), 1.87 – 1.81 (m, 1H, H-4''), 1.51 (dt, J = 13.8, 11.3 Hz, 1H, H-2''), 1.36 (d, J = 6.3 Hz, 3H, H-16). **(1, 3-trans)** δ 7.85 – 7.81 (m, 2H, H-13), 7.57 – 7.55 (m, 1H, H-7), 7.52 – 7.50 (m, 2H, H-9, H-11), 7.45 – 7.42 (m, 1H, H-15), 7.41 (t, J = 7.7 Hz, 1H, H-10), 7.39– 7.35 (m, 2H, H-14), 4.41(qddd, J = 6.4, 5.8, 4.3, 0.1, 1H, H-$1_{equitorial}$), 4.20 (ddtd, J = 9.4, 7.0, 4.0, 0.5, 1H, H-3_{axial}), 3.02 (dd, J = 9.0, 5.2 Hz, 1H, H-5'), 2.94 – 2.85 (m, 1H, H-5''), 2.00 (dtd, J = 13.7, 9.4, 5.2, 1H, H-4'), 1.93 – 1.82 (m, 3H, H-2', H-2'', H-4''), 1.37 (d, J = 6.5 Hz, 3H, H-16).

^{13}C NMR (176 MHz, $CDCl_3$): **(1, 3-cis)** δ 143.6 (C-6), 133.9 (C-13), 133.4 (C-11), 132.2 (C-7), 130.8 (C-15), 129.9 (C-9), 129.4 (C-10), 127.7 (C-14), 119.2 (C-17), 112.6 (C-8), 70.6 (C-3), 68.2 (C-1), 40.9 (C-2), 38.6 (C-4), 31.2 (C-5), 23.3 (C-16). **(1, 3-trans)** δ 143.4 (C-6), 133.9 (C-13), 133.4 (C-11), 132.2 (C-7), 130.8 (C-15), 129.9 (C-9), 129.4 (C-10), 127.7 (C-14), 119.2 (C-17), 112.6 (C-8), 67.2 (C-3), 65.2 (C-1), 38.3 (C-4), 37.9 (C-2), 31.6 (C-5), 22.8 (C-16). Note: the boron-bound carbon (C-12) was not detected, likely due to quadrupolar relaxation.

^{11}B NMR (225 MHz, $CDCl_3$): δ 27.0.

HRMS (ESI): $C_{19}H_{21}BNO_2$ $[M+H]^+$: calculated 306.1660, found 306.1658.

IR ν_{max} (neat/cm^{-1}): 3076 (aryl C-H), 2975 (alkyl C-H), 2228 (C≡N), 1303 (C-O).

tert-Butyl _N_-[3-(2-pyrimidin-5-ylphenoxy)propyl]carbamate, 229

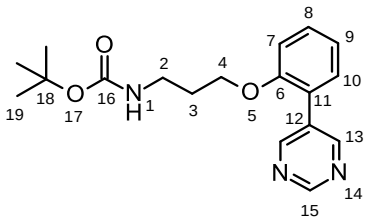

To a stirred solution of 2-(pyrimidin-5-yl)phenol (584 mg, 3.39 mmol, 1 eq.) in DMF (7 mL) was added *tert*-butyl *N*-(3-chloropropyl)carbamate (788 mg, 4.07 mmol, 1.2 eq.), potassium carbonate (516 mg, 3.73 mmol, 1.1 eq.), a catalytic amount of potassium iodide (113 mg, 0.68 mmol, 0.2 eq.). The resulting suspension was stirred at 90 °C for 18h. The reaction mixture was then cooled to rt, diluted with H_2O (20 mL) and extracted with EtOAc (3 × 30 mL). The combined organic extracts were dried over $MgSO_4$, filtered and concentrated *in vacuo*. The resulting crude residue was purified by flash column chromatography to afford **229** (690 mg, 62%) as a beige solid.

^{1}H NMR (700 MHz, $CDCl_3$): δ 9.14 (s, 1H, H-15), 8.90 (s, 2H, H-13), 7.40 (t, *J* = 7.5 Hz, 1H, H-8), 7.32 (dd, *J* = 7.5, 1.5 Hz, 1H, H-10), 7.08 (t, *J* = 7.5 Hz, 1H, H-9), 7.01 (d, *J* = 7.5 Hz, 1H, H-7), 4.59 (br s, 1H, H-1), 4.06 (t, *J* = 6.1 Hz, 2H, H-4), 3.20 (q, *J* = 6.1 Hz, 2H, H-2), 1.94 (qn, *J* = 6.1 Hz, 2H, H-3), 1.41 (s, 9H, H-19).

^{13}C NMR (176 MHz, $CDCl_3$): δ 157.0 (C-15), 156.9 (C-13), 156.0 (two coinciding peaks, C-6 and C-16), 132.3 (C-12), 130.7 (C-8), 130.5 (C-10), 123.6 (C-11), 121.6 (C-9), 112.4 (C-7), 79.4 (C-18), 66.3 (C-4), 37.9 (C-2), 29.8 (C-3), 28.5 (C-19).

HRMS (ESI): $C_{18}H_{24}N_3O_3$ $[M+H]^+$: calculated 330.1812, found 330.1811.

IR ν_{max} (neat/cm^{-1}): 3311 (N-H), 3004 (aryl C-H), 2952 (alkyl C-H), 1699 (C=O).

m.p. 165-167 °C.

3-(2-Pyrimidin-5-ylphenoxy)propan-1-amine, 230

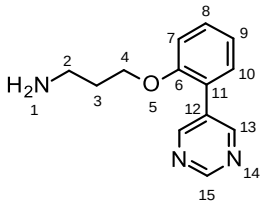

To a stirred solution of **229** (541 mg, 1.64 mmol, 1 eq.) in dioxane (10 mL) was added 2M HCl (ether solution, 10 mL). The resulting white suspension was stirred at rt at 18 h and then concentrated *in vacuo* to afford the hydrochloride salt of the amine. To this was added 2M NaOH (10mL) and the mixture was stirred at rt for 3 h. H_2O (20 mL) was then added to the reaction mixture and then extracted with $CHCl_3$ (3 × 30 mL). The combined organic extracts were dried over $MgSO_4$, filtered and concentrated *in vacuo* to furnish the free amine **230** (359 mg, 95%) as a yellow oil.

^{1}H NMR (700 MHz, $CDCl_3$): δ 9.12 (s, 1H, H-15), 8.89 (s, 2H, H-13), 7.41 – 7.37 (m, 1H, H-8), 7.30 (dd, *J* = 7.5, 1.7 Hz, 1H, H-10), 7.06 (td, *J* = 7.5, 0.9 Hz, 1H, H-9), 7.02 (d, *J* = 8.3 Hz, 1H, H-7), 4.09 (t, *J* = 6.7 Hz, 2H, H-4), 2.79 (t, *J* = 6.7 Hz, 2H, H-2), 1.87 (qn, *J* = 6.7 Hz, 2H, H-3).

^{13}C NMR (176 MHz, $CDCl_3$): δ 157.0 (C-15), 156.9 (C-13), 156.1 (C-6), 132.3 (C-12), 130.6 (C-8), 130.4 (C-10), 123.6 (C-11), 121.4 (C-9), 112.4 (C-7), 66.3 (C-4), 39.1 (C-2), 32.9 (C-3).

HRMS (ESI): $C_{13}H_{16}N_3O$ $[M+H]^+$: calculated 230.1288, found 230.1286.

IR ν_{max} (neat/cm^{-1}): 3311 (N-H), 3042 (aryl C-H), 2942 (alkyl C-H), 2870 (alkyl C-H).

2-Amino-*N*-[3-(2-pyrimidin-5-ylphenoxy)propyl]benzamide, 231

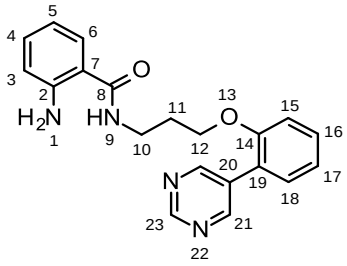

To a stirred solution of **230** (304 mg, 1.33 mmol, 1 eq.) in MeCN (8 mL) was added isatoic anhydride (227 mg, 1.39 mmol, 1.05 eq.) and the resulting suspension was stirred at rt for 18 h. The reaction mixture was then concentrated *in vacuo* and the resulting crude residue was purified by flash column chromatography to afford **231** (202 mg, 44%) as a colourless oil.

^{1}H NMR (700 MHz, $CDCl_3$): δ 9.13 (s, 1H, H-23), 8.93 (s, 2H, H-21), 7.40 (td, *J* = 8.2, 1.7 Hz, 1H, H-16), 7.33 (dd, *J* = 7.5, 1.7 Hz, 1H, H-18), 7.18 (ddd, J = 8.4, 7.3, 1.5 Hz, 1H, H-4), 7.14 (dd, J = 7.3, 1.4 Hz, 1H, H-6), 7.10 (td, *J* = 7.5, 0.9 Hz, 1H, H-17), 7.03 (d, *J* = 8.2 Hz, 1H, H-15), 6.65 (dd, *J* = 8.4, 0.7 Hz, 1H, H-3), 6.60 (t, *J* = 7.3 Hz, 1H, H-5), 6.14 (br s, 1H, H-9), 5.49 (br s, 2H, H-1), 4.12 (t, *J* = 6.7 Hz, 2H, H-12), 3.50 (q, *J* = 6.7 Hz, 2H, H-10), 2.08 (qn, *J* = 6.4 Hz, 2H, H-11).

^{13}C NMR (176 MHz, $CDCl_3$): δ 169.6 (C-8), 157.0 (C-23), 156.9 (C-21), 155.9 (C-14), 148.8 (C-2), 132.4 (C-4), 132.3 (C-20), 130.7 (C-16), 130.5 (C-18), 127.0 (C-6), 123.6 (C-19), 121.7 (C-17), 117.4 (C-3), 116.8 (C-5), 115.9 (C-7), 112.6 (C-15), 66.5 (C-12), 37.2 (C-10), 29.5 (C-11).

HRMS (ESI): $C_{20}H_{21}N_4O_2$ $[M+H]^+$: calculated 349.1659, found 349.1659.

IR ν_{max} (neat/cm^{-1}): 3429 (N-H), 3313 (N-H), 3166 (aryl C-H), 2965 (alkyl C-H), 2928 (alkyl C-H), 1628 (C=O).

2-Phenyl-3-[3-(2-pyrimidin-5-ylphenoxy)propyl]-1H-1,3,2-benzodiazaborinin-4-one, 225

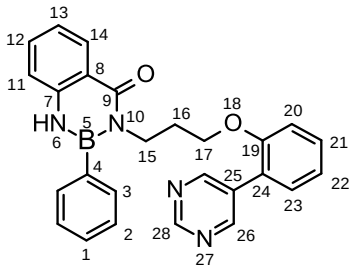

To **231** (202 mg, 0.58 mmol, 1 eq.) was added phenylboronic acid (85 mg, 0.70 mmol, 1.2 eq.) in one portion and stirred neat at 150 °C for 3 h. The reaction mixture was then cooled to rt and was purified by flash column chromatography to afford **225** (25 mg, 10%) as a colourless oil.

^{1}H NMR (700 MHz, $CDCl_3$): δ 9.04 (s, 1H, H-28), 8.68 (s, 2H, H-26), 8.25 (dd, *J* = 7.2, 1.2 Hz, 1H, H-14), 7.51 – 7.48 (m, 1H, H-12), 7.42 (d, *J* = 6.7 Hz, 2H, H-3), 7.37 – 7.33 (m, 1H, H-22), 7.33 – 7.30 (m, 1H, H-1), 7.27 – 7.23 (m, 3H, (2H, H-2), (1H, H-20)) 7.15 (t, *J* = 7.2 Hz, 1H, H-13), 7.04 (td, *J* = 7.5, 0.8 Hz, 1H, H-21), 6.98 (d, *J* = 8.0 Hz, 1H, H-11), 6.89 (d, *J* = 8.2 Hz, 1H, H-23), 6.64 (br s, 1H, H-6), 3.95 (t, *J* = 6.9 Hz, 2H, H-17), 3.89 (t, *J* = 6.9 Hz, 2H, H-15), 2.07 (qn, *J* = 6.9 Hz, 2H, H-16).

^{13}C NMR (126 MHz, $CDCl_3$): δ 166.8 (C-9), 156.8 (C-28), 156.7 (C-26), 155.8 (C-19), 143.2 (C-7), 133.5 (C-12), 132.2 (C-25), 131.8 (C-3), 130.5 (two coinciding peaks, C-20 and C-22), 129.5 (two coinciding peaks, C-1 and C-14), 128.2 (C-2), 123.4 (C-24), 121.9 (C-13), 121.2 (C-21), 119.2 (C-8), 117.2 (C-11), 112.2 (C-23), 66.1 (C-17), 41.4 (C-15), 29.7 (C-16). Note: the boron-bound carbon (C-4) was not detected, likely due to quadrupolar relaxation.

^{11}B NMR (225 MHz, $CDCl_3$): δ 31.9.

HRMS (ESI): $C_{26}H_{24}BN_4O_2$ $[M+H]^+$: calculated 435.1987, found 435.1987.

IR ν_{max} (neat/cm^{-1}): 3322 (N-H), 3029 (aryl C-H), 2969 (alkyl C-H), 2941 (alkyl C-H), 1740 (C=O).

2-[3-(4-Oxo-2-phenyl-1H-1,3,2-benzodiazaborinin-3-yl)propoxy]benzonitrile, 239

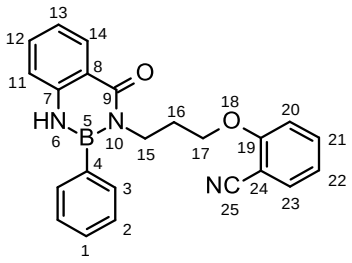

To the corresponding alkylated anthranilamide (338 mg, 1.14 mmol, 1 eq.) was added phenylboronic acid (167 mg, 1.37 mmol, 1.2 eq.) in one portion and stirred neat at 150 °C for 3 h before cooling to rt. The resulting crude residue was directly purified by flash column chromatography to afford **239** (111 mg, 25%) as a white solid.

^{1}H NMR (500 MHz, $CDCl_3$): δ 8.27 (dd, *J* = 7.6, 1.4 Hz, 1H, H-14), 7.56 – 7.53 (m, 2H, H-21, H-23), 7.50 (t, *J* = 7.6 Hz, 1H, H-12) 7.46 (d, *J* = 7.6 Hz, 2H, H-3), 7.17 (t, *J* = 7.6 Hz, 1H, H-13), 7.00 (d, *J* = 7.6 Hz, 1H, H-11), 6.94 (td, *J* = 7.6, 0.8 Hz, 1H, H-22), 6.82 (d, *J* = 8.2 Hz, 1H, H-20), 6.57 (br s, 1H, H-6), 4.05 (t, *J* = 6.5 Hz, 2H, H-15), 4.02 (t, *J* = 6.5 Hz, 2H, H-17), 2.18 (qn, *J* = 6.5 Hz, 2H, H-16).

^{13}C NMR (126 MHz, $CDCl_3$): δ 166.6 (C-9), 160.0 (C-19), 142.9 (C-7), 133.8 (C-23), 133.4 (C-12), 133.2 (C-21), 131.6 (C-3), 129.1 (two coinciding peaks, C-1 and C-14), 128.1 (C-2), 121.6 (C-13), 120.2 (C-22), 118.8 (C-8), 116.8 (C-11), 115.9 (C-25), 111.7 (C-20), 101.7 (C-24), 66.3 (C-17), 40.7 (C-15), 29.2 (C-16). Note: the boron-bound carbon (C-4) was not detected, presumably due to quadrupolar relaxation.

^{11}B NMR (225 MHz, $CDCl_3$): δ 30.8.

HRMS (ESI): $C_{23}H_{21}BN_3O_2$ $[M+H]^+$: calculated 382.1721, found 381.1727.

IR ν_{max} (neat/cm^{-1}): 3316 (N-H), 3003 (aryl C-H), 2938 (alkyl C-H), 2228 (C≡N), 1620 (C=O).

m.p. 157 – 158 °C.

Tetrabutylammonium (4'-methyl-[2,2'-bipyridin]-5-yl)methanesulfonate, L1

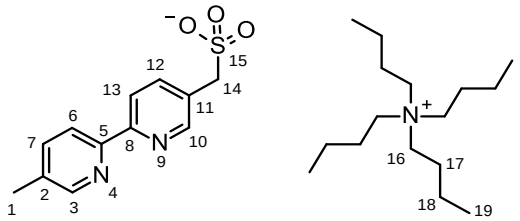

Sodium sulfite (260 mg, 2.07 mmol, 1.2 eq.) was added to a solution of 5-(bromomethyl)-5'-methyl-2,2'-bipyridine (453 mg, 1.72 mmol, 1 eq.) in a mixture of acetone and water (2:3, 10 mL). The resulting solution was heated at reflux at 100 °C for 2 h then allowed to cool to rt. The reaction mixture was concentrated in vacuo and the resulting residue was redissolved in water (4 mL), then washed with DCM (4 mL) and Et_2O (4 mL). DCM (4 mL), tetrabutyl ammonium hydrogen sulfate (462 mg, 1.36 mmol, 0.8 eq.) and NaOH (54 mg, 1.36 mmol, 0.8 eq.) was added, and the mixture stirred vigorously for 1 h. The two layers were then separated, and the aqueous layer extracted with DCM (3 × 5 mL). The combined organic layers were washed with H_2O (3 × 5 mL) to remove excess tetrabutyl ammonium. The organic layer was dried over $MgSO_4$ and concentrated *in vacuo* to afford **L1** (247 mg, 25%) as a white solid.

^{1}H NMR (500 MHz, $CDCl_3$): δ 8.69 (d, *J* = 1.8 Hz, 1H, H-10), 8.47 (dd, *J* = 1.5, 0.7 Hz, 1H, H-3), 8.29 – 8.26 (m, 2H, H-6 and H-13), 7.97 (dd, *J* = 8.1, 2.2 Hz, 1H, H-12), 7.59 (ddd, *J* = 8.1, 2.2, 0.6 Hz, 1H, H-7), 4.12 (s, 2H, H-14), 3.11 – 3.05 (m, 8H, H-16), 2.37 (s, 3H, H-1), 1.53 – 1.43 (m, 8H, H-17), 1.39 – 1.29 (m, 8H, H-18), 0.93 (t, *J* = 7.3 Hz, 12H, H-19).

^{13}C NMR (126 MHz, $CDCl_3$): δ 153.8 (C-8), 153.7 (C-5z), 150.7 (C-10), 149.3 (C-3), 138.6 (C-12), 137.1 (C-7), 132.7 (C-2), 130.9 (C-11), 120.0 (two coinciding peaks, C-6 and C-13), 58.2 (C-16), 54.5 (C-14), 23.6 (C-17), 19.4 (C-18), 18.0 (C-1), 13.3 (C-19).

HRMS (ESI): $C_{12}H_{13}BN_2O_3S$ $[M+H]^+$: calculated 265.0641, found 265.0636.

IR ν_{max} (neat/cm^{-1}): 3375 (O-H), 2961 (alkyl C-H), 2872 (alkyl C-H), 1492 (S=O).

m.p. 98 – 100 °C.

1-Methyl-2-phenyl-3H-1,3,2-benzodiazaborinin-4-one, 249

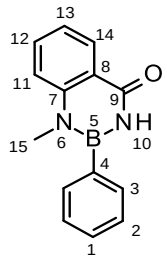

To a suspension of 2-methylaminobenzamide (431 mg, 2.87 mmol, 1 eq.) in toluene (10 mL) was added phenylboronic acid (350 mg, 2.87 mmol, 1 eq.) and heated at reflux at 110 °C for 3 h. The resulting light-yellow solution was allowed to cool to rt and concentrated in vacuo. The resulting off-white solid was washed with Et_2O to afford **249** (500 mg, 74%) as a white solid.

^{1}H NMR (700 MHz, $CDCl_3$): δ 8.36 (dd, *J* = 7.8, 1.7 Hz, 1H, H-14), 7.68 (t, *J* = 7.8 Hz, 1H, H-12), 7.58 (dd, *J* = 6.4, 3.0 Hz, 2H, H-3), 7.48 – 7.45 (m, 3H, (1H, H-1), (2H, H-2)), 7.32 (d, *J* = 7.8 Hz, 1H, H-11), 7.25 (t, *J* = 7.8 Hz, 2H, H-13), 7.25 (br s, 1H, NH), 3.40 (s, 3H, H-15).

^{13}C NMR (176 MHz, $CDCl_3$): δ 166.0 (C-9), 146.9 (C-7), 134.2 (C-12), 132.7 (C-3), 129.7 (two coinciding peaks, C-1 and C-14), 128.4 (C-2), 121.9 (C-13), 120.2 (C-8), 114.9 (C-11), 34.8 (C-15). Note: the boron-bound carbon (C-4) was not detected, presumably due to quadrupolar relaxation.

^{11}B NMR (128 MHz, $CDCl_3$): δ 30.3.

HRMS (ESI): $C_{14}H_{14}BN_2O$ $[M+H]^+$: calculated 237.1194, found 237.1196.

IR ν_{max} (neat/cm^{-1}): 3194 (N-H), 3078 (aryl C-H), 3019 (aryl C-H), 2892 (alkyl C-H), 1658 (C=O).

m.p. 169 – 171 °C.

4.3.2 Synthesis of diazaboroles via halomethyl boronates

3-Cyclohexyl-2,7,7,8,8-pentamethyl-6,9-dioxa-1,3-diaza-5λ^4-boraspiro[4.4]non-1-ene, 307

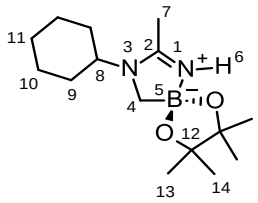

General procedure **C** was carried out with cyclohexylamine (208 µL, 2 eq.) as the amine, MeCN (2 mL) as the nitrile, and bromomethylboronic acid pinacol ester (220 mg, 1 mmol, 1 eq.). Silica gel column chromatography eluted with EtOAc/MeOH/NEt_3 (90:8:2) delivered **307** (167 mg, 66%) as a white solid.

^{1}H NMR (700 MHz, $CDCl_3$): δ 5.52 (br s, 1H, H-6), 3.33 – 3.27 (m, 1H, H-8), 2.29 (s, 2H, H-4), 2.02 (s, 3H, H-7), 1.79 (br d, 2H, *J* = 13.6 Hz, H-10), 1.65 – 1.59 (m, 1H, H-11'), 1.60 – 1.52 (m, 4H, H-9), 1.27 – 1.20 (m, 3H, (2H, H-10), (1H, H-11'')), 1.11 (s, 6H, s, H-13), 1.08 (6H, s, H-14).

^{13}C NMR (176 MHz, $CDCl_3$): δ 165.5 (C-2), 78.7 (C-12), 56.0 (C-8), 40.3 – 39.0 (m, C-4), 30.9 (C-9), 25.6 (C-10), 25.2 (two coinciding peaks, C-11 and C-13), 25.1 (C-14), 15.5 (C-7).

^{11}B NMR (225 MHz, $CDCl_3$): δ 7.5.

HRMS (ESI): $C_{15}H_{30}BN_2O_2$ $[M+H]^+$: calculated 281.2395, found 281.2393.

IR ν_{max} (neat/cm^{-1}): 3256 (N–H), 2965 (alkyl C–H), 2932 (alkyl C–H), 2857 (alkyl C–H), 1596 (C=N), 1162 (C–O), 1045 (C–O).

m.p. 212 – 213 °C.

2,2,3,3,7-Pentamethyl-8-propyl-1,4-dioxa-6,8-diaza-5lambda4-boraspiro[4.4]non-6-ene, 308

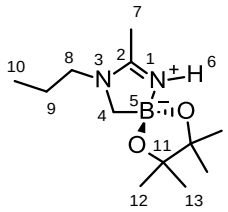

General procedure **C** was carried out with *n*-propylamine (164 µL, 2 eq.) as the amine, MeCN (2 mL) as the nitrile, and bromomethylboronic acid pinacol ester (220 mg, 1 mmol, 1 eq.). Silica gel column chromatography eluted with EtOAc/MeOH/NEt_3 (90:8:2) afforded **308** (153 mg, 64%) as a white solid.

^{1}H NMR (700 MHz, $CDCl_3$): δ 5.55 (br s, 1H, H-6), 3.16 (t, *J* = 7.3 Hz, 2H, H-8), 2.39 (s, 2H, H-4), 2.03 (s, 3H, H-7), 1.59 (sext, *J* = 7.3 Hz, 2H, H-9), 1.13 (s, 6H, H-12), 1.10 (s, 6H, H-13), 0.87 (t, *J* = 7.3 Hz, 3H, H-10).

^{13}C NMR (176 MHz, $CDCl_3$): δ 166.3 (C-2), 78.8 (C-11), 50.3 (C-8), 46.4 – 44.7 (m, C-4), 25.3 (C-12), 25.1 (C-13), 21.1 (C-9), 15.4 (C-7), 11.3 (C-10).

^{11}B NMR (160 MHz, $CDCl_3$): δ 7.6.

HRMS (ESI): $C_{12}H_{26}BN_2O_2$ $[M+H]^+$: calculated 241.2082, found 241.2084.

IR ν_{max} (neat/cm^{-1}): 3286 (N–H), 2988 (alkyl C–H), 2920 (alkyl C–H), 1561 (C=N).

m.p. 108 – 109 °C.

3-(Propylamino)but-2-enenitrile, 311

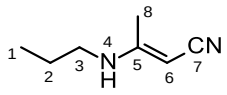

n-Propylamine (146 µL, 1.78 mmol, 1 eq.) and MeCN (2 mL) were added to a flame-dried vial and cooled to 0 °C. *n*-BuLi (1.6 M in hexanes, 1.1 mL, 1.78 mmol, 1 eq.) was then added dropwise and the reaction mixture was stirred at 0 °C for a further 20 minutes and then allowed to slowly warm to room temperature over 18 h. The resulting yellow solution was then diluted with sat. aq. NH_4Cl (10 mL) and then extracted with DCM (3 × 20 mL). The combined organic extracts were dried over $MgSO_4$, filtered and concentrated *in vacuo*. The crude residue was then purified by flash column chromatography to afford **311** (49 mg, 23%) as a colourless oil.

^{1}H NMR (600 MHz, $CDCl_3$): δ 4.30 (br s, 1H, H-4), 3.76 (s, 1H, H-6), 2.89 (td, *J* = 7.3, 5.3 Hz, 2H, H-3), 2.09 (s, 3H, H-8), 1.59 (sext, *J* = 7.3 Hz, 2H, H-2), 0.95 (t, J = 7.3 Hz, 3H, H-1).

^{13}C NMR (126 MHz, $CDCl_3$): δ 160.1 (C-5), 122.3 (C-7), 60.3 (C-6), 45.4 (C-3), 21.7 (C-2), 20.5 (C-8), 11.7 (C-1).

HRMS (ESI): $C_7H_{13}N_2$ $[M+H]^+$: calculated 125.1073, found 125.1072.

IR ν_{max} (neat/cm^{-1}): 3320 (N–H), 3079 (=C–H), 2964 (alkyl C–H), 2933 (alkyl C–H), 2876 (alkyl C–H), 2185 (C≡N), 1594 (C=C), 1541.

3-(Cyclohexylamino)but-2-enenitrile, 313

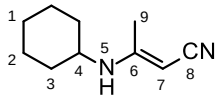

Cyclohexylamine (116 µL, 1.01 mmol, 1 eq.) and MeCN (2 mL) were added to a flame-dried vial and cooled to 0 °C. *n*-BuLi (1.6 M in hexanes, 630 µL, 1.01 mmol, 1 eq.) was then added dropwise and the reaction mixture was stirred at 0 °C for a further 20 minutes and allowed to slowly warm to room temperature over 18 h. The resulting yellow solution was then diluted with sat. aq. NH_4Cl (10 mL) and extracted with DCM (3 × 20 mL). The combined organic extracts were dried over $MgSO_4$, filtered and concentrated *in vacuo*. The crude residue was then purified by flash column chromatography to afford **313** (31 mg, 19%) as a colourless oil.

^{1}H NMR (600 MHz, $CDCl_3$): δ 4.24 (br s, 1H, H-5), 3.78 (s, 1H, H-7), 3.10 – 2.95 (m, 1H, H-3), 2.06 (s, 3H, H-9), 1.94 (dd, *J* = 12.1, 2.2 Hz, 2H, H-3), 1.77 – 1.67 (m, 2H, H-2), 1.66 – 1.57 (m, 1H, H-1'), 1.35 – 1.25 (m, 2H, H-2), 1.23 – 1.06 (m, 3H, (2H, H-3), (1H, H-1'')).

^{13}C NMR (126 MHz, $CDCl_3$): δ 158.8 (C-6), 122.5 (C-8), 60.0 (C-7), 51.9 (C-4), 32.3 (C-3), 25.7 (C-1), 24.8 (C-2), 20.9 (C-9).

HRMS (ESI): $C_{10}H_{16}N_2$ $[M+H]^+$: calculated 165.1386, found 165.1385.

IR ν_{max} (neat/cm^{-1}): 3302 (N–H), 3085 (=C–H), 2929 (alkyl C–H), 2856 (alkyl C–H), 2179 (C≡N), 1589 (C=C), 1546.

2,2,3,3,7-Pentamethyl-3-butyl-1,4-dioxa-6,8-diaza-5λ^4-boraspiro[4.4]non-6-ene, 321

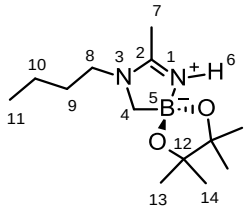

General procedure **C** was carried out with *n*-butylamine (180 µL, 2 eq.) as the amine, MeCN (2 mL) as the nitrile, and bromomethylboronic acid pinacol ester (220 mg, 1 mmol, 1 eq.). Silica gel column chromatography eluted with EtOAc/MeOH/NEt_3 (90:8:2) delivered **321** (145 mg, 63%) as a white solid.

^{1}H NMR (700 MHz, $CDCl_3$): δ 5.51 (br s, 1H, H-6), 3.17 (t, *J* = 7.3 Hz, 2H, H-8), 2.37 (s, 2H, H-4), 2.00 (s, 3H, H-7), 1.58 – 1.46 (m, 2H, H-9), 1.26 (sext, *J* = 7.3 Hz, 2H, H-10), 1.12 (s, 6H, H-13), 1.08 (s, 6H, H-14), 0.88 (t, *J* = 7.3 Hz, 3H, H-11).

^{13}C NMR (176 MHz, $CDCl_3$): δ 166.1 (C-2), 78.7 (C-12), 48.4 (C-8), 46.6 – 44.8 (m, C-4), 29.9 (C-9), 25.3 (C-13), 25.2 (C-14), 20.0 (C-10), 15.4 (C-7), 13.8 (C-11).

^{11}B NMR (160 MHz, $CDCl_3$): δ 7.6.

HRMS (ESI): $C_{13}H_{28}BN_2O_2$ $[M+H]^+$: calculated 255.2238, found 255.2235.

IR ν_{max} (neat/cm^{-1}): 3231 (N–H), 2960 (alkyl C–H), 2930 (alkyl C–H), 2858 (alkyl C–H), 1601 (C=N), 1161 (C–O), 1055 (C–O).

m.p. 120 – 121 °C.

2,2,3,3,7-Pentamethyl-8-(*p*-tolyl)-1,4-dioxa-6,8-diaza-5λ^4-boraspiro[4.4]non-6-ene, 322

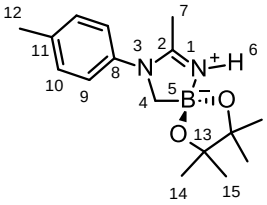

General procedure **C** was carried out with *p*-toluidine (213 mg, 2 eq.) as the amine, MeCN (2 mL) as the nitrile, and bromomethylboronic acid pinacol ester (220 mg, 1 mmol, 1 eq.). Silica gel column chromatography eluted with EtOAc/MeOH/NEt_3 (90:8:2) delivered **322** (174 mg, 61%) as a colourless oil.

^{1}H NMR (700 MHz, $CDCl_3$): δ 7.15 (d, *J* = 8.2 Hz, 2H, H-10), 6.99 (d, *J* = 8.2 Hz, 2H, H-9), 5.97 (br s, 1H, H-6), 2.84 (s, 2H, H-4), 2.34 (s, 3H, H-12), 1.95 (s, 3H, H-7), 1.17 (s, 6H, H-14), 1.11 (s, 6H, H-15).

^{13}C NMR (176 MHz, $CDCl_3$): δ 166.8 (C-2), 138.9 (C-8), 137.6 (C-11), 130.2 (C-10), 125.6 (C-9), 78.9 (C-13), 51.5 – 50.1 (m, C-4), 25.3 (C-14), 25.1 (C-15), 21.2 (C-12), 16.2 (C-7).

^{11}B NMR (225 MHz, $CDCl_3$): δ 7.8.

HRMS (ESI): $C_{16}H_{26}BN_2O_2$ $[M+H]^+$: calculated 289.2082, found 289.2085.

IR ν_{max} (neat/cm^{-1}): 3231 (N–H), 2993 (alkyl C–H), 2919 (alkyl C–H), 2876 (alkyl C–H), 1576 (C=N), 1102 (C–O), 1076 (C–O).

8-[(4-Methoxyphenyl)methyl]-2,2,3,3,7-pentamethyl-1,4-dioxa-6,8-diaza-5λ^4-boraspiro[4.4]non-6-ene, 323

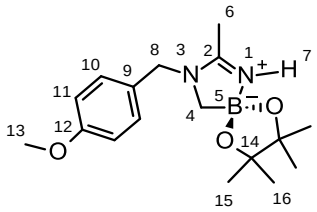

General procedure **C** was carried out with 4-methoxybenzylamine (178 µL, 2 eq.) as the amine, MeCN (2 mL) as the nitrile, and bromomethylboronic acid pinacol ester (220 mg, 1 mmol, 1 eq.). Silica gel column chromatography eluted with EtOAc/MeOH/NEt_3 (90:8:2) delivered **323** (134 mg, 43%) as a colourless oil.

^{1}H NMR (600 MHz, $CDCl_3$): δ 7.07 (d, *J* = 8.5 Hz, 2H, H-10), 6.84 (d, *J* = 8.5 Hz, 2H, H-11), 5.70 (br s, 1H, H-7), 4.36 (s, 2H, H-8), 3.79 (s, 3H, H-13), 2.39 (s, 2H, H-4), 2.12 (s, 3H, H-6), 1.13 (s, 6H, H-15), 1.07 (s, 6H, H-16).

^{13}C NMR (151 MHz, $CDCl_3$): δ 166.5 (C-2), 159.3 (C-12), 128.7 (C-10), 127.5 (C-9), 114.3 (C-11), 78.7 (C-14), 55.4 (C-13) 52.0 (C-8), 25.2 (C-15), 25.0 (C-16), 15.6 (C-6). Note: the boron-bound carbon (C-4) was not detected, presumably due to quadrupolar relaxation.

^{11}B NMR (225 MHz, $CDCl_3$): δ 7.6.

HRMS (ESI): $C_{17}H_{28}BN_2O_3$ $[M+H]^+$: calculated 319.2188, found 319.2183.

IR ν_{max} (neat/cm^{-1}): 3240 (N-H), 3068 (aryl C-H), 2922 (alkyl C-H), 1591 (C=N).

8-Benzyl-2,2,3,3,7-pentamethyl-1,4-dioxa-6,8-diaza-5λ^4-boraspiro[4.4]non-6-ene, 324

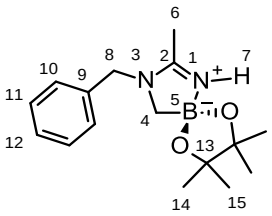

General procedure **C** was carried out with benzylamine (198 μL, 2 eq.) as the amine, MeCN (2 mL) as the nitrile, and bromomethylboronic acid pinacol ester (220 mg, 1 mmol, 1 eq.). Silica gel column chromatography eluted with EtOAc/MeOH/NEt_3 (90:8:2) delivered **324** (100 mg, 39%) as a colourless oil.

^{1}H NMR (700 MHz, $CDCl_3$): δ 7.30 – 7.25 (m, 2H, H-11), 7.23 (t, *J* = 7.3 Hz, 1H, H-12), 7.10 (d, *J* = 7.3 Hz, 2H, H-10), 5.73 (br s, 1H, H-7), 4.38 (s, 2H, H-8), 2.38 (s, 2H, H-4), 2.07 (s, 3H, H-6), 1.10 (s, 6H, H-14), 1.03 (s, 6H, H-15).

^{13}C NMR (176 MHz, $CDCl_3$): δ 166.8 (C-2), 135.6 (C-9), 129.0 (C-11), 127.9 (C-12), 127.2 (C-10), 78.8 (C-13), 52.6 (C-8), 47.5 – 46.3 (m, C-4), 25.3 (C-14), 25.1 (C-15), 15.6 (C-6).

^{11}B NMR (225 MHz, $CDCl_3$): δ 7.7.

HRMS (ESI): $C_{16}H_{26}BN_2O_2$ $[M+H]^+$: calculated 289.2082, found 289.2076.

IR ν_{max} (neat/cm^{-1}): 3216 (N–H), 3088 (aryl C–H), 3064 (aryl C–H), 2962 (alkyl C–H), 2924 (alkyl C–H), 2866 (alkyl C–H), 15994 (C=N), 1163 (C–O), 1052 (C–O).

2,2,3,3,7-Pentamethyl-8-(2-phenylethyl)-1,4-dioxa-6,8-diaza-5λ^4-boraspiro[4.4]non-6-ene, 325

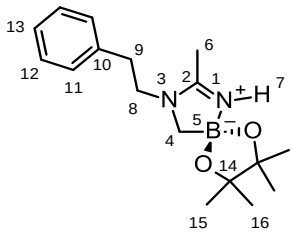

General procedure **C** was carried out with phenethylamine (228 µL, 2 eq.) as the amine, MeCN (2 mL) as the nitrile, and bromomethylboronic acid pinacol ester (220 mg, 1 mmol, 1 eq.). Silica gel column chromatography eluted with EtOAc/MeOH/NEt_3 (90:8:2) delivered **325** (147 mg, 54%) as a white solid.

^{1}H NMR (600 MHz, $CDCl_3$): δ 7.25 (t, *J* = 7.3 Hz, 2H, H-12), 7.18 (t, *J* = 7.3 Hz, 1H, H-13), 7.10 (d, *J* = 7.3 Hz, 2H, H-11), 5.51 (br s, 1H, H-7), 3.40 (t, *J* = 7.2 Hz, 2H, H-8), 2.80 (t, *J* = 7.2 Hz, 2H, H-9), 2.48 (s, 2H, H-4), 1.67 (s, 3H, H-6), 1.11 (s, 6H, H-15), 1.09 (s, 6H, H-16).

^{13}C NMR (151 MHz, $CDCl_3$): δ 166.5 (C-4), 138.3 (C-10), 128.8 (two coinciding peaks, C-11 and C-12), 126.8 (C-13), 78.7 (C-14), 50.7 (C-8), 46.4 – 44.0 (m, C-4), 34.1 (C-9), 25.2 (C-15), 25.1 (C-16), 15.0 (C-6).

^{11}B NMR (160 MHz, $CDCl_3$): δ 7.6.

HRMS (ESI): $C_{17}H_{28}BN_2O_2$ $[M+H]^+$: calculated 303.2238, found 303.2238.

IR ν_{max} (neat/cm^{-1}): 3216 (N–H), 3064 (aryl C–H), 2962 (alkyl C–H), 2923 (alkyl C–H), 2866 (alkyl C–H), 1554 (C=N), 1163 (C–O), 1051 (C–O).

m.p. 170 – 173 °C.

8-(2,2-Dimethoxyethyl)-2,2,3,3,7-pentamethyl-1,4-dioxa-6,8-diaza-5λ^4-boraspiro[4.4]non-6-ene, 326

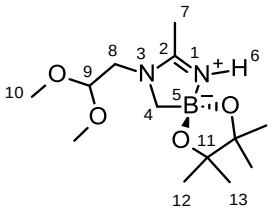

General procedure **C** was carried out with aminoacetaldehyde dimethyl acetal (197 µL, 2 eq.) as the amine, MeCN (2 mL) as the nitrile, and bromomethylboronic acid pinacol ester (220 mg, 1 mmol, 1 eq.). Silica gel column chromatography eluted with EtOAc/MeOH/NEt_3 (90:8:2) delivered **326** (34 mg, 13%) as a white solid.

^{1}H NMR (700 MHz, $CDCl_3$): δ 5.65 (br s, 1H, H-6), 4.46 (t, *J* = 5.3 Hz, 1H, H-9), 3.37 (s, 6H, H-10), 3.30 (d, *J* = 5.3 Hz, 2H, H-8), 2.46 (s, 2H, H-4), 2.07 (s, 3H, H-7), 1.14 (s, 6H, H-12), 1.10 (s, 6H, H-13).

^{13}C NMR (176 MHz, $CDCl_3$): δ 167.9 (C-2), 102.2 (C-9), 78.8 (C-11), 55.4 (C-10), 51.6 (C-8), 25.3 (C-12), 25.1 (C-13), 15.8 (C-7). Note: the boron-bound carbon (C-4) was not detected, presumably due to quadrupolar relaxation.

^{11}B NMR (160 MHz, $CDCl_3$): δ 7.6.

HRMS (ESI): $C_{13}H_{28}BN_2O_4$ $[M+H]^+$: calculated 287.2137, found 287.2128.

IR ν_{max} (neat/cm^{-1}): 3248 (N–H), 2965 (alkyl C–H), 2929 (alkyl C–H), 2892 (alkyl C–H), 1560 (C=N), 1183 (C–O), 1056 (C–O).

m.p. 173 – 175 °C.

***tert*-Butyl 2-(2,2,3,3,7-pentamethyl-1,4-dioxa-6,8-diaza-5λ^4-boraspiro[4.4]non-6-en-8-yl)acetate, 327**

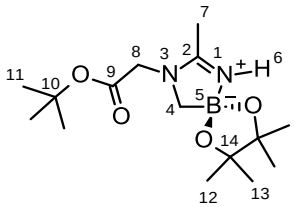

General procedure **C** was carried out with glycine *tert*-butyl ester (261 µL, 2 eq.) as the amine, MeCN (2 mL) as the nitrile, and bromomethylboronic acid pinacol ester (220 mg, 1 mmol, 1 eq.). Silica gel column chromatography eluted with EtOAc/MeOH/NEt_3 (90:8:2) delivered **327** (120 mg, 39%) as a white solid.

^{1}H NMR (500 MHz, $CDCl_3$): δ 5.84 (br s, 1H, H-6), 3.85 (s, 2H, H-8), 2.47 (s, 2H, H-4), 2.05 (s, 3H, H-7), 1.45 (s, 9H, H-11), 1.14 (s, 6H. H-12), 1.10 (s, 6H, H-13).

^{13}C NMR (176 MHz, $CDCl_3$): δ 168.1 (C-2), 167.1 (C-9), 82.9 (C-10), 78.9 (C-14), 51.3 (C-8), 49.0 – 47.8 (m, C-4), 28.1 (C-11), 25.2 (C-12), 25.0 (C-13), 15.4 (C-7).

^{11}B NMR (225 MHz, $CDCl_3$): δ 7.7.

HRMS (ESI): $C_{15}H_{30}BN_2O_4$ $[M+H]^+$: calculated 313.2293, found 313.2289.

IR ν_{max} (neat/cm^{-1}): 3233 (N-H), 2970 (alkyl C-H), 2928 (alkyl C-H), 1743 (C=O).

m.p. 197 – 198 °C.

8-Butyl-7-ethyl-2,2,3,3-tetramethyl-1,4-dioxa-6,8-diaza-5λ^4-boraspiro[4.4]non-6-ene, 328

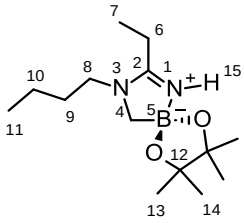

General procedure **C** was carried out with *n*-butylamine (200 µL, 2 eq.) as the amine, propionitrile (388 µL) as the nitrile, and bromomethylboronic acid pinacol ester (220 mg, 1 mmol, 1 eq.). Silica gel column chromatography eluted with EtOAc/MeOH/NEt_3 (90:8:2) delivered **328** (102 mg, 42%) as an off-white solid.

^{1}H NMR (700 MHz, $CDCl_3$): δ 5.59 (br s, 1H, H-15), 3.18 (t, *J* = 7.4 Hz, 2H, H-8), 2.41 (s, 2H, H-4), 2.32 (q, *J* = 7.6 Hz, 2H, H-6), 1.56 – 1.51 (m, 2H, H-9), 1.30 – 1.24 (m, 2H, H-10), 1.20 (t, *J* = 7.6 Hz, 3H, H-7), 1.15 (s, 6H, H-13), 1.11 (s, 6H, H-14), 0.90 (t, *J* = 7.4 Hz, 3H, H-11).

^{13}C NMR (176 MHz, $CDCl_3$): δ 170.5 (C-2), 78.9 (C-12), 47.9 (C-8), 29.9 (C-9), 25.3 (C-13), 25.1 (C-14), 21.5 (C-6), 20.1 (C-10), 13.9 (C-11), 10.0 (C-7). Note: the boron-bound carbon (C-4) was not detected, presumably due to quadrupolar relaxation.

^{11}B NMR (225 MHz, $CDCl_3$): δ 7.7.

HRMS (ESI): $C_{14}H_{30}BN_2O_2$ $[M+H]^+$: calculated 269.2395, found 269.2395.

IR ν_{max} (neat/cm^{-1}): 3232 (N–H), 2959 (alkyl C–H), 2929 (alkyl C–H), 2873 (alkyl C–H), 1601 (C=N), 1206 (C–O), 1050 (C–O).

m.p. 105 – 108 °C.

8-Butyl-7-isopropyl-2,2,3,3-tetramethyl-1,4-dioxa-6,8-diaza-5λ^4-boraspiro[4.4]non-6-ene, 329

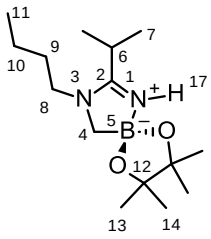

General procedure **C** was carried out with *n*-butylamine (200 µL, 2 eq.) as the amine, isobutyronitrile (534 µL) as the nitrile, and bromomethylboronic acid pinacol ester (220 mg, 1 mmol, 1 eq.). Silica gel column chromatography eluted with EtOAc/MeOH/NEt_3 (90:8:2) delivered **329** (12 mg, 4%) as a colourless oil.

^{1}H NMR (700 MHz, $CDCl_3$): δ 5.48 (br s, 1H. H-17), 3.19 (t, *J* = 7.5 Hz, 2H, H-8), 2.69 (heptet, *J* = 6.8 Hz, 1H, H-6), 2.38 (s, 2H. H-4), 1.55 (dt, *J* = 15.1, 7.5 Hz, 2H, H-9), 1.27 (sext, *J* = 7.5 Hz, 2H, H-10), 1.18 (d, *J* = 6.8 Hz, 6H, H-7), 1.13 (s, 6H, H-13), 1.09 (s, 6H, H-14), 0.90 (t, *J* = 7.5 Hz, 3H, H-11).

^{13}C NMR (176 MHz, $CDCl_3$): δ 174.0 (C-2), 78.7 (C-12), 47.8 (C-8), 30.2 (C-9), 26.5 (C-6), 25.3 (C-13), 25.1 (C-14), 20.1 (C-10), 20.0 (C-7), 13.9 (C-11). Note: the boron-bound carbon (C-4) was not detected, presumably due to quadrupolar relaxation.

^{11}B NMR (225 MHz, $CDCl_3$): δ 7.6.

HRMS (ESI): $C_{15}H_{32}BN_2O_2$ $[M+H]^+$: calculated 283.2551, found 283.2546.

IR ν_{max} (neat/cm^{-1}): 3306 (N–H), 2963 (alkyl C–H), 2933 (alkyl C–H), 2877 (alkyl C–H), 1581 (C=N), 1162 (C–O), 1041 (C–O).

***tert*-Butyl *N*-[(8-butyl-2,2,3,3-tetramethyl-1,4-dioxa-6,8-diaza-5λ^4-boraspiro[4.4]non-6-en-7-yl)methyl]carbamate, 331**

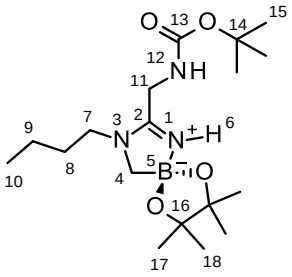

General procedure **C** was carried out with *n*-butylamine (200 µL, 2 eq.) as the amine, *N*-(*tert*-butoxycarbonyl)-2-aminoacetonitrile (848 mg) as the nitrile, and bromomethylboronic acid pinacol ester (220 mg, 1 mmol, 1 eq.). Silica gel column chromatography eluted with EtOAc/MeOH/NEt_3 (90:8:2) delivered **331** (105 mg, 31%) as a white solid.

^{1}H NMR (700 MHz, $CDCl_3$): δ 6.27 (br s, 1H, H-6), 5.99 (br s, 1H, H-12), 3.98 (d, *J* = 5.1 Hz, 2H, H-11), 3.15 (t, *J* = 7.4 Hz, 2H, H-7), 2.42 (s, 2H, H-4), 1.53 (qn, *J* = 7.4 Hz, 2H, H-8), 1.46 (s, 9H, H-15), 1.27 (sext, *J* = 7.4 Hz, 2H, H-9), 1.17 (s, 6H, H-17), 1.12 (s, 6H, H-18), 0.90 (t, *J* = 7.4 Hz, 3H, H-10).

^{13}C NMR (176 MHz, $CDCl_3$): δ 167.5 (C-2), 155.5 (C-13), 81.0 (C-14), 79.1 (C-16), 47.8 (C-7), 37.6 (C-11), 29.9 (C-8), 28.5 (C-15), 25.2 (C-17), 25.0 (C-18), 20.1 (C-9), 13.9 (C-10). Note: the boron-bound carbon (C-4) was not detected, presumably due to quadrupolar relaxation.

^{11}B NMR (225 MHz, $CDCl_3$): δ 7.8.

HRMS (ESI): $C_{18}H_{37}BN_3O_4$ $[M+H]^+$: calculated 370.2872, found 370.2863.

IR ν_{max} (neat/cm^{-1}): 3552 (N–H), 3230 (N–H), 2975 (alkyl C–H), 2954 (alkyl C–H), 2925 (alkyl C–H), 2873 (alkyl C–H), 1675 (C=O),1595 (C=N), 1161 (C–O), 1051 (C–O).

m.p. 199 – 200 °C.

8-Butyl-2,2,3,3-tetramethyl-7-phenyl-1,4-dioxa-6,8-diaza-5λ^4-boraspiro[4.4]non-6-ene, 332

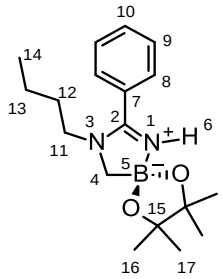

General procedure **C** was carried out with *n*-butylamine (200 µL, 2 eq.) as the amine, benzonitrile (308 µL) as the nitrile, and bromomethylboronic acid pinacol ester (220 mg, 1 mmol, 1 eq.). Silica gel column chromatography eluted with EtOAc/MeOH/NEt_3 (90:8:2) delivered **332** (51 mg, 16%) as a colourless oil.

^{1}H NMR (700 MHz, $CDCl_3$): δ 7.47 (t, *J* = 7.4 Hz, 1H, H-10), 7.42 (t, *J* = 7.4 Hz, 2H, H-9), 7.34 (d, *J* = 7.4 Hz, 2H. H-8), 5.72 (s, 1H, H-6), 3.10 (t, *J* = 7.4 Hz, 2H, H-11), 2.51 (s, 2H, H-4), 1.50 (qn, *J* = 7.4 Hz, 2H, H-12), 1.17 – 1.13 (m, 2H, H-13), 1.12 (s, 6H, H-16), 1.10 (s, 6H, H-17), 0.75 (t, *J* = 7.4 Hz, 3H, H-14).

^{13}C NMR (176 MHz, $CDCl_3$): δ 168.7 (C-2), 131.1 (C-10), 129.6 (C-7), 129.1 (C-9), 127.4 (C-8), 78.9 (C-15), 49.1 (C-11), 30.0 (C-12), 25.2 (C-16), 25.1 (C-17), 19.8 (C-13), 13.7 (C-14). Note: the boron-bound carbon (C-4) was not detected, presumably due to quadrupolar relaxation.

^{11}B NMR (225 MHz, $CDCl_3$): δ 8.0.

HRMS (ESI): $C_{18}H_{30}BN_2O_2$ $[M+H]^+$: calculated 317.2395, found 317.2391.

IR ν_{max} (neat/cm^{-1}): 3302 (N–H), 2980 (alkyl C–H), 2931 (alkyl C–H), 2892 (alkyl C–H), 1583 (C=N), 1152 (C–O), 1058 (C–O).

7-Benzyl-8-butyl-2,2,3,3-tetramethyl-1,4-dioxa-6,8-diaza-5λ^4-boraspiro[4.4]non-6-ene, 333

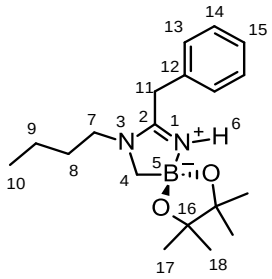

General procedure **C** was carried out with *n*-butylamine (200 µL, 2 eq.) as the amine, phenylacetonitrile (629 µL) as the nitrile, and bromomethylboronic acid pinacol ester (220 mg, 1 mmol, 1 eq.). Silica gel column chromatography eluted with EtOAc/MeOH/NEt_3 (90:8:2) delivered **333** (40 mg, 15%) as a colourless oil.

^{1}H NMR (700 MHz, $CDCl_3$): δ 7.34 (t, *J* = 7.2 Hz, 2H, H-14), 7.30 (t, *J* = 7.2 Hz, 1H, H-15), 7.18 (d, *J* = 7.2 Hz, 2H, H-13), 5.40 (br s, 1H, H-6), 3.61 (s, 2H, H-11), 3.21 (t, *J* = 7.4 Hz, 2H, H-7), 2.44 (s, 2H, H-4), 1.52 – 1.46 (m, 2H, H-8), 1.26 (sext, *J* = 7.4 Hz, 2H, H-9), 1.07 (s, 6H, H-17), 1.04 (s, 6H, H-18), 0.86 (t, *J* = 7.4 Hz, 3H, H-10).

^{13}C NMR (176 MHz, $CDCl_3$): δ 167.9 (C-2), 132.5 (C-12), 129.4 (C-13), 129.3 (C-14), 128.1 (C-15), 78.7 (C-16), 48.2 (C-7), 35.1 (C-11), 29.8 (C-8), 25.2 (C-17), 25.1 (C-18), 20.0 (C-9), 13.9 (C-10). Note: the boron-bound carbon (C-4) was not detected, presumably due to quadrupolar relaxation.

^{11}B NMR (225 MHz, $CDCl_3$): δ 7.7.

HRMS (ESI): $C_{19}H_{32}BN_2O_2$ $[M+H]^+$: calculated 331.2551, found 331.2542.

IR ν_{max} (neat/cm^{-1}): 3207 (N–H), 2962 (alkyl C–H), 2928 (alkyl C–H), 2867 (alkyl C–H), 1601 (C=N), 1161 (C–O), 1053 (C–O).

2-[Chloro-(4-methoxyphenyl)methyl]-4,4,5,5-tetramethyl-1,3,2-dioxaborolane, 334

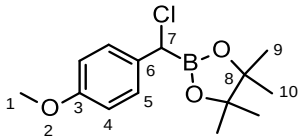

To a stirred solution of DCM (393 µL, 6.15 mmol, 1.6 eq.) and THF (5 mL) at -100 °C, was added *n*-BuLi (1.6 M in hexanes, 2.88 mL, 4.61 mmol, 1.2 eq.) dropwise and a white precipitate formed towards the end of the BuLi addition. Subsequently, 4-methoxyphenylboronic acid pinacol ester (900 mg, 3.84 mmol, 1 eq.) in THF (5 mL) was added dropwise and the reaction mixture was allowed to warm to rt over 18 h and then concentrated *in vacuo*. Cold hexane (10 mL) was added to the residue and the suspension stirred for 10 min followed by filtration. The filtrate was concentrated *in vacuo* to afford compound **334** (938 mg, 86%) as a pale-yellow oil.

^{1}H NMR (700 MHz, $CDCl_3$): δ 7.38 (d, *J* = 8.7 Hz, 2H, H-5), 6.86 (d, *J* = 8.7 Hz, 2H, H-4), 4.46 (s, 1H, H-7), 3.79 (s, 3H, H-1), 1.29 (s, 6H, H-9), 1.28 (s, 6H, H-10).

^{13}C NMR (176 MHz, $CDCl_3$): δ 159.5 (C-3), 130.9 (C-6), 130.3 (C-5), 114.2 (C-4), 84.8 (C-8), 55.3 (C-1), 24.7 (C-9), 24.6 (C-10). Note: the boron-bound carbon (C-7) was not detected, presumably due to quadrupolar relaxation.

^{11}B NMR (225 MHz, $CDCl_3$): δ 31.0

LRMS (ESI): $C_{14}H_{21}BClO_3$ $[M+H]^+$: calculated 283.13, found 283.11.

2-(1-Chloro-2-phenyl-ethyl)-4,4,5,5-tetramethyl-1,3,2-dioxaborolane, 335

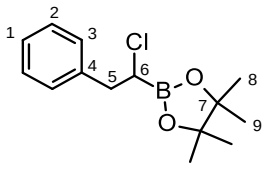

To a stirred solution of DCM (394 µL, 6.16 mmol, 1.6 eq.) and THF (5 mL) at -100 °C, was added *n*-BuLi (1.6 M in hexanes, 3.13 mL, 5.01 mmol, 1.3 eq.) dropwise and a white precipitate formed towards the end of the BuLi addition. Subsequently, benzylboronic acid pinacol ester (840 mg, 3.85 mmol, 1 eq.) in THF (5 mL) was added dropwise and the reaction mixture was allowed to warm to rt over 18 h and then concentrated *in vacuo*. Cold hexane (10 mL) was added to the residue and the suspension stirred for 10 min followed by filtration. The filtrate was concentrated *in vacuo* to afford compound **335** (720 mg, 67%) as a pale-yellow oil.

^{1}H NMR (700 MHz, $CDCl_3$): δ 7.29 (t, *J* = 7.1 Hz, 2H, H-2), 7.26 (d, *J* = 7.1 Hz, 2H, H-3), 7.23 (t, *J* = 7.1 Hz, 1H, H-1), 3.60 (t, *J* = 8.2 Hz, 1H, H-6), 3.18 (dd, *J* = 13.8, 8.2 Hz, 1H, H-5'), 3.10 (dd, *J* = 13.8, 8.2 Hz, 1H, H-5''), 1.24 (s, 6H, H-8), 1.22 (s, 6H, H-9)

^{13}C NMR (176 MHz, $CDCl_3$): δ 138.4 (C-4), 129.3 (C-2), 128.4 (C-3), 126.8 (C-1), 84.5 (C-7), 40.3 (C-5), 24.7 (C-8), 24.6 (C-9). Note: the boron-bound carbon (C-6) was not detected, presumably due to quadrupolar relaxation.

^{11}B NMR (225 MHz, $CDCl_3$): δ 32.0

HRMS (ESI): $C_{14}H_{19}BClO_2$ $[M–H]^-$: calculated 265.1172, found 265.1244.

2-(1-Chloro-3-phenyl-propyl)-4,4,5,5-tetramethyl-1,3,2-dioxaborolane, 336

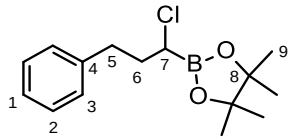

To a stirred solution of DCM (204 µL, 3.20 mmol, 1.6 eq.) and THF (5 mL) at -100 °C, was added *n*-BuLi (1.6 M in hexanes, 1.50 mL, 2.40 mmol, 1.2 eq.) dropwise and a white precipitate formed towards the end of the BuLi addition. Subsequently, 2-phenylethyl-1-boronic acid pinacol ester (464 mg, 2.00 mmol, 1 eq.) in THF (5 mL) was added dropwise and the reaction mixture was allowed to warm to rt over 18 h and then concentrated *in vacuo*. Cold hexane (10 mL) was added to the residue and the suspension stirred for 10 min followed by filtration. The filtrate was concentrated *in vacuo* to afford compound **336** (289 mg, 53%) as a colourless oil.

^{1}H NMR (600 MHz, $CDCl_3$): δ 7.28 (t, *J* = 7.5 Hz, 2H, H-2), 7.23 – 7.16 (m, 3H, H-1 and H-3), 3.41 (t, *J* = 7.7 Hz, 1H, H-7), 2.84 (dt, *J* = 14.5, 7.7 Hz, 1H, H-5'), 2.75 (dt, *J* = 14.5, 7.7 Hz, 1H, H-5''), 2.12 (dd, *J* = 14.5, 7.7 Hz, 2H, H-6), 1.28 (s, 12H, H-9).

^{13}C NMR (151 MHz, $CDCl_3$): δ 141.2 (C-4), 128.8 (two coinciding peaks, C-2 and C-3), 126.2 (C-1), 84.6 (C-8), 35.8 (C-6), 33.4 (C-5), 24.7 (C-9). Note: the boron-bound carbon (C-7) was not detected, presumably due to quadrupolar relaxation.

^{11}B NMR (225 MHz, $CDCl_3$): δ 31.5.

2-(1-Bromo-1-methyl-ethyl)-4,4,5,5-tetramethyl-1,3,2-dioxaborolane, 338

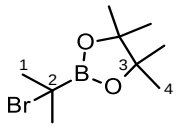

To a solution of isopropoxyboronic acid pinacol ester (1.01 g, 1.11 mL, 5.94 mmol, 1.1 eq.) in DCM (20 mL) was added Br_2 (864 mg, 277 µL, 5.40 mmol, 1 eq.) under an argon atmosphere and the reaction was stirred art room temperature for 3 h. The reaction mixture was then concentrated in vacuo to afford **338** (1.4 g, quantitative yield) as a light-yellow oil which was used for the next step without further purification.

^{1}H NMR (700 MHz, $CDCl_3$): δ 1.76 (s, 6H, H-1), 1.27 (s, 12H, H-4).

^{13}C NMR (126 MHz, $CDCl_3$): δ 84.4 (C-3), 30.4 (C-1), 24.5 (C-4). Note: the boron-bound carbon (C-2) was not detected, presumably due to quadrupolar relaxation.

^{11}B NMR (225 MHz, $CDCl_3$): δ 28.0.

HRMS (ESI): $C_9H_{19}BBrO_2$ $[M+H]^+$: calculated 249.0656, found 249.0651.

8-Cyclohexyl-9-methyl-2,2,3,3,7-pentamethyl-1,4-dioxa-6,8-diaza-5λ^4-boraspiro[4.4]non-6-ene, 340

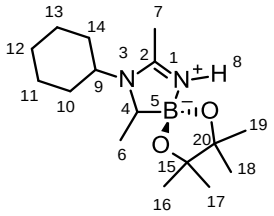

General procedure **C** was carried out with cyclohexylamine (228 µL, 2 mmol, 2 eq.) as the amine, MeCN (2 mL) as the nitrile, and 2-(1-bromoethyl)-4,4,5,5-tetramethyl-1,3,2-dioxaborolane (190 mg, 1 mmol, 1 eq.). Silica gel column chromatography eluted with EtOAc/MeOH/NEt_3 (90:8:2) delivered **340** (229 mg, 78%) as a white solid.

^{1}H NMR (700 MHz, Acetone-d_6): δ 6.64 (br s, 1H, H-8), 3.48 (tt, *J* = 12.0, 3.8 Hz, 1H, H-9), 2.46 (q, *J* = 6.7 Hz, 1H, H-4), 2.14 (s, 3H, H-7), 1.86 – 1.80 (m, 2H, H-10’ and H-11’), 1.79 – 1.74 (m, 2H, H-10’’ and H-13’), 1.70 (qd, *J* =12.4, 3.8 Hz, 1H, H-13’’), 1.64 (d, *J* = 11.8 Hz, 1H, H-12’), 1.60 (qd, *J* = 12.4, 3.8 Hz, 1H, H-11’’), 1.40 – 1.28 (m, 2H, H-14’ and H-14’’), 1.18 (qt, *J* = 12.4, 3.8 Hz, 1H, H-12’’), 1.09 (d, *J* = 6.7 Hz, 3H, H-6), 1.01 (s, 3H, H-16), 1.00 (s, 3H, H-17), 0.99 (s, 3H, H-18), 0.96 (s, 3H, H-19).

^{13}C NMR (176 MHz, Acetone-d_6): δ 166.7 (C-2), 78.3 (C-15), 78.1 (C-20), 57.0 (C-9), 34.5 (C-11), 31.2 (C-13), 26.5 (C-14), 26.4 (C-10), 26.1 (C-16), 26.0 (C-12), 25.9 (C-17), 25.7 (C-18), 25.6 (C-19), 18.0 (C-6), 15.3 (C-7). Note: the boron-bound carbon (C-4) was not detected, presumably due to quadrupolar relaxation.

^{11}B NMR (225 MHz, Acetone-d_6): δ 7.9.

HRMS (ESI): $C_{16}H_{32}BN_2O_2$ $[M+H]^+$: calculated 295.2551, found 295.2552.

IR ν_{max} (neat/cm^{-1}): 3269 (N–H), 2967 (alkyl C–H), 2949 (alkyl C–H), 2856 (alkyl C–H), 1584 (C=N), 1165 (C–O), 1048 (C–O).

m.p. 164 – 165 °C.

8-Butyl-9-methyl-2,2,3,3,7-pentamethyl-1,4-dioxa-6,8-diaza-5λ^4-boraspiro[4.4]non-6-ene, 341

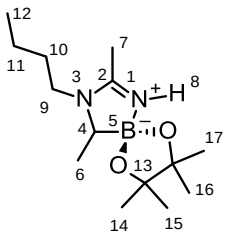

General procedure **C** was carried out with *n*-butylamine (197 µL, 2 mmol, 2 eq.) as the amine, MeCN (2 mL) as the nitrile, and 2-(1-bromoethyl)-4,4,5,5-tetramethyl-1,3,2-dioxaborolane (190 mg, 1 mmol, 1 eq.). Silica gel column chromatography eluted with EtOAc/MeOH/NEt_3 (90:8:2) delivered **341** (191 mg, 71%) as a white solid as well as a small amount of inseparable pinacol.

^{1}H NMR (700 MHz, $CDCl_3$): δ 5.52 (s, 1H, H-8), 3.26 – 3.14 (m, 2H, H-9), 2.61 – 2.54 (m, 1H, H-4), 2.02 (s, 3H, H-7), 1.60 – 1.52 (m, 1H, H-10'), 1.47 – 1.40 (m, 1H, H-10''), 1.34 – 1.24 (m, 2H, H-11), 1.16 – 1.08 (m, 15H, H-6, H-14, H-15, H-16, H-17), 0.94 – 0.88 (m, 3H, H-12).

^{13}C NMR (176 MHz, $CDCl_3$): δ 165.6 (C-2), 78.9 (C-13), 43.6 (C-9), 30.3 (C-10), 25.5 (C-14), 25.4 (two coinciding peaks, C-15, C-16), 25.3 (C-17), 20.2 (C-11), 15.6 (C-7), 13.9 (C-12), 13.8 (C-6). Note: the boron-bound carbon (C-4) was not detected, presumably due to quadrupolar relaxation.

^{11}B NMR (225 MHz, $CDCl_3$): δ 7.8.

HRMS (ESI): $C_{14}H_{30}BN_2O_2$ $[M+H]^+$: calculated 269.2395, found 269.2392.

IR ν_{max} (neat/cm^{-1}): 3225 (N–H), 2959 (alkyl C–H), 2938 (alkyl C–H), 2855 (alkyl C–H), 1591 (C=N), 1164 (C–O), 1054 (C–O).

m.p. 198 – 200 °C.

8-Butyl-9,9-dimethyl-2,2,3,3,7-pentamethyl-1,4-dioxa-6,8-diaza-5λ^4-boraspiro[4.4]non-6-ene, 342

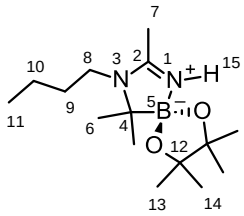

General procedure **C** was carried out with *n*-butylamine (200 µL, 2 eq.) as the amine, MeCN (2 mL) as the nitrile, and UHS-553 (250 mg, 1 mmol, 1 eq.). Silica gel column chromatography eluted with EtOAc/MeOH/NEt_3 (90:8:2) delivered **342** (66 mg, 23%) as a white solid.

^{1}H NMR (700 MHz, $CDCl_3$): δ 5.43 (br s, 1H, H-15), 3.12 – 3.07 (m, 2H, H-8), 2.00 (s, 3H, H-7), 1.51 – 1.45 (m, 2H, H-9), 1.31 (sext, *J* = 7.4 Hz, 2H, H-10), 1.13 (s, 6H, H-6), 1.08 (s, 6H, H-13), 1.08 (s, 6H, H-14), 0.92 (t, *J* = 7.4 Hz, 3H, H-11).

^{13}C NMR (176 MHz, $CDCl_3$): δ 165.0 (C-2), 78.5 (C-12), 41.2 (C-8), 33.4 (C-9), 25.7 (C-13), 25.5 (C-14), 23.4 (C-6), 20.6 (C-10), 15.7 (C-7), 13.8 (C-11). Note: the boron-bound carbon (C-4) was not detected, presumably due to quadrupolar relaxation.

^{11}B NMR (225 MHz, $CDCl_3$): δ 8.0.

HRMS (ESI): $C_{15}H_{32}BN_2O_2$ $[M+H]^+$: calculated 283.2551, found 283.2545.

IR ν_{max} (neat/cm^{-1}): 3239 (N–H), 2961 (alkyl C–H), 2929 (alkyl C–H), 2873 (alkyl C–H), 1595 (C=N), 1153 (C–O), 1044 (C–O).

m.p. 100 – 102 °C.

8-Benzyl-9-methyl-2,2,3,3,7-pentamethyl-1,4-dioxa-6,8-diaza-5λ^4-boraspiro[4.4]non-6-ene, 343

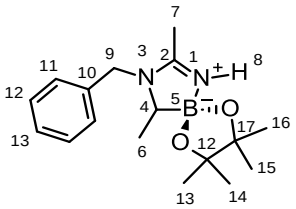

General procedure **C** was carried out with benzylamine (280 µL, 2 mmol, 2 eq.) as the amine, MeCN (2 mL) as the nitrile, and 2-(1-bromoethyl)-4,4,5,5-tetramethyl-1,3,2-dioxaborolane (190 mg, 1 mmol, 1 eq.). Silica gel column chromatography eluted with EtOAc/MeOH/NEt_3 (90:8:2) delivered **343** (163 mg, 54%) as a white solid.

^{1}H NMR (700 MHz, $CDCl_3$): δ 7.31 (t, *J* = 7.4 Hz, 2H, H-12), 7.27 – 7.24 (m, 1H, H-13), 7.16 (d, *J* = 7.4 Hz, 2H, H-11), 5.71 (br s, 1H, H-8), 4.50 – 4.43 (m, 2H, H-9), 2.58 (q, *J* = 6.8 Hz, 1H, H-4), 2.04 (s, 3H, H-7), 1.17 – 1.13 (m, 9H, contains H-6 (3H), H-13 (3H) and H-14 (3H)), 1.10 (s, 3H, H-15), 1.08 (s, 3H, H-16).

^{13}C NMR (176 MHz, $CDCl_3$): δ 166.6 (C-2), 136.3 (C-10), 129.0 (C-12), 127.8 (C-13), 127.0 (C-11), 78.8 (C-12), 78.5 (C-17), 51.6 – 50.2 (m, C-4), 47.9 (C-9), 25.5 (two coinciding peaks, C-13 and C-14), 25.5 (C-15), 25.4 (C-16), 16.1 (C-7), 14.0 (C-6).

^{11}B NMR (225 MHz, $CDCl_3$): δ 7.9.

HRMS (ESI): $C_{17}H_{28}BN_2O_2$ $[M+H]^+$: calculated 303.2238, found 303.2225.

IR ν_{max} (neat/cm^{-1}): 3235 (N–H), 3031 (aryl C–H), 2964 (alkyl C–H), 2941 (alkyl C–H), 2915 (alkyl C–H), 1594 (C=N).

m.p. 161 – 163 °C.

8-(*p*-Tolyl)-9-methyl-2,2,3,3,7-pentamethyl-1,4-dioxa-6,8-diaza-5λ^4-boraspiro[4.4]non-6-ene, 344

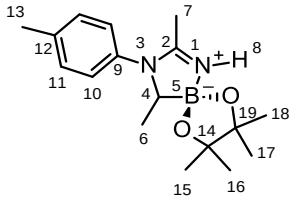

General procedure **C** was carried out with *p*-toluidine (214 mg, 2 mmol, 2 eq.) as the amine, MeCN (2 mL) as the nitrile, and 2-(1-bromoethyl)-4,4,5,5-tetramethyl-1,3,2-dioxaborolane (190 mg, 1 mmol, 1 eq.). Silica gel column chromatography eluted with EtOAc/MeOH/NEt_3 (90:8:2) delivered **344** (162 mg, 53%) as a white solid.

^{1}H NMR (700 MHz, $CDCl_3$): δ 7.17 (d, *J* = 8.2 Hz, 2H, H-11), 6.95 (d, *J* = 8.2 Hz, 2H, H-10), 5.91 (s, 1H, H-8), 2.96 (q, *J* = 7.2 Hz, 1H, H-4), 2.35 (s, 3H, H-13), 1.89 (s, 3H, H-7), 1.19 (s, 6H, H-15, H-16), 1.14 (s, 3H, H-17), 1.13 (s, 3H, H-18), 0.98 (d, *J* = 7.2 Hz, 3H, H-6).

^{13}C NMR (176 MHz, $CDCl_3$): δ 166.2 (C-2), 137.9 (C-12), 136.2 (C-9), 130.2 (C-11), 127.2 (C-10), 79.1 (C-14), 78.8 (C-19), 25.5 (two coinciding peaks; C-15, C-16), 25.4 (C-17), 25.3 (C-18), 21.2 (C-13), 16.4 (C-7), 14.4 (C-6). Note: the boron-bound carbon (C-4) was not detected, presumably due to quadrupolar relaxation.

^{11}B NMR (225 MHz, $CDCl_3$): δ 8.0.

HRMS (ESI): $C_{17}H_{28}BN_2O_2$ $[M+H]^+$: calculated 303.2238, found 303.2238.

IR ν_{max} (neat/cm^{-1}): 3239 (N–H), 3096 (aryl C–H), 2966 (alkyl C–H), 2925 (alkyl C–H), 2864 (alkyl C–H), 1593 (C=N), 1066 (C–O), 1017 (C–O).

m.p. 197 – 198 °C.

8-(2-Phenylethyl)-9-methyl-2,2,3,3,7-pentamethyl-1,4-dioxa-6,8-diaza-5λ^4-boraspiro[4.4]non-6-ene, 345

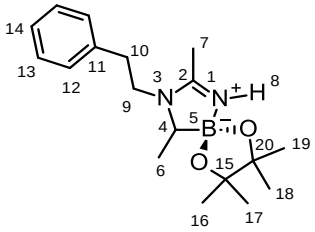

General procedure **C** was carried out with phenethylamine (251 µL, 2 mmol, 2 eq.) as the amine, MeCN (2 mL) as the nitrile, and 2-(1-bromoethyl)-4,4,5,5-tetramethyl-1,3,2-dioxaborolane (190 mg, 1 mmol, 1 eq.). Silica gel column chromatography eluted with EtOAc/MeOH/NEt_3 (90:8:2) delivered **345** (141 mg, 45%) as an off-white solid.

^{1}H NMR (700 MHz, $CDCl_3$): δ 7.30 (t, *J* = 7.5 Hz, 2H, H-13), 7.23 (t, *J* = 7.3 Hz, 1H, H-14), 7.16 (d, *J* = 7.5 Hz, 2H, H-12), 5.54 (br s, 1H, H-8), 3.49 (ddd, *J* = 14.5, 9.2, 5.3 Hz, 1H, H-9'), 3.43 – 3.36 (m, 1H, H-9''), 2.89 (ddd, *J* = 14.5, 9.2, 5.3 Hz, 1H, H-10'), 2.73 – 2.68 (m, 2H, H-10'' and H-4), 1.81 (s, 3H, H-7), 1.19 (d, *J* = 7.3 Hz, 3H, H-6), 1.16 (s, 6H, H-16 and H-17), 1.12 (s, 6H, H-18 and H-19).

^{13}C NMR (176 MHz, $CDCl_3$): δ 165.9 (C-2), 138.4 (C-11), 128.9 (C-12), 128.8 (C-13), 126.9 (C-14), 78.8 (C-15), 78.5 (C-20), 45.9 (C-9), 34.8 (C-10), 25.6 (C-16 and C17), 25.5 (C-18), 25.4 (C-19), 15.5 (C-7), 14.0 (C-6). Note: the boron-bound carbon (C-4) was not detected, presumably due to quadrupolar relaxation.

^{11}B NMR (225 MHz, $CDCl_3$): δ 7.9.

HRMS (ESI): $C_{18}H_{30}BN_2O_2$ $[M+H]^+$: calculated 317.2395, found 317.2393.

IR ν_{max} (neat/cm^{-1}): 3220 (N–H), 3091 (aryl C–H), 2963 (alkyl C–H), 2921 (alkyl C–H), 2860 (alkyl C–H), 1597 (C=N), 1164 (C–O), 1056 (C–O).

m.p. 239 – 242 °C.

8-Cyclohexyl-9-(2-phenylethyl)-2,2,3,3,7-pentamethyl-1,4-dioxa-6,8-diaza-5λ^4-boraspiro[4.4]non-6-ene, 347

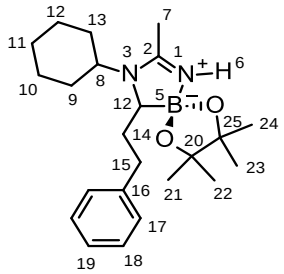

To a scintillation vial, cyclohexylamine (131 µL, 2 eq.) and MeCN (2 mL) was added followed by 2-(1-chloro-3-phenyl-propyl)-4,4,5,5-tetramethyl-1,3,2-dioxaborolane (160 mg, 1 mmol, 1 eq.). The reaction mixture was then stirred at room temperature for 18 h. The resulting suspension was diluted with sat. aq. $NaHCO_3$ (20 mL), extracted with DCM (3 × 20 mL) and washed with brine (20 mL). The combined organic extracts were dried over $MgSO_4$, filtered and concentrated *in vacuo*. The resultant crude residue was then purified by flash column chromatography to afford **347** (38 mg, 17%) as a beige solid.

^{1}H NMR (700 MHz, $CDCl_3$): δ 7.24 (t, *J* = 7.4 Hz, 2H, H-18), 7.20 (d, *J* = 7.4 Hz, 2H, H-17), 7.13 (t, *J* = 7.4 Hz, 1H, H-19), 5.58 (br s, 1H, H-6), 3.28 (tt, *J* = 12.2, 3.3 Hz, 1H, H-8), 2.97 (td, *J* = 12.9, 5.1 Hz, 1H, H-15'), 2.73 (d, *J* = 6.0 Hz, 1H, H-12), 2.57 (td, *J* = 12.9, 4.3 Hz, 1H, H-15''), 2.09 (s, 3H, H-7), 2.02 – 1.94 (m, 1H, H-14'), 1.91 – 1.76 (m, 5H, (1H, H-9'), (1H, H-10'), (1H, H-12'), (1H, H-13'), (1H, H-14'')), 1.69 – 1.55 (m, 3H, (1H, H-10'), (1H, H-11'), (1H, H-12'')), 1.29 – 1.21 (m, 2H, H-9'' and H-13''), 1.17 (s, 3H, H-21), 1.14 (s, 3H, H-22), 1.13 (s, 3H, H-23), 1.12 (s, 3H, H-24), 1.11 – 1.07 (m, 1H, H-11'').

^{13}C NMR (176 MHz, $CDCl_3$): δ 166.6 (C-2), 144.3 (C-16), 128.5 (C-17), 128.3 (C-18), 125.4 (C-19), 78.8 (C-20), 78.4 (C-25), 57.7 (C-8), 54.6 – 53.4 (m, C-12), 33.8 (C-10), 33.5 (C-14), 32.0 (C-15), 30.9 (C-12), 26.3 (two coinciding peaks, C-9 and C-13), 25.8 (two coinciding peaks, C-21 and C-22), 25.6 (two coinciding peaks, C-23 and C-24), 25.5 (C-11), 16.4 (C-7).

^{11}B NMR (225 MHz, $CDCl_3$): δ 7.8.

HRMS (ESI): $C_{23}H_{38}BN_2O_2$ $[M+H]^+$: calculated 385.3021, found 385.3010.

IR ν_{max} (neat/cm^{-1}): 3340 (N–H), 3028 (aryl C–H), 2981 (alkyl C–H), 2937 (alkyl C–H), 1586 (C=N).

m.p. 111 – 113 °C.

8-Propyl-9-benzyl-2,2,3,3,7-pentamethyl-1,4-dioxa-6,8-diaza-5λ^4-boraspiro[4.4]non-6-ene, 348

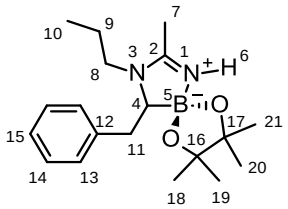

To a scintillation vial, *n*-propylamine (75 µL, 2 eq.) and MeCN (2 mL) was added followed by 2-(1-chloro-2-phenyl-ethyl)-4,4,5,5-tetramethyl-1,3,2-dioxaborolane (122 mg, 1 mmol, 1 eq.). The reaction mixture was then stirred at room temperature for 18 h. The resulting suspension was diluted with sat. aq. $NaHCO_3$ (20 mL), extracted with DCM (3 × 20 mL) and washed with brine (20 mL). The combined organic extracts were dried over $MgSO_4$, filtered, and concentrated *in vacuo*. The resultant crude residue was then purified by flash column chromatography to afford **348** (43 mg, 28%) as an off-white solid.

^{1}H NMR (500 MHz, $CDCl_3$): δ 7.30 (d, *J* = 7.5 Hz, 2H, H-13), 7.24 (t, *J* = 7.5 Hz, 2H, H-14), 7.13 (t, *J* = 7.5 Hz, 1H, H-15), 5.56 (br s, 1H, H-6), 3.25 (dd, *J* = 15.4, 3.7 Hz, 1H, H-11'), 2.98 (dd, J = 9.5, 3.7 Hz, 1H, H-4), 2.92 (ddd, *J* = 14.4, 9.9, 6.7 Hz, 1H, H-8'), 2.83 (ddd, *J* = 14.4, 9.9, 4.6 Hz, 1H, H-8''), 2.58 (dd, *J* = 15.4, 9.5 Hz, 1H, H-11''), 1.99 (s, 3H, H-7), 1.37 – 1.29 (m, 1H, H-9'), 1.21 – 1.16 (m, 1H, H-9''), 1.15 (s, 3H, H-18), 1.13 (s, 3H, H-19), 1.10 (s, 3H, H-20), 1.00 (s, 3H, H-21), 0.53 (t, *J* = 7.4 Hz, 3H, H-10).

^{13}C NMR (176 MHz, $CDCl_3$): δ 165.9 (C-2), 143.5 (C-12), 128.8 (C-13), 128.3 (C-14), 125.6 (C-15), 78.9 (C-16), 78.6 (C-17), 55.8 – 54.3 (m, C-4), 47.1 (C-8), 36.9 (C-11), 25.8 (C-18), 25.7 (C-19), 25.4 (C-20), 25.3 (C-21), 21.0 (C-9), 15.7 (C-7), 11.1 (C-10).

^{11}B NMR (225 MHz, $CDCl_3$): δ 7.7.

HRMS (ESI): $C_{19}H_{32}BN_2O_2$ $[M+H]^+$: calculated 331.2551, found 331.2548.

IR ν_{max} (neat/cm^{-1}): 3273 (N–H), 3028 (aryl C–H), 2968 (alkyl C–H), 2934 (alkyl C–H), 1593 (C=N).

m.p. 141 – 142 °C.

5 References

(1) Ishihara, K.; Yamamoto, H. Arylboron Compounds as Acid Catalysts in Organic Synthetic Transformations. *European J. Org. Chem.* **1999**, *1999*, 527–538. https://doi.org/10.1002/(SICI)1099-0690(199903)1999:3<527::AID-EJOC527>3.0.CO;2-R.

(2) Dasgupta, A.; Babaahmadi, R.; Slater, B.; Yates, B. F.; Ariafard, A.; Melen, R. L. Borane-Catalyzed Stereoselective C–H Insertion, Cyclopropanation, and Ring-Opening Reactions. *Chem* **2020**, *6*, 2364–2381. https://doi.org/10.1016/j.chempr.2020.06.035.

(3) Carden, J. L.; Dasgupta, A.; Melen, R. L. Halogenated Triarylboranes: Synthesis, Properties and Applications in Catalysis. *Chem. Soc. Rev.* **2020**, *49*, 1706–1725. https://doi.org/10.1039/c9cs00769e.

(4) Ishihara, K. Chiral B(III) Lewis Acids. In *Lewis Acids in Organic Synthesis*; John Wiley & Sons, Ltd, 2000; pp 135–190. https://doi.org/10.1002/9783527618309.ch5.

(5) Ishihara, K. Achiral B(III) Lewis Acids. In *Lewis Acids in Organic Synthesis*; John Wiley & Sons, Ltd, 2000; pp 89–133. https://doi.org/10.1002/9783527618309.ch4.

(6) Ma, Y.; Wang, B.; Zhang, L.; Hou, Z. Boron-Catalyzed Aromatic C-H Bond Silylation with Hydrosilanes. *J. Am. Chem. Soc.* **2016**, *138*, 3663–3666. https://doi.org/10.1021/jacs.6b01349.

(7) Sabatini, M. T.; Boulton, L. T.; Sheppard, T. D. Borate Esters: Simple Catalysts for the Sustainable Synthesis of Complex Amides. *Sci. Adv.* **2017**, *3*, e1701028. https://doi.org/10.1126/sciadv.1701028.

(8) Kirschner, S.; Peters, M.; Yuan, K.; Uzelac, M.; Ingleson, M. J. Developing Organoboranes as Phase Transfer Catalysts for Nucleophilic Fluorination Using CsF. *Chem. Sci.* **2022**, *13*, 2661–2668. https://doi.org/10.1039/D2SC00303A.

(9) Brown, H.; Rao, B. C. Communications - Hydroboration of Olefins. A Remakably Fast Room-Temperature Addition of Diborane to Olefins. *J. Org. Chem.* **1957**, *22*, 1136–1137. https://doi.org/10.1021/jo01360a625.

(10) Brown, H. C.; Zweifel, G. A stereospecific cis hydration of the double bond in cyclic derivatives. *J. Am. Chem. Soc.* **1959**, *81*, 247. https://doi.org/10.1021/ja01510a059.

(11) Brown, H. C.; Mandal, A. K.; Kulkarni, S. U. Hydroboration. 45. New, Convenient Preparations of Representative Borane Reagents Utilizing Borane-Methyl Sulfide. *J. Org. Chem.* **1977**, *42*, 1392–1398. https://doi.org/10.1021/jo00428a028.

(12) Miyaura, N.; Yamada, K.; Suzuki, A. A New Stereospecific Cross-Coupling by the Palladium-Catalyzed Reaction of 1-Alkenylboranes with 1-Alkenyl or 1-Alkynyl Halides. *Tetrahedron Lett.* **1979**, *20*, 3437–3440. https://doi.org/10.1016/S0040-4039(01)95429-2.

(13) Miyaura, N.; Suzuki, A. Stereoselective Synthesis of Arylated (E)-Alkenes by the Reaction of Alk-1-Enylboranes with Aryl Halides in the Presence of Palladium Catalyst. *J. Chem. Soc., Chem. Commun.* **1979**, No. 19, 866–867. https://doi.org/10.1039/C39790000866.

(14) Mukaiyama, T.; Inomata, K.; Yamamoto, S. The Reactions of Thioboronite. *Tetrahedron Lett.* **1971**, *12*, 1097–1100. https://doi.org/10.1016/S0040-4039(01)96636-5.

(15) Fenzl, W.; Köster, R.; Zimmerman, H. J. Justus Liebigs Ann. Chem. **1975**.

(16) Brown, H. C.; Dhar, R. K.; Bakshi, R. K.; Pandiarajan, P. K.; Singaram, B. Major Effect of the Leaving Group in Dialkylboron Chlorides and Triflates in Controlling the Stereospecific Conversion of Ketones into Either [E]- or [Z]-Enol Borinates. *J. Am. Chem. Soc.* **1989**, *111*, 3441–3442. https://doi.org/10.1021/ja00191a058.

(17) Paterson, I.; Lombart, H.-G.; Allerton, C. Total Synthesis of Elaiolide Using a Copper(I)-Promoted Stille Cyclodimerization Reaction. *Org. Lett.* **1999**, *1*, 19–22. https://doi.org/10.1021/ol990004c.

(18) Schlesinger, H. I.; Brown, H. C. Metallo Borohydrides. III. Lithium Borohydride. *J. Am. Chem. Soc.* **1940**, *62*, 3429–3435. https://doi.org/10.1021/ja01869a039.

(19) Chaikin, S. W.; Brown, W. G. Reduction of Aldehydes, Ketones and Acid Chlorides by Sodium Borohydride. *J. Am. Chem. Soc.* **1949**, *71*, 122–125. https://doi.org/10.1021/ja01169a033.

(20) Luche, J. L. Lanthanides in Organic Chemistry. 1. Selective 1,2 Reductions of

Conjugated Ketones. *J. Am. Chem. Soc.* **1978**, *100*, 2226–2227. https://doi.org/10.1021/ja00475a040.

(21) Hütter, R.; Keller-Schierlein, W.; Knüsel, F.; Prelog, V.; Rodgers Jr, G. C.; Suter, P.; Vogel, G.; Voser, W.; Zähner, H. The Metabolic Products of Microorganisms. Boromycin. *Helv. Chim. Acta* **1967**, *50*, 1533–1539.

(22) Kohno, J.; Kawahata, T.; Otake, T.; Morimoto, M.; Mori, H.; Ueba, N.; Nishio, M.; Kinumaki, A.; Komatsubara, S.; Kawashima, K. Boromycin, an Anti-HIV Antibiotic. *Biosci. Biotechnol. Biochem.* **1996**, *60*, 1036–1037. https://doi.org/10.1271/bbb.60.1036.

(23) Hemscheidt, T.; Puglisi, M. P.; Larsen, L. K.; Patterson, G. M. L.; Moore, R. E.; Rios, J. L.; Clardy, J. Structure and Biosynthesis of Borophycin, a New Boeseken Complex of Boric Acid from a Marine Strain of the Blue-Green Alga Nostoc Linckia. *J. Org. Chem.* **1994**, *59*, 3467–3471. https://doi.org/10.1021/jo00091a042.

(24) Okami, Y.; Okazaki, T.; Kitahara, T.; Umezawa, H. Studies on Marine Microorganisms. V. A New Antibiotic, Aplasmomycin, Produced by a Streptomycete Isolated from Shallow Sea Mud. *J. Antibiot. (Tokyo).* **1976**, *29*, 1019–1025. https://doi.org/10.7164/antibiotics.29.1019.

(25) Schummer, D.; Irschik, H.; Reichenbach, H.; Höfle, G. Antibiotics from Gliding Bacteria, LVII. Tartrolons: New Boron-containing Macrodiolides from Sorangium Cellulosum. *Liebigs Ann. der Chemie* **1994**, *1994*, 283–289. https://doi.org/10.1002/jlac.199419940310.

(26) Sato, K.; Okazaki, T.; Maeda, K.; Okami, Y. New Antibiotics, Aplasmomycins B and C. *J. Antibiot. (Tokyo).* **1978**, *31*, 632–635. https://doi.org/10.7164/antibiotics.31.632.

(27) Elshahawi, S. I.; Trindade-Silva, A. E.; Hanora, A.; Han, A. W.; Flores, M. S.; Vizzoni, V.; Schrago, C. G.; Soares, C. A.; Concepcion, G. P.; Distel, D. L.; Schmidt, E. W.; Haygood, M. G. Boronated Tartrolon Antibiotic Produced by Symbiotic Cellulose-Degrading Bacteria in Shipworm Gills. *Proc. Natl. Acad. Sci.* **2013**, *110*, E295–E304. https://doi.org/10.1073/pnas.1213892110.

(28) Accardi, F.; Toscani, D.; Bolzoni, M.; Dalla Palma, B.; Aversa, F.; Giuliani, N. Mechanism of Action of Bortezomib and the New Proteasome Inhibitors on Myeloma

Cells and the Bone Microenvironment: Impact on Myeloma-Induced Alterations of Bone Remodeling. *Biomed Res. Int.* **2015**, 172458. https://doi.org/10.1155/2015/172458.

(29) Finch, J. J.; Jinna, S. Spotlight on Tavaborole for the Treatment of Onychomycosis. *Drug Des. Devel. Ther.* **2015**, *9*, 6185. https://doi.org/10.2147/DDDT.S81944.

(30) Adams, S.; Miller, G. T.; Jesson, M. I.; Watanabe, T.; Jones, B.; Wallner, B. P. PT-100, a Small Molecule Dipeptidyl Peptidase Inhibitor, Has Potent Antitumor Effects and Augments Antibody-Mediated Cytotoxicity via a Novel Immune Mechanism. *Cancer Res.* **2004**, *64*, 5471–5480. https://doi.org/10.1158/0008-5472.CAN-04-0447.

(31) Patel, B. D.; Ghate, M. D. Recent Approaches to Medicinal Chemistry and Therapeutic Potential of Dipeptidyl Peptidase-4 (DPP-4) Inhibitors. *Eur. J. Med. Chem.* **2014**, *74*, 574–605. https://doi.org/10.1016/j.ejmech.2013.12.038.

(32) Murahashi, S. Synthesis of phthalimidines from schiff bases and carbon monoxide. *J. Am. Chem. Soc.* **1955**, *77*, 6403–6404. https://doi.org/10.1021/ja01628a120.

(33) Boström, J.; Brown, D. G.; Young, R. J.; Keserü, G. M. Expanding the Medicinal Chemistry Synthetic Toolbox. *Nat. Rev. Drug Discov.* **2018**, *17*, 709–727. https://doi.org/10.1038/nrd.2018.116.

(34) Zaitsev, V. G.; Shabashov, D.; Daugulis, O. Highly Regioselective Arylation of Sp3 C-H Bonds Catalyzed by Palladium Acetate. *J. Am. Chem. Soc.* **2005**, *127*, 13154–13155. https://doi.org/10.1021/ja054549f.

(35) Wan, L.; Dastbaravardeh, N.; Li, G.; Yu, J. Q. Cross-Coupling of Remote Meta -c-h Bonds Directed by a u-Shaped Template. *J. Am. Chem. Soc.* **2013**, *135*, 18056–18059. https://doi.org/10.1021/ja410760f.

(36) Ackermann, L.; Vicente, R.; Althammer, A. Assisted Ruthenium-Catalyzed C-H Bond Activation: Carboxylic Acids as Cocatalysts for Generally Applicable Direct Arylations in Apolar Solvents. *Org. Lett.* **2008**, *10*, 2299–2302. https://doi.org/10.1021/ol800773x.

(37) Hartwig, J. F. Regioselectivity of the Borylation of Alkanes and Arenes. *Chem. Soc. Rev.* **2011**, *40*, 1992–2002. https://doi.org/10.1039/c0cs00156b.

(38) Murai, S.; Kakiuchi, F.; Sekine, S.; Tanaka, Y.; Kamatani, A.; Sonoda, M.; Chatani, N.

Efficient Catalytic Addition of Aromatic Carbon-Hydrogen Bonds to Olefins. *Nature* **1993**, *366*, 529–531. https://doi.org/10.1038/366529a0.

(39) Sonoda, M.; Kakiuchi, F.; Chatani, N.; Murai, S. Ruthenium-Catalyzed Addition of Carbon–Hydrogen Bonds in Aromatic Ketones to Olefins. The Effect of Various Substituents at the Aromatic Ring. *Bull. Chem. Soc. Jpn.* **1997**, *70*, 3117–3128. https://doi.org/10.1246/bcsj.70.3117.

(40) Lim, Y.-G.; Kang, J.-B.; Kim, Y. H. Regioselective Alkylation of 2-Phenylpyridines with Terminal Alkenes via C–H Bond Activation by a Rhodium Catalyst. *J. Chem. Soc., Perkin Trans. 1* **1996**, No. 17, 2201–2206. https://doi.org/10.1039/P19960002201.

(41) Oi, S.; Fukita, S.; Inoue, Y. Rhodium-Catalysed Direct Ortho Arylation of 2-Arylpyridines with Arylstannanes via C–H Activation. *Chem. Commun.* **1998**, No. 22, 2439–2440. https://doi.org/10.1039/A806790B.

(42) Kakiuchi, F.; Kan, S.; Igi, K.; Chatani, N.; Murai, S. A Ruthenium-Catalyzed Reaction of Aromatic Ketones with Arylboronates: A New Method for the Arylation of Aromatic Compounds via C−H Bond Cleavage. *J. Am. Chem. Soc.* **2003**, *125*, 1698–1699. https://doi.org/10.1021/ja029273f.

(43) Dick, A. R.; Hull, K. L.; Sanford, M. S. A Highly Selective Catalytic Method for the Oxidative Functionalization of C−H Bonds. *J. Am. Chem. Soc.* **2004**, *126*, 2300–2301. https://doi.org/10.1021/ja031543m.

(44) Desai, L. V; Hull, K. L.; Sanford, M. S. Palladium-Catalyzed Oxygenation of Unactivated Sp3 C−H Bonds. *J. Am. Chem. Soc.* **2004**, *126*, 9542–9543. https://doi.org/10.1021/ja046831c.

(45) Hartwig, J. F. Carbon- Heteroatom Bond-Forming Reductive Eliminations of Amines, Ethers, and Sulfides. *Acc. Chem. Res.* **1998**, *31*, 852–860.

(46) Han, R.; Hillhouse, G. L. Carbon−Oxygen Reductive-Elimination from Nickel(II) Oxametallacycles and Factors That Control Formation of Ether, Aldehyde, Alcohol, or Ester Products. *J. Am. Chem. Soc.* **1997**, *119*, 8135–8136. https://doi.org/10.1021/ja9714999.

(47) Williams, B. S.; Goldberg, K. I. Studies of Reductive Elimination Reactions To Form

Carbon−Oxygen Bonds from Pt(IV) Complexes. *J. Am. Chem. Soc.* **2001**, *123*, 2576–2587. https://doi.org/10.1021/ja003366k.

(48) Båckvall, J. E. Pure and Appl. Chem. 1992, 64, 429--437;(c) J.-E. Båckvall. *Acc. Chem. Res* **1983**, *16*, 335–342.

(49) Ryabov, A. D.; Sakodinskaya, I. K.; Yatsimirsky, A. K. Kinetics and Mechanism of Ortho-Palladation of Ring-Substituted NN-Dimethylbenzylamines. *J. Chem. Soc., Dalt. Trans.* **1985**, *12*, 2629–2638. https://doi.org/10.1039/DT9850002629.

(50) Canty, A. J.; van Koten, G. Mechanisms of D8 Organometallic Reactions Involving Electrophiles and Intramolecular Assistance by Nucleophiles. *Acc. Chem. Res.* **1995**, *28*, 406–413. https://doi.org/10.1021/ar00058a002.

(51) Davies, D. L.; Donald, S. M. A.; Macgregor, S. A. Computational Study of the Mechanism of Cyclometalation by Palladium Acetate. *J. Am. Chem. Soc.* **2005**, *127*, 13754–13755. https://doi.org/10.1021/ja052047w.

(52) Jonasson, C.; Horváth, A.; Bäckvall, J.-E. Intramolecular Palladium(II)-Catalyzed 1,2-Addition to Allenes. *J. Am. Chem. Soc.* **2000**, *122*, 9600–9609. https://doi.org/10.1021/ja001748k.

(53) Bay, K. L.; Yang, Y.-F.; Houk, K. N. Multiple Roles of Silver Salts in Palladium-Catalyzed C–H Activations. *J. Organomet. Chem.* **2018**, *864*, 19–25. https://doi.org/10.1016/j.jorganchem.2017.12.026.

(54) Wang, D.-H.; Mei, T.-S.; Yu, J.-Q. Versatile Pd(II)-Catalyzed C−H Activation/Aryl−Aryl Coupling of Benzoic and Phenyl Acetic Acids. *J. Am. Chem. Soc.* **2008**, *130*, 17676–17677. https://doi.org/10.1021/ja806681z.

(55) Giri, R.; Maugel, N.; Li, J.-J.; Wang, D.-H.; Breazzano, S. P.; Saunders, L. B.; Yu, J.-Q. Palladium-Catalyzed Methylation and Arylation of Sp2 and Sp3 C−H Bonds in Simple Carboxylic Acids. *J. Am. Chem. Soc.* **2007**, *129*, 3510–3511. https://doi.org/10.1021/ja0701614.

(56) Chiong, H. A.; Pham, Q.-N.; Daugulis, O. Two Methods for Direct Ortho-Arylation of Benzoic Acids. *J. Am. Chem. Soc.* **2007**, *129*, 9879–9884. https://doi.org/10.1021/ja071845e.

(57) Dogan, Ö.; Gürbüz, N.; Özdemir, İ.; Çetinkaya, B. Palladium N-Heterocyclic-

Carbene-Catalyzed Ortho-Arylation of Benzaldehyde Derivatives. *Heteroat. Chem.* **2008**, *19*, 569–574. https://doi.org/10.1002/hc.20479.

(58) Wang, D.-H.; Wasa, M.; Giri, R.; Yu, J.-Q. Pd(II)-Catalyzed Cross-Coupling of Sp3 C−H Bonds with Sp2 and Sp3 Boronic Acids Using Air as the Oxidant. *J. Am. Chem. Soc.* **2008**, *130*, 7190–7191. https://doi.org/10.1021/ja801355s.

(59) Giri, R.; Liang, J.; Lei, J.-G.; Li, J.-J.; Wang, D.-H.; Chen, X.; Naggar, I. C.; Guo, C.; Foxman, B. M.; Yu, J.-Q. Pd-Catalyzed Stereoselective Oxidation of Methyl Groups by Inexpensive Oxidants under Mild Conditions: A Dual Role for Carboxylic Anhydrides in Catalytic C□H Bond Oxidation. *Angew. Chemie Int. Ed.* **2005**, *44*, 7420–7424. https://doi.org/10.1002/anie.200502767.

(60) De Almeida, M. V; Barton, D. H. R.; Bytheway, I.; Ferreira, J. A.; Hall, M. B.; Liu, W.; Taylor, D. K.; Thomson, L. Preparation and Thermal Decomposition of N,N'-Diacyl-N,N'-Dialkoxyhydrazines: Synthetic Applications and Mechanistic Insights. *J. Am. Chem. Soc.* **1995**, *117*, 4870–4874. https://doi.org/10.1021/ja00122a018.

(61) Yus Gabriel; Alonso, Francisco, M. R. Lithium/DTBB-Induced Reduction of N-Alkoxyamides and Acyl Azides. *Synthesis (Stuttg).* **2001**, *2001*, 914–918. https://doi.org/10.1055/s-2001-13415.

(62) Zaitsev, V. G.; Shabashov, D.; Daugulis, O. Highly Regioselective Arylation of Sp3 C−H Bonds Catalyzed by Palladium Acetate. *J. Am. Chem. Soc.* **2005**, *127*, 13154–13155. https://doi.org/10.1021/ja054549f.

(63) Engle, K. M.; Mei, T.-S.; Wasa, M.; Yu, J.-Q. Weak Coordination as a Powerful Means for Developing Broadly Useful C–H Functionalization Reactions. *Acc. Chem. Res.* **2012**, *45*, 788–802. https://doi.org/10.1021/ar200185g.

(64) Lucas, E. L.; Lam, N. Y. S.; Zhuang, Z.; Chan, H. S. S.; Strassfeld, D. A.; Yu, J.-Q. Palladium-Catalyzed Enantioselective β-C(Sp3)–H Activation Reactions of Aliphatic Acids: A Retrosynthetic Surrogate for Enolate Alkylation and Conjugate Addition. *Acc. Chem. Res.* **2022**, *55*, 537–550. https://doi.org/10.1021/acs.accounts.1c00672.

(65) O' Donovan, D. H.; De Fusco, C.; Spring, D. R. The Reductive Cleavage of Picolinic Amides. *Tetrahedron Lett.* **2016**, *57*, 2962–2964. https://doi.org/10.1016/j.tetlet.2016.05.068.

(66) Takamatsu, K.; Hirano, K.; Miura, M. Copper-Mediated Decarboxylative Coupling of Benzamides with Ortho-Nitrobenzoic Acids by Directed C−H Cleavage. *Angew. Chemie Int. Ed.* **2017**, *56*, 5353–5357. https://doi.org/10.1002/anie.201701918.

(67) Kanyiva, K. S.; Kuninobu, Y.; Kanai, M. Palladium-Catalyzed Direct C–H Silylation and Germanylation of Benzamides and Carboxamides. *Org. Lett.* **2014**, *16*, 1968–1971. https://doi.org/10.1021/ol500519y.

(68) Berger, M.; Chauhan, R.; Rodrigues, C. A. B.; Maulide, N. Bridging C−H Activation: Mild and Versatile Cleavage of the 8-Aminoquinoline Directing Group. *Chem. – A Eur. J.* **2016**, *22*, 16805–16808. https://doi.org/10.1002/chem.201604344.

(69) Landge, V. G.; Shewale, C. H.; Jaiswal, G.; Sahoo, M. K.; Midya, S. P.; Balaraman, E. Nickel-Catalyzed Direct Alkynylation of C(Sp2)–H Bonds of Amides: An "Inverse Sonogashira Strategy" to Ortho-Alkynylbenzoic Acids. *Catal. Sci. Technol.* **2016**, *6*, 1946–1951. https://doi.org/10.1039/C5CY01299F.

(70) Li, B. T. Y.; White, J. M.; Hutton, C. A. Synthesis of the LeuTrp Component of the Celogentin Family of Cyclic Peptides Through a CH ActivationCross-Coupling Strategy. *Aust. J. Chem.* **2010**, *63*, 438–444.

(71) Taylor, R. D.; MacCoss, M.; Lawson, A. D. G. Rings in Drugs. *J. Med. Chem.* **2014**, *57*, 5845–5859. https://doi.org/10.1021/jm4017625.

(72) Kalyani, D.; Deprez, N. R.; Desai, L. V; Sanford, M. S. Oxidative C−H Activation/C−C Bond Forming Reactions: Synthetic Scope and Mechanistic Insights. *J. Am. Chem. Soc.* **2005**, *127*, 7330–7331. https://doi.org/10.1021/ja051402f.

(73) Deprez, N. R.; Sanford, M. S. Reactions of Hypervalent Iodine Reagents with Palladium: Mechanisms and Applications in Organic Synthesis. *Inorg. Chem.* **2007**, *46*, 1924–1935. https://doi.org/10.1021/ic0620337.

(74) Chen, Z.-B.; Zhang, F.-L.; Yuan, Q.; Chen, H.-F.; Zhu, Y.-M.; Shen, J.-K. α-Iminonitrile: A New Cyanating Agent for the Palladium Catalyzed C–H Cyanation of Arenes. *RSC Adv.* **2016**, *6*, 64234–64238. https://doi.org/10.1039/C6RA14512D.

(75) Zhao, X.; Dimitrijević, E.; Dong, V. M. Palladium-Catalyzed C−H Bond Functionalization with Arylsulfonyl Chlorides. *J. Am. Chem. Soc.* **2009**, *131*, 3466–3467. https://doi.org/10.1021/ja900200g.

(76) Liu, X.; Yi, Z.; Wang, J.; Liu, G. Decarboxylative Acylation of Arenes with Mandelic Acid Derivatives via Palladium-Catalyzed Oxidative Sp2 C–H Activation. *RSC Adv.* **2015**, *5*, 10641–10646. https://doi.org/10.1039/C4RA14107E.

(77) Chu, J.-H.; Lin, P.-S.; Wu, M.-J. Palladium(II)-Catalyzed Ortho Arylation of 2-Phenoxypyridines with Potassium Aryltrifluoroborates via C−H Functionalization. *Organometallics* **2010**, *29*, 4058–4065. https://doi.org/10.1021/om100494p.

(78) Kinuta, H.; Tobisu, M.; Chatani, N. Rhodium-Catalyzed Borylation of Aryl 2-Pyridyl Ethers through Cleavage of the Carbon–Oxygen Bond: Borylative Removal of the Directing Group. *J. Am. Chem. Soc.* **2015**, *137*, 1593–1600. https://doi.org/10.1021/ja511622e.

(79) Li, J.; Wang, Z.-X. Nickel-Catalyzed Amination of Aryl 2-Pyridyl Ethers via Cleavage of the Carbon–Oxygen Bond. *Org. Lett.* **2017**, *19*, 3723–3726. https://doi.org/10.1021/acs.orglett.7b01549.

(80) Chernyak, N.; Dudnik, A. S.; Huang, C.; Gevorgyan, V. PyDipSi: A General and Easily Modifiable/Traceless Si-Tethered Directing Group for C−H Acyloxylation of Arenes. *J. Am. Chem. Soc.* **2010**, *132*, 8270–8272. https://doi.org/10.1021/ja1033167.

(81) Huang, C.; Chernyak, N.; Dudnik, A. S.; Gevorgyan, V. The Pyridyldiisopropylsilyl Group: A Masked Functionality and Directing Group for Monoselective Ortho-Acyloxylation and Ortho-Halogenation Reactions of Arenes. *Adv. Synth. \& Catal.* **2011**, *353*, 1285–1305. https://doi.org/10.1002/adsc.201000975.

(82) Richter, H.; Beckendorf, S.; Mancheño, O. G. Modifiable Sulfur Tethers as Directing Groups for Aromatic C-H Acetoxylation Reactions. *Adv. Synth. \& Catal.* **2011**, *353*, 295–302. https://doi.org/10.1002/adsc.201000941.

(83) García-Rubia, A.; Fernández-Ibáñez, M. Á.; Gómez Arrayás, R.; Carretero, J. C. 2-Pyridyl Sulfoxide: A Versatile and Removable Directing Group for the PdII-Catalyzed Direct C-H Olefination of Arenes. *Chem. – A Eur. J.* **2011**, *17*, 3567–3570. https://doi.org/10.1002/chem.201003633.

(84) Shi, B.-F.; Maugel, N.; Zhang, Y.-H.; Yu, J.-Q. PdII-Catalyzed Enantioselective Activation of C(Sp2)-H and C(Sp3)-H Bonds Using Monoprotected Amino Acids as Chiral Ligands. *Angew. Chemie Int. Ed.* **2008**, *47*, 4882–4886.

https://doi.org/10.1002/anie.200801030.

(85) Mo, F.; Trzepkowski, L. J.; Dong, G. Synthesis of Ortho-Acylphenols through the Palladium-Catalyzed Ketone-Directed Hydroxylation of Arenes. *Angew. Chemie Int. Ed.* **2012**, *51*, 13075–13079. https://doi.org/10.1002/anie.201207479.

(86) Li, G.; Wan, L.; Zhang, G.; Leow, D.; Spangler, J.; Yu, J.-Q. Pd(II)-Catalyzed C–H Functionalizations Directed by Distal Weakly Coordinating Functional Groups. *J. Am. Chem. Soc.* **2015**, *137*, 4391–4397. https://doi.org/10.1021/ja5126897.

(87) Mei, T.-S.; Giri, R.; Maugel, N.; Yu, J.-Q. PdII-Catalyzed Monoselective Ortho Halogenation of C-H Bonds Assisted by Counter Cations: A Complementary Method to Directed Ortho Lithiation. *Angew. Chemie Int. Ed.* **2008**, *47*, 5215–5219. https://doi.org/10.1002/anie.200705613.

(88) Zhang, Y.-H.; Yu, J.-Q. Pd(II)-Catalyzed Hydroxylation of Arenes with 1 Atm of O2 or Air. *J. Am. Chem. Soc.* **2009**, *131*, 14654–14655. https://doi.org/10.1021/ja907198n.

(89) Giri, R.; Yu, J.-Q. Synthesis of 1,2- and 1,3-Dicarboxylic Acids via Pd(II)-Catalyzed Carboxylation of Aryl and Vinyl C−H Bonds. *J. Am. Chem. Soc.* **2008**, *130*, 14082–14083. https://doi.org/10.1021/ja8063827.

(90) Zhang, Y.-H.; Shi, B.-F.; Yu, J.-Q. Palladium(II)-Catalyzed Ortho Alkylation of Benzoic Acids with Alkyl Halides. *Angew. Chemie Int. Ed.* **2009**, *48*, 6097–6100. https://doi.org/10.1002/anie.200902262.

(91) Lu, Y.; Wang, D.-H.; Engle, K. M.; Yu, J.-Q. Pd(II)-Catalyzed Hydroxyl-Directed C−H Olefination Enabled by Monoprotected Amino Acid Ligands. *J. Am. Chem. Soc.* **2010**, *132*, 5916–5921. https://doi.org/10.1021/ja101909t.

(92) Strassfeld, D. A.; Chen, C.-Y.; Park, H. S.; Phan, D. Q.; Yu, J.-Q. Hydrogen-Bond-Acceptor Ligands Enable Distal C(Sp3)–H Arylation of Free Alcohols. *Nature* **2023**, *622*, 80–86. https://doi.org/10.1038/s41586-023-06485-8.

(93) Wang, X.; Lu, Y.; Dai, H.-X.; Yu, J.-Q. Pd(II)-Catalyzed Hydroxyl-Directed C−H Activation/C−O Cyclization: Expedient Construction of Dihydrobenzofurans. *J. Am. Chem. Soc.* **2010**, *132*, 12203–12205. https://doi.org/10.1021/ja105366u.

(94) Ping, Y.; Wang, L.; Ding, Q.; Peng, Y. Nitrile as a Versatile Directing Group for C(Sp2)–H Functionalizations. *Adv. Synth. Catal.* **2017**, *359*, 3274–3291.

https://doi.org/10.1002/adsc.201700684.

(95) Yoo, E. J.; Ma, S.; Mei, T.-S.; Chan, K. S. L.; Yu, J.-Q. Pd-Catalyzed Intermolecular C–H Amination with Alkylamines. *J. Am. Chem. Soc.* **2011**, *133*, 7652–7655. https://doi.org/10.1021/ja202563w.

(96) Chan, K. S. L.; Wasa, M.; Wang, X.; Yu, J.-Q. Palladium(II)-Catalyzed Selective Monofluorination of Benzoic Acids Using a Practical Auxiliary: A Weak-Coordination Approach. *Angew. Chemie Int. Ed.* **2011**, *50*, 9081–9084. https://doi.org/10.1002/anie.201102985.

(97) Li, G.; Leow, D.; Wan, L.; Yu, J.-Q. Ether-Directed Ortho-C–H Olefination with a Palladium(II)/Monoprotected Amino Acid Catalyst. *Angew. Chemie Int. Ed.* **2013**, *52*, 1245–1247. https://doi.org/10.1002/anie.201207770.

(98) Engle, K. M.; Yu, J.-Q. Developing Ligands for Palladium(II)-Catalyzed C–H Functionalization: Intimate Dialogue between Ligand and Substrate. *J. Org. Chem.* **2013**, *78*, 8927–8955. https://doi.org/10.1021/jo400159y.

(99) Shao, Q.; Wu, K.; Zhuang, Z.; Qian, S.; Yu, J.-Q. From Pd(OAc)2 to Chiral Catalysts: The Discovery and Development of Bifunctional Mono-N-Protected Amino Acid Ligands for Diverse C–H Functionalization Reactions. *Acc. Chem. Res.* **2020**, *53*, 833–851. https://doi.org/10.1021/acs.accounts.9b00621.

(100) García-Cuadrado, D.; Braga, A. A. C.; Maseras, F.; Echavarren, A. M. Proton Abstraction Mechanism for the Palladium-Catalyzed Intramolecular Arylation. *J. Am. Chem. Soc.* **2006**, *128*, 1066–1067. https://doi.org/10.1021/ja056165v.

(101) Lafrance, M.; Rowley, C. N.; Woo, T. K.; Fagnou, K. Catalytic Intermolecular Direct Arylation of Perfluorobenzenes. *J. Am. Chem. Soc.* **2006**, *128*, 8754–8756. https://doi.org/10.1021/ja062509l.

(102) Cheng, G.-J.; Yang, Y.-F.; Liu, P.; Chen, P.; Sun, T.-Y.; Li, G.; Zhang, X.; Houk, K. N.; Yu, J.-Q.; Wu, Y.-D. Role of N -Acyl Amino Acid Ligands in Pd(II)-Catalyzed Remote C–H Activation of Tethered Arenes. *J. Am. Chem. Soc.* **2014**, *136*, 894–897. https://doi.org/10.1021/ja411683n.

(103) Engle, K. M.; Wang, D.-H.; Yu, J.-Q. Ligand-Accelerated C−H Activation Reactions: Evidence for a Switch of Mechanism. *J. Am. Chem. Soc.* **2010**, *132*, 14137–14151.

https://doi.org/10.1021/ja105044s.

(104) Wang, D.-H.; Engle, K. M.; Shi, B.-F.; Yu, J.-Q. Ligand-Enabled Reactivity and Selectivity in a Synthetically Versatile Aryl C–H Olefination. *Science (80-.).* **2010**, *327*, 315–319. https://doi.org/10.1126/science.1182512.

(105) Shabashov, D.; Daugulis, O. Auxiliary-Assisted Palladium-Catalyzed Arylation and Alkylation of Sp 2 and Sp3 Carbon-Hydrogen Bonds. *J. Am. Chem. Soc.* **2010**, *132*, 3965–3972. https://doi.org/10.1021/ja910900p.

(106) Frutos-Pedreño, R.; García-Sánchez, E.; Oliva-Madrid, M. J.; Bautista, D.; Martínez-Viviente, E.; Saura-Llamas, I.; Vicente, J. C-H Activation in Primary 3-Phenylpropylamines: Synthesis of Seven-Membered Palladacycles through Orthometalation. Stoichiometric Preparation of Benzazepinones and Catalytic Synthesis of Ureas. *Inorg. Chem.* **2016**, *55*, 5520–5533. https://doi.org/10.1021/acs.inorgchem.6b00542.

(107) Nadres, E. T.; Santos, G. I. F.; Shabashov, D.; Daugulis, O. Scope and Limitations of Auxiliary-Assisted, Palladium-Catalyzed Arylation and Alkylation of Sp2 and Sp3 C-H Bonds. *J. Org. Chem.* **2013**, *78*, 9689–9714. https://doi.org/10.1021/jo4013628.

(108) Meng, G.; Lam, N. Y. S.; Lucas, E. L.; Saint-Denis, T. G.; Verma, P.; Chekshin, N.; Yu, J. Q. Achieving Site-Selectivity for C-H Activation Processes Based on Distance and Geometry: A Carpenter's Approach. *J. Am. Chem. Soc.* **2020**, *142*, 10571–10591. https://doi.org/10.1021/jacs.0c04074.

(109) Leow, D.; Li, G.; Mei, T. S.; Yu, J. Q. Activation of Remote Meta-C-H Bonds Assisted by an End-on Template. *Nature* **2012**, *486*, 518–522. https://doi.org/10.1038/nature11158.

(110) Patra, T.; Watile, R.; Agasti, S.; Naveen, T.; Maiti, D. Sequential Meta-C-H Olefination of Synthetically Versatile Benzyl Silanes: Effective Synthesis of Meta-Olefinated Toluene, Benzaldehyde and Benzyl Alcohols. *Chem. Commun.* **2016**, *52*, 2027–2030. https://doi.org/10.1039/c5cc09446a.

(111) Bag, S.; Patra, T.; Modak, A.; Deb, A.; Maity, S.; Dutta, U.; Dey, A.; Kancherla, R.; Maji, A.; Hazra, A.; Bera, M.; Maiti, D. Remote Para-C–H Functionalization of Arenes by a D-Shaped Biphenyl Template-Based Assembly. *J. Am. Chem. Soc.* **2015**,

137, 11888–11891. https://doi.org/10.1021/jacs.5b06793.

(112) Jayarajan, R.; Das, J.; Bag, S.; Chowdhury, R.; Maiti, D. Diverse Meta-C−H Functionalization of Arenes across Different Linker Lengths. *Angew. Chemie - Int. Ed.* **2018**, *57*, 7659–7663. https://doi.org/10.1002/anie.201804043.

(113) Zhang, L.; Zhao, C.; Liu, Y.; Xu, J.; Xu, X.; Jin, Z. Activation of Remote Meta-C−H Bonds in Arenes with Tethered Alcohols: A Salicylonitrile Template. *Angew. Chemie - Int. Ed.* **2017**, *56*, 12245–12249. https://doi.org/10.1002/anie.201705495.

(114) Ihara, H.; Koyanagi, M.; Suginome, M. Anthranilamide: A Simple, Removable Ortho - Directing Modifier for Arylboronic Acids Serving Also as a Protecting Group in Cross-Coupling Reactions. *Org. Lett.* **2011**, *13*, 2662–2665. https://doi.org/10.1021/ol200764g.

(115) Ihara, H.; Suginome, M. Easily Attachable and Detachable Ortho-Directing Agent for Arylboronic Acids in Ruthenium-Catalyzed Aromatic C-H Silylation. *J. Am. Chem. Soc.* **2009**, *131*, 7502–7503. https://doi.org/10.1021/ja902314v.

(116) Ihara, H.; Ueda, A.; Suginome, M. Ruthenium-Catalyzed CH Silylation of Methylboronic Acid Using a Removable α-Directing Modifier on the Boron Atom. *Chem. Lett.* **2011**, *40*, 916–918. https://doi.org/10.1246/cl.2011.916.

(117) Yamamoto, T.; Ishibashi, A.; Suginome, M. Rhodium-Catalyzed C(Sp2)–H Addition of Arylboronic Acids to Alkynes Using a Boron-Based, Convertible Ortho-Directing Group. *Chem. Lett.* **2017**, *46*, 1169–1172. https://doi.org/10.1246/cl.170404.

(118) Yamamoto, T.; Ishibashi, A.; Suginome, M. Regioselective Synthesis of O-Benzenediboronic Acids via Ir-Catalyzed o-C-H Borylation Directed by a Pyrazolylaniline-Modified Boronyl Group. *Org. Lett.* **2017**, *19*, 886–889. https://doi.org/10.1021/acs.orglett.7b00041.

(119) Yamamoto, T.; Ishibashi, A.; Suginome, M. Boryl-Directed, Ir-Catalyzed C(Sp3)-H Borylation of Alkylboronic Acids Leading to Site-Selective Synthesis of Polyborylalkanes. *Org. Lett.* **2019**, *21*, 6235–6240. https://doi.org/10.1021/acs.orglett.9b02112.

(120) Ihara, H.; Koyanagi, M.; Suginome, M. Anthranilamide: A Simple, Removable Ortho-Directing Modifier for Arylboronic Acids Serving Also as a Protecting Group in

Cross-Coupling Reactions. *Org. Lett.* **2011**, *13*, 2662–2665. https://doi.org/10.1021/ol200764g.

(121) Coomber, C. E.; Benhamou, L.; Bučar, D. K.; Smith, P. D.; Porter, M. J.; Sheppard, T. D. Silver-Free Palladium-Catalyzed C(Sp 3)-H Arylation of Saturated Bicyclic Amine Scaffolds. *J. Org. Chem.* **2018**, *83*, 2495–2503. https://doi.org/10.1021/acs.joc.7b02665.

(122) Van Steijvoort, B. F.; Kaval, N.; Kulago, A. A.; Maes, B. U. W. Remote Functionalization: Palladium-Catalyzed C5(Sp3)-H Arylation of 1-Boc-3-Aminopiperidine through the Use of a Bidentate Directing Group. *ACS Catal.* **2016**, *6*, 4486–4490. https://doi.org/10.1021/acscatal.6b00841.

(123) Lennox, A. J. J.; Lloyd-Jones, G. C. Selection of Boron Reagents for Suzuki–Miyaura Coupling. *Chem. Soc. Rev.* **2014**, *43*, 412–443. https://doi.org/10.1039/C3CS60197H.

(124) Williams, A. F.; White, A. J. P.; Spivey, A. C.; Cordier, C. J. Meta -Selective C-H Functionalisation of Aryl Boronic Acids Directed by a MIDA-Derived Boronate Ester. *Chem. Sci.* **2020**, *11*, 3301–3306. https://doi.org/10.1039/d0sc00230e.

(125) Noguchi, H.; Hojo, K.; Suginome, M. Boron-Masking Strategy for the Selective Synthesis of Oligoarenes via Iterative Suzuki-Miyaura Coupling. *J. Am. Chem. Soc.* **2007**, *129*, 758–759. https://doi.org/10.1021/ja067975p.

(126) Cabrera, P. J.; Lee, M.; Sanford, M. S. Second-Generation Palladium Catalyst System for Transannular C-H Functionalization of Azabicycloalkanes. *J. Am. Chem. Soc.* **2018**, *140*, 5599–5606. https://doi.org/10.1021/jacs.8b02142.

(127) Ackermann, L.; Diers, E.; Manvar, A. Ruthenium-Catalyzed C-H Bond Arylations of Arenes Bearing Removable Directing Groups via Six-Membered Ruthenacycles. *Org. Lett.* **2012**, *14*, 1154–1157. https://doi.org/10.1021/ol3000876.

(128) Rodríguez, M.; Ramos-Ortíz, G.; Alcalá-Salas, M. I.; Maldonado, J. L.; López-Varela, K. A.; López, Y.; Domínguez, O.; Meneses-Nava, M. A.; Barbosa-García, O.; Santillan, R.; Farfán, N. One-Pot Synthesis and Characterization of Novel Boronates for the Growth of Single Crystals with Nonlinear Optical Properties. *Dye. Pigment.* **2010**, *87*, 76–83. https://doi.org/10.1016/j.dyepig.2010.02.007.

(129) Beesly, R. M.; Ingold, C. K.; Thorpe, J. F. CXIX.- The formation and stability of

spiro-compounds. Part I. spiro-Compounds from cyclohexane. *J. Chem. Soc., Trans.* **1915**, *107*, 1080–1106. https://doi.org/10.1039/CT9150701080.

(130) Lennox, A. J. J.; Lloyd-Jones, G. C. Selection of Boron Reagents for Suzuki-Miyaura Coupling. *Chem. Soc. Rev.* **2014**, *43*, 412–443. https://doi.org/10.1039/c3cs60197h.

(131) Chen, J.; Cammers-Goodwin, A. 2-(Fluorophenyl)Pyridines by the Suzuki-Miyaura Method: Ag2O Accelerates Coupling over Undesired Ipso Substitution (SNAr) of Fluorine. *Tetrahedron Lett.* **2003**, *44*, 1503–1506. https://doi.org/10.1016/S0040-4039(02)02793-4.

(132) Wang, P.; Verma, P.; Xia, G.; Shi, J.; Qiao, J. X.; Tao, S.; Cheng, P. T. W.; Poss, M. A.; Farmer, M. E.; Yeung, K.-S.; Yu, J.-Q. Ligand-Accelerated Non-Directed C–H Functionalization of Arenes. *Nature* **2017**, *551*, 489–493. https://doi.org/10.1038/nature24632.

(133) Achar, T. K.; Zhang, X.; Mondal, R.; Shanavas, M. S.; Maiti, S.; Maity, S.; Pal, N.; Paton, R. S.; Maiti, D. Palladium-Catalyzed Directed Meta-Selective C−H Allylation of Arenes: Unactivated Internal Olefins as Allyl Surrogates. *Angew. Chemie Int. Ed.* **2019**, *58*, 10353–10360. https://doi.org/10.1002/anie.201904608.

(134) Porey, S.; Zhang, X.; Bhowmick, S.; Kumar Singh, V.; Guin, S.; Paton, R. S.; Maiti, D. Alkyne Linchpin Strategy for Drug:Pharmacophore Conjugation: Experimental and Computational Realization of a Meta-Selective Inverse Sonogashira Coupling. *J. Am. Chem. Soc.* **2020**, *142*, 3762–3774. https://doi.org/10.1021/jacs.9b10646.

(135) Mihai, M. T.; Davis, H. J.; Genov, G. R.; Phipps, R. J. Ion Pair-Directed C–H Activation on Flexible Ammonium Salts: Meta-Selective Borylation of Quaternized Phenethylamines and Phenylpropylamines. *ACS Catal.* **2018**, *8*, 3764–3769. https://doi.org/10.1021/acscatal.8b00423.

(136) Davis, H. J.; Genov, G. R.; Phipps, R. J. Meta-Selective C−H Borylation of Benzylamine-, Phenethylamine-, and Phenylpropylamine-Derived Amides Enabled by a Single Anionic Ligand. *Angew. Chemie Int. Ed.* **2017**, *56*, 13351–13355. https://doi.org/10.1002/anie.201708967.

(137) Hofmann, A. W. Zur Kenntniss Des Piperidins Und Pyridins. *Berichte der Dtsch. Chem. Gesellschaft* **1879**, *12*, 984–990. https://doi.org/10.1002/cber.187901201254.

(138) Löffler, K.; Freytag, C. Über Eine Neue Bildungsweise von N-Alkylierten Pyrrolidinen. *Berichte der Dtsch. Chem. Gesellschaft* **1909**, *42*, 3427–3431. https://doi.org/10.1002/cber.19090420377.

(139) Löffler, K. Über Eine Neue Bildungsweise N-Alkylierter Pyrrolidine. *Berichte der Dtsch. Chem. Gesellschaft* **1910**, *43*, 2035–2048. https://doi.org/10.1002/cber.191004302146.

(140) Lewis, G. N. *Valence and the Structure of Atoms and Molecules*; Chemical Catalog Company, Incorporated: New York, 1923.

(141) Lowry, T. M. The Uniqueness of Hydrogen. *J. Soc. Chem. Ind.* **1923**, *42*, 43–47. https://doi.org/10.1002/jctb.5000420302.

(142) Brönsted, J. N. Einige Bemerkungen Über Den Begriff Der Säuren Und Basen. *Recl. des Trav. Chim. des Pays-Bas* **1923**, *42*, 718–728. https://doi.org/10.1002/recl.19230420815.

(143) Brown, H. C.; Kanner, B. Preparation and Reactions of 2,6-Di-t-Butylpyridine and Related Hindered Bases. A Case of Steric Hindrance toward the Proton1,2. *J. Am. Chem. Soc.* **1966**, *88*, 986–992. https://doi.org/10.1021/ja00957a023.

(144) Brown, H. C.; Schlesinger, H. I.; Cardon, S. Z. Studies in Stereochemistry. I. Steric Strains as a Factor in the Relative Stability of Some Coördination Compounds of Boron. *J. Am. Chem. Soc.* **1942**, *64*, 325–329. https://doi.org/10.1021/ja01254a031.

(145) Welch, G. C.; San Juan, R. R.; Masuda, J. D.; Stephan, D. W. Reversible, Metal-Free Hydrogen Activation. *Science (80-.).* **2006**, *314*, 1124–1126. https://doi.org/10.1126/science.1134230.

(146) Chase, P. A.; Welch, G. C.; Jurca, T.; Stephan, D. W. Metal-Free Catalytic Hydrogenation. *Angew. Chemie Int. Ed.* **2007**, *46*, 8050–8053. https://doi.org/10.1002/anie.200702908.

(147) Greb, L.; Oña-Burgos, P.; Schirmer, B.; Grimme, S.; Stephan, D. W.; Paradies, J. Metal-Free Catalytic Olefin Hydrogenation: Low-Temperature H2 Activation by Frustrated Lewis Pairs. *Angew. Chemie Int. Ed.* **2012**, *51*, 10164–10168. https://doi.org/10.1002/anie.201204007.

(148) Meng, W.; Feng, X.; Du, H. Asymmetric Catalysis with Chiral Frustrated Lewis Pairs.

Chinese J. Chem. **2020**, *38*, 625–634. https://doi.org/10.1002/cjoc.202000011.

(149) Chen, D.; Klankermayer, J. Metal-Free Catalytic Hydrogenation of Imines with Tris(Perfluorophenyl)Borane. *Chem. Commun.* **2008**, No. 18, 2130–2131. https://doi.org/10.1039/B801806E.

(150) Chen, D.; Wang, Y.; Klankermayer, J. Enantioselective Hydrogenation with Chiral Frustrated Lewis Pairs. *Angew. Chemie Int. Ed.* **2010**, *49*, 9475–9478. hhttps://doi.org/10.1002/anie.201004525.

(151) Liu, Y.; Du, H. Chiral Dienes as "Ligands" for Borane-Catalyzed Metal-Free Asymmetric Hydrogenation of Imines. *J. Am. Chem. Soc.* **2013**, *135*, 6810–6813. https://doi.org/10.1021/ja4025808.

(152) Lindqvist, M.; Borre, K.; Axenov, K.; Kótai, B.; Nieger, M.; Leskelä, M.; Pápai, I.; Repo, T. Chiral Molecular Tweezers: Synthesis and Reactivity in Asymmetric Hydrogenation. *J. Am. Chem. Soc.* **2015**, *137*, 4038–4041. https://doi.org/10.1021/ja512658m.

(153) Gao, B.; Feng, X.; Meng, W.; Du, H. Asymmetric Hydrogenation of Ketones and Enones with Chiral Lewis Base Derived Frustrated Lewis Pairs. *Angew. Chemie Int. Ed.* **2020**, *59*, 4498–4504. https://doi.org/10.1002/anie.201914568.

(154) Florides, G. A.; Christodoulides, P. Global Warming and Carbon Dioxide through Sciences. *Environ. Int.* **2009**, *35*, 390–401. https://doi.org/10.1016/j.envint.2008.07.007.

(155) Stips, A.; Macias, D.; Coughlan, C.; Garcia-Gorriz, E.; Liang, X. S. On the Causal Structure between CO2 and Global Temperature. *Sci. Rep.* **2016**, *6*, 21691. https://doi.org/10.1038/srep21691.

(156) Mömming, C. M.; Otten, E.; Kehr, G.; Fröhlich, R.; Grimme, S.; Stephan, D. W.; Erker, G. Reversible Metal-Free Carbon Dioxide Binding by Frustrated Lewis Pairs. *Angew. Chemie Int. Ed.* **2009**, *48*, 6643–6646. https://doi.org/10.1002/anie.200901636.

(157) Berkefeld, A.; Piers, W. E.; Parvez, M. Tandem Frustrated Lewis Pair/Tris(Pentafluorophenyl)Borane-Catalyzed Deoxygenative Hydrosilylation of Carbon Dioxide. *J. Am. Chem. Soc.* **2010**, *132*, 10660–10661. https://doi.org/10.1021/ja105320c.

(158) Ashley, A. E.; Thompson, A. L.; O'Hare, D. Non-Metal-Mediated Homogeneous Hydrogenation of CO2 to CH3OH. *Angew. Chemie Int. Ed.* **2009**, *48*, 9839–9843. https://doi.org/10.1002/anie.200905466.

(159) Courtemanche, M.-A.; Pulis, A. P.; Rochette, É.; Légaré, M.-A.; Stephan, D. W.; Fontaine, F.-G. Intramolecular B/N Frustrated Lewis Pairs and the Hydrogenation of Carbon Dioxide. *Chem. Commun.* **2015**, *51*, 9797–9800. https://doi.org/10.1039/C5CC03072B.

(160) Légaré, M. A.; Courtemanche, M. A.; Rochette, É.; Fontaine, F. G. Metal-Free Catalytic C-H Bond Activation and Borylation of Heteroarenes. *Science (80-.).* **2015**, *349*, 513–516. https://doi.org/10.1126/science.aab3591.

(161) Shang, M.; Cao, M.; Wang, Q.; Wasa, M. Enantioselective Direct Mannich-Type Reactions Catalyzed by Frustrated Lewis Acid/Brønsted Base Complexes. *Angew. Chemie Int. Ed.* **2017**, *56*, 13338–13341. https://doi.org/10.1002/anie.201708103.

(162) Cross, M. Novel Approaches to Aromatic C–H Borylation, University College London, 2023.

(163) Biedrzycki, M.; Scouten, W. H.; Biedrzycka, Z. Derivatives of Tetrahedral Boronic Acids. *J. Organomet. Chem.* **1992**, *431*, 255–270. https://doi.org/10.1016/0022-328X(92)83330-K.

(164) Nizioł, J.; Zieliński, Z.; Leś, A.; Dąbrowska, M.; Rode, W.; Ruman, T. Synthesis, Reactivity and Biological Activity of N(4)-Boronated Derivatives of 2′-Deoxycytidine. *Bioorg. Med. Chem.* **2014**, *22*, 3906–3912. https://doi.org/10.1016/j.bmc.2014.06.014.

(165) Oba, T.; Takahashi, H.; Roppongi, M.; Miyata, K. 1,4,2-Diazaborole-Type Heterocycle from 2H-Azirine-2-Carboxylate and [(Alkylamino)Methyl]Trifluoroborate. *Tetrahedron Lett.* **2022**, *102*, 153953. https://doi.org/10.1016/j.tetlet.2022.153953.

(166) Garget, T. A.; Kiefel, M. J.; Houston, T. A. Perfluorinated Pinacol Promotes Efficient Amidination of 2-Aminophenylboronic Acid. *ARKIVOC* **2022**, *2022*, 143–153. https://doi.org/10.24820/ark.5550190.p011.834.

(167) Hu, N.; Zhao, G.; Zhang, Y.; Liu, X.; Li, G.; Tang, W. Synthesis of Chiral α-Amino Tertiary Boronic Esters by Enantioselective Hydroboration of α-Arylenamides. *J. Am.*

Chem. Soc. **2015**, *137*, 6746–6749. https://doi.org/10.1021/jacs.5b03760.

(168) Baron, H.; Remfry, F. G. P.; Thorpe, J. F. CLXXV.—The Formation and Reactions of Imino-Compounds. Part I. Condensation of Ethyl Cyanoacetate with Its Sodium Derivative. *J. Chem. Soc., Trans.* **1904**, *85*, 1726–1761. https://doi.org/10.1039/CT9048501726.

(169) Li, Z.; Zhang, L.; Nishiura, M.; Luo, G.; Luo, Y.; Hou, Z. CO2 Activation by Lewis Pairs Generated Under Copper Catalysis Enables Difunctionalization of Imines. *J. Am. Chem. Soc.* **2020**, *142*, 1966–1974. https://doi.org/10.1021/jacs.9b11423.

(170) Wood, J. L.; Marciasini, L. D.; Vaultier, M.; Pucheault, M. Iron Catalysis and Water: A Synergy for Refunctionalization of Boron. *Synlett* **2014**, *25*, 551–555. https://doi.org/10.1055/s-0033-1340500.

(171) Slabber, C. A.; Grimmer, C. D.; Robinson, R. S. Solution-State 15N NMR and Solid-State Single-Crystal XRD Study of Heterosubstituted Diazaboroles and Borinines Prepared via an Effective and Simple Microwave-Assisted Solvent-Free Synthesis. *J. Organomet. Chem.* **2013**, *723*, 122–128. https://doi.org/10.1016/j.jorganchem.2012.09.018.

(172) Ding, S.; Ma, Q.; Zhu, M.; Ren, H.; Tian, S.; Zhao, Y.; Miao, Z. Direct Transformation from Arylamines to Aryl Naphthalene-1,8-Diamino Boronamides: A Metal-Free Sandmeyer-Type Process. *Molecules* **2019**, *24*, 1–12. https://doi.org/10.3390/molecules24030377.

(173) Xu, L.; Li, P. Direct Introduction of a Naphthalene-1,8-Diamino Boryl [B(Dan)] Group by a Pd-Catalysed Selective Boryl Transfer Reaction. *Chem. Commun.* **2015**, *51*, 5656–5659. https://doi.org/10.1039/c5cc00231a.

(174) Yang, H.; Li, Y.; Jiang, M.; Wang, J.; Fu, H. General Copper-Catalyzed Transformations of Functional Groups from Arylboronic Acids in Water. *Chem. - A Eur. J.* **2011**, *17*, 5652–5660. https://doi.org/10.1002/chem.201003711.

(175) Bunce, R. A.; Nammalwar, B. 4(1H)-Quinolinones by a Tandem Reduction-Addition-Elimination Reaction. *Org. Prep. Proced. Int.* **2010**, *42*, 557–563. https://doi.org/10.1080/00304948.2010.526512.

(176) Prebil, R.; Kralj, D.; Golobic, A.; Stare, K.; Dahmann, G.; Stanovnik, B.; Svete, J.;

Janjić, M.; Prebil, R.; Grošelj, U.; Kralj, D.; Malavašič, Č.; Golobič, A.; Stare, K.; Dahmann, G.; Stanovnik, B.; Svete, J. A Simple Synthesis of 5- (2-Aminophenyl) -1 H -Pyrazoles. *Helv. Chim. Acta* **2011**, *94*, 1703–1717. https://doi.org/10.1002/hlca.201100055.

(177) Maiti, D.; Buchwald, S. L. Orthogonal Cu- and Pd-Based Catalyst Systems for the O- and N-Arylation of Aminophenols. *J. Am. Chem. Soc.* **2009**, *131*, 17423–17429. https://doi.org/10.1021/ja9081815.

(178) Wang, G.; Xu, L.; Li, P. Double N,B-Type Bidentate Boryl Ligands Enabling a Highly Active Iridium Catalyst for C-H Borylation. *J. Am. Chem. Soc.* **2015**, *137*, 8058–8061. https://doi.org/10.1021/jacs.5b05252.

(179) Wright, A. C.; Du, Y. E.; Stoltz, B. M. Small-Scale Procedure for Acid-Catalyzed Ketal Formation. *J. Org. Chem.* **2019**, *84*, 11258–11260. https://doi.org/10.1021/acs.joc.9b01541.